ISJET

INTERNATIONAL SCIENTIFIC JOURNAL OF ENGINEERING AND TECHNOLOGY

Volume 10 No. 2 July-December 2026

ISSN 2586-8527 (Online)

Panyapiwat Institute of Management

Indexed in the Thai-Journal Citation Index (TCI 1)

INTERNATIONAL SCIENTIFIC JOURNAL OF ENGINEERING AND TECHNOLOGY (ISJET)

Volume 10 No. 2 July-December 2026

ISSN 2586-8527 (Online)
PANYAPIWAT INSTITUTE OF MANAGEMENT

INTERNATIONAL SCIENTIFIC JOURNAL OF ENGINEERING AND TECHNOLOGY (ISJET)
Volume 10 No. 2 July-December 2026
ISSN 2586-8527 (Online)

Copyright
Panyapiwat Institute of Management
85/1 Moo 2, Chaengwattana Rd.,
Bang Talat, Pakkred,
Nonthaburi, 11120, Thailand
Tel. +66 2855 1560
E-mail: isjet@pim.ac.th
Website: https://ph02.tci-thaijo.org/index.php/isjet/index

Copyright©2017, Panyapiwat Institute of Management

INTERNATIONAL SCIENTIFIC JOURNAL OF ENGINEERING AND TECHNOLOGY (ISJET)

Volume 10 No. 2 July-December 2026 ISSN 2586-8527 (Online)

THE INTERNATIONAL SCIENTIFIC JOURNAL OF ENGINEERING AND TECHNOLOGY (ISJET), with online ISSN 2586-8527, has been published since 2017. It is currently a journal accredited by the Thai-Journal Citation Index Centre (TCI), classified in Tier 1 for the field of Science and Technology.

Aim and Scope:

The purpose of publishing and disseminating academic articles in the fields of Engineering, Logistics, Agricultural Science, Food Science, and other areas of Science and Technology. Fields for academics, researchers, instructors, students, and the general.

The ISJET submissions are welcome from both the Panyapiwat Institute of Management (PIM) and other institutions in Thailand and abroad.

Peer Review Process
Reviewing Policy:

1. Any manuscript to be accepted for publication must have been reviewed and approved by at least two peer reviewers in that particular field or related fields. The Journal has a double-blind peer review policy, which means that neither the peer reviewer nor the author knows the identity of the other.
2. The submitted manuscript must have never been published in any other periodical, and must not be in the approval process for publication by any other periodical. Also, the author must not plagiarize others' work.
3. The article, expression, illustrations, and tables that are published in the Journal are the sole responsibility of the author and not that of the Panyapiwat Institute of Management.
4. The Editorial Board of the ISJET reserves the right to change or revise the name(s) and unit(s) of the author(s) in all cases after the issuance of the letter.
5. The Editorial Board of the ISJET reserves the right to cancel the publication that has been issued a certification of publication in the Panyapiwat Journal.
6. The Editorial Board of the ISJET reserves the right to decide on publishing an article in the Journal.

Type of Articles:

Research article: Original full-length research papers that have not been published previously. These are articles where authors report on studies they conducted. The length should exceed 15 pages, excluding references.

Academic articles: These are critical evaluations of studies in particular areas that have already been published, or theoretical articles in which the authors aim to formulate new theories on existing research. The length should exceed 15 pages, excluding references.

Review articles: Will be accepted in areas of topical interest and will normally focus on literature published over the previous five years. A review article typically includes: Abstract, Introduction, Main Body, Discussion, Conclusion, and References. The length should exceed 15 pages, excluding references.

Language:

The ISJET accepts manuscripts in English. All submissions must be well-written and adhere to correct, standard, and academically appropriate language. For English manuscripts, proofreading by a native speaker is required to ensure clarity and quality.

To maintain the Journal's high standards and publication ethics, the editorial board has implemented the Turnitin Program for all submitted manuscripts to address plagiarism issues.

Frequency of Publication: 2 issues/ Year
The first issue: January - June
The second issue: July – December

Number of articles: 10 articles per issue

Publication and Access Charges:

The author is required to pay a publication fee of 4,000 Baht/article via direct transfer to the Panyapiwat Institute of Management account only. This payment should be made after receiving notification that the article has passed the preliminary review by the editorial board.

Workflow of Journal:

https://drive.google.com/file/d/1bUeIYuL7nOsAfvIUB0h3AtEcNHKtuQRg/view?usp=drive_link

Open Access Policy:

All articles published in ISJET are open access and freely available for reading, downloading, and sharing. However, proper citations of these articles are required for their reproduction and public distribution by any medium.

Ownership and Management:

The ISJET is published by the Research and Development Department at Panyapiwat Institute of Management, Thailand, with financial support provided by the Institute. The journal's operation is led by the Editor-in-Chief and the Associate Editor-in-Chief, who work closely with the editorial team and staff. This funding ensures that the journal maintains high standards of publishing and a thorough peer-review process, and remains freely accessible to researchers globally. The INTERNATIONAL SCIENTIFIC JOURNAL OF ENGINEERING AND TECHNOLOGY (ISJET) is dedicated to fostering innovation and scientific advancement, and its support of this journal helps promote the exchange of knowledge and encourages collaborations both within Thailand and internationally.

Publisher:

The Office of Research and Development, Panaypiwat Institute of Management (PIM), is responsible for preparing and publishing the INTERNATIONAL SCIENTIFIC JOURNAL OF ENGINEERING AND TECHNOLOGY (ISJET).

The Address of the Institute is:

85/1 Moo 2, Chaengwattana RD., Bang Talat, Pakkred, Nonthaburi 11120, Thailand
Email: isjet@pim.ac.th Tel. +66 855 1560

Copyright and Licensing:

Prospective authors should be aware that all submissions must be original and be accompanied by the consent form listing all named authors. Additionally, authors must obtain official permission to include texts, figures, data, or any other information attributable to others.

Upon submission, the authors grant ISJET the right to publish the article without restrictions. However, the authors retain the copyright to their work and the right to reproduce, distribute, and display it. Authors may use the articles in their academic work or share them with their students, while the ISJET Journal controls how they are disseminated.

Revenue Sources:

The entire publication process is fee-free. The ISJET relies solely on the support of Panyapiwat Institute of Management (PIM) to generate revenue and encourage scholars and researchers to publish their valuable work.

Advertising:

In alignment with its policy, the journal does not accept any form of advertisement funding. Relevant information about academic conferences, journal updates, or research projects may be shared on the journal's official website when deemed appropriate. The inclusion of such content does not compromise the journal's ethical principles.

Direct Marketing:

The journal does not engage in direct marketing practices. Announcements, such as calls for papers or journal promotions, are made available through official channels, including the journal's website, social media, or affiliated organizations. These communications adhere to ethical guidelines and respect individual privacy.

INTERNATIONAL SCIENTIFIC JOURNAL OF ENGINEERING AND TECHNOLOGY (ISJET)
Volume 10 No. 2 July-December 2026
ISSN 2586-8527 (Online)

Advisors Board

Assoc. Prof. Dr. Somrote Komolavanij	Panyapiwat Institute of Management, Thailand
Assoc. Prof. Dr. Voravit Siripholvat	Panyapiwat Institute of Management, Thailand
Prof. Dr. Jakrapong Kaewkhao	Nakhon Pathom Rajabhat University, Thailand
Assoc. Prof. Dr. Paritud Bhandhubanyong	Independent Scholar, Thailand
Assoc. Prof. Dr. Pisit Charnkeitkong	Independent Scholar, Thailand

Editor-in-chief

Assoc. Prof. Dr. Parinya Sanguansat	Panyapiwat Institute of Management, Thailand

Associate Editors

Asst. Prof. Dr. Anupong Thuengnaitham	Panyapiwat Institute of Management, Thailand
Asst. Prof. Dr. Nivet Chirawichitchai	Panyapiwat Institute of Management, Thailand
Asst. Prof. Dr. Phannachet Na Lamphun	Panyapiwat Institute of Management, Thailand
Dr. Wirin Sonsrettee	Panyapiwat Institute of Management, Thailand

Editorial Board

Prof. Dr. Anand Marya	University of Puthisastra, Cambodia
Prof. Dr. Arnulfo P. Azcarraga	De La Salle University, Philippines
Prof. Dr. Bob Rastall	University of Reading, UK
Prof. Dr. Chidchanok Lursinsap	Chulalongkorn University, Thailand
Prof. Dr. Kyoko Kato	Aoyama Gakuin University, Japan
Prof. Dr. Feng Wang	University of California, Berkeley, USA
Prof. Dr. Methi Wecharatana	New Jersey Institute of Technology, USA
Prof. Dr. Nigel Scollan	Queen's University Belfast, UK
Prof. Dr. Ninshu Ma	University of Osaka, Japan
Prof. Dr. Panich Intra	Rajamangala University of Technology Lanna, Thailand
Prof. Dr. Parames Chutima	Chulalongkorn University, Thailand
Prof. Dr. Phadungsak Rattanadecho	Thammasat University, Thailand
Prof. Dr. Prabhas Chongstitvatana	Chulalongkorn University, Thailand
Prof. Dr. Prasanta Kumar Dey	Aston Business School, Aston University, UK
Prof. Dr. Rattikorn Hewett	Texas Tech University, USA
Prof. Dr. Rosemary R. Seva	De La Salle University, Philippines
Prof. Dr. Sandhya Babel	Sirindhorn International Institute of Technology, Thammasat University, Thailand
Prof. Dr. Saraju Mohanty	University of North Texas, USA
Prof. Dr. Stephen Beck	University of Sheffield, UK
Prof. Dr. Takashi Yukawa	Nagaoka University of Technology, Japan
Prof. Dr. Thanaruk Theeramunkong	Sirindhon International Institute of Technology, Thammasat University, Thailand
Prof. Dr. Venkata Seshachala Sarma Yadavalli	University of Pretoria, South Africa
Prof. Dr. Vira Chankong	Case Western Reserve University, USA
Prof. Dr. Yap Bee Wah	Institute of Big Data Analytics and Artificial Intelligence, Malaysia
Prof. Chen Wei Ning, William	Nanyang Technological University, Singapore
Prof. Duane P. Bartholomew	University of Hawaii at Manoa, Honolulu, USA
Prof. Jun Li	Curtin University, Australia
Prof. Yizhen Yang	Nanjing Tech University Pujiang Institute, China
Assoc. Prof. Bo Jing	Nanjing Audit University, China
Assoc. Prof. Dr. Chawalit Jeenanunta	Sirindhon International Institute of Technology, Thammasat University, Thailand
Assoc. Prof. Dr. Ivan Henderson V. Gue	De La Salle University, Philippines
Assoc. Prof. Dr. Nattapon Chantarapanich	Kasetsart University, Sriracha Campus, Thailand
Assoc. Prof. Dr. Wilaiporn Lee	King Mongkut's University of Technology North Bangkok, Thailand
Asst. Prof. Dr. Adisak Joomwong	Maejo University, Thailand

Asst. Prof. Dr. Rangsima Chanphana — Chulalongkorn University, Thailand
Dr. Jochen Hermann Josef Amrehn — Nanjing Tech University Pujiang Institute, China
Dr. Muhammad Akhsin Muflikhun — Gadjah Mada University, Indonesia
Dr. Risdy Risdiyono — Islamic University of Indonesia, Indonesia
Dr. Viet Hoang — Van Lang University, Vietnam

Journal Secretary
Ms. Suchinda Chaluai — Panyapiwat Institute of Management, Thailand

INTERNATIONAL SCIENTIFIC JOURNAL OF ENGINEERING AND TECHNOLOGY (ISJET)
Volume 10 No. 2 July-December 2026
ISSN 2586-8527 (Online)

Peer Reviewers

Prof. Dr. Parames Chutima	Chulalongkorn University, Thailand
Assoc. Prof. Dr. Chana Raksiri	Kasetsart University, Thailand
Assoc. Prof. Dr. Chanboon Sathitwiriyawong	King Mongkut's Institute of Technology Ladkrabang, Thailand
Assoc. Prof. Dr. Nattapon Chantarapanich	Kasetsart University Sriracha Campus, Thailand
Assoc. Prof. Dr. Nikorn Sirivongpaisal	Prince of Songkla University, Hat Yai Campus, Thailand
Assoc. Prof. Dr. Nivit Charoenchai	Chiang Mai University, Thailand
Assoc. Prof. Dr. Panomkhawn Riyamongkol	Naresuan University, Thailand
Assoc. Prof. Dr. Papot Jaroenapibal	Khon Kaen University, Thailand
Assoc. Prof. Dr. Siriporn Supratid	Rangsit University, Thailand
Assoc. Prof. Dr. Sunan Pansakorn	Rajamangala University of Technology Thanyaburi, Thailand
Assoc. Prof. Dr. Thananya Wasusri	Mahidol University, Thailand
Assoc. Prof. Dr. Werasak Kurutach	Mahanakorn University of Technology, Thailand
Assoc. Prof. Dr. Wilaiporn Lee	King Mongkut's University of Technology North Bangkok, Thailand
Assoc. Prof. Chaiyan Junsiri	Khon Khen University, Thailand
Asst. Prof. Dr. Adisak Joomwong	Maejo University, Thailand
Asst. Prof. Dr. Chutima Beokhaimook	Rangsit University, Thailand
Asst. Prof. Dr. Korawit Chaisu	Chiang Mai University, Thailand
Asst. Prof. Dr. Narongdech Keeratipranon	Chulalongkorn University, Thailand
Asst. Prof. Dr. Satien Janpla	Suan Sunandha Rajabhat University, Thailand
Asst. Prof. Dr. Sukumal Kitisin	Kasetsart University, Thailand
Asst. Prof. Dr. Sumeth Yuenyong	Mahidol University, Thailand
Asst. Prof. Dr. Wongkot Sriurai	Ubon Ratchathani University, Thailand

INTERNATIONAL SCIENTIFIC JOURNAL OF ENGINEERING AND TECHNOLOGY (ISJET)
Volume 10 No. 2 July-December 2026
ISSN 2586-8527 (Online)

Dear Colleagues,

Welcome to the second issue of the 10th volume of the International Scientific Journal of Engineering and Technology (ISJET). As we complete our tenth volume, the ten papers in this issue share a practical purpose: Making engineering cleaner, safer, and more efficient in the settings where it is actually used. The contributions range from biodegradable packaging and factory-floor process improvement to autonomous vehicles, machine vision, and nanoparticle instrumentation, and many draw on Thai industrial and institutional case studies.

Sustainability runs through this issue. One study develops biodegradable cushioning for delivery packaging by blending sago starch with sodium alginate or kappa carrageenan. Drop-and-transport tests show that sago-to-hydrogel ratios of 80:20 and 60:40 provide the best structural stability and impact absorption, with alginate favoring impact resistance and carrageenan favoring flexibility. At the institutional level, another paper proposes 26 Sustainable Performance Indicators, linked to 81 SDG indicators, to measure how Thailand's science, technology, and innovation organizations—NRCT, NSTDA, and TSRI—contribute to the Sustainable Development Goals.

Several papers turn to the efficiency and reliability of everyday operations. Applying the ECRS principle to pineapple peeling knife sharpening, one team introduces a work-holding jig and a single, harder grinding wheel, cutting processing time from 151 to 86 minutes per unit and grinding costs from 22,400 to 7,200 THB per month. A complementary study treats human error in agricultural and automotive manufacturing as a systemic Man–Machine–Material–Method (4M) issue, using Quality Function Deployment and the House of Quality to translate employer requirements into workforce competency specifications. In the service sector, an automated OCR system with rule-based post-processing helps a non-profit organization verify electronic bank transfer slips; with final operator verification, it reaches full accuracy and saves more than 41 hours of work.

In autonomous mobility, a real-environment comparison of two SLAM solutions, Gmapping and Cartographer, identifies cumulative error as the key factor limiting mapping accuracy and highlights the importance of loop detection. Working in the CARLA simulator, another team integrates Adaptive Cruise Control and Lane Departure Warning: the cruise control tracks the lead vehicle's speed with 97.9% accuracy, while lane warnings remain reliable on clear markings but produce false positives above 30% in heavy rain or on dashed lines. Continuing a line of work featured in our previous issue, a review of the DonkeyCar platform surveys explainable image captioning for autonomous driving and replicates the ADAPT model alongside lane-following and obstacle-avoidance tasks on low-cost hardware.

Finally, two papers advance measurement and inspection. An image-based system for hen egg grading combines maximum-likelihood classification in HSV color space with least-squares ellipse fitting and RANSAC, reaching true positive rates of 97% and 96% on training and test data from 150 eggs graded to Thai agricultural standards. At the nanometer scale, a miniaturized parallel-plate electrostatic size classifier for aerosol particles up to 300 nm shows close agreement between experiment and its design model, pointing toward more portable aerosol instruments.

We sincerely thank our authors for entrusting their work to ISJET, our peer reviewers for their careful and timely evaluations, and the editorial board and journal staff who make each issue possible. As ISJET marks ten volumes of publication, we warmly invite researchers in Thailand and abroad to continue submitting their research, academic, and review articles. We hope this issue sparks new ideas and continued cross-disciplinary collaboration within the engineering and technology community.

With kind regards,

Assoc. Prof. Dr. Parinya Sanguansat
Editor-in-chief
isjet@pim.ac.th

INTERNATIONAL SCIENTIFIC JOURNAL OF ENGINEERING AND TECHNOLOGY (ISJET)
Volume 10 No. 2 July-December 2026
ISSN 2586-8527 (Online)

CONTENTS

- **A Guideline for Sustainable Material Selection in Product Packaging Design: Development and Testing of Packaging Made from Environmentally Friendly Material** 1
  Suchada Rianmora, Chaiyut Suwannakan, Sirawich Chanchiewvichai, Kantarat Sreeprasert, and Supavich Vongvivat

- **Application of an Automated OCR System for Data Processing of Banking Electronic Transfer Slips: A Case Study of a Non-Profit Organization in Thailand** 18
  Dhammanit Buddhakulsomsiri, Laddawan Suwannachote, Jirachai Buddhakulsomsiri, and Parthana Parthanadee

- **Comparing Two SLAM Solutions to Improve the Perception Accuracy of Autonomous Vehicles** 34
  Yu Jiand and Jian Qu

- **From Human Error Prevention to QFD-Based Preventive System Design in Thailand's Agricultural and Automotive Manufacturing Systems** 40
  Wichapol Chanchiewvichai, Suchada Rianmora, Thiti Mahaboonpachai, Chatchai Vorathanawat, and Sirawich Chanchiewvichai

- **Image Analysis for Hen Egg Classification and Size Estimation** 56
  Supawadee Chaivivatrakul and Jednipat Moonrinta

- **Increasing Efficiency in Pineapple Peeling Knife Sharpening through ECRS Principles** 68
  Pipat Lertkowit, Poom Jatunitanon, and Bundit Inseemeesak

- **Integrated Lane Departure Warning and Adaptive Cruise Control for Enhanced Driving Safety in Advanced Driver Assistance Systems: A Simulation Study** 79
  Tanakorn Mongkondatsawat, Panumat Rergngam, Wutthichai Imwong, Namchai Sokai, and Nakorn Indra-Payoong

- **Measuring What Matters: Sustainable Performance Indicators and STI's Role in Achieving the SDGs** 87
  Kaewkarn Manosudprasit, Suchada Rianmora, and Pisal Yenradee

- **Miniaturized Electrostatic Size Classifier (mESC): Development and Validation of Nanometer Aerosol Classification** 103
  Papol Sardyoung and Panich Intra

- **Review of DonkeyCar Platform: From Deep Learning to Autonomous Driving Implementation** 114
  Ning Wang and Jian Qu

A Guideline for Sustainable Material Selection in Product Packaging Design: Development and Testing of Packaging Made from Environmentally Friendly Material

Suchada Rianmora[1*], Chaiyut Suwannakan[2], Sirawich Chanchiewvichai[3], Kantarat Sreeprasert[4], and Supavich Vongvivat[5]

[1,2,3,4,5]School of Manufacturing Systems and Mechanical Engineering (MSME), Sirindhorn International Institute of Technology, Thammasat University, Pathumthani, Thailand

E-mail: suchada@siit.tu.ac.th*, m6822040801@g.siit.tu.ac.th, d6722300305@g.siit.tu.ac.th, m6722041081@g.siit.tu.ac.th, kong@smilingmaddog.com

Received: December 16, 2025 / Revised: April 3, 2026 / Accepted: April 3, 2026

***Abstract*—This study investigates biodegradable cushioning materials for delivery packaging based on sago starch combined with hydrogel-based biopolymers. The research aims to address damage, environmental pollution, and packaging waste associated with conventional petroleum-based cushioning materials. Researchers developed biodegradable cushion samples by blending sago starch with sodium alginate and kappa carrageenan. We used a Design of Experiments approach to examine how material ratio and hydrogel type affect cushioning performance. We evaluated impact resistance, flexibility, and durability through material formulation, drop testing, and transport simulation. The results show that material composition strongly influences cushioning behavior, with sago-to-hydrogel ratios of 80:20 and 60:40 showing improved structural stability and impact absorption compared with other formulations. Alginate-based composites exhibited superior impact resistance and stable cushioning performance, whereas carrageenan-based composites offered greater flexibility.**

***Index Terms*—Sustainable Packaging, Biodegradable Cushion, Sago Starch, Hydrogel Material, Delivery Impact Protection, Customer Satisfaction**

I. Introduction

As e-commerce and direct-to-consumer deliveries grow, packaging design plays an increasingly critical role in protecting products during transit and maintaining customer satisfaction. While sellers can ensure product quality, external factors during delivery—such as rough handling or inadequate cushioning—often damage, deform, or contaminate goods. These issues not only reduce customer satisfaction but can also lead to return requests, refunds, and increased operational costs [1], [2].

In recent years, ready-to-drink beverages in glass containers have become popular due to their premium look, product visibility, and perceived safety, especially for sensitive containers and products. However, several pain points remain, including fragility, weight, thermal discomfort, and slippery surfaces due to condensation, all of which reduce usability and safety. To address these issues, design strategies should focus on improving functionality and user experience through protective sleeves, ergonomic shapes, and thermal insulation. Hybrid materials and innovative structures can also reduce weight while maintaining glass's aesthetic appeal. By translating these pain points into design requirements, beverage containers can be improved to enhance convenience, safety, and overall customer satisfaction.

In this context, understanding consumer expectations and delivery-related requirements is essential to guiding the development of effective packaging solutions.

Conventional packaging materials such as foam, bubble wrap, and plastic fillers are widely used for their lightweight and cushioning properties. However, these materials contribute to long-term environmental problems, including landfill waste and plastic pollution. As sustainability becomes a growing priority among consumers and logistics providers, the packaging industry is increasingly shifting toward biodegradable alternatives derived from renewable resources [3].

Natural materials such as cornstarch, mushroom mycelium, and seaweed-derived alginate have shown potential in providing protective functions comparable to synthetic materials while reducing environmental impact. Sago starch, extracted from palm pith, is another promising biopolymer due to its biodegradability and film-forming properties. When combined with hydrogels such as alginate or carrageenan, sago-based composites can be engineered to achieve flexibility, shock absorption, and durability, which are critical performance requirements for cushioning

materials used to deliver perishable and fragile products.

Motivated by consumer expectations for safety, sustainability, and usability in delivery packaging, this study integrates consumer insights with experimental evaluation to establish guidelines for selecting sustainable cushioning mats based on sago starch and hydrogels. The study first analyzes consumer feedback to identify key performance and usability requirements for delivery applications. The study then translates these requirements into material selection criteria and evaluates them through controlled formulation and testing. This approach supports the systematic development of biodegradable cushioning materials that balance protective performance with environmental sustainability and practical applicability in real-world delivery systems.

II. Research Background

To achieve the objective of this study, which focuses on identifying an effective approach for managing loads during transportation and organizing stacked sago bags, various factors will be considered. These include the types of sago available in the industry, waste management, user-friendliness, ergonomic considerations, relevant research findings from similar case studies, and overall performance within the sago bag supply chain.

A. Sustainable Protective Packaging

Conventional foams and plastics protect goods well, but create persistent waste and microplastics. Biobased, compostable materials are being pursued to replace EPS/EPE while maintaining protective performance in transit. Hydrogels and polysaccharide films are attractive because they're non-toxic, form energy-dissipating networks, and can be processed into films/coatings or skins around products, especially food [4], [5]. Recent reviews highlight alginate's crosslinking with divalent ions (e.g., Ca^{2+}) to create strong, flexible, edible films suitable for food contact and active packaging [6].

B. Packaging Design and Material Selection for Sustainable Cushioning

In packaging design, material selection is a critical decision that directly affects protection performance, environmental impact, cost, and user acceptance [7]. Previous studies on sustainable packaging design emphasize selecting environmentally friendly materials that balance mechanical performance, biodegradability, food safety, moisture resistance, and compatibility with delivery and logistics systems. Design-oriented research highlights the importance of translating user and delivery requirements into measurable material properties, such as impact absorption, flexibility, durability, and ease of handling [8]. In this context, biodegradable materials such as starch-based polymers and hydrogels have been increasingly explored as alternatives to petroleum-based cushioning materials due to their tunable mechanical behavior and environmental benefits [9]. However, existing studies often evaluate these materials in isolation, with limited integration of user-driven design criteria or systematic selection methods. This gap motivates a survey-guided approach in which consumer expectations inform material selection and experimental evaluation for packaging applications.

C. Hydrogels in Packaging

Calcium alginate hydrogels: Ionically crosslinked networks with tunable mechanical strength, moisture retention, and barrier properties; widely explored for edible/biodegradable films and coatings that can cushion, conform, and reduce bruising of fresh produce [6], [10]. Kappa-carrageenan: A sulfated galectin that forms clear, film-forming gels; when plasticized or composited, it yields protective films used in the preservation and transport of fruits/vegetables. Crosslinkers or hybrid blends can address mechanical limitations in neat carrageenan and enhance toughness [11].

D. Starch Biopolymers

Sago starch (from tropical palms) is abundant in SE Asia, low-cost, and film-forming. Starch films alone can be brittle and moisture-sensitive; hybridizing starch with hydrogel systems (alginate/kappa) improves flexibility, toughness, and processing latitude for biodegradable packaging [10], [12]. Ongoing studies and pilots evaluate sago-based films for carrier bags and food packaging, including recent formulations that incorporate functional additives [13].

E. Target Customers & Service Expectations (Delivery/E-Commerce)

With the growth of e-commerce, cushion packaging is now a core part of logistics performance. Customers prioritize: Timeliness, accuracy, product condition, security, communication/traceability, convenience, and cost [14], [15]. Firms respond with reliable carriers, tracking, proactive updates, flexible options, high-quality packaging, and fast issue resolution (improving satisfaction and loyalty) [16], [17].

Moreover, decision influencers and product affinities align closely across segments, with each type responding to distinct cues. Food bloggers emphasize trends, health, and sustainability, appealing most to the Self-Absorbed segment, which seeks validation of trends. Eco-celebrities highlight lifestyle and visible impact, resonating with the Self-Centered segment that frames personal benefits as "green." [18], [19]. Nutrition experts focus on facts,

safety, and shelf life, aligning with the Self-Confident segment, which values evidence and standards. Likewise, product categories map naturally: Organic foods (trend and prestige) fit the Self-Absorbed, health-conscious foods (functional and clean label) suit the Self-Centered, and sustainable foods (eco-pack and ethical sourcing) align with the Self-Confident [20]-[22].

Although many studies have investigated biodegradable packaging materials such as starch and hydrogel-based biopolymers, most existing research focuses on films, coatings, or broader sustainability aspects rather than on packaging systems specifically designed to protect products from impact during delivery. Only a limited number of studies have quantitatively evaluated biodegradable cushioning materials under simulated transport and drop conditions using systematic optimization methods such as Design of Experiments (DoE). Furthermore, the relationship among material composition, cushioning performance, and practical delivery requirements for fragile and perishable products remains underexplored. As a result, a clear research gap remains in developing biodegradable cushioning packaging that integrates material optimization, impact protection, and real-world delivery conditions. To address this gap, this study proposes an alternative and supportive cushioning design approach under the "send-with-safe" concept, in which sago starch and hydrogel composites are systematically selected, tested, and optimized to provide safe, sustainable, and reliable protection for delivery packaging applications.

III. Research Concepts

After the research team collected data through mechanical testing of various cushion materials using different methods, they summarized the results to reflect common types of cushioning packaging used to protect items during shipping and handling. These materials include bubble wrap, plastic packs, cardboard, and foam packaging. Table I presents detailed descriptions of each cushioning type.

Bubble wrap is a plastic packaging material with small, air-filled bubbles that offer excellent cushioning against impacts. It is lightweight and customizable but raises environmental concerns because it is made of plastic. Plastic packs, made from durable plastics, are versatile, lightweight, and suitable for various products; however, they contribute to plastic pollution and may not adequately protect heavy items. Cardboard packaging is lightweight, customizable, and eco-friendly; however, it can be weakened when exposed to moisture and has limited durability. Foam packaging, available at various densities, provides high protection and shock absorption but is bulky and difficult to recycle [23], [24].

Moreover, in existing cushion packaging designs, key terms and concerns often center on three main aspects: Effectiveness, sustainability, and cost-effectiveness. Packaging must effectively protect the product during transit, including cushioning against impacts, vibrations, and compressive forces, particularly for fragile items, while accommodating various product shapes and sizes for a secure fit. Sustainable packaging solutions are increasingly emphasized, including eco-friendly materials and reduced packaging waste, with a preference for reusable or easily recyclable designs.

Additionally, packaging design should be cost-effective and optimize material usage without compromising protection. User experience is also important, with a focus on easy-to-open designs, clear labeling, and minimalistic packaging. Designs must comply with regulatory standards regarding packaging materials, labeling, and environmental impact [2]. To stand out in the market, packaging designs can incorporate innovative features that differentiate them from competitors, such as unique shapes, colors, or additional functionalities that enhance the overall product experience [18].

TABLE I
COMMON TYPES OF A CUSHION PACKAGE

Type	Features	Pros	Cons
Bubble Warp	• *Structure:* Comprises numerous small air-filled bubbles encapsulated within a plastic film. These bubbles are typically uniform in size and closely spaced. • *Material:* Usually made from polyethylene, which is a type of plastic known for its flexibility and durability. • *Transparency:* Often transparent, allowing for easy identification of the wrapped item. • *Customizability:* Available in various sizes and bubble densities. Some types also have anti-static properties, ideal for electronic products.	• *Protection:* Offers excellent cushioning against impacts, vibrations, and compressive forces. • *Lightweight:* Its air-filled design makes it extremely light. • *Custom:* Suitable for wrapping a wide range of product shapes and sizes.	• *Environmental Concerns:* Traditional bubble wrap is made from plastic. • *Limited Protection for Heavy Items:* While excellent for fragile items, it is not suitable for heavy items.
Plastic Packs	• *Material Composition:* Typically made from various types of plastics such as polyethylene, polypropylene, or PVC, known for their durability and flexibility. • *Customizable Sizes and Shapes:* Can be manufactured in a range of sizes and shapes, tailored to specific products or purposes. • *Variety of Forms:* Available in multiple forms, including bags, pouches, and containers.	• *Versatility:* Suitable for packaging a diverse array of products, from food items to electronics, due to their adaptable nature. • *Lightweight and Durable:* Offers a lightweight yet sturdy solution, reducing shipping costs and resisting tears and punctures.	• *Environmental Impact:* Major contributors to plastic pollution. • *Chemical Contamination Risk:* Certain plastics can leach chemicals, particularly when used for food packaging. • *Limited Durability for Heavy Items:* May not provide adequate protection for heavy or sharp items.
Cardboard Packaging	• *Lightweight yet Sturdy:* Cardboard is lightweight but provides sufficient strength and durability for a variety of packaging needs. • *Easily Customizable:* Can be cut and folded into a multitude of shapes and sizes, accommodating a wide range of products.	• *Eco-Friendly:* Often made from recycled materials. • *Cost-Effective:* Generally, less expensive than other packaging materials. • *Lightweight:* Reduces shipping costs due to its light weight	• *Susceptibility to Moisture:* Cardboard can weaken when exposed to moisture or humidity. • *Limited Durability:* Not as durable as some other materials. • *Limited Reusability:* Its structural integrity may diminish with repeated use. • *Flammability:* Being a paper product, it is more susceptible to fire hazards.
Foam Packaging	• *Density and Firmness Variability:* Available in various densities and firmness levels. • *Moldability:* Can be molded or cut into an array of shapes and sizes. • *Shock Absorption:* Highly effective in absorbing shocks and vibrations	• *High Protection Level:* Provides excellent cushioning and shock absorption. • *Lightweight:* Adds minimal weight to the overall package. • Versatile Applications: Suitable for a wide range of products. • *Customization:* Easily customized to fit the shape and size of various products	• *Environmental Impact:* Can be difficult to recycle, contributing to environmental pollution. • *Space Consumption:* Bulky and can take up considerable storage space. • *Cost Considerations:* Generally, more expensive than other packaging materials. • *Chemical Sensitivity:* Certain foam materials can degrade when under certain environmental conditions.

A. Classification of Fruits by Peel Hardness

Classifying fruits by peel hardness helps match packaging and handling protocols to mechanical risk during transport. Three broad classes are useful for logistics and cushioning design: hard-peel, medium-hard peel, and soft-peel fruits. Peel hardness can be assessed via (i) puncture/penetration (penetrometer or texture analyzer), (ii) peel thickness (micrometer or caliper), and (iii) impact resistance (drop/pendulum tests), often complemented by non-destructive firmness/elasticity methods for quality control. Together, these tests indicate resistance to bruising, tearing, and cuticle failure under mechanical stress.

Hard-peel fruits have thick, tough rinds/exocarps that offer strong mechanical protection in transit—e.g., coconut (Cocos nucifera) with a highly toughened endocarp; pomegranate (Punica granatum) with a leathery exocarp; and watermelon (Citrullus lanatus) with a thick, impact-modulating rind where rind thickness is a key trait. *Medium-hard-peel fruits*, such as citrus (orange/lemon), have multilayered peels (flavedo/albedo) rich in essential oils, providing moderate mechanical protection while remaining workable in packing lines. Avocado has a leathery, medium-thick peel; mango exhibits peel firmness that decreases during ripening, so protection needs to

scale with maturity. *Soft-peel fruits* have thin, fragile skins that bruise/tear easily and require the most protective packaging—e.g., banana (notoriously bruise-prone) and tomato (cuticle/peel easily punctured; peel mechanics strongly linked to impact injury). Stone fruit, like peaches, also bruise readily as the peel/flesh softens.

B. Fruit Transportation in Logistics

Cold-chain logistics. Maintaining target temperatures reduces respiration, microbial growth, and waste—but raises energy demand and environmental burden; recent reviews highlight energy intensity and sustainability gaps in perishable food cold chains. Real-time monitoring (IoT/5G/NB-IoT, flexible sensors, anomaly detection) is increasingly used to control temperatures, detect failures early, and enable shelf-life-driven distribution while addressing device life, accuracy, and data-loss constraints. Multimodal transportation. Combining modes (road/rail/sea) can cut costs and emissions for long-haul perishables when routing accounts for time–temperature sensitivity, carbon, and food-waste objectives. Recent models and case studies show multi-objective planning (time, cost, CO_2, cargo loss) outperforms unimodal baselines. Joint distribution. Consolidating flows from multiple shippers into shared routes/depots reduces redundant trips, improves vehicle utilization, and can materially lower both economic and environmental costs in urban delivery networks.

C. Innovative Natural Material

Innovative natural packaging materials must meet several key criteria to satisfy customer expectations and ensure product protection and environmental sustainability. Customers demand packaging that effectively cushions fragile items against shocks, impacts, and vibrations during transit to prevent damage or loss. Packaging durability is paramount; it must withstand wear and tear, maintain structural integrity, and provide long-lasting protection, especially under challenging transport conditions. Lighter packaging is preferred to reduce shipping costs and environmental impacts by lowering carbon emissions. Water resistance is essential for preventing water or moisture from reaching the product and causing damage. Sustainability and reusability are becoming increasingly significant, with customers favoring materials that are recyclable, biodegradable, or reusable. Affordability also matters, as customers want packaging that balances quality and price. Customers prefer easy packaging and unpacking and look for user-friendly packaging that does not require specialized tools. Protection against external forces, such as impacts during transit or storage, is vital for maintaining product integrity. Finally, sanitization and contamination prevention are essential for product safety and consumer health.

D. Data Collection and Translated Needs

This research focuses on designing and developing an alternative support method for a food delivery platform using the *Product Design and Development (PDD)* method. Feedback and perceptions from target customers were gathered exclusively to capture their perspectives, without involving health or medical testing. The goal was to translate customer viewpoints, considered "intangible data," into "a physical design" for a new delivery support item. Questions and activities were non-harmful, focusing on opinions, perceptions, and experiences related to their cultures or societies, without extensively requesting personal or sensitive data. The primary focus was on functional requirements and feedback from customers using related delivery services or cushion products to keep items secure within containers. During that period, ethical considerations were less strict, allowing researchers to ask about the technical terms of engineering designs rather than specific personal information. Official consent forms with strict signature requirements were not required; participants only needed to provide consent by saying 'Yes' or 'No' to giving information, either in writing or verbally, before starting tasks. This research was conducted between 2019 and 2025. After the target users agreed to participate, the authors distributed the questionnaires and carefully reviewed them to ensure adherence to general ethical standards and the absence of conflicts of interest. In the early stages of this study, formal rules on data consent and personal information were neither clearly stated nor widely followed in Thailand.

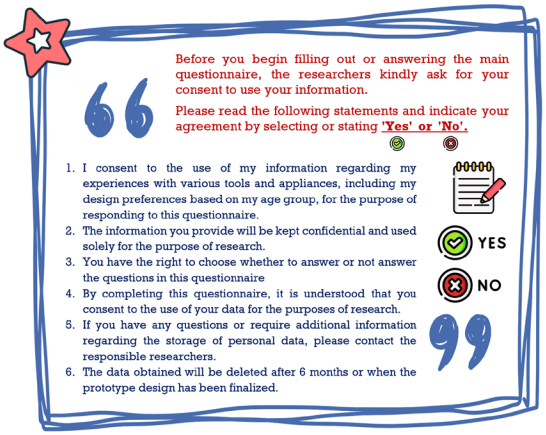

Fig. 1. Statements regarding the issue of consent

From the authors' perspective, using simple words and short explanations was the best way to ask for consent and help participants feel comfortable. Therefore, the ethics statement clearly notes that *"no formal ethics approval was required,"* as consent was obtained from all participants. It also confirms that all participants gave informed consent and that their participation was voluntary and anonymous.

The research followed these steps, as illustrated in Fig. 1, which shows how consent was handled. In this study, data collection involved participants completing a survey through both online platforms and physical posters with QR codes. The questionnaire was designed to be concise, respecting participants' time while still extracting relevant data, with an estimated completion time of 5-10 minutes. We used Google Forms for online data collection because it is accessible, easy to use, and can reach a broad population. For on-site data collection, we strategically placed QR codes linked to the same Google Form in crowded areas, such as common spaces where delivery riders assemble and student dormitories. This approach targeted a specific demographic segment, university students, who are often more environmentally aware and likely to be early adopters of sustainable products.

Key points: To gather detailed insights into the target requirements for the delivery platform in online purchasing, businesses should conduct user surveys to understand online shoppers' preferences and pain points regarding delivery times, packaging, tracking options, and return processes. Additionally, organizing focus group discussions with a diverse group of shoppers can help explore their experiences and opinions on delivery services. One-on-one interviews with frequent online shoppers will also help researchers better understand their motivations, concerns, and specific requirements related to delivery services, without probing into personal information. The researchers investigated the perceptions and behaviors of people living in the Bangkok metropolitan area. The survey focused on consumer views regarding the safety, sustainability, and design of cushion packaging—particularly for food and health-related items. To determine the required sample size, we used the standard formula for sample size calculation (Equation (1) [25].

$$\left(\frac{(Z)^2 \, x \, p \, x \, q}{(e)^2}\right) = n, \qquad (1)$$

where

e is the desired level of precision (the margin of error, or confidence interval)

p is the estimated proportion of the population that has the attribute in question

Z is the standard normal value corresponding to the selected confidence level

Therefore, in this study, $p = 0.5$ indicates 95% confidence and at least ±7 % precision. A 95% confidence level gave Z values of 1.96, per the normal tables, giving

$$\left(\frac{(1.96)^2 \, x \, 0.5 \, x \, 0.5}{(0.07)^2}\right) = 196.$$

Thus, we needed at least 196 responses. To ensure sufficient data, we distributed 250 online questionnaires via social media and institutional email networks. Despite accessibility challenges, the researchers collected 175 valid responses (approximately 70%) during the initial phase. These responses informed the development of a conceptual model for biodegradable cushion packaging to enhance safety during delivery. The value 196 refers to the *minimum required sample size* calculated using Cochran's sample size formula to achieve a 95% confidence level. However, this study collected and analyzed 175 valid questionnaire responses. Therefore, all statistical analyses and design translations reported in the manuscript are based on 175 participants.

In the detailed design phase, 92 participants—mainly professionals and academics in engineering, packaging, and logistics—were interviewed to evaluate usability and design-related issues, with a particular focus on the form, fit, and function (3Fs) of the proposed biodegradable cushion packaging. These insights helped refine the design to meet practical needs better. Before the full survey, the researchers conducted a small trial run with 30 respondents to test the questionnaire. This trial, known as a pilot test, helped identify any confusing or unclear questions, allowing the researchers to improve the survey's clarity and structure.

The finalized structured survey consisted of three main sections: *"Customer Preferences"*, *"Packaging Safety and Environmental Perceptions"*, and *"User Experience with Delivery Services"*.

IV. Results

The survey included multiple-choice, Likert-scale, and *open-ended questions* to gather both quantitative and qualitative feedback. The survey was distributed to a sample of 175 participants aged 15 to 55, with 39% male and 61% female. Most respondents were university students or regular delivery service users, providing relevant perspectives for evaluating packaging used in e-commerce and food/health-related logistics. This comprehensive approach allowed the research team to assess consumer perceptions regarding durability, sustainability, ease of use, and hygiene, and to make informed design improvements based on both survey data and expert interviews.

A. Adjective Words with 7-Point Semantic Differential Scale

The responses from the 175 participants were analyzed using SPSS, considering three main factors. Adjective words were paired with images to clarify the design's specific characteristics that might meet customer requirements (Fig. 3).

B. Kaiser-Meyer-Olkin Measure of Sampling Adequacy

The Kaiser-Meyer-Olkin Measure of Sampling Adequacy checks the validity of the data for *Factor Analysis*. The value should be above 0.5 to ensure data reliability and suitability for *Factor Analysis*. The results obtained in this step are shown in Fig. 2.

C. Bartlett's Test of Sphericity

The results were used to test the hypothesis. For this test, the following hypothesis is proposed:

H_0: Correlation Matrix is equal to one

H_1: The Correlation Matrix is not equal to one

When the significance value was < 0.05, we rejected H0. We conclude that the Correlation Matrix is 1. The results of this test are shown in Fig. 2.

KMO and Bartlett's Test		
Kaiser-Meyer-Olkin Measure of Sampling Adequacy		.878
Bartlett's Test of Sphericity	Approx. Chi-Square	688.919
	df	55
	Sig.	<.001

Fig. 2. Kaiser-Meyer-Olkin Measure of Sampling Adequacy result

D. Rotated Component Matrix

The *Rotated Component Matrix* is a statistical output from the factor analysis that shows the relationships between variables (such as survey questions or test items) and the underlying factors (or components) identified by the analysis. The matrix is "rotated" to simplify interpretation of the factor loadings, making it easier to see which variables relate most strongly to each factor. This matrix is a valuable tool for determining how factors should be grouped, as it assesses each factor's loading, with the highest loading indicating the group to which the factor should belong. The scree plot (Fig. 4) shows eigenvalues on the y-axis against component numbers on the x-axis.

	Like more				Neutral			Like more
	Heavy	-3	-2	-1	0	1	2	3	Light
	Rigidity	-3	-2	-1	0	1	2	3	Deformation
	Straighten	-3	-2	-1	0	1	2	3	Flexibility
	Ephemeral	-3	-2	-1	0	1	2	3	Sustainability
	Water absorbed	-3	-2	-1	0	1	2	3	Waterproof
	Unaffordable	-3	-2	-1	0	1	2	3	Affordable
	Manual	-3	-2	-1	0	1	2	3	Automation
	Sealed	-3	-2	-1	0	1	2	3	Easy to open
	Thickness(Thin)	-3	-2	-1	0	1	2	3	Thickness(Thick)
	Dark color	-3	-2	-1	0	1	2	3	Bright color
	Compact size	-3	-2	-1	0	1	2	3	Large size

Fig. 3. Adjective words with 7-point semantic differential scale

TABLE II
THE ADJECTIVE WORDS RECOMMENDED (LEFT SIDE)

Product Characteristics (Left Side)	Definition
Heavy	Cushion packaging has substantial mass, making it feel weighty when lifted or moved, which can enhance stability and balance and reduce the risk of tipping or being easily displaced by external forces.
Rigidity	Cushion packaging's structure is stiff and does not bend or flex easily under force.
Straighten/Form-Fitted	Cushion packaging is designed to attain a precise, straight configuration, tailored to conform to specific packaging shapes.
Ephemeral	Cushion packaging is intended for short-term use and may not be long-lasting.
Water Absorbed	Cushion packaging is not waterproof and allows water to permeate and be retained.
Unaffordable	Cushion packaging is priced at a level considered high or inaccessible to the average consumer.
Manual	The operation of Cushion packaging requires human effort or intervention without automation.
Sealed	Cushion packaging is tightly enclosed to prevent substances, including air, water, or other materials, from entering or escaping.
Thickness (Thin)	Cushion packaging has a small distance between its two opposite sides, making it not bulky or chunky.
Dark Color	Cushion packaging has a color that is closer to black than white on the color spectrum and absorbs more light than it reflects.
Compact Size	Cushion packaging is designed to occupy a small volume, taking up minimal space and is often portable.

TABLE III
THE ADJECTIVE WORDS RECOMMENDED (RIGHT SIDE)

Product Characteristics (Right Side)	Definition
Light	Cushion packaging is lightweight, making it easy to handle and reducing shipping costs.
Deformation	Cushion packaging can be bent without breaking, allowing it to adapt to various shapes and impacts, indicating a certain level of malleability while maintaining structural integrity.
Flexibility	Cushion packaging is flexible enough to wrap around various items, akin to bubble wrap, providing a snug fit and protective cushioning for a range of parcel shapes and sizes.
Sustainability	Cushion packaging is designed for repeated use and minimal environmental impact, highlighting reusability and resource conservation, often integrating recycled materials and being recyclable or compostable at the end of its life cycle.
Waterproof	Cushion packaging is impervious to water, preventing moisture penetration.
Affordable	Cushion packaging is reasonably priced, making it accessible to a wide range of consumers.
Automation	Cushion packaging is compatible with machine processing and integrates seamlessly into automated packing systems, reducing packing time and improving operational efficiency.
Easy to Open	Cushion packaging is designed with features that allow for easy access to its item, enhancing user convenience.
Thickness (Thick)	Cushion packaging has a substantial distance between its two opposite surfaces, which may contribute to durability and protection.
Bright Color	Cushion packaging features a highly saturated and vivid hue, which increases visibility and may have aesthetic.
Large Size	Cushion packaging is significant in dimensions, providing ample space or volume for its intended use.

An Eigenvalue greater than one indicates the importance of the component number, which is then recorded. The scree plot typically shows a downward curve, and the point where the slope levels off indicates the number of factors the analysis should generate. In some cases, both criteria may suggest too many factors. In this study, the scree plot suggested two components (groups of design), as these two were above the eigenvalue threshold of 1.

Thus, factor analysis reduces the many variables that describe a complex concept, such as economic status, to a few interpretable latent factors. In other words, we want to find a smaller set of interpretable factors that explain as much variability in the data as possible. The cushion design can be separated into two groups (Fig. 3). Furthermore, to ensure the design team is on the same page, we provide clear, concise definitions of each adjective used to specify the product characteristics (cushion design). Tables II and III present the recommended adjective words to support the selection of a cushion platform, with the conceptual ideas grouped according to the results of the "*Rotated Component Matrix*."

E. Scree plot and Total Variance

The scree plot always displays a downward curve. The point at which the curve's slope clearly levels off indicates the number of factors to be generated by the analysis (Fig. 4).

Component 1 explained 53.013% of the variance and included attributes related to the packaging's aesthetic and functional appeal, such as color, waterproofing, and reusability. This component reflects consumers' desire for packaging that is visually appealing and that offers practical benefits. The high color loading (0.793) suggests that visual appeal is significant. The prominence of waterproofing (0.783) and reusability (0.762) underscores consumer preferences for durability and environmental consciousness, aligning with the increasing trend of sustainability in product packaging [24].

Component 2 explains 13.714% of the variance and is characterized by variables related to ease of use and functionality, such as thickness and security (ease of opening). The negative loading of thickness on this factor (-0.863) may indicate a preference for thinner, less bulky packaging, which aligns with the need for convenience and space efficiency. The strong positive loading of security (0.852) highlights the importance of easy access to packaging products.

F. Component Transformation

The rotated component matrix (Fig. 5), obtained with varimax rotation, further clarified the factor structure and provided a more interpretable solution. From Table IV, the positive correlation between the factors (0.735) indicates that the first group concerns how the packaging looks and feels (aesthetics) and whether it is environmentally friendly and reusable (practicality). Moreover, the second group (0.678) includes factors such as whether the packaging is easy to open and not too bulky or heavy (functionality). This means people do not want to struggle with opening their packaging or have it take up too much space) Since these scores are positive and not too low or too high, it suggests that while these groups differ (one focuses on looking good and being useful again, and the other on being easy to use), they are connected. It is like saying that people care about both how the packaging looks and how it works; they are different aspects, but both matter to the consumer.

Principal Component Analysis (PCA) was used to identify the key underlying characteristics in the survey data and reduce a large set of correlated variables into a smaller set of meaningful components. Varimax rotation with Kaiser normalization was applied to enhance the interpretability of the extracted components by maximizing factor separation and ensuring balanced variable contributions across factors. This procedure preserves the original data structure while improving the clarity and stability of the factor solution, thereby enabling more effective interpretation and application of the resulting components in the design of biodegradable cushion packaging.

Table V lists the guided and recommended materials used as cushions to support the delivery platform [26].

TABLE IV
COMPONENT TRANSFORMATION MATRIX

Component Transformation Matrix		
Component	**1**	**2**
1	0.735	0.678
2	0.678	-.0735

*Extraction Method: Principal Component Analysis Rotation Method: Varimax With Kaiser Normalization

TABLE V
THE CONCEPTUAL IDEAS OBTAINED FOR THE NEW MATERIAL

No.	**Idea**	**Product Specification**	**Customer's Requirement**
1	Product 1 is Sago	Reusable, Water-Resistant, Weight	Size, Color
2	Product 2 is Alginate	Thickness, Method of Packing, Firmness	Security, Fits in Shape



Fig. 4. The Scree Plot

Rotated Component Matrix

Kansei word			Component	
Positive	Negative		1	2
Sustainability	Ephemeral	Reusable	.809	
Large size	Compact size	Size	.805	
Bright color	Dark color	Color	.795	
Waterproof	Water absorbed	Water-resistant	.782	
Light	Heavy	Weight	.773	
Affordable	Unaffordable	Price		
Thickness(Thick)	Thickness(Thin)	Thickness		-.863
Easy to open	Sealed	Security (Easy-to-open)		.852
Automation	Manual	Method packing		.820
Flexibility	Straighten	Fits in shape with packages		.700
Deformation	Rigidity	Firmness (Hardness or Softness)		.681

Fig. 5. Rotated Component Matrix

V. Product Design and Development

Product Design and Development (PDD) transforms customer needs and market opportunities into a functional, manufacturable, and marketable product. It involves defining product requirements, creating and testing design concepts, selecting suitable materials and manufacturing methods, and refining the product to ensure quality, usability, and cost efficiency [5], [8].

Product development typically requires five main phases: Conceptual development, system-level design, detailed design, testing and refinement, and production ramp-up. In this study, the concept development phase appears in the Results section, where questionnaire-based responses are translated into descriptive terms representing key customer requirements. Building on this, the manuscript moves to the second phase of PDD, system-level design, in which it identifies and discusses the key factors and specifications of the design platform.

A. System-Level Design

This stage explains how the biodegradable cushion packaging is organized into its main parts and how these parts work together as one system. The goal is to make the design easy to understand before moving to detailed design and testing. The packaging system is made up of three main parts:

Core Cushion Layer – This middle layer absorbs impact and protects the product during transport. It is made from a mix of sago starch and hydrogel materials such as alginate or kappa-carrageenan. The hydrogel helps spread and reduce the force when the package is dropped, while the sago starch adds structure and keeps the layer light and affordable.

Surface Film Layer – This thin outer film touches the product. It gives a smooth surface, keeps the cushion clean, and prevents moisture from entering. The film can also be printed or labeled if needed.

Outer Wrap or Holder Layer – This part surrounds the cushion and connects it to the delivery box or container. It helps keep the cushion in place and makes it easier to pack, handle, and recycle after use.

B. Detailed Design

A Design of Experiments approach systematically evaluated how material composition affects cushioning performance. The DOE followed a two-factor, two-level full factorial design with replication. Factor A was the sago-to-hydrogel mixing ratio, and Factor B was the hydrogel type (sodium alginate or kappa carrageenan). We prepared each factor-level combination as a cushion sample according to the run matrix. We evaluated performance using two response variables: impact absorption from drop testing and flexibility from bending evaluation. We analyzed the resulting data using analysis of variance to determine which factors significantly influenced each response. Main-effects plots visualized trends across factor levels, and we selected the final formulation through multi-response optimization to maximize impact absorption and flexibility, prioritizing impact absorption because of the risk of delivery damage.

- **Experimental Factors and Levels**

Two independent factors were selected based on preliminary studies and material feasibility:

Factor A – Material Ratio (Sago Starch: Hydrogel)

Level 1: 20:80

Level 2: 40:60

Factor B – Hydrogel Type

Level 1: Sodium Alginate

Level 2: Kappa Carrageenan

This creates a 2 x 2 full factorial design with two replications (Table VI).

TABLE VI
A 2 X 2 Full Factorial Design with Two Replications

Run	Ratio (Sago: Hydrogel)	Hydrogel Type
1	20:80	Alginate
2	20:80	Carrageenan
3	40:60	Alginate
4	40:60	Carrageenan
5	20:80	Alginate
6	20:80	Carrageenan
7	40:60	Alginate
8	40:60	Carrageenan

- **Impact Resistance (Drop Test)**

Impact resistance was evaluated through a series of controlled drop tests designed to replicate shocks and vibrations commonly experienced in logistics and delivery systems. Each biodegradable cushion sample was subjected to repeated drops from a height of 60 cm, using a fixed weight (500 g) to simulate packaged consumer goods. We then examined the surfaces for cracks, deformation, or fragmentation. We calculated energy absorption by measuring the reduction in rebound height and visible damage. These findings suggest that alginate provides superior shock resistance because its cross-linked gel structure disperses kinetic energy more effectively than carrageenan. Increasing sago content from 20% to 40% slightly improved the stability of alginate composites, while carrageenan samples showed decreased performance and became more brittle under impact.

- **Flexibility**

Flexibility testing assessed the cushion packaging's ability to bend, stretch, and recover under external forces without compromising its protective

properties. Samples underwent manual bending tests at 45° and 90°. Carrageenan samples scored higher flexibility values (7-8) across both sago levels, showing better adaptability to bending and deformation. Alginate, while stronger in impact absorption, displayed lower flexibility (scores 4-6 at 40% sago and 5-6 at 20% sago). This indicates that carrageenan provides more elastic cushioning.

C. Testing and Refinement

The testing and refinement stage involved validating the DOE results and using them to optimize the biodegradable cushion prototypes. A 2^2 full factorial design with two replications was applied, investigating the effects of sago concentration (20% vs 40%) and hydrogel type (carrageenan vs alginate) on impact absorption and flexibility

Analysis of Variance

Source	DF	Adj SS	Adj MS	F-Value	P-Value
Model	3	12.375	4.1250	11.00	0.021
Linear	2	11.250	5.6250	15.00	0.014
Sago	1	1.125	1.1250	3.00	0.158
Hydrogel	1	10.125	10.1250	27.00	0.007
2-Way Interactions	1	1.125	1.1250	3.00	0.158
Sago*Hydrogel	1	1.125	1.1250	3.00	0.158
Error	4	1.500	0.3750		
Total	7	13.875			

Fig. 6. ANOVA (impact absorption)

Analysis of Variance

Source	DF	Adj SS	Adj MS	F-Value	P-Value
Model	3	11.3750	3.7917	6.07	0.057
Linear	2	10.2500	5.1250	8.20	0.038
Sago	1	0.1250	0.1250	0.20	0.678
Hydrogel	1	10.1250	10.1250	16.20	0.016
2-Way Interactions	1	1.1250	1.1250	1.80	0.251
Sago*Hydrogel	1	1.1250	1.1250	1.80	0.251
Error	4	2.5000	0.6250		
Total	7	13.8750			

Fig. 7. ANOVA (flexibility)

The two-factor, two-level full factorial design with replication provided clear evidence of how material composition affects the cushioning properties of the biodegradable packaging. For impact absorption (Fig. 6), the regression model was statistically significant ($p = 0.021$), with hydrogel type emerging as the dominant factor ($p = 0.007$). Alginate consistently achieved higher impact absorption values, maintaining average scores around 8.5 regardless of sago content. In contrast, carrageenan performed worse, and its impact resistance decreased further at higher starch levels, suggesting increased brittleness. Although sago concentration itself was not statistically significant ($p = 0.158$), practical differences were observed; higher starch slightly improved the stability of alginate composites while reducing the cushioning effectiveness of carrageenan. The regression model expressed in uncoded units confirmed this trend, showing only a small negative coefficient for sago. These findings indicate that alginate provides a more robust matrix for dissipating kinetic energy, making it the preferred material for fragile, impact-sensitive goods.

For flexibility (Fig.7), the model approached significance ($p = 0.057$), with hydrogel type again playing the key role ($p = 0.016$). Carrageenan cushions achieved higher flexibility scores, typically between 7 and 8, demonstrating better adaptability to bending and deformation. Alginate, by contrast, was stiffer, with flexibility scores ranging from 4 to 6, though this rigidity provided structural support under load. Sago concentration and interaction effects were not statistically significant for flexibility. Still, factorial plots showed that carrageenan maintained higher elasticity across both levels, while alginate performed more consistently but was less adaptable. This confirms the trade-off between the two hydrogel systems: alginate optimizes impact absorption at the expense of flexibility, while carrageenan maximizes adaptability but sacrifices toughness.

The factorial analysis highlighted material-compatibility differences: alginate maintained stable performance across sago levels, whereas carrageenan showed sensitivity to starch increases, with clear deterioration in impact absorption (Fig. 8). Although interaction effects were not statistically significant, these plots provided practical insights into how each hydrogel behaves in combination with starch. Such visual interpretation is important for guiding refinements, as it demonstrates the robustness of alginate systems relative to the variability of carrageenan composites (Fig. 9).

The optimization process further reinforced these conclusions. Because both flexibility and impact absorption were set as maximization targets (Fig. 10), with impact absorption weighted twice as much as flexibility, the optimal solution was 20% sago with alginate hydrogel. This condition provided predicted performance values of 8.5 for impact absorption and 5.5 for flexibility, representing the most balanced outcome for real-world applications. While carrageenan was more flexible, its poor impact absorption at higher sago levels made it less suitable as a universal solution. Therefore, the optimization validated alginate as the superior choice for protective packaging, while carrageenan could be used selectively for irregularly shaped or delicate goods requiring adaptability.

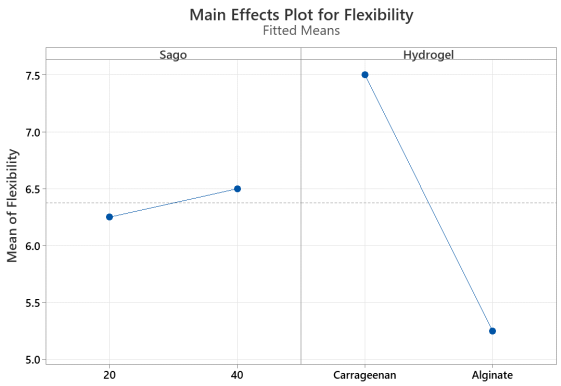

Fig. 8. Main effects plot for impact absorption

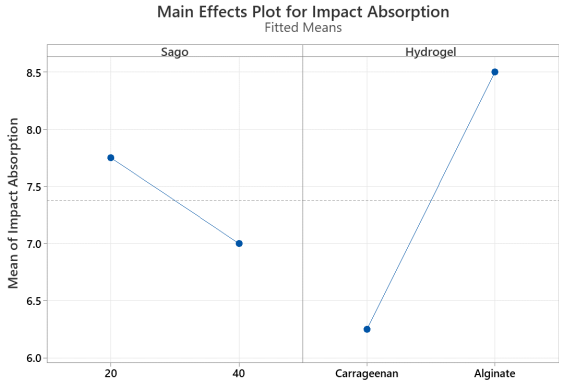

Fig. 9. Main effects plot for flexibility

Solution

Solution	Sago	Hydrogel	Flexibility Fit	Impact Absorption Fit	Composite Desirability
1	20	Alginate	5.5	8.5	0.659704

Fig. 10. Optimization information

D. Production Ramp-up

The logo and print on the product package play an important role in communicating brand identity and messages to consumers—additional information on how packaging and branding strategies are finalized during the production ramp-up phase.

(1) Logo Design: The logo serves as a visual representation of the brand (Arctic Circle) and is prominently featured in the product package. During the production ramp-up phase, we pay careful attention to ensure the logo is visually appealing, memorable, and effectively communicates the brand's values and identity. We carefully choose design elements such as color, typography, and imagery to resonate with the target audience and differentiate the product from competitors. This is achieved by considering "*eye-catching and universal symbol concepts*."

(2) Print Design: In addition to the logo, the print design of the product package includes various elements such as product name, key features, usage instructions, and branding messages. These elements are strategically placed to enhance overall visual appeal and communicate important information to consumers. The print design was thoroughly tested and refined to ensure readability, clarity, and consistency across different packaging formats and sizes.

(3) Branding Strategies: During the production ramp-up phase, branding strategies are finalized to create a cohesive brand experience across all touchpoints. This involves aligning the packaging design with the overall brand identity and marketing strategy. "*Key considerations*" include brand positioning, messaging hierarchy, visual aesthetics, and emotional appeal. By seamlessly integrating branding elements into product packaging, companies aim to create a strong brand presence and foster consumer loyalty.

(4) Market Readiness: Ensuring that product packaging is market-ready is a critical aspect of the production ramp-up phase. This involves conducting market research, gathering focus-group feedback, and analyzing consumer trends to inform decisions on packaging design and branding strategies. The goal is to create packaging that attracts attention, clearly communicates the product's value proposition, and resonates with the target audience.

(5) Quality Control: Quality control measures are implemented throughout the production process to maintain consistency and ensure that the final product meets the highest quality standards. This includes conducting rigorous inspections of packaging materials, printing techniques, and finished products to identify defects or inconsistencies. By adhering to strict quality control protocols, companies can mitigate risks and uphold their reputations for delivering premium products.

Key point: In this study, the "*production ramp-up phase"* represents a critical stage in the product development process, where packaging and branding strategies are finalized to prepare the product for market launch. By investing time and resources in optimizing packaging design and branding, companies can enhance the perceived value of their products and gain a competitive edge in the marketplace. Fig. 11 illustrates the logo and print design, which serve as guidelines for the desired product.

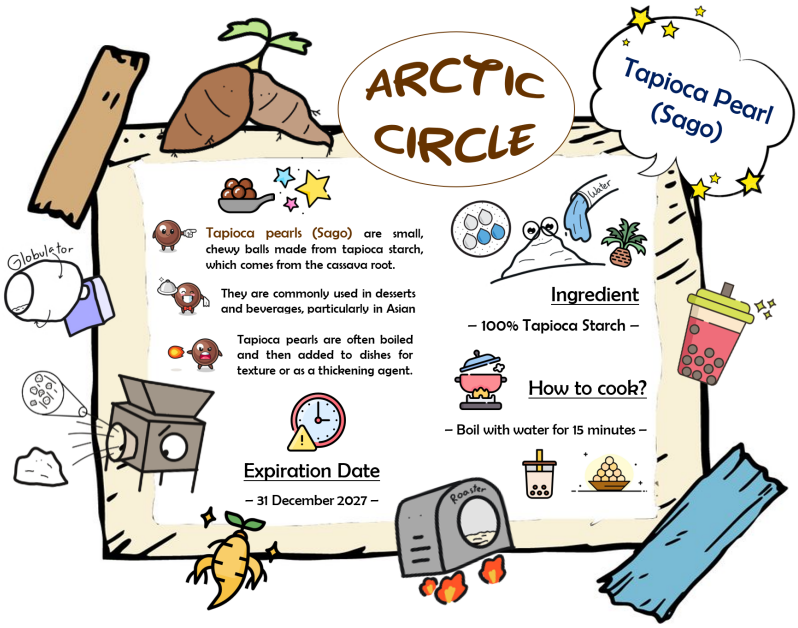

Fig. 11. The logo and print design applied to support the packaging design platform

VI. Conclusion and Contribution

This study demonstrates the feasibility of biodegradable cushioning materials based on sago starch and hydrogel biopolymers as sustainable alternatives to conventional petroleum-based packaging for delivery applications. Using a design of experiments approach with a 2 × 2 full factorial design, we systematically evaluated the effects of material composition and hydrogel type on impact absorption and flexibility, revealing hydrogel type as the dominant performance factor. Alginate-based composites consistently provided superior and stable impact absorption across sago concentration levels, while carrageenan-based composites exhibited greater flexibility but reduced shock resistance at higher sago contents. Multi-response optimization, which weighted impact absorption twice as heavily as flexibility to reflect the risk of delivery damage, identified 20% sago starch combined with alginate hydrogel as the optimal formulation, offering the most balanced performance for real-world use. While carrageenan may suit applications requiring greater adaptability, its lower impact resistance limits its effectiveness as a general-purpose cushioning material.

VII. Scope and Limitations

This study was limited to testing two sago concentration levels and two hydrogel systems. Future research should expand to include a wider range of formulation ratios and explore cross-linkers such as calcium ions, plasticizers, or hybrid fibers to enhance structural toughness and stability. Moreover, understanding the relationships among temperature, stress, and material separation is crucial for predicting the long-term performance of biopolymer-based systems under varying thermal and mechanical conditions [27], [28].

This knowledge can help minimize cracking, delamination, and deformation during storage, handling, and transportation, ensuring safe, damage-free delivery in practical logistics environments. Long-term evaluations are also needed to examine the effects of humidity, temperature cycling, microbial degradation, and real-world transport-route conditions, such as vibration and impact profiles. Future studies should also address logistics and cost considerations—including material availability, production scalability, and transportation efficiency—to improve the feasibility and economic viability of applying the developed systems in real-world operations [29], [30].

For *"fragile or expensive"* products that require careful handling, especially when cost is not a concern, use an alginate-based cushion. Alginate can be molded to fit the contours of the product's surface, providing optimal protection. However, it is important to study and address the sensitivity of the organic or natural materials used in such cushions to ensure their effectiveness and durability.

VIII. Implications

Practical Implications: This study's findings have several practical implications for the delivery industry. By adopting organic materials such as alginate and tapioca starch for packaging, delivery companies can enhance the security and hygiene of their products, especially for health-related and food items. This could increase customer satisfaction and loyalty, as customers would receive their products in their original condition. Additionally, using organic materials

aligns with sustainability goals, as these materials are biodegradable and environmentally friendly. The key point is that implementing these findings could improve delivery quality and contribute to a more sustainable future.

Social implications: This research has significant implications for consumers' health and well-being. By using organic packaging, delivery companies can reduce contamination risk and ensure customers receive safe, hygienic products. This is particularly important for health-related items, where synthetic materials can pose health risks. Additionally, using organic materials aligns with consumer preferences for environmentally friendly products, potentially enhancing delivery companies' reputations and attracting environmentally conscious customers. The key point is that the social implications of this research underscore the importance of using sustainable, safe materials in the delivery process to protect consumer health and the environment.

Acknowledgement

The authors thank the School of Industrial Engineering and Technology (SIIT), Thammasat University, for providing research facilities and academic support throughout the study. The authors would like to express sincere appreciation to Dr. Thiti Mahaboonpachai for his valuable suggestions and insightful discussions on key aspects of interfacial mechanics and fracture behavior of concrete and composite materials, particularly focusing on Polymer-Cement Mortar (PCM) applications, finite element modeling of structural interfaces, and experimental characterization and validation of material performance. Grateful acknowledgment is also extended to Mr. Pannawit Ngaochai from The Siam Refractory Industry Co., Ltd. (SRIC), a subsidiary of the Siam Cement Public Company Limited (SCG), for his kind support and professional guidance on material selection for the hot-air drying machine used in the food industry. His recommendations were particularly helpful in ensuring that the selected materials enhance the quality and reliability of sago starch as a cushioning medium under the "send-with-safe" concept. The 2nd author acknowledges the Faculty's Quota Scholarship awarded by Sirindhorn International Institute of Technology, Thammasat University.

References

[1] A. D. Do, V. L. Ta, P. T. Bui, N. T. Do, Q. T. Dong, and H. T. Lam, "The impact of the quality of logistics services in e-commerce on the satisfaction and loyalty of Generation Z customers," *Sustainability*, vol. 15, no. 21, Art. no. 15294, Nov. 2023, https://doi.org/10.3390/su152115294

[2] P. Ravula, "Impact of delivery performance on online review ratings: The role of temporal distance of ratings," *J. Mark. Anal.*, vol. 11, no. 2, pp. 149-159, May 2022, https://doi.org/10.1057/s41270-022-00168-5

[3] M. Rastegarpour, M. Sina, S. Hasanvand, E. Khanniri, S. Shojaee-Aliabadi, and A. M. Mortazavian, "Investigating sustainable and renewable sources of carbon quantum dots for utilization in food packaging systems: A review," *Appl. Food Res.*, vol. 6, no. 1, Art. no. 101600, Jun. 2025, https://doi.org/10.1016/j.afres.2025.101600

[4] B. Niemczyk-Soczynska and P. Ł. Sajkiewicz, "Hydrogel-based systems as smart food packaging: A review," *Polymers*, vol. 17, no. 8, Art. no. 1005, Apr. 2025, https://doi.org/10.3390/polym17081005

[5] T. S. Parreidt, K. Müller, and M. Schmid, "Alginate-based edible films and coatings for food packaging applications," *Int. J. Biol. Macromol.*, vol. 107, no. 10, Art. no.170, Oct. 2018, https://doi.org/10.3390/foods7100170

[6] C. Metha, S. Pawar, and V. Suvarna, "Recent advancements in alginate-based films for active food packaging applications," *Sustain. Food Technol.*, vol. 2, no. 5, pp. 1246-1265, Jul. 2024, https://doi.org/10.1039/D3FB00216K

[7] L. Magnier and D. Crié, "Communicating packaging eco-friendliness: An exploration of consumers' perceptions of eco-designed packaging," *Int. J. Retail Distrib. Manag.*, vol. 43, nos. 4-5, pp. 350-366, 2015, https://doi.org/10.1108/IJRDM-04-2014-0048

[8] K. T. Ulrich and S. D. Eppinger, *Product Design and Development*, 7th ed. New York, NY, USA: McGraw-Hill, 2020.

[9] J. Rydz and M. Musioł, "Applications of novel biodegradable polymeric materials," *Materials*, vol. 15, no. 23, Art. no. 8411, Nov. 2022, https://doi.org/10.3390/ma15238411

[10] A. Fazilah, M. Maizura, A. A. Karim, U. Uthumporn, B. K. Chew, and R. Bhat, "Physical and mechanical properties of sago starch–alginate films incorporated with calcium chloride," *Int. Food Res. J.*, vol. 18, no. 3, pp. 1027-1033, 2011.

[11] C. Cheng et al., "Recent advances in carrageenan-based films for food packaging applications," *Front. Nutr.*, vol. 9, Art. no. 1004588, Sep. 2022, https://doi.org/10.3389/fnut.2022.1004588

[12] P. M. Arockianathan, S. Sekar, S. S. Sankar, B. Kumaran, and T. P. Sastry, "Evaluation of biocomposite films containing alginate and sago starch impregnated with silver nano particles," *Carbohydr. Polym.*, vol. 90, no. 1, pp. 717-724, Sep. 2012, https://doi.org/10.1016/j.carbpol.2012.06.003

[13] A. Bagher Abiri, H. Baghaei, and A. M. Nafchi, "Preparation and application of active bionanocomposite films based on sago starch reinforced with a combination of TiO_2 nanoparticles and *Peganum harmala* extract for preserving chicken fillets," *Polymers*, vol. 15, no. 13, Art. no. 2889, Jun. 2023, https://doi.org/10.3390/polym15132889

[14] S. Horng and P. Yenradee, "Delivery service management system using Google Maps for SMEs in emerging countries," *Comput. Mater. Contin.*, vol. 75, no. 3, pp. 6119-6143, Apr. 2023, https://doi.org/10.32604/cmc.2023.038764

[15] S. Cha-Ume and N. Chiadamrong, "Simulation of retail supply chain behaviour and financial impact in an uncertain environment," *Int. J. Logist. Syst. Manag.*, vol. 13, no. 2, pp. 162-186, 2012, https://doi.org/10.1504/IJLSM.2012.048934

[16] S. Kunnapapdeelert, J. V. Johnson, and P. Phalitnonkiat, "Green last-mile route planning for efficient e-commerce distribution," *Eng. Manag. Prod. Serv.*, vol. 14, no. 1, pp. 1-12, Mar. 2022, https://doi.org/10.2478/emj-2022-0001

[17] S. Kunnapapdeelert and R. Klinsrisuk, "Determination of green vehicle routing problem via differential evolution," *Int. J. Logist. Syst. Manag.*, vol. 34, no. 3, pp. 395-410, 2019, https://doi.org/10.1504/IJLSM.2019.103091

[18] P. Pinthanon, S. Rianmora, and P. Yenradee, "Sustainable design concept for a trendy beverage container," *Int. J. Sustain. Eng.*, vol. 18, no. 1, Art. no. 2492158, Apr. 2025, https://doi.org/10.1080/19397038.2025.2492158

[19] J. L. Vázquez, A. Lanero, J. A. García, and X. Moraño, "Segmentation of consumers based on awareness, attitudes and use of sustainability labels in the purchase of commonly used products," *Sustain. Prod. Consum.*, vol. 38, pp. 115-129, Jun. 2023, https://doi.org/10.1016/j.spc.2023.03.025
[20] S. Verma and D. Kapoor, "Sustainability on the plate: How influencers and social norms transform food choices," *Br. Food J.*, vol. 127, no. 6, pp. 1942-1958, Apr. 2025, https://doi.org/10.1108/BFJ-11-2024-1202
[21] S. Rianmora, L. Sukjitsakunchai, and T. Tachawatanawisal, "Designing and developing a platform called 'rest at restaurant' to support the basic needs of senior adults," *Cogent Bus. Manag.*, vol. 11, no. 1, Art. no. 2301798, Feb. 2024, https://doi.org/10.1080/23311975.2024.2301798
[22] W. Chanchiewvichai, S. Rianmora, and N. Patmayothin, "Designing everyday essentials: A guide for user-friendly accessibility using quality function deployment," *Cogent Eng.*, vol. 11, no. 1, Art. no. 2387826, Aug. 2024, https://doi.org/10.1080/23311916.2024.2387826
[23] N. Kassim et al., "Sustainable packaging design for molded expanded polystyrene cushion," *Materials*, vol. 16, no. 4, Art. no. 1723, Feb. 2023, https://doi.org/10.3390/ma16041723
[24] S. P. Singh, V. Chonhenchob, and G. Burgess, "Comparison of various loose-fill cushioning materials based on protective and environmental performance," *Packag. Technol. Sci.*, vol. 7, no. 5, pp. 229-241, Sep./Oct. 1994, https://doi.org/10.1002/pts.2770070504
[25] Statistics How To, "Sample size in statistics (how to find it): Excel, Cochran's formula, general tips," *Statistics How To*, 2025. [Online]. Available: https://www.statisticshowto.com/probability-and-statistics/find-sample-size/ [Accessed: Dec. 25, 2025].
[26] S. Rianmora, D. Padnoi, T. Rattanopas, and B. Yantabutr, "Alternative design for salad spinner-Sallatë," *Int. Sci. J. Eng. Technol.*, vol. 3, no. 2, pp. 1-14, Dec. 2019, https://ph02.tci-thaijo.org/index.php/isjet/article/view/231741
[27] T. Mahaboonpachai, Y. Kuromiya, and T. Matsumoto, "Experimental investigation of adhesion failure of the interface between concrete and polymer-cement mortar in an external wall tile structure under a thermal load," *Constr. Build. Mater.*, vol. 22, no. 9, pp. 2001-2006, Sep. 2008, https://doi.org/10.1016/j.conbuildmat.2007.07.002
[28] T. Mahaboonpachai, T. Matsumoto, and Y. Inaba, "Investigation of interfacial fracture toughness between concrete and adhesive mortar in an external wall tile structure," *Int. J. Adhes. Adhes.*, vol. 30, no. 1, pp. 1-9, Jan. 2010, https://doi.org/10.1016/j.ijadhadh.2009.06.005
[29] X. Yang, H. Li, Y. Sun, Y. Cai, H. Zhou, and F. Zhong, "Research on the design method of cushioning packaging for products with unbalanced mass," *Appl. Sci.*, vol. 13, no. 15, Art. no. 8632, Jul. 2023, https://doi.org/10.3390/app13158632
[30] M. Zhao et al., "Food packaging films from natural polysaccharides and protein hydrogels: A comprehensive review," *Food Chem. X*, vol. 25, Art. no. 102174, Jan. 2025, https://doi.org/10.1016/j.fochx.2025.102174

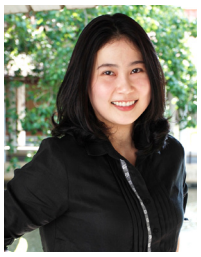

Suchada Rianmora is a lecturer in the School of Manufacturing Systems and Mechanical Engineering (MSME), Sirindhorn International Institute of Technology, Thammasat University, Thailand. She received her D.Eng. from the Asian Institute of Technology, Thailand. Her research interests are reverse engineering, rapid prototyping, image processing, industrial instruments and controlling systems, design and development, design for manufacture and assembly, maintenance engineering, and manufacturing processes.



Chaiyut Suwannakan received his B.Eng. in the Industrial Engineering Program at the School of Manufacturing Systems and Mechanical Engineering (MSME), Sirindhorn International Institute of Technology, Thammasat University, Thailand. He is currently pursuing a Master of Engineering in Logistics and Supply Chain Systems Engineering (LSCSE) at Sirindhorn International Institute of Technology. His research interests include product design and development, design of experiments, process improvement, and machine learning.



Sirawich Chanchiewvichai received his B.Eng. (1st class honors) in the Industrial Engineering Program at the School of Manufacturing Systems and Mechanical Engineering (MSME), Sirindhorn International Institute of Technology, Thammasat University, Thailand. He received a Master of Engineering in Logistics and Supply Chain Systems Engineering (LSCSE) from Sirindhorn International Institute of Technology. He is currently pursuing a Doctor of Philosophy (Engineering and Technology) at the same institute. His research interests include fault analysis, manufacturing process design, artificial intelligence, and product design and development.



Kantarat Sreeprasert received her B.Eng. in Chemical Engineering from the School of Bio-Chemical Engineering and Technology (BCET), Sirindhorn International Institute of Technology, Thammasat University, Thailand. She recently completed her M.Eng. in Logistics and Supply Chain Systems Engineering (LSCSE) at the same institute. Her research interests include bio-composite packaging materials, sustainable product development, and environmentally friendly logistics systems.



Supavich Vongvivat is the Founder of Smiling Mad Dog Co., Ltd. He received his Bachelor of Engineering in Industrial Engineering from the School of Manufacturing Systems and Mechanical Engineering (MSME), Sirindhorn International Institute of Technology (SIIT), Thammasat University, Thailand. He also obtained a Master of Business Administration (MBA) with a concentration in Finance from the University of Portland, Oregon, USA. His research interests include design and business development, human error analysis, customer typologies, next-generation product innovation, beverage systems, agricultural-based materials, and delivery platforms.

Application of an Automated OCR System for Data Processing of Banking Electronic Transfer Slips: A Case Study of a Non-Profit Organization in Thailand

Dhammanit Buddhakulsomsiri[1], Laddawan Suwannachote[2], Jirachai Buddhakulsomsiri[3], and Parthana Parthanadee[4*]

[1,2]Kasetsart University Laboratory School, Center for Educational Research and Development, Kasetsart University, Bangkok, Thailand

[3]Sirindhorn International Institute of Technology, Thammasat University, Pathum Thani, Thailand

[4]Department of Agro-Industrial Technology, Faculty of Agro-Industry, Kasetsart University, Bangkok, Thailand

E-mail: dhammanit@gmail.com, laddawan.su@ku.ac.th, jirachai@siit.tu.ac.th, parthana.p@ku.th*

Received: September 15, 2025 / Revised: July 16, 2026 / Accepted: July 21, 2026

***Abstract*—This article presents an application of an automated optical character recognition system developed to process transactional data from electronic bank transfer slips. Target users include small businesses, non-profit organizations, and individuals who manually process electronic transfer slips from customers. The objective is to help operators screen transfer slips, enter data, and correct and verify it using a post-OCR algorithm. The Main contribution of this study is the development of the integrated man-machine system, consisting of an OCR tool and rule-based post-OCR scripts that generate data as input for operators' final verification. Challenges include incorrect transfer slips, low-quality slip images, and diverse slip formats from various mobile banking applications. A numerical test of the automated OCR system uses a case study dataset from a non-profit organization. The dataset contains 2,603 submitted transfer-slip images from 10,924 transactions over about one month of operations. The results indicate that the OCR system can achieve 78% accuracy in processing the slips and 90% accuracy in monetary values. With final verification by operators, the system achieves 100% accuracy, saving over 41 hours of operator time.**

***Index Terms*—Optical Character Recognition (OCR), Man-Machine System, Electronic Transfer Slip, Transactional Data, Mobile Banking Application, Operations Efficiency Improvement**

I. Introduction

This article presents the development of an automated Optical Character Recognition (OCR) system specifically to process data from electronic transfer slips in mobile banking applications. The motivation comes from a non-profit organization's need to process and verify many financial transactions daily by hand. In the past decade, businesses, industries, and society have integrated digital technology into daily activities, such as banking, shopping, and donations. The widespread adoption of mobile banking has shifted consumer behavior across diverse demographic groups, including adolescents, working professionals, and older adults. The expansion of online commerce through mobile applications and social media platforms has significantly accelerated the volume of digital financial activities.

In today's mobile banking practices, senders typically provide recipients with proof of payment, most commonly in the form of electronic transfer slips automatically generated by mobile banking applications. These digital documents serve as preliminary evidence of financial transactions and require recipients to manually verify transaction details before executing subsequent operations, such as dispatching goods, confirming delivery schedules, or maintaining financial records. However, the manual verification process poses several operational challenges. It is inherently time-consuming and prone to human error, particularly under high transaction volumes. The task's repetitiveness, combined with cognitive fatigue, increases the likelihood of misprocessing and can result in financial errors and/or significant delays. These issues underscore the need for more efficient, automated verification mechanisms to improve transaction reliability and streamline operational workflows.

To mitigate the inefficiencies associated with manual verification in financial transactions, OCR technology has gained increasing interest as a means of automating the reading and extraction of relevant data from digital financial documents. While OCR can

enhance operational efficiency, its adoption among small-scale enterprises and individual users remains constrained by technical and practical challenges. First, OCR performance depends on image quality. Documents captured at low resolution, with visible folds, shadowing, or glare, often result in inaccurate data extraction. Additionally, diverse transfer slip formats issued by different financial institutions pose a significant barrier to developing universally compatible OCR systems. In addition, conventional OCR algorithms lack contextual awareness and, to some extent, cannot reliably differentiate between similar-looking data elements, such as account numbers and monetary values, or identify essential fields based on functional relevance rather than visual characteristics. These limitations underscore the necessity for more sophisticated, context-specific OCR systems or tools to improve reliability and generalizability across diverse use cases.

Although many free OCR tools are available online, they typically allow users to process only one image at a time. This constraint makes them insufficient for high-volume use cases, such as extracting data from multiple electronic transfer slips. Moreover, these tools often output unstructured text extracted in a linear sequence based on the visual arrangement of text within the image. This format lacks proper organization and does not facilitate efficient data retrieval or further analysis.

For practical applications, particularly in financial workflows, accurate extraction, recording, and storage of information in structured formats such as spreadsheets or databases are often required. Without structured data management, users face inefficiencies when handling large datasets, including duplication risks and difficulty retrieving specific transaction details. Furthermore, most standard OCR tools lack verification mechanisms to cross-reference extracted data with internal records, such as invoices or prior transaction logs. This limitation compromises data integrity and hinders downstream operational accuracy. In addition, reliance on cloud-based or third-party OCR platforms raises serious privacy concerns, as electronic transfer slips frequently contain sensitive personal and financial information, such as account details, sender identities, and transaction amounts. While commercial OCR solutions with enhanced capabilities exist, implementing them often requires substantial financial investment in licensing and customization. Alternatively, developing in-house OCR tools or systems requires specialized technical expertise and significant resources, which may be prohibitive for small-scale businesses, non-profit organizations, and individual users.

In this article, we develop an automated OCR system that integrates OCR technology for image processing and data entry with human judgment for data verification. The system balances efficiency, accuracy, and reliability. By implementing rule-based verification post-OCR scripts, the system facilitates rapid extraction of transaction details, such as sender and recipient information, account numbers, transaction amounts, and timestamps, while allowing human operators to perform targeted verification and review of key information when the OCR system detects anomalies or discrepancies. This verification model reduces cognitive load on users and improves scalability across diverse operational settings. In particular, the OCR system supports customization to specific organizational needs, making it feasible to deploy in resource-constrained environments. Additionally, by storing extracted and validated data in structured formats compatible with spreadsheet applications or database systems, the approach supports traceability, audit readiness, and integration into existing financial workflows. Developing such a system also supports broader efforts to democratize access to intelligent financial tools by providing smaller organizations and general users with affordable, practical solutions for handling critical documentation tasks.

Although OCR technology has advanced considerably and has been successfully applied to financial documents such as invoices, receipts, and bank slips, existing research has primarily focused on improving text detection and recognition accuracy through machine learning and deep learning techniques. Comparatively less attention has been given to developing integrated systems that support the complete operational workflow required for transaction verification, including automated data extraction, structured data management, rule-based validation, and efficient human-assisted verification. This study addresses this gap by developing a customizable OCR-based transaction processing system that integrates these components into a unified workflow for electronic transfer slips generated by mobile banking applications. Beyond improving recognition performance, the proposed system emphasizes practical deployment by supporting efficient processing of large transaction volumes, structured record management, and privacy-preserving operation suitable for resource-constrained organizations and individual users.

II. Literature Review

This section contains recent developments in OCR technology and its implementation across various fields. This section reviews research studies on OCR for handwritten text to identify ongoing research directions and trends [1]. Because OCR systems digitize handwritten and printed text, the outputs often contain inaccuracies, necessitating post-processing or post-OCR techniques to correct errors. [2] This

survey reviews cutting-edge post-OCR methods, evaluation metrics, and available datasets and tools. These methods are categorized as manual, (semi-) automatic, and automatic techniques, further divided into isolated-word and context-specific approaches. To address language-specific challenges, a mask Region-Based Convolutional Neural Network (R-CNN)-based model was proposed to detect text bounding boxes in Thai-language documents such as ID cards, passports, and bank slips [3]. This approach outperforms the Character-Region Awareness for Text Detection (CRAFT) model in both accuracy and efficiency, contributing to improving OCR preprocessing for non-Latin scripts. [4] proposed an OCR framework for Vietnamese identity cards. The authors use a pretrained multi-language Connectionist Text Proposal Network (CTPN) to crop all text regions in both training and testing images. To capture Vietnamese tone marks, they expand the cropped regions by 20%. A customized Convolutional Recurrent Neural Network (CRNN) is then employed for recognition and model training. The framework achieves over 96.7% character-level accuracy and 89.7% word-level accuracy.

In finance and banking, a hybrid of OCR and artificial intelligence/machine learning has gained prominence to streamline labor-intensive accounting processes. For example, OCR has been applied to recognize digits and capital letters in cheque processing, achieving high accuracy using a model trained on the extended Modified National Institute of Standards and Technology (EMNIST) dataset [5]. [6] Extended the application of OCR to financial reimbursement. The study presents a smartphone-based intelligent reimbursement system that uses deep learning to automate invoice processing. The system achieves an average OCR accuracy of 99.1% and employs a regular matching and Recursive Segmentation (RMRS) algorithm.

Beyond identity verification and reimbursement, a growing body of research explores OCR for financial ticket recognition, including receipts and invoices; see [7]-[9]. In addition, the challenge of diverse financial ticket layouts and mixed Chinese-English text was addressed by proposing an all-content recognition method that combines a Pixel Aggregation Network (PAN) for text detection with a Financial Ticket Character Recognition Framework (FTCRF) based on faster R-CNN [10]. Their system achieves 91.75% accuracy at the string level and 87% at the whole-ticket level, demonstrating how OCR overcomes ticket variability to enhance automation and compliance in financial documentation. Nacsoft OCR, a deep learning-based engine optimized for Turkish receipts, was later developed [11]. The system combines ResNet34-Unet for receipt area detection, YOLOv4 for text localization, and a C-RNN for word recognition. Nacsoft OCR achieves the highest accuracy on Turkish receipts (93.89% Character Error Rate CER) and competitive results on English datasets, while also offering faster processing speeds. In retail applications, OCR supports tasks such as reading receipts, interpreting price tags, and capturing inventory labels, reducing manual input and improving operational speed. A transformer-based OCR model, SRRNet, is introduced in [12] to recognize text from shopping receipts while preserving the two-dimensional spatial layout. SRRNet achieves high accuracy on large-scale receipt datasets and public scene-text benchmarks, effectively handling distorted and irregular text. Similarly, [13] integrates OCR into a multimodal product recognition system for real-time inventory tracking, automated checkout, and stock monitoring, achieving 94.6% accuracy and demonstrating OCR's utility in retail automation for standardizing extracted data.

Advanced post-OCR techniques are essential for extracting structured data from documents with complex layouts. In [14], OCRMiner, a rule-based system, is proposed to identify key invoice fields by leveraging both textual and layout features. [15] explores language-specific customization, addressing limitations of standard OCR engines like Tesseract for Turkish-language invoices. The proposed system integrates template-matching techniques and significantly outperforms baseline models, validating the importance of language adaptation. However, challenges remain in generalizing across diverse invoice templates and image qualities, highlighting broader issues such as sensitivity to layout variations, visual inconsistencies, and low-resolution scans. Data quality remains a critical constraint in OCR-based systems.

[16] presents a web-based invoice processing platform featuring an annotation tool and an extraction module. The system utilizes OpenCV for image preprocessing and a fine-tuned Tesseract engine for text extraction, achieving 85-95% accuracy across more than 25 invoice formats. In [17], multimodal models are evaluated by fine-tuning LayoutXLM on OCR-extracted tokens from 1,503 scanned German Company records. The model outperforms unimodal and large language model baselines in document classification tasks.

In the retail domain, [18] addresses OCR-induced errors in product names from receipts by introducing a graph-based agglomerative clustering method using Levenshtein distance to group similar name variants. Tested on synthetic data, the method effectively identifies coarse-grained relationships such as product categories and families. Additionally, [19] combines OCR output with text classification and Mondrian conformal prediction to detect anomalies like barcode switching and mis-scans in grocery store

data. The system demonstrates OCR's value not only in text extraction but also as a reliable foundation for anomaly detection and classification, helping reduce shrinkage loss.

Overall, the reviewed studies demonstrate that recent OCR research has achieved substantial improvements in text detection and recognition accuracy through deep learning, transformer-based models, language-specific adaptations, and advanced post-processing techniques. However, most existing studies evaluate OCR performance primarily at the character, word, or document level, emphasizing recognition accuracy for specific document types and benchmark datasets. Comparatively less attention has been given to developing integrated transaction-processing systems that combine OCR with rule-based validation, structured data management, and human-assisted verification to support real-world financial workflows. Furthermore, many reported systems are designed for specific document templates or languages, which may limit their adaptability to diverse electronic transfer slips generated by different banking applications. These observations indicate the need for a practical OCR-based system that extends beyond text recognition to support reliable transaction verification and structured financial data management in real-world applications.

III. Problem Statement

The design, development, and implementation of the automated data processing system utilize OCR technology to extract and manage information from electronic fund transfer slips. The system's primary functions include extraction, preliminary validation, and structured data writing from transfer slips. The test data are from a non-profit organization in Thailand, referred to as "the user." The organization receives financial contributions, referred to as "donations," from a wide range of individual and institutional donors across Thailand.

Donations are typically made through two channels: a direct deposit over the counter at a bank or through a mobile banking application. With the mobile banking application, a donor can choose a direct transfer to the user's savings account (select the user's bank, enter the account number, and specify the transfer amount), or an electronic donation, so-called "e-donation," by scanning a QR code that the bank issues to the user. The Revenue Department, Ministry of Finance, facilitates e-donations through an official platform that enables donors to claim tax exemptions for donations to registered non-profit entities. After completing a transaction on the mobile banking application, the system automatically generates an electronic transfer slip and stores it on the donor's mobile device.

A non-profit organization can manage multiple good cause projects and initiatives, prompting donors to specify the intended purpose of their donations. A donor can choose to submit their transfer slip to the user and state the donation's intended purpose. In other words, the user must accurately verify and categorize a submitted transfer slip according to its designated donation purpose. In contrast, a transaction made without submitting the slip is counted as a general donation, which the user can use for any purpose.

This article's case study uses one specific donation purpose as a representative example to illustrate the operational challenges. To count as a donation for the purpose, the donor must state their intention and submit an image of the electronic transfer slip through the user's social media channels, Facebook or Line Applications. On any given day, fewer slips are usually submitted than the total number of donations made. To use the donation funds for the intended purpose, the user must accurately total the donation amounts from the submitted slips. Currently, this process is performed manually by human operators, who have other full-time job and only help out as volunteers The OCR system is, therefore, developed to perform preliminary tasks of screening, verifying, and recording critical transaction details, including the date and time of transfer, the accuracy of the user's bank and account number, and the donation amount to assist human operators, to improve efficiency of the process.

IV. Data Collection and Operational Challenges

The OCR system inputs image files of transfer slips generated by mobile banking applications. Figs. 1 to 4 show examples of electronic transfer slips from various mobile banking applications that the OCR system and post-OCR scripts can process easily. Key information identifying the user and the donor is blurred for confidentiality reasons. Transfer slips vary in format because each bank uses its own slip design. Additionally, most mobile banking applications permit users to personalize the background of their transfer slips, further contributing to format variability. The size and quality of these images also vary considerably, largely depending on the donors' technical proficiency.

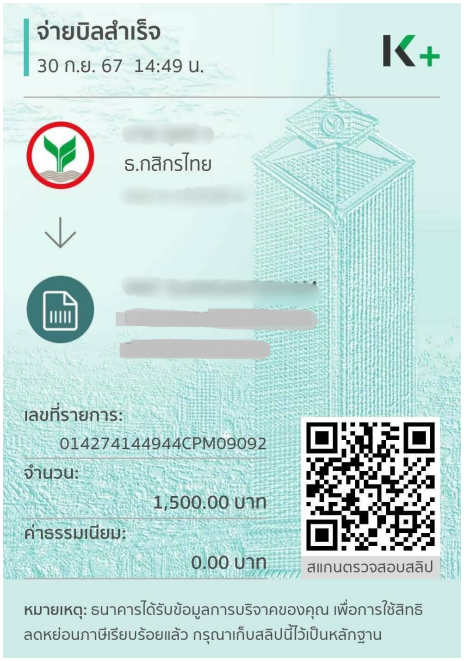

Fig 1. Examples of electronic transfer slips from the K-Bank mobile application

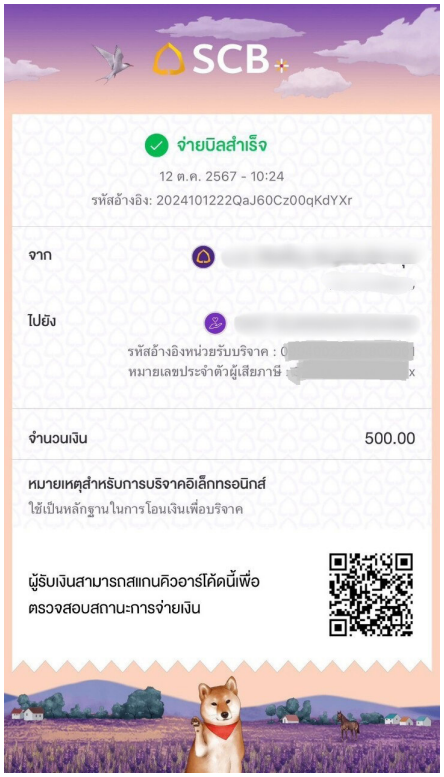

Fig 2. Examples of electronic transfer slips from the SCB mobile application



Fig 3. Examples of electronic transfer slips from the KTB mobile application



Fig 4. Examples of electronic transfer slips from the K-Bank mobile application with a personalized background

In addition, donors with limited experience using mobile devices often submit low-resolution images with small file sizes, resulting in unclear or partially legible text and numbers. Moreover, some submitted slips are not generated by the mobile banking application. Instead, some donors manually take pictures using their devices' camera function and submit the images as proof of transactions. Representative examples of such transfer slips are shown in Figs. 5 to 8.

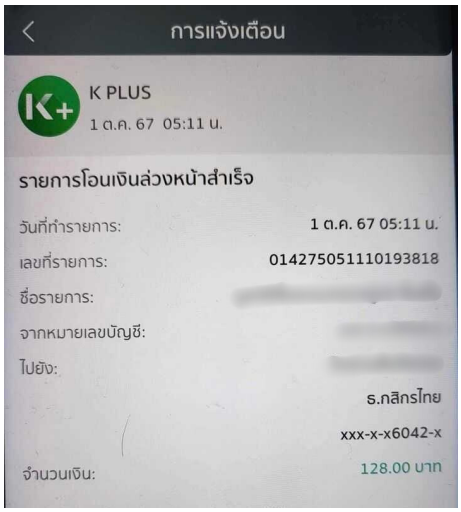

Fig 5. Picture of a complete transaction taken from the screen of a mobile banking application



Fig 6. Picture of a printed transfer slip from an ATM

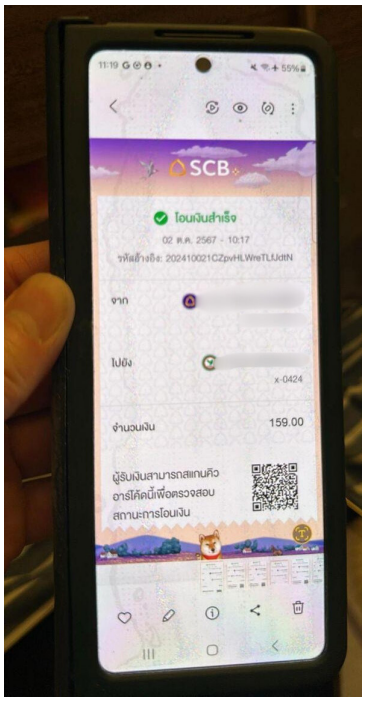

Fig 7. A picture showing the whole mobile device

As shown in the figures, some submitted transfer slips not generated by mobile banking applications are highly inconsistent and have poor image quality, which directly impacts the OCR system's performance.

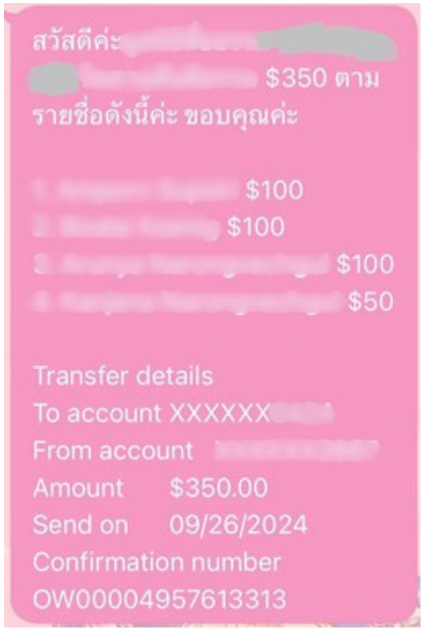

Fig 8. Picture of an SMS notification via chat message with a USD amount instead of a THB amount

In Fig. 5, instead of downloading or sending the transfer slip directly from their mobile device, the donor took a picture of the mobile banking application screen showing a completed transaction, which results in poor image quality. Fig. 6 shows a printed transfer slip from an ATM. Fig. 7 is another example of the donor using a different mobile device to take a picture of their own mobile device, showing the mobile banking application screen with a completed transaction. Fig. 8 shows a text message stating that four donors are making four donations in USD.

In manual verification scenarios, poor image quality or incorrect slips can prolong inspection times, complicate the review process, and contribute to operator fatigue. With an automated OCR system, low-quality images may lead to recognition errors or incomplete data extraction. Preliminary analysis reveals that low-resolution and partially legible images typically have file sizes below 100 kilobytes (kB).

The user collects transfer slip images submitted by donors through social media platforms daily. The user reviews, records, and stores these images in a folder categorized by the slip submission date. However, the transaction date indicated on the slip may differ from the submission date, as donors do not always submit their slips on the same day after completing a transaction. This discrepancy often results in mismatches between the actual transaction date and the date of the folder used for image storage. Following the collection and review process, several operational challenges have been identified:

- High number of image submissions: Each day, there are over 300 transactions. Approximately 90 transfer slips are received, with over ten formats varying across different banks.
- Low image quality: Many slips are difficult to read due to poor resolution. Some submissions are screenshots with blurred text and figures rather than the original digital files.
- Incorrect account number: Some slips contain transactions directed to incorrect bank accounts.
- Duplicate submissions: Repeated uploads of the same transfer slip can lead to double-counting and errors in data entry and verification.

In the case study dataset, 2,603 slips were submitted out of 10,924 total transactions (24%). Each channel has approximately the same number of transactions. The table shows that the number of submitted slips on each day can vary significantly, from a minimum of 13 slips on 26 September 2024 to a maximum of 726 slips on 19 October 2024, which is the day before a particular event organized by the user (i.e., the reason the number of submitted slips surges). The user and its operators face the challenge that all slips must be processed manually, and many arrive the day before an important event. Table I shows the number of transactions from each donation channel and the number of submitted slips.

TABLE I
NUMBER OF TRANSACTIONS IN EACH CHANNEL AND NUMBER OF SUBMITTED SLIPS IN THE CASE STUDY DATASET

Date	e-Donation (Transactions)	Direct Transfer (Transactions)	Total Number of Transactions	Number of Submitted Slips	Percentage
21 September 24	622	256	878	271	31%
22 September 24	248	196	444	117	26%
23 September 24	170	186	356	110	31%
24 September 24	117	147	264	54	20%
25 September 24	192	217	409	68	17%
26 September 24	95	138	233	13	6%
27 September 24	85	137	222	66	30%
28 September 24	105	145	250	32	13%
29 September 24	132	142	274	19	7%
30 September 24	102	160	262	17	6%
1 October 24	100	212	312	90	29%
2 October 24	106	204	310	42	14%
3 October 24	74	147	221	30	14%
4 October 24	91	136	227	35	15%
5 October 24	130	153	283	34	12%
6 October 24	106	148	254	40	16%

TABLE I
NUMBER OF TRANSACTIONS IN EACH CHANNEL AND NUMBER OF SUBMITTED SLIPS IN THE CASE STUDY DATASET (CON.)

Date	e-Donation (Transactions)	Direct Transfer (Transactions)	Total Number of Transactions	Number of Submitted Slips	Percentage
7 October 24	87	133	220	42	19%
8 October 24	73	148	221	26	12%
9 October 24	65	144	209	44	21%
10 October 24	105	161	266	38	14%
11 October 24	75	126	201	39	19%
12 October 24	121	132	253	41	16%
13 October 24	169	180	349	46	13%
14 October 24	169	155	324	112	35%
15 October 24	122	171	293	92	31%
16 October 24	144	189	333	95	29%
17 October 24	208	239	447	100	22%
18 October 24	279	189	468	164	35%
19 October 24	1451	690	2,141	726	34%
Total	**5543**	**5381**	**10,924**	**2,603**	**24%**

V. DESCRIPTION OF THE OCR SYSTEM

The automated OCR system is developed using Python. EasyOCR was selected as the OCR engine because it is an open-source framework that supports multilingual text recognition, including Thai and English, without requiring language-specific model development. EasyOCR framework provides pretrained deep learning models that can be readily integrated into Python applications, making it suitable for rapid system development and deployment. Furthermore, EasyOCR performs robustly on digital images captured from mobile devices and offers sufficient recognition accuracy for electronic transfer slips while allowing local execution without relying on cloud-based services. This local processing capability is important for preserving the privacy of sensitive financial information contained in transfer slips. Fig. 9 presents the system logic diagram. The system description uses the notation below.

Notation

l: Index of image files

m: The total number of images for a given day, $l = 1, 2, \ldots, m$

Notation (Continued)

i: Index of extracted text elements in a list called *test*, where an element is a set of strings read by the OCR

n: The total number of elements, $i = 1, 2, \ldots, n$

count: Counter for image files

file: A list containing the image file names

test: Raw data of elements read from slips by the OCR

info: A list containing important elements to be written to a spreadsheet, *info* = [Name, ID, Amount, Time]

main: A master list containing all elements in *info* read from all slips on a given day

suc_read: A list containing file names that the OCR can successfully read

failed_read: A list containing file names that the OCR cannot accurately read

The system description in Fig. 3 is written as pseudo-code as follows:

The system begins by importing six required open-source libraries of OCR tools (i.e., *easyOCR*), data management, and file management.

The system loads a function (i.e., a post-OCR script) called Tester, created specifically for this system. It post-processes the output by removing unwanted text and correcting text read by *the easyOCR* package.

- To record the computational time required to process a set of images, the *timer* is triggered to start.

- Next, the folder containing all images to be processed for a given day is loaded.

- Six lists, including *file*, *test*, *info*, *main*, *suc_read*, and *failed_read*, are initialized

- Index of image files, *l*, is set to zero.

- The system checks whether all images have been processed, i.e., $l > m$. If not, the system proceeds to (A); otherwise, it goes to (B).

(A) There are images remaining to be processed:

- The current image file, indexed by number *l*, is processed by the easyOCR tool, and the extracted elements are stored in the list called *test*. The index *i*

for the extracted text elements in *test* and the image-file counter are set to zero.

- The name of the current file being processed is recorded in the first entry of the list *info*, and the *count* is increased by one.

- [Checkpo[Checkpoint 1] The system checks whether all the elements are recorded, i.e., $i > n$. If $i > n$, then proceed to [Checkpoint 2]. Otherwise, it proceeds to the *post-OCR* scripts.

- [Checkpoint 2] The system checks whether the information in the list *info* is complete.

• Complete information in the *info* is recorded as a successful reading by the OCR tool, where the file name of the current image is recorded in the *suc_read* list.

• Incomplete information in the *info* is recorded as a failed reading by the easyOCR tool, where the file name of the current image is recorded in the *failed_read* list.

• Information (complete or incomplete) read by easyOCR is appended to the *main* list. The *test* list and *info* list are reset to be empty lists, ready for the next image to be processed.

• Index *l* is increased by one, and the OCR tool proceeds to the next image.

- Post-OCR scripts: If i<n, i.e., not all the elements are already recorded, then the post-OCR script proceeds to perform the following checkpoints sequentially:

• [Checkpoint 3] whether the currently read element's data type is a date type. If it is a date type, the system records the date data in the 4th entry of the info list and increases the count by one. Increment i, and return to [Checkpoint 1]. Otherwise, go to [Checkpoint 4].

• [Checkpoint 4] The system checks whether the current element is the last, i.e., *count* = 4. If so, the system proceeds to [Checkpoint 2]. If not, it proceeds to [Checkpoint 5].

[Checkpoint 5] checks whether the currently read element contains the correct account number, i.e., the read element contains a 13-digit string that represents an e-donation (i.e., 099x00xxxxxxx, note that X marks are used to mask the non-profit organization ID), or contains a 10-digit string that represents a direct transfer to a savings account (i.e., xxx-x-x6042-x). If it is the correct account information, the system records the account number data in the 2nd entry of the info list and increases the count by one. The system increments i and returns to [Checkpoint 1]. Otherwise, go to [Checkpoint 6].

• [Checkpoint 6] The system checks whether the current element is the last, i.e., *count* = 4. If so, the system proceeds to [Checkpoint 2]. If not, it proceeds to [Checkpoint 7].

• [Checkpoint 7] The system checks whether the currently read element is a valid donation amount. The Tester function performs this check. If it is a valid amount, then the *amount* data is recorded in the 3rd entry of the *info* list, and the *count* is increased by one. Then, increment i, and return to [Checkpoint 1]. Otherwise, go to [Checkpoint 8].

• [Checkpoint 8] The system checks whether the current element is the last, i.e., *count* = 4. If so, the system proceeds to [Checkpoint 2]. If not, the system increases index i by one and returns to [Checkpoint 1].

(A) All images are already processed:

- Two sub-folders, [Successful Reading] and [Failed Reading], are created to essentially separate the image files, which are successfully read and unsuccessfully read, to facilitate the operators during verification of the transfer slips accordingly.

- All the image files that the OCR tool and post-OCR scripts can process completely, whose file names are recorded in the list *suc_read*, are copied to the [Successful Reading] folder.

- In addition, all the image files that cannot be read completely, whose file names are kept in the list *failed_read*, are copied to the [Failed Reading] folder.

- All the texts processed by the system are recorded into a spreadsheet file, ready to be verified by the operators.

- Finally, the *timer* is stopped, and the computational time is recorded.

In addition, the *Tester* function corrects the donation amount based on common errors read by *easyOCR,* as listed below.

-Replace the English alphabet "l" with a numeric "1" (one)

- Replace the English alphabet "n" with the Thai alphabet "ท"

- Replace the English alphabet "o" with a numeric "0" (zero)

- Replace the English alphabet "s" with a numeric "5" (five)

- Replace the punctuation mark comma "," with a punctuation mark period "."

- Replace the English alphabet "s" with a numeric "5" (five)

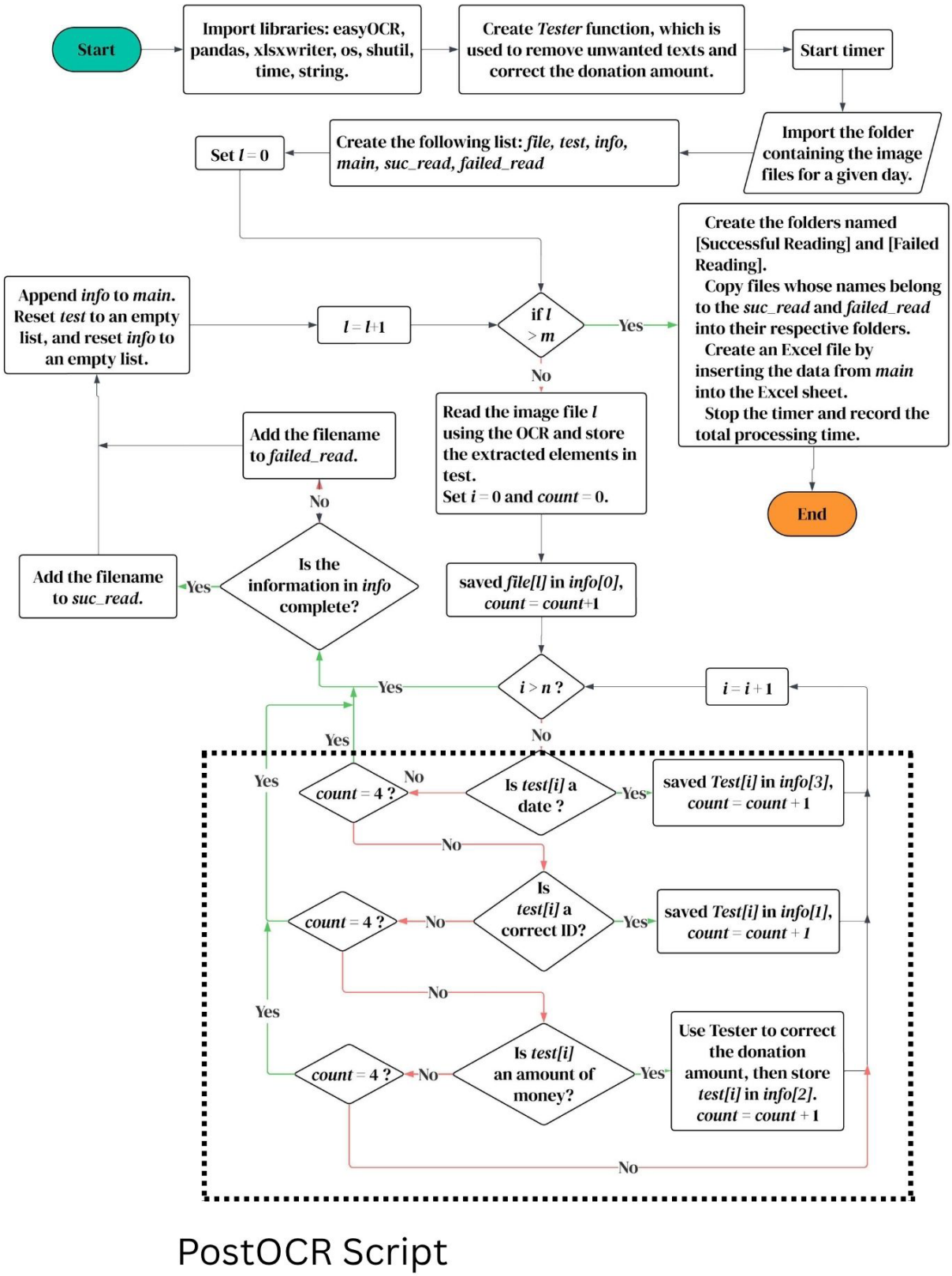

Fig. 9. Logic diagram of the automated OCR system

VI. Computational Test Results and Discussion

A. Overall Performance of the Automated OCR System

After processing all the image files, examples of results are shown in Table II. The 1st example indicates that the ID (i.e., account number) cannot be read. In the 2nd example, the system incorrectly reads the donation amount as zero, and it cannot read the date.

TABLE II
Examples of Incorrect Reading and Correct Reading by The System

Filename	ID	Amount	Date	Remark
LINE_ALBUM_xxxxxx_11.jpg	ID Pass	500	7 October 24	Cannot read ID
LINE_ALBUM_xxxxxx_40.jpg	xxx-x-x6042-x	0	Time Or Day	Amount is 0, and cannot read the date
LINE_ALBUM_xxxxxx_161.jpg	099x00xxxxxxx	200.008	10 October 24	Incorrect amount (Read B as 8)
LINE_ALBUM_xxxxxx_30.jpg	099x00xxxxxxx	2000	13 October 24	Correct reading

The third example shows that the donation amount, which is 200.00B (B is for Thai Baht), is read incorrectly as 200.008. The last example is a correct reading and the most typical result. The performance of the developed automated OCR system, which features post-OCR scripts, is evaluated in terms of the accuracy and efficiency of slip screening and reading using the test dataset.

B. Accuracy Analysis of the Automated OCR System

Table III presents the system's accuracy in terms of the number and percentage of slips read correctly, total donation amount, and daily computational time. In total, 2,603 images (slips) are processed, of which 2,031 slips are processed correctly, i.e., the four key pieces of information are read and recorded in a spreadsheet. This gives an overall accuracy of 78.03%, where percent accuracy is the ratio of accurately read slips to the total number of slips. Similarly, donation amount accuracy is the ratio of the read amount to the actual transaction amount. Although slip-level accuracy is moderate at 78.03%, donation-amount accuracy reached 90.04%, indicating that the system extracts the most critical financial information in most cases. This difference suggests that many OCR failures involve secondary fields (e.g., account numbers or dates) rather than monetary values, making the system suitable as a preprocessing tool before human verification.

TABLE III
Percent Accuracy of The OCR Tool and Computational Time

Date	OCR Reading Accuracy (Slips)			OCR Reading Accuracy (%)		Run-Time (s)
	Incorrect	Correct	Total	Slips	Donation Amount	
21 September 24	68	203	271	74.91%	86.24%	1,941.6
22 September 24	24	93	117	79.49%	86.87%	1,052.7
23 September 24	32	78	110	70.91%	75.48%	871.0
24 September 24	18	36	54	66.67%	78.19%	425.9
25 September 24	13	55	68	80.88%	97.38%	568.6
26 September 24	2	11	13	84.62%	41.40%	119.2
27 September 24	15	51	66	77.27%	95.45%	471.8
28 September 24	6	26	32	81.25%	88.82%	319.3
29 September 24	3	16	19	84.21%	79.73%	160.4
30 September 24	3	14	17	82.35%	88.92%	153.3
1 October 24	24	66	90	73.33%	60.26%	647.6
2 October 24	14	28	42	66.67%	85.87%	336.0
3 October 24	7	23	30	76.67%	89.24%	251.3
4 October 24	6	29	35	82.86%	86.19%	274.0

TABLE III
PERCENT ACCURACY OF THE OCR TOOL AND COMPUTATIONAL TIME (CON.)

Date	OCR Reading Accuracy (Slips)			OCR Reading Accuracy (%)		Run-Time (s)
	Incorrect	Correct	Total	Slips	Donation Amount	
5 October 24	6	28	34	82.35%	92.95%	237.9
6 October 24	11	29	40	72.50%	91.52%	322.8
7 October 24	8	34	42	80.95%	87.39%	320.6
8 October 24	9	17	26	65.38%	88.03%	198.8
9 October 24	14	30	44	68.18%	46.69%	340.9
10 October 24	12	26	38	68.42%	71.92%	324.8
11 October 24	4	35	39	89.74%	97.71%	345.7
12 October 24	8	33	41	80.49%	99.19%	291.7
13 October 24	1	45	46	97.83%	99.69%	347.2
14 October 24	28	84	112	75.00%	82.31%	845.3
15 October 24	16	16	92	82.61%	98.33%	722.9
16 October 24	20	75	95	78.95%	95.44%	694.5
17 October 24	13	87	100	87.00%	48.27%	715.4
18 October 24	21	143	164	87.20%	98.30%	1,318.3
19 October 24	166	560	726	77.13%	94.31%	10,833.6
Total	**572**	**2,031**	**2,603**	**78.03%**	**90.04%**	**25,453.1**

Unlike many OCR-based document processing systems that rely on OCR confidence scores to decide whether to accept recognition results, the proposed framework instead performs deterministic, rule-based validation followed by mandatory human verification. This design suits financial transactions, where even a single undetected recognition error may lead to monetary loss.

Detailed inspection of failed cases revealed that most errors stemmed from poor image quality, including low resolution, compression artifacts, partial cropping, glare, and non-transfer-slip images. These conditions reduce OCR recognition accuracy, and the rule-based post-OCR algorithm cannot fully correct them.

C. Efficiency Improvement of the Operators with the Assistance of the Automated OCR System

For operational efficiency, the OCR system demonstrates clear time savings over manual processing. Based on operator experience, manual handling of transfer slips, including reading, verifying, and all data entry, typically takes an average of one minute per slip. With the OCR system, the same task requires 25,453.10 seconds (i.e., 7 hours, 4 minutes, and 13.1 seconds), or 9.78 seconds of computer time per slip. This is followed by a brief manual verification requiring, on average, three seconds of operator time per correctly processed slip, or 15 seconds for incorrectly processed slips (including non-transfer slips that are submitted), and these estimated average times per slip come from operators' actual time to do their jobs, with and without the automated OCR system. Table IV estimates operator time savings with the system.

TABLE IV
ESTIMATED OPERATOR'S TIME SAVINGS

Method	No. of Slips	Operator Time (min)
Manual work	2,603	2,603
Automated OCR system		
Correctly processed	2,031	101.55
Incorrectly processed	572	143
Total	**2,603**	**244.55**
Savings	**-**	**2,358.45**

From the table, estimated operator-time savings are 2,358.45 minutes (39 hours and 18 minutes), representing over 90% savings for the case study dataset of 2,603 submitted slips. The results demonstrate an important operational tradeoff. Rather than eliminating human involvement, the proposed framework substantially reduces repetitive manual work while preserving human oversight for critical financial verification. Consequently, operator effort

is reduced without compromising the reliability required in financial applications.

D. Factors Affecting OCR System Performance

Further analysis of image file sizes helps clarify the impact of input image quality on OCR system performance. Table V provides details on the OCR system accuracy with respect to image file size. The results show that average accuracy increases with larger image files. Very small-sized images (<100 kB) exhibited a high error rate of about 51.25%, indicating that low-resolution images significantly affect reading accuracy. Only slightly larger images (at least 100 kB) generally perform better. Overall, medium-to-high resolution images (i.e., at least 200 kB) are recommended for more accurate results. Distributions of the number of incorrect readings, the total number of slips, and the correct reading percentages are shown in Figs. 10 to 12, respectively.

TABLE V
PERCENT ACCURACY OF THE OCR TOOL BY FILE SIZE

Date	Number of Incorrect Readings (Slips) of Each Size (kB)						Number of Images (Slips) of Each Size (kB)						Correct Reading Percentage					
	< 100 kB	100 kB	200 kB	300 kB	400 kB	500 kB	< 100 kB	100 kB	200 kB	300 kB	400 kB	500 kB	< 100 kB	100 kB	200 kB	300 kB	400 kB	500 kB
21 Sep 24	2	24	30	12	0	0	5	89	107	57	12	1	60.0%	73.0%	72.0%	79.0%	100.0%	100.0%
22 Sep 24	2	7	12	3	0	0	2	29	57	25	3	1	0.0%	75.9%	79.0%	88.0%	100.0%	100.0%
23 Sep 24	1	10	14	6	1	0	1	30	43	29	7	0	0.0%	66.7%	67.4%	79.3%	85.7%	-
24 Sep 24	0	5	9	3	0	1	1	12	22	14	3	2	100.0%	58.3%	59.1%	78.6%	100.0%	50.0%
25 Sep 24	0	4	5	4	0	0	1	19	29	16	3	0	100.0%	79.0%	82.8%	75.0%	100.0%	-
26 Sep 24	0	2	0	0	0	0	0	10	3	0	0	0	-	80.0%	100.0%	-	-	-
27 Sep 24	0	6	7	2	0	0	0	22	24	16	4	0	-	72.7%	70.8%	87.5%	100.0%	-
28 Sep 24	1	1	2	2	0	0	1	4	14	9	4	0	0.0%	75.0%	85.7%	77.8%	100.0%	-
29 Sep 24	0	2	0	0	1	0	0	3	6	6	4	0	-	33.3%	100.0%	100.0%	75.0%	-
30 Sep 24	0	2	1	0	0	0	0	5	8	4	0	0	-	60.0%	87.5%	100.0%	-	-
1 Oct 24	0	11	9	3	1	0	0	27	42	17	2	2	-	59.3%	78.6%	82.4%	50.0%	100.0%
2 Oct 24	3	1	7	3	0	0	4	10	15	11	2	0	25.0%	90.0%	53.3%	72.7%	100.0%	-
3 Oct 24	0	2	3	1	1	0	0	9	13	5	2	1	-	77.8%	76.9%	80.0%	50.0%	100.0%
4 Oct 24	1	1	3	1	0	0	1	5	16	11	2	0	0.0%	80.0%	81.3%	90.9%	100.0%	-
5 Oct 24	0	2	3	1	0	0	0	10	19	4	1	0	-	80.0%	84.2%	75.0%	100.0%	-
6 Oct 24	0	5	5	1	0	0	0	8	19	12	1	0	-	37.5%	73.7%	91.7%	100.0%	-
7 Oct 24	1	4	2	1	0	0	2	13	21	6	0	0	50.0%	69.2%	90.5%	83.3%	-	-
8 Oct 24	0	4	2	3	0	0	0	9	7	9	1	0	-	55.6%	71.4%	66.7%	100.0%	-
9 Oct 24	0	2	10	0	2	0	2	11	21	6	3	1	100.0%	81.8%	52.4%	100.0%	33.3%	100.0%
10 Oct 24	0	5	4	3	0	0	0	10	18	8	1	1	-	50.0%	77.8%	62.5%	100.0%	100.0%
11 Oct 24	0	1	2	0	0	1	0	8	12	14	3	1	-	87.5%	83.3%	100.0%	100.0%	100.0%
12 Oct 24	2	3	3	0	0	0	2	19	14	6	0	0	0.0%	84.2%	78.6%	100.0%	-	-
14 Oct 24	0	9	14	3	2	0	2	34	53	19	4	0	100.0%	73.5%	73.6%	84.2%	50.0%	-
15 Oct 24	1	7	7	1	0	0	4	30	40	14	4	0	75.0%	76.7%	82.5%	92.9%	100.0%	-
16 Oct 24	2	0	14	4	0	0	2	25	49	14	5	0	0.0%	100.0%	71.4%	71.4%	100.0%	-
17 Oct 24	3	5	5	0	0	0	4	26	47	18	5	0	25.0%	80.8%	89.4%	100.0%	100.0%	-
18 Oct 24	4	3	10	4	0	0	7	39	80	34	4	0	42.9%	92.3%	87.5%	88.2%	100.0%	-
19 Oct 24	17	59	65	22	3	0	38	246	314	110	17	1	55.3%	76.0%	79.3%	80.0%	82.4%	100.0%
Total	**41**	**187**	**248**	**83**	**11**	**2**	**80**	**776**	**1131**	**502**	**101**	**12**	**48.8%**	**75.9%**	**78.1%**	**83.5%**	**89.1%**	**91.7%**

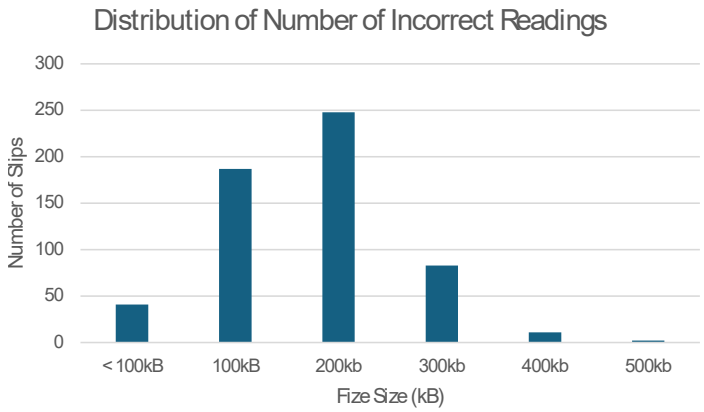

Fig 10. Distribution of the incorrect readings

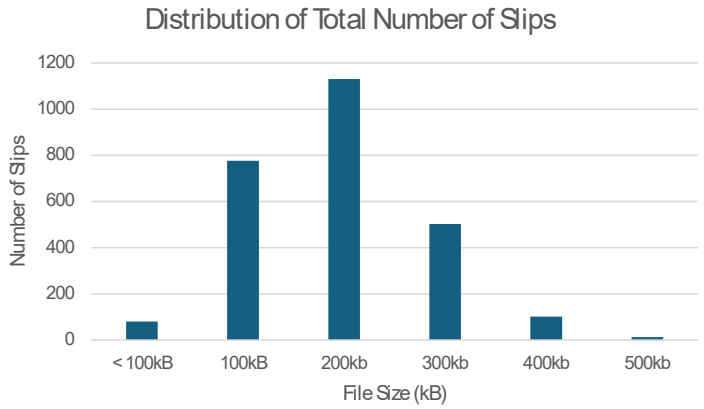

Fig 11. Distribution of the total number of slips

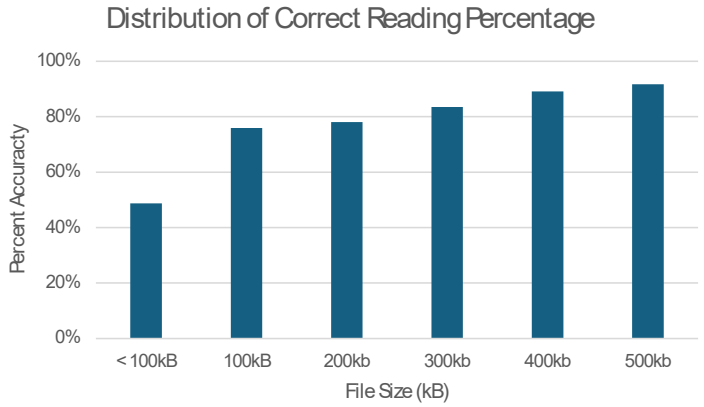

Fig 12. Distribution of the correct reading percentage

From Figs. 10 and 11, the distributions look similar, with more slips at lower file sizes than at the average file size. Fig. 12 clearly shows that a higher accuracy percentage can be achieved for larger file sizes

The observed trend suggests that image resolution is a dominant factor affecting OCR performance. Larger image files generally contain more visual detail, allowing character boundaries to be recognized more reliably. Consequently, image acquisition guidelines specifying a minimum image quality may substantially improve OCR performance without modifying the recognition algorithm. From an operational perspective, encouraging users to upload higher-quality images may represent a more cost-effective strategy than developing increasingly sophisticated OCR algorithms. Similar to previous studies, OCR accuracy is strongly influenced by image quality. However, unlike studies focusing solely on OCR recognition performance, the proposed framework demonstrates that combining OCR with rule-based post-processing and reliability required for financial document processing human verification can substantially improve operational efficiency while maintaining the VII.

VII. Conclusion

This article demonstrates the development and application of an automated OCR tool with a post-OCR algorithm to improve accuracy performance. Computational test results indicate that OCR technology, as a pre-processing tool for human operators, has acceptable accuracy in both the number of slips and the monetary amount. While manual review by operators, when executed meticulously, may yield near-perfect accuracy, it remains highly time- and labor-intensive. Although the OCR tool exhibits slightly reduced accuracy, it offers substantial gains in slip-processing efficiency. This work introduces a practical framework that integrates an OCR tool, a post-OCR correction algorithm, and human verification into a unified operational workflow for real-world financial document processing. Within this workflow, the OCR tool and post-OCR algorithm perform the initial data extraction and correction. At the same time, human operators conduct the final verification, leveraging the complementary strengths of automation and human oversight. This integrated workflow enables near-zero verification errors while reducing manual workload by approximately 95%, making it especially effective for this problem, which requires both scalability and reliability. Experimental results confirm the OCR tool's robust, consistent performance. Based on the evaluated dataset, which is 29 days of operations, the man-machine approach produces reliable outputs, indicating its potential for full deployment.

Overall, this study demonstrates that the proposed human-in-the-loop OCR framework offers a practical solution for improving document-processing efficiency while preserving data accuracy. By combining automated OCR with targeted human verification, the framework remains effective despite variations in document quality, making it particularly suitable for resource-constrained organizations that require scalable and reliable document processing. Future research should evaluate the proposed framework across similar applications to establish its generalizability further and identify context-specific errors. Sources that can guide the development of improved post-OCR algorithms.

Acknowledgment

The authors thank the non-profit organization that provided the case study problem and test dataset for this article.

References

[1] J. Memon, M. Sami, R. A. Khan, and M. Uddin, "Handwritten Optical Character Recognition (OCR): A comprehensive Systematic Literature Review (SLR)," *IEEE Access*, vol. 8, pp. 142642-142668, Jan. 2020, https://doi.org/10.1109/ACCESS.2020.3012542

[2] T. T. H. Nguyen, A. Jatowt, M. Coustaty, and A. Doucet, "Survey of post-OCR processing approaches," *ACM Comput. Surv.*, vol. 54, no. 6, Art. no. 129, pp. 1-37, Jul. 2021, https://doi.org/10.1145/3453476

[3] P. Kiatphaisansophon, D. Wanvarie, and N. Cooharojananone, "Efficient text bounding box identification using Mask R-CNN: Case of Thai documents," *IEEE Access*, vol. 12, pp. 49306-49328, Feb. 2024, https://doi.org/10.1109/ACCESS.2024.3383911

[4] D. P. V. Hoai, H. -T. Duong, and V. T. Hoang, "Text recognition for Vietnamese identity card based on deep features network," *Int. J. Doc. Anal. Recognit.*, vol. 24, no. 2, pp. 123-131, Feb. 2021, https://doi.org/10.1007/s10032-021-00363-7

[5] S. Srivastava, J. Priyadarshini, S. Gopal, S. Gupta, and H. S. Dayal, "Optical character recognition on bank cheques using 2-D convolutional neural network," in *Applications of Artificial Intelligence Techniques in Engineering*, H. Malik, S. Srivastava, Y. R. Sood, and A. Ahmad, Eds. Singapore: Springer, 2019, pp. 589-596, https://doi.org/10.1007/978-981-13-1822-1_55

[6] Y. Meng, R. Wang, J. Wang, J. Yang, and G. Gui, "IRIS: Smartphone-aided intelligent reimbursement system using deep learning," *IEEE Access*, vol. 7, pp. 165635-165645, Nov. 2019, https://doi.org/10.1109/ACCESS.2019.2953501

[7] R. B. Palm, O. Winther, and F. Laws, "Cloudscan - A configuration-free invoice analysis system using recurrent neural networks," in *Proc. 14th IAPR Int. Conf. Document Anal. Recognit. (ICDAR)*, 2017, pp. 406-413, https://doi.org/10.1109/ICDAR.2017.74

[8] Y. Sun, X. Mao, S. Hong, W. Xu, and G. Gui, "Template matching-based method for intelligent invoice information identification," *IEEE Access*, vol. 7, pp. 28392-28401, Feb. 2019, https://doi.org/10.1109/ACCESS.2019.2901943

[9] F. Yi et al., "Dual model medical invoices recognition," *Sensors*, vol. 19, no. 20, Art. no. 4370, Oct. 2019, https://doi.org/10.3390/s19204370

[10] H. Zhang, B. Dong, Q. Zheng, B. Feng, B. Xu, and H. Wu, "All-content text recognition method for financial ticket images," *Multimedia Tools Appl.*, vol. 81, pp. 28327-28346, Mar. 2022, https://doi.org/10.1007/s11042-022-12741-2

[11] C. Sayallar, A. Sayar, and N. Babalık, "An OCR engine for printed receipt images using deep learning techniques," *Int. J. Adv. Comput. Sci. Appl.*, vol. 14, no. 2, pp. 833-840, Feb. 2023, https://doi.org/10.14569/IJACSA.2023.0140295

[12] H. Zhou, L. Shao, and H. Zhang, "SRRNet: A transformer structure with adaptive 2D spatial attention mechanism for cell phone-captured shopping receipt recognition," *IEEE Trans. Consum. Electron.*, vol. 70, no. 1, pp. 3289-3298, Feb. 2024, https://doi.org/10.1109/TCE.2022.3229438

[13] S. Patel, "Multi-Modal product recognition in retail environments: Enhancing accuracy through integrated vision and OCR approaches," *World J. Adv. Res. Rev.*, vol. 25, no. 1, pp. 1837-1844, Jan. 2025, https://doi.org/10.30574/wjarr.2025.25.1.0122

[14] H. T. Ha and A. Horák, "Information extraction from scanned invoice images using text analysis and layout features," *Signal Process. Image Commun.*, vol. 102, Art. no. 116601, Mar. 2022, https://doi.org/10.1016/j.image.2021.116601
[15] H. Arslan, "End to end invoice processing application based on key fields extraction," *IEEE Access*, vol. 10, pp. 78398-78413, Jul. 2022, https://doi.org/10.1109/ACCESS.2022.31932828
[16] A. M. Akanksh et al., "Automated invoice data extraction using image processing," *IAES Int. J. Artif. Intell.*, vol. 12, no. 2, pp. 514-521, Jun. 2023, https://doi.org/10.11591/ijai.v12.i2.pp514-521
[17] C. Gerling and S. Lessmann, "Multimodal document analytics for banking process automation," *Inf. Fusion*, vol. 118, Art. no. 102973, Jun. 2025, https://doi.org/10.1016/j.inffus.2025.102973
[18] J. R. Ilagan and J. B. Ilagan, "Graph-partitioning entity resolution for resolving noisy product names in OCR scans of retail receipts," *Procedia Comput. Sci.*, vol. 239, pp. 338-345, Oct. 2024, https://doi.org/10.1016/j.procs.2024.06.180
[19] R. Oucheikh, T. Pettersson, and T. Löfström, "Product verification using OCR classification and Mondrian conformal prediction," *Expert Syst. Appl.*, vol. 188, Art. no. 115942, Feb. 2022, https://doi.org/10.1016/j.eswa.2021.115942



Dhammanit Buddha-kulsomsiri is currently a Matthayom 6 (Grade 12) student in the Science Program at the Kasetsart University Laboratory School, Center for Educational Research and Development, Bangkok, Thailand. His research interests include data analytics applications using Python. The automated OCR system application presented in this paper was developed for a case-study non-profit organization as part of the author's graduation project.



Laddawan Suwannachote is a teacher in the Technology Subgroup of the Science and Technology Subject Learning Group at the Kasetsart University Laboratory School, Center for Educational Research and Development, Bangkok, Thailand. She received a Master of Education in Educational Communications and Technology from Kasetsart University in 2003. She has served as a student advisor on several projects related to information technology and data analysis.



Jirachai Buddhakulsomsiri is an associate professor with the School of Manufacturing Systems and Mechanical Engineering, Sirindhorn International Institute of Technology, Thammasat University, Thailand. He received his Ph.D. from Oregon State University, USA, in 2003. His research interests include logistics and supply chain systems engineering, with a focus on inventory optimization, supply chain network design, sustainable vehicle routing, and demand forecasting using time-series and machine-learning models.



Parthana Parthanadee is an associate professor at the Department of Agro-Industrial Technology, Faculty of Agro-Industry, Kasetsart University, Bangkok, Thailand. She received her Ph.D. in industrial engineering from Oregon State University, USA, in 2004. Her research interests include applied operations research in agro-industry, vehicle routing, production planning, and agri-food supply chain and logistics management.

Comparing Two SLAM Solutions to Improve the Perception Accuracy of Autonomous Vehicles

Yu Ji[1] and Jian Qu[2*]
[1,2]Faculty of Engineering and Technology, Panyapiwat Institute of Management, Nonthaburi, Thailand
E-mail: 6672100059@stu.pim.ac.th, jianqu@pim.ac.th[*]

Received: November 8, 2024 / Revised: March 24, 2025 / Accepted: May 28, 2025

***Abstract*— Sensing the environment through sensors has always been vital in realizing autonomous driving tasks. Environmental perception performance directly affects autonomous driving performance. Autonomous driving vehicles perceive the surrounding environment based on sensor data, and environmental perception is usually achieved through mapping and positioning. Two traditional perception methods exist: (1) Relying on existing map information and collecting data to calculate the location problem. (2) Relying on known positioning coordinates to infer map information. The real-time performance of these two methods is abysmal and cannot meet the needs of continuous autonomous driving. This paper analyzes the accuracy of two SLAM solutions, Gmapping and Cartographer, through a comparison experiment in which a car perceives maps and obstacles in a real environment, and concludes that cumulative error is a key factor affecting accuracy. This has drawn attention to loop detection.**

***Index Terms*—Autonomous Driving, Obstacle Avoidance, Environmental Awareness, Map Construction**

I. Introduction

Autopilot can be realized in many ways, but many problems affect its robustness when moving from virtual to real-world deployment. Existing autopilot systems are generally divided into a perception layer, a decision-making layer, and an executive layer. The perception layer executes environment-aware commands and is the core technology enabling interaction between the vehicle and the external environment. At the perceptual level, the algorithm may classify a piece of transparent glass as a non-obstacle, but it still exists. If self-driving cars cannot detect problematic obstacles, then self-driving cannot be achieved. Therefore, improving self-driving perception has long been a focus of research. Once perception is solved, obstacle avoidance becomes much easier. In addition, real-time perception is also important. Self-driving cars do not need to collect road data before driving. SLAM scheme can improve self-driving vehicles' perception and real-time performance [1]. SLAM (Simultaneous Localization and Mapping), also known as CML (Concurrent Mapping and Localization), involves real-time positioning and map construction. It solves positioning, navigation, obstacle avoidance, and related problems in unfamiliar environments. The SLAM system framework is divided into five modules: sensor data, visual odometer, back-end, mapping, and loop detection [2]. Based on sensors, SLAM falls into three categories: visual SLAM, lidar SLAM, and Multi-sensor fusion SLAM. This paper aims to deploy a self-driving car in a real scene to test its environmental awareness and verify the SLAM scheme's reliability.

II. Research Objective

In specific environments, self-driving cars can rely on a single camera to perceive the environment and piece together different areas based on the real-world layout through boundary features. However, in harsh environments, a single sensor is powerless. Moreover, multimodal perception algorithms have a threshold. If objects in the real environment fall below the threshold during calculation, the self-driving car may make mistakes. We aim to improve self-driving perception technology by comparing it with current standard SLAM methods.

III. Literature Review

A debate has long existed about the strengths of visual and non-visual SLAM schemes. Generally, vision schemes have advantages and can provide rich environmental texture information. However, vision schemes require significant computation and are easily affected by external light [3]-[5], reducing the robustness of self-driving cars. Radar offers more accurate range, stable operation in strong light, and easier information processing. However, the radar scheme loses detail.

A. Vision SLAM

Vision SLAM collects data using monocular [4]-[6], binocular, or stereoscopic cameras, or other vision sensors. A visual SLAM system has five parts: Data reading, front end, back end, loop detection, and drawing. The system's workflow usually involves the sensor collecting image data and delivering it to the front end, which extracts image features to build the local map and independently locate the vehicle. Then, the back end optimizes the front-end information. Loop detection combines maps generated by different parts of the same scene, using known locations, coordinates, and other information to complete a large map.

B. Laser SLAM

Laser SLAM is a SLAM scheme in which self-driving vehicles estimate their position and pose from point cloud information fed back by lidar and build maps of the surrounding environment [2], [7]. Laser SLAM falls into two categories: filter-based and optimization-based. Representative examples include the Gmapping and Cartographer algorithms.

1) Gmapping

Gmapping, proposed by Grisetti G and others [8], [9], is based on the particle filter method to estimate the posture of the self-driving vehicle, propagates each particle with the kinematic model, calculates the propagated particles with the weight of the observation model, and constructs the map according to the measured pose of the self-driving vehicle. It can achieve better mapping in small environments. When using particle filters to estimate the pose of a self-driving car, each particle stores a specific time track of the self-driving car and a map of the environment at a particular time. This inevitably leads to particle resampling. The longer it takes to build the map, the more particles are resampled, and even if all particles are copied from one particle, the particles' diversity is lost entirely. To reduce memory use from resampling, Gmapping reduces the number of resamplings and uses a threshold to measure the difference between the predicted and actual distributions. [9], [10]. When the difference is minimal, it performs no resampling. When the difference is significant, it resamples. However, mapping treats all particles equally when the odometer model propagates, leading to particle degradation, such as replacing high-quality particles with low-quality particles. Therefore, odometer information is essential for the Gmapping solution, and odometer accuracy determines the quality of the map constructed.

Gmapping uses particle filtering to estimate the robot's position and posture. Each particle represents a possible robot trajectory, and a weight represents its credibility. The robot's state (position and posture) is (1-1), where x and y are positions and θ is the direction.

The particle filter formula is (1-2), where $x_{1:t}^{i}$ is the state trajectory of the i-th particle. ω_t^i is the weight of the i-th particle. $\delta(\cdot)$ is the Dirac delta function, indicating that the state of the particle is discrete.

The particle weight is updated using the observation data zt, as shown in formulas (1-3). Among them, $p(z_t|x_t^i, m_{t-1}^i)$ is the observation model, representing the probability of observing z_t under particle I and map m_{t-1}^i.

To avoid particle degradation (some particles have too large weights), Gmapping periodically resamples, discards low-weight particles, and copies high-weight particles. Each particle independently maintains a map, and the map update is based on the current observation data, as shown in the formula (1-4). Maps are usually represented using an Occupancy Grid Map, where the probability of each grid is updated using observed data.

$$x_t = (x, y, \theta) \tag{1-1}$$

$$p(x_{1:t}|z_{1:t}, u_{1:t}) = \sum_{i=1}^{N} \cdot \omega_t^i \delta(x_{1:t} - x_{1:t}^i) \tag{1-2}$$

$$\omega_t^i \propto \omega_{1:t}^i \cdot p\left(z_t \middle| x_t^i, m_{t-1}^i\right) \tag{1-3}$$

$$p(m|x_{1:t}, z_{1:t}) = \Pi_{i=1}^{N} \cdot p\left(m \middle| x_{1:t}^i, z_{1:t}\right) \tag{1-4}$$

2) Cartographer

The Cartographer algorithm is Google's open-source solution. Its core is creating local sub-images fused with multi-sensor data and a scan-matching strategy for closed-loop detection [11].

In this scheme, the front-end scan-matching algorithm combines Correlative Scan Matching (CSM) and gradient optimization. After generating a sub-map, it performs local closed-loop detection; once all sub-maps are constructed, it performs global closed-loop detection using a branch-and-bound algorithm and a pre-calculated grid to speed it up. However, Cartographer does not verify results during closed-loop detection, which can lead to errors in closed-loop maps when the robot perceives similar boundaries.

Cartographer represents the robot's pose and observation data as nodes and edges in a graph and solves the SLAM problem by optimizing the graph structure.

Each node represents the robot's pose at a particular moment $x_t = (x, y, \theta)$, where x,y are positions and θ is the direction. Edges represent constraints between poses, such as relative poses from odometers or loop-closure detection. Cartographer optimizes the graph structure by minimizing the error function, as shown in formula (2-1), where $e_{ij}(x)$ is the error function representing the difference between the actual observation and the predicted value

between node i and node j. Ω_{ij} is the information matrix, which means the confidence of the constraint.

For pose constraints, the formula of the error function is as follows (2-2), where $\ominus$ represents the relative transformation of pose and z_{ij} is the observed relative pose.

$$\hat{x} = \arg\min_{x} \sum_{i,j} e_{ij}(x)^{T} \Omega_{ij} e_{ij}(x) \quad (2\text{-}1)$$

$$e_{ij}(x) = x_i \ominus x_j - z_{ij} \quad (2\text{-}2)$$

A cartographer performs loop detection by matching the current laser scan data with the historical map data and finding possible loops. The probability model formula for loop detection can be expressed as (2-3), where π_k is the mixing weight and $N(z_t|\mu_k, \sum_k)$ is the Gaussian distribution, which indicates the matching degree between the observed data z_t and the map m.

$$p(z_t|x_t, m) = \sum_{k=1}^{K} \pi_k N(z_t|\mu_k, \sum_k) \quad (2\text{-}3)$$

Cartographer uses sub-maps to manage large-scale environments. Each submap is a local map constructed by local optimization. The global map is composed of multiple sub-maps aligned by global optimization.

C. *Multi-sensor Fusion SLAM*

When comparing perception capabilities without considering factors such as price and operating speed, multi-sensor fusion SLAM technology outperforms single-sensor SLAM technology (including visual SLAM and radar SLAM). [12]-[15]. Multi-sensor fusion SLAM technology can provide information redundancy. In simple terms, when an object falls below a particular sensor's recognition threshold, another sensor fills the gap, making map building more comprehensive and accurate.

1) RTAB-Map

Given the urgent need for multi-sensor technology in the scientific research community, Michaud et al. proposed RTAB-Map. Real-Time Appearance-Based mapping (RTAB-Map) is an appearance-based closed-loop detection method that integrates visual and lidar SLAM solutions and supports real-time positioning and navigation of most current sensors in unknown environments.

SLAM emphasizes accurate, real-time mapping and positioning. When computer performance is limited, these two requirements often conflict. We must carefully balance them in the program to achieve the best practical results.

SLAM methods must identify when to revisit past locations (loop detection) to correct the map. Dynamic environments, lighting changes, geometric changes, and repeated environments can lead to incorrect positioning or positioning failures. Therefore, the method should be robust to the above problems.

Currently, robot navigation methods are based on grid maps. For static large scene maps, effective map management involves map sessions and call and memory management during positioning to reduce map maintenance time.

When the robot does not know its relative position to the previously created map or loses its position, it cannot plan a path to a previously visited location. To avoid restarting mapping from scratch or positioning itself in a previously built map, multi-session mapping allows the system to initialize a new map at startup and then merge the two maps when it encounters a previously visited location.

IV. Methodology

This section introduces the laser SLAM algorithm Cartographer and completes mapping and positioning through experiments [16]-[20]. The experimental steps include: 1) constructing the model car; 2) selecting the real environment; 3) collecting data; and 4) evaluating. The experiment aims to build the model car in a real environment, collect feedback data to generate map information and model vehicle location information, and ultimately enable environmental perception.

A. *ROS2 System Model Car*

The model car is equipped with the ROS2 operating system, an Astra Pro depth camera, a lidar, an IMU, a Jetson Orin Nano development board, a ROS car expansion version, a USB UHB expansion version, an Ackerman backplane, and a touch screen.



Fig .1. ROS2 autonomous driving car

TABLE I
AUTONOMOUS DRIVING CAR CONFIGURATION

Classification	Detailed
Operating System	ROS2
	Astra Pro Depth Camera
Sensor	Lida
	IMU
GPU	Jeston Orin Nano 8GB
Extended board	ROS Car Expansion Board
	USB Expansion Board
Base Plate	Ackerman baseboard
Operation board	Touch Screen

B. Data Collection

To intuitively observe the effect of mapping [16], [19], we chose a closed rectangular space, arranged four obstacles in the space, and divided them into one easy-to-identify obstacle and three difficult-to-identify obstacles based on recognition difficulty. Then, we set up two scenes in the same rectangular space. In Scene 1, the self-driving car is in the middle of the rectangular space, with an obstacle in each of the four directions. In Scene 2, place obstacles only in front of and to the left of the self-driving car. Use this to observe SLAM results and calibrate the real environment and obstacles in the SLAM map [21], [22]. Rely on vehicle radar to measure the barriers and feed them to the map. For this reason, I used another algorithm, Gmapping, to compare its effects with Cartographer. Both Gmapping and Cartographer algorithms rely on radar sensors.

1) Experimental Purpose

To test and compare the accuracy of autonomous vehicles in perceiving the environment and detecting closed loops on maps using Cartographer and GMapping algorithms, we designed the following experiment: placing the autonomous vehicle in an unfamiliar environment and placing obstacles in the four directions of the scene, allowing it to restore the scene and obstacles as much as possible on the 2D grid map. Based on the real environment, the advantages and disadvantages of the two algorithms are analyzed, and a better perception algorithm is proposed for the future.

2) Obstacle Classification

LiDAR does not perform well in identifying transparent objects and may fail to identify them. However, it performs well in identifying non-transparent objects. Therefore, we classify transparent obstacles as challenging to locate and non-transparent obstacles as easy to identify.

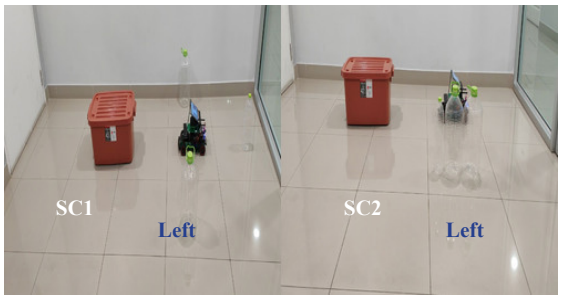

Fig. 2. Scene layout

C. Evaluation Method

While keeping the experimental environment and equipment unchanged, we tested the Gmapping and Cartographer algorithms once each, recorded their results for perceiving maps and obstacles in the experimental environment, and plotted them in a table. If the surrounding environment is successfully perceived to form a raster map, we write a checkmark in the environment column; if a simple obstacle is successfully identified, we write a checkmark in the simple column; if N difficult obstacles are successfully identified, we write the corresponding N in the problematic column [23]-[24].

TABLE II
ALGORITHM RELIABILITY

Algo	Sce	Env	Easy	Hard
Cartographer	1	√	√	2
	2	√	√	√
Gmapping	1	√	√	1
	2	√	√	√

V. RESULT

Through the map comparison, we find that both Cartographer and Gmapping can restore the actual scene and identify obstacles that are easy to locate. However, Cartographer performs better at identifying three difficult-to-find barriers. In scene 1, Cartographer identified the easily identifiable obstacles directly in front and the challenging obstacles on the left and rear. In scenario 2, the Cartographer can identify three stacked barriers that are difficult to locate. When using the Gmapping algorithm, Gmapping recognizes the easy-to-identify obstacles in front of scene 1 but does not identify the problematic obstacles on the left, right, and rear. In scene 2, the Cartographer can identify three stacks of challenging obstacles.

When Gmapping performs loop Detection, computational complexity increases with the number of particles, particle degradation occurs, and accuracy

decreases after long-term operation. Cartographer uses scan matching for loop detection. Although the calculation is complex, the accuracy is more stable and does not change over time.

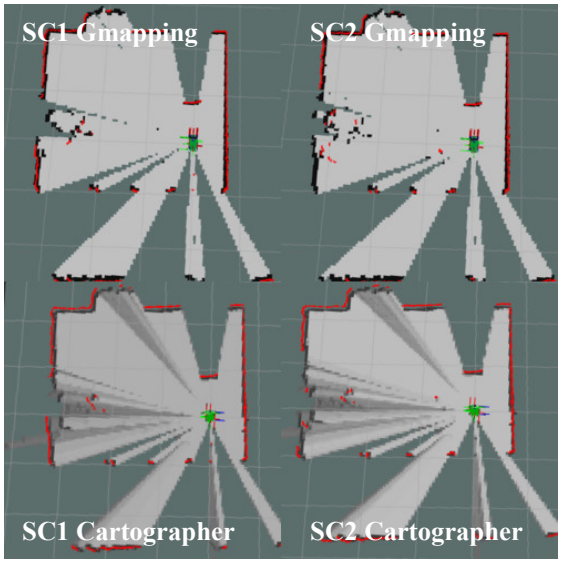

Fig. 3. Mapping

, vol. 22, no. 6, Art. no. 013, 2022, https://doi.

VI. Conclusion

This article introduces the SLAM framework, classification, and laser SLAM methods. Generally, no matter the algorithm, relying on a single sensor to achieve full environmental awareness is very difficult. Neither Cartographer nor Gmapping can detect all obstacles, but at this stage, Cartographer detects more obstacles, giving it a perception advantage.

For 2D LiDAR SLAM, perceiving obstacles below the radar is impossible. Highly transparent objects can cause the laser-point return trajectory to deviate, so the radar may scan the object and fail to identify it as an obstacle. At this point, we need other sensors to improve autonomous vehicle perception. We could design relevant experiments based on sensor capabilities. Still, in complex real environments, achieving autonomous driving by relying on a single sensor is difficult. Therefore, in SLAM research, multi-sensor fusion provides better perception than a single sensor, which cannot be achieved by improving the algorithm alone.

In subsequent SLAM research, we should pay more attention to global optimization. Accumulated error reduces accuracy, and loop detection can eliminate it.

Author Contributions

Conceptualization, Y. J. and J. Q.; Methodology, Y. J. and J. Q.; Software, Y. J. and J. Q.; Validation, Y. J. and J. Q.; Formal analysis, Y. J. and J. Q.; Investigation, Y. J. and J. Q.; Data Curation, Y. J. and J. Q.; Writing—Original Draft Preparation, Y. J. and J. Q.; Writing—Review and Editing, Y. J. and J. Q.; Visualization, Y. J. and J. Q.; Supervision, J. Q.; All authors have read and agreed to the published version of the manuscript.

The first author received scholarship support from CPALL for conducting this research in PIM.

References

[1] A. Dwijotomo, M. A. Abdul Rahman, M. H. M. Ariff, H. Zamzuri, and W. M. H. Wan Azree, "Cartographer SLAM method for optimization with an adaptive multi-distance scan scheduler," *Appl. Sci.*, vol. 10, no. 1, Art. no. 347, Jan. 2020, https://doi.org/10.3390/app10010347

[2] S. Macenski and I. Jambrecic, "SLAM Toolbox: SLAM for the dynamic world," *J. Open Source Softw.*, vol. 6, no. 61 p. 2783, May 2021, https://doi.org/10.21105/joss.02783

[3] Ł. Sobczak, K. Filus, J. Domańska, and A. Domański, "Finding the best hardware configuration for 2D SLAM in indoor environments via simulation based on Google Cartographer," *Sci. Rep.*, vol. 12, Art. no. 18815, Nov. 2022, https://doi.org/10.1038/s41598-022-22938-y

[4] Z. Liu, Z. Cui, Y. Li, and W. Wang, "Parameter optimization analysis of Gmapping algorithm based on improved RBPF particle filter," *J. Phys.: Conf. Ser.*, vol. 1646, no. 1, p. 012004, Sep. 2020, https://doi.org/10.1088/1742-6596/1646/1/012004

[5] X. Liu, G. Gong, X. Hu, G. Shang, and H. Zhu, "Cognitive enhancement of robot path planning and environmental perception based on Gmapping algorithm optimization," *Electronics*, vol. 13, no. 5, Art. no. 818, Feb. 2024, https://doi.org/10.3390/electronics13050818

[6] P. Wang, Z. Chen, Q. Zhang, and J. Sun, "A loop closure improvement method of Gmapping for low cost and resolution laser scanner," *IFAC-PapersOnLine*, vol. 49, no. 12, pp. 168-173, 2016, https://doi.org/10.1016/j.ifacol.2016.07.569

[7] Y. Li and J. Qu, "Intelligent road tracking and real-time acceleration-deceleration for autonomous driving using modified convolutional neural networks," *Curr. Appl. Sci. Technol.*, vol. 22, no. 6, Art. no. 013, 2022, https://doi.org/10.55003/cast.2022.06.22.013

[8] C. Tian, H. Liu, Z. Liu, H. Li, and Y. Wang, "Research on multi-sensor fusion SLAM algorithm based on improved Gmapping," *IEEE Access*, vol. 11, pp. 13690-13703, 2023, https://doi.org/10.1109/ACCESS.2023.3243633

[9] Q. Lin, Z. Ke, S. Bi, S. Xu, Y. Liang, F. Hong, and L. Feng, "Indoor mapping using Gmapping on embedded system," in *Proc. 2017 IEEE Int. Conf. Robotics and Biomimetics (ROBIO)*, 2017, pp. 2444-2449, https://doi.org/10.1109/ROBIO.2017.8324786

[10] C. Kim, H. Kim, and W. K. Chung, "Exactly Rao-Blackwellized unscented particle filters for SLAM," in *Proc. IEEE Int. Conf. Robotics and Automation (ICRA)*, 2011, pp. 3589-3594, https://doi.org/10.1109/ICRA.2011.5980086

[11] B. Vincke, A. Elouardi, and A. Lambert, "Design and evaluation of an embedded system based SLAM applications," in *Proc. IEEE/SICE Int. Symp. System Integration (SII)*, 2010, p. 345, https://doi.org/10.1109/SII.2010.5708329

[12] W. G. Teame, W. Zhongmin, and Y. Yu, "Optimization of SLAM Gmapping based on simulation," *Int. J. Eng. Res. Technol.*, vol. 9, no. 4, pp. 74-81, Apr. 2020, https://pdfs.semanticscholar.org/c075/14524528655b397b19f1596a71597b38bf3e.pdf

[13] S. Lee, G. Tewolde, J. Lim, and J. Kwon, "2D SLAM solution for low-cost mobile robot based on embedded single board computer," in *Proc. World Congress on Advances in Nano, Bio, Robotics and Energy (ANBRE17)*, 2017, https://jrkwon.com/woordpress/wp-content/uploads/2023/02/YP.06RR1712_3813F5.pdf?utm_source=chatgpt.com

[14] M. Mazuran, G. D. Tipaldi, L. Spinello, W. Burgard, and C. Stachniss, "A statistical measure for map consistency in SLAM," in *Proc. IEEE Int. Conf. Robotics and Automation (ICRA)*, 2014, pp. 3650-3655, https://doi.org/10.119/ICRA.2014.6907387

[15] S. Ding and J. Qu, "Smart car with road tracking and obstacle avoidance based on ResNet18-CBAM," in *Proc. 7th Int. Conf. Business and Industrial Research (ICBIR)*, 2022, pp. 582-585, https://doi.org/10.1109/ICBIR54589.2022.9786406

[16] B. L. E. A. Balasuriya et al., "Outdoor robot navigation using Gmapping based SLAM algorithm," in *Proc. Moratuwa Engineering Research Conf. (MERCon)*, 2016, pp. 403-408, https://doi.org/10.1109/MERCon.2016.7480175

[17] W. Zhang, Q. Zhang, K. Sun, and S. Guo, "A laser-SLAM algorithm for indoor mobile mapping," *Int. Arch. Photogramm. Remote Sens. Spatial Inf. Sci.*, vol. XLI-B4, pp. 351-355, 2016, https://doi.org/10.5194/isprs-archives-XLI-B4-351-2016

[18] Z. Zhang, H. Guo, G. Nejat, and P. Huang, "Finding disaster victims: A sensory system for robot-assisted 3D mapping of urban search and rescue environments," in *Proc. IEEE Int. Conf. Robotics and Automation (ICRA)*, 2007, pp. 3889-3894, https://doi.org/10.1109/ROBOT.2007.364075

[19] P. Yang, "Efficient particle filter algorithm for ultrasonic sensor-based 2D range-only simultaneous localisation and mapping application," *IET Wireless Sens. Syst.*, vol. 2, no. 4, pp. 394-401, Dec. 2012, https://doi.org/10.1049/iet-wss.2011.0129

[20] S. Ding and J. Qu, "Research on self-driving based on dynamic recognition of traffic signs," in *Proc. 6th Int. Conf. Information Technology (InCIT)*, 2022, pp. 64-68, https://doi.org/10.1109/InCIT56086.2022.10067858

[21] A. V. Kanhere and G. X. Gao, "LiDAR SLAM utilizing normal distribution transform and measurement consensus," in *Proc. 32nd Int. Tech. Meeting Satellite Div. Inst. Navig. (ION GNSS+ 2019)*, 2019, pp. 2228-2240, https://doi.org/10.33012/2019.16954

[22] M. Rojas-Fernandez, D. Mújica-Vargas, M. Matuz-Cruz, and D. Lopez-Borreguero, "Performance comparison of 2D SLAM techniques available in ROS using a differential drive robot," in *Proc. Int. Conf. Electronics, Communications and Computers (CONIELECOMP)*, 2018, pp. 50-58, https://doi.org/10.1109/CONIELECOMP.2018.8327175

[23] T. J. Chong, X. J. Tang, C. H. Leng, M. Yogeswaran, O. E. Ng, and Y. Z. Chong, "Sensor technologies and Simultaneous Localization and Mapping (SLAM)," *Procedia Comput. Sci.* vol. 76, pp. 174-179, Dec. 2015, https://doi.org/10.1016/j.procs.2015.12.336

[24] Q. Shen, H. Sun, and P. Ye, "Research of large-scale offline map management in visual SLAM," in *Proc. 4th Int. Conf. Systems and Informatics (ICSAI)*, 2017, pp. 215-219.



Yu Ji is pursuing a master's degree in the Faculty of Engineering and Technology, Panyapiwat Institute of Management, Thailand. Our research mainly focuses on autonomous driving, with a a special emphasis on multi-sensor fusion technology. We are also working on autonomous driving systems based on image recognition.



Jian Qu is a full-time lecturer in the Faculty of Engineering and Technology, Panyapiwat Institute of Management. He received a Ph.D. with Outstanding Performance award from the Japan Advanced Institute of Science and Technology, Japan, in 2013. He received a B.B.A. with Summa Cum Laude honours from the Institute of International Studies of Ramkhamhaeng University, Thailand, in 2006, and an M.S.I.T. from Sirindhorn International Institute of Technology, Thammasat University, Thailand, in 2010. His research interests are natural language processing, intelligent algorithms, machine learning, machine translation, information retrieval, and image processing.

From Human Error Prevention to QFD-Based Preventive System Design in Thailand's Agricultural and Automotive Manufacturing Systems

Wichapol Chanchiewvichai[1], Suchada Rianmora[2*], Thiti Mahaboonpachai[3], Chatchai Vorathanawat[4], and Sirawich Chanchiewvichai[5]
[1,2,5]School of Manufacturing Systems and Mechanical Engineering (MSME),
Sirindhorn International Institute of Technology, Thammasat University, Pathumthani, Thailand
[3]Pakdee College of Commerce and Technology Vocational College, Muang Kamphaengphet, Thailand
[4]Thaisangcharoen Service Co., Ltd. (TSS), District, Samutprakarn, Thailand
E-mail: d6722300040@g.siit.tu.ac.th, suchada@siit.tu.ac.th*, thiti@pcct.ac.th, chatchai@sctc.co.th
d6722300305@g.siit.tu.ac.th

Received: January 9, 2026 / Revised: February 27, 2026 / Accepted: March 25, 2026

***Abstract*—Traditional agricultural and automotive manufacturing systems still rely heavily on manual operations and maintenance, making human error a major source of process instability, product quality variation, and equipment failure. In Thailand, educational pathways strongly shape workforce capability in these industries. Technical and Vocational Education and Training (TVET) programs emphasize hands-on skills, equipment operation, and practical problem-solving, whereas general academic education focuses primarily on theoretical knowledge, often resulting in weaker alignment with operational requirements. In this study, human error is defined as a systemic issue arising from interactions among Man, Machine, Material, and Method (4M), rather than as isolated individual mistakes. Quality Function Deployment (QFD) and the House of Quality (HoQ) translate manufacturer and business owner requirements into explicit workforce competency specifications to prevent human error. By linking organizational priorities with skill-based design requirements, the proposed framework supports a shift from corrective responses to preventive system design, enhancing reliability, safety, and sustainability in agricultural and automotive manufacturing environments.**

***Index Terms*—Human Error Prevention, Agricultural Manufacturing Systems, Quality Function Deployment (QFD), House of Quality (HoQ), Technical and Vocational Education (TVET), Maintenance Engineering**

I. Introduction

Agricultural manufacturing industries transform raw agricultural products into materials suitable for food, industrial, and consumer applications. Among these industries, starch-based manufacturing represents a vital link between agriculture and downstream production, supplying inputs for food, pharmaceuticals, packaging, and bio-based products. While technological advances have enabled high efficiency and automation in modern plants, much of agricultural manufacturing—particularly starch, sago, and cassava processing—still relies on traditional factories characterized by manual operations and human-centered decision-making. In these environments, humans remain central to daily production and maintenance activities. Operators and technicians handle machine setup, material handling, inspection, adjustment, and repair. As a result, human error significantly affects process stability, product quality, equipment reliability, and safety in agricultural manufacturing systems. Unlike discrete manufacturing sectors, agricultural processing uses biological raw materials that vary in moisture content, particle size, and contamination levels. This variability increases process complexity and places additional demands on workers. Small human errors—such as incorrect machine settings, delayed maintenance, unnoticed vibration, or improper cleaning—can propagate through the production chain, leading to quality loss, energy waste, or equipment damage [1]-[3].

A. Human Error Overview

In traditional factories, these errors are often treated as isolated incidents rather than indicators of systemic weaknesses. Agricultural manufacturing systems can be examined using the 4M framework: Man, Machine, Material, and Method. Within this framework, human error intersects with all dimensions. Workers (Man) possess experiential knowledge but may lack formal training in error

prevention. Machines (Machine) are often aging and not designed to tolerate improper use or maintenance mistakes. Materials (Material), being natural and variable, increase the impact of incorrect handling or processing. Lastly, methods (Method) often rely on tradition rather than standardized procedures, making it difficult to detect and correct deviations early. While previous studies have addressed productivity improvement, equipment redesign, and material utilization in agricultural industries, human error—particularly in routine operations and maintenance—has received limited attention. Errors are commonly addressed only after breakdowns or quality failures occur, reinforcing a corrective rather than preventive approach. This reactive practice limits the long-term sustainability and competitiveness of agricultural manufacturing industries [4].

B. Literature Review

Historically, Thailand's labor market has been shaped by demographic transition and structural economic change. In earlier decades, a large share of the workforce was concentrated in agriculture and informal sectors, where demand for certified technical competencies or standardized vocational qualifications was limited. However, as Thailand industrialized and integrated into global supply chains, the need for technical skills increased, particularly in manufacturing and service sectors. Despite this shift, relatively fewer students pursue technical career pathways than general academic tracks, creating a persistent mismatch between labor market demands and available technical competencies. The Technical and Vocational Education and Training (TVET) system has long been recognized as a key mechanism for addressing this skills gap. OECD reports indicate that approximately 14% of Thai secondary students are enrolled in TVET programs, higher than the ASEAN average of 8% but still insufficient to fully meet industry demand. While TVET graduates generally show stronger employment outcomes and wage premiums than those with only general secondary education, the supply of vocational graduates remains insufficient to meet growing demand for skilled technical workers in key sectors [5].

Despite these enrollment trends, Thailand continues to struggle with a mismatch between educational outputs and labor market demand. Employers report shortages of skilled technicians and operators—particularly in industrial sectors— a skills mismatch remains a significant barrier to productivity and competitiveness. Rapid technological change and evolving job requirements intensify the problem, demanding not only basic technical skills but also strong problem-solving abilities, critical thinking, and digital literacy [6].

Thailand's labor market is undergoing structural change driven by digital transformation and automation. AI and related technologies are increasingly automating routine tasks, while new roles require stronger digital and cognitive competencies. However, AI cannot fully replace human labor. Manufacturing and maintenance activities still require human judgment, hands-on skills, and experiential knowledge that cannot be fully codified into algorithms. Operational settings involve variability and uncertainty, demanding contextual decision-making and practical problem-solving. In addition, creativity, craftsmanship, and professional responsibility remain human-centered capabilities that automated systems cannot replicate. While AI improves efficiency through data analysis and system monitoring, sustainable industrial development depends on integrating AI technologies with skilled workers to enhance performance, reduce human error, and strengthen system reliability [7]-[8].

Despite ongoing policy efforts to promote vocational education, recent data show a continuous decline in TVET enrollment in Thailand. National statistics (2018-2025) (Fig. 1) indicate that total enrollment peaked at approximately 1,028,961 students in 2563 before declining steadily to 898,442 students in 2568. This represents a decline of about 130,519 students, or 12.7% over five academic years. The downward trend suggests more students are shifting from vocational pathways to general academic education. This situation raises concerns about the future supply of technically skilled workers. A continued reduction in TVET enrollment may worsen skill shortages in operational and maintenance roles, increasing the risk of human error in manufacturing sectors that rely heavily on practical technical competencies.

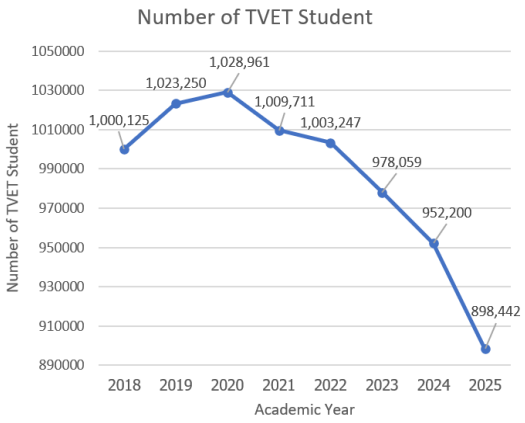

Fig. 1. Number of TVET students vs. academic year [10]

Therefore, enhancing the attractiveness of vocational education and integrating emerging technologies, such as AI, into training programs are

essential for maintaining industrial reliability and long-term competitiveness [9]-[10].

C. Human Error Examples

Human error also plays a significant role in agricultural machinery accidents, particularly with tractors and other equipment. A case study in Italy examined how human error affects agricultural tractor operations and integrated these findings into risk assessment procedures for vineyard cultivation. The research highlighted that operator failures—such as incorrect handling, delayed responses, and misjudging hazardous conditions—substantially contribute to accidents and injuries, despite stringent safety regulations. The study emphasized the need for user-centered approaches in hazard analysis and safety interventions to mitigate risks associated with human error during agricultural machinery operation, including hazard identification and ergonomic factors that influence operator performance [11].

D. Thailand's Workforce Structure

Thailand's workforce structure clearly divides Technical and Vocational Education and Training (TVET) graduates from those from general academic pathways (upper secondary and non-engineering university programs). TVET curricula emphasize hands-on training, machine operation, maintenance practices, and compliance with Standard Operating Procedures (SOPs), while general academic education prioritizes theoretical knowledge and progression to higher education. This divergence directly affects workforce readiness in manufacturing environments where error prevention depends on practical competence [12], [13].

E. Current Trend

Recent evidence from both automotive manufacturing and agricultural industries indicates that workers with vocational or technical backgrounds are better prepared to perform error-sensitive operational and maintenance tasks. In contrast, graduates from general academic pathways often require longer adaptation periods and closer supervision, increasing the likelihood of operational deviations and maintenance-related errors during the early stages of employment [14]-[16].

F. Research Gap

This research addresses this gap by positioning human error as a central concern in agricultural manufacturing systems. By integrating human error considerations into a structured framework based on the 4M model, the study aims to support more reliable, preventive, and sustainable manufacturing processes in agriculture-based industries. This research aims to identify and analyze sources of human error in agricultural manufacturing operations and maintenance, examine their interactions with machinery condition, material variability, and production methods, and propose design- and maintenance-oriented strategies that shift management practices from corrective to preventive approaches, thereby improving reliability, safety, and sustainability in starch-based and similar agricultural industries through a 4M-based framework that systematically integrates human capability (Man), maintainable and error-tolerant equipment (Machine), robustness to raw material variability (Material), and standardized preventive methods with early error detection (Method), while acknowledging that validation is primarily limited to starch processing systems and influenced by organizational, cultural, and resource constraints.

II. Problem Statement

A. System Platform

Agricultural manufacturing systems, especially those that use traditional processing methods, operate under conditions in which human judgment and manual intervention dominate daily activities. Over time, repeated exposure to the same processes normalizes deviations, shortcuts, and minor mistakes [17]. Maintenance actions often rely on experience rather than documented procedures, and workers rarely record or analyze errors such as incomplete inspections, improper adjustments, or delayed repairs [18]. Human error in these systems typically results not from negligence but from systemic conditions such as time pressure during harvest seasons, fatigue from long working hours, limited training, and inadequate machine design. These factors increase the likelihood of errors during operation and maintenance, particularly in processes such as drying, milling, separation, and material transfer.

B. Equipment Platform

In many agricultural factories, maintenance remains largely corrective. Equipment is repaired only after failure, often under urgent conditions that increase the risk of error. Without structured error detection or early-warning mechanisms, latent errors remain unnoticed. Over time, these errors lead to equipment breakdowns, safety incidents, or quality nonconformities that disrupt production and increase costs [19]-[21]. In addition, growing regulatory requirements for food safety, traceability, and environmental performance further pressure agricultural manufacturing systems [22]. Human errors during cleaning, calibration, or maintenance can cause contamination, excessive energy use, or noncompliance with standards. Despite these challenges, few traditional factories have frameworks that explicitly link human error with maintenance engineering and process management. Therefore,

an integrated approach is needed that recognizes human error as an inherent part of agricultural manufacturing and manages it systematically through design, training, maintenance planning, and process standardization.

III. Research Background

In Thailand, educational pathways differ significantly in how well they align with labor market needs, particularly in practical skills and workforce readiness. Technical and Vocational Education and Training (TVET) programs are specifically designed to develop hands-on competencies, technical skills, and industry-relevant knowledge, especially at the upper secondary and post-secondary levels [23]-[24]. About one-third of Thai upper secondary students are enrolled in vocational tracks, and vocational programs also account for a substantial share of post-secondary enrolment, reflecting TVET's important role in workforce preparation [25]. Evidence indicates that vocational education in Thailand is associated with more favorable employment outcomes compared with general academic education at the same level. Graduates from vocational and technical programs tend to have higher employment rates, improved job matching, and a lower likelihood of working in informal or low-skilled occupations than graduates from general academic tracks [26].

Fig. 2 shows how operator overconfidence (10 years of experience) during welding can directly affect finished-part quality, leading to a *Short Trim Line* defect [27]. Process improvement can be achieved through proper training and retraining, even for skilled workers who have graduated from vocational tracks and possess strong operational competencies. Although these workers have substantial experience, long-term involvement in the same operation may lead to overconfidence and reduced adherence to standard procedures.

In this case, targeted retraining and upskilling programs can help reinforce best practices, improve process discipline, and reduce defect rates.

Graduates from vocational and technical education pathways in Thailand consistently align more closely with labor market requirements in manufacturing sectors than those from general academic education at the same level. Vocational education emphasizes practical training, machine operation, and real-world problem-solving, which directly supports employment in industrial and agricultural manufacturing environments. In contrast, general academic pathways prioritize theoretical knowledge and preparation for higher education, often resulting in weaker job–specific skills for operational roles. These differences explain why technical and vocational graduates are more frequently employed in manufacturing positions, experience lower informality risk, and demonstrate higher operational efficiency in practice-oriented industries.

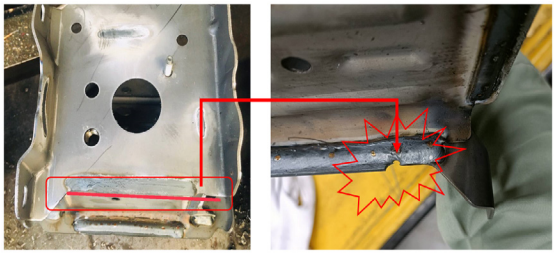

Fig. 2. Defect found during the task – welding process [27]

Table I presents data on enrollment and graduation among Thai Technical and Vocational Education and Training (TVET) students. The statistics indicate that Thailand's TVET system remains a major source of industrial labor, particularly for production and maintenance roles. On average, more than 170,000 students are admitted annually to the vocational certificate level and over 129,000 to the higher vocational diploma level, for a total of almost 300,000 students per year. Meanwhile, graduates from the vocational certificate level exceed 126,000 per year, while approximately 117,000 graduate from the higher vocational diploma level, for a combined output of about 240,000 graduates per year. This sustained supply highlights TVET institutions' critical role in supporting labor-intensive and error-sensitive industries such as automotive manufacturing and agricultural processing. Because TVET education is hands-on, students learn through workshop-based training, direct interaction with industrial equipment, and exposure to real operational constraints. As a result, graduates tend to develop stronger procedural discipline, practical problem-solving ability, and familiarity with standard operating procedures earlier than those following general academic education pathways, which primarily emphasize theoretical knowledge. [28].

Moreover, vocational education has been shown to increase the probability of employment in industrial and manufacturing sectors, where practical skills and operational competence are critical. These findings suggest that graduates of technical or vocational schools are often better prepared for practical manufacturing tasks than those from general academic pathways. This distinction matters especially in agricultural manufacturing, where daily operations depend heavily on equipment handling, routine maintenance, and process adjustment, and where stronger technical training can improve efficiency and reduce human error. Table II presents a comparative overview of education pathways in Thailand and their employment outcomes, emphasizing workforce readiness for manufacturing and agricultural industries.

TABLE I
ENROLLMENT AND GRADUATION STATISTICS FOR THAI TECHNICAL AND VOCATIONAL EDUCATION AND TRAINING (TVET) [28]

Academic Year	New Admissions (Vocational Certificate)	Graduates (Vocational Certificate)	New Admissions (Higher Vocational Diploma)	Graduates (Higher Vocational Diploma)
2017	165,766	80,875	112,229	87,858
2018	72,202	124,732	51,048	122,771
2019	N/A	130,116	N/A	118,489
2020	166,557	140,755	116,126	122,585
2021	229,380	148,351	166,310	141,981
2022	218,798	106,781	160,928	95,976
2023	213,652	155,873	168,746	130,054
Average	**177,652**	**126,783**	**129,231**	**117,102**

TABLE II
COMPARISON OF EDUCATION LEVELS AND EMPLOYMENT OUTCOMES IN THAILAND

Education Level	Training Focus	Practical Skill Intensity	Employment Rate (Relative)	Manufacturing Employment Likelihood	Job–Skill Match	Informality Risk
Lower Secondary (Junior High School)	Basic general education	Very Low	Low	Very Low	Poor	High
Upper Secondary (General Academic)	Academic knowledge	Low	Moderate	Low	Moderate–Poor	Moderate–High
Upper Secondary (Vocational/Technical)	Hands-on technical skills	High	High	High	Good	Low–Moderate
Post-Secondary Vocational Diploma (TVET)	Advanced technical skills	Very High	Very High	Very High	Very Good	Low
University Degree (General)	Theoretical knowledge	Moderate	High	Moderate	Moderate	Low
University Degree (Engineering)	Applied technical theory	High	High	High	Good	Low

A. House of Quality (HoQ) Framework

House of Quality (HoQ) framework has been created to support the research on human error prevention in agricultural and starch-based manufacturing, where:

Customer = Manufacturer or business owner

Customer Requirements (CRs) = Expectations related to smooth operations and effective maintenance performance

Technical Characteristics (Roof/Specifications) = Specific worker skills and competencies required to prevent human error

We obtained all data used in the House of Quality (HoQ) framework through structured interviews with experienced business owners in the agricultural and starch-based manufacturing sectors. We derived the customer requirements, technical skills, importance ratings, and relationship levels directly from their expert insights and operational experience.

We collected the data used in the House of Quality (HoQ) framework through structured interviews with experienced business owners in the agricultural and starch-based manufacturing sectors. We systematically derived all Customer Requirements (CR1-CR6) (Table III), Technical Skills (TS1-TS7) (Table IV), importance ratings, and relationship levels (Table V) from their expert knowledge and operational experience.

Interviews focused on operational stability and maintenance effectiveness to identify Customer Requirements and their corresponding 1-5 importance ratings. The team synthesized technical skills from expert input on the competencies needed to prevent operational errors and equipment failures. Experts

determined the relationship levels within the HoQ matrix through interviews, in which participants assessed how each technical skill supports each customer requirement.

Because human error arises from interactions among workforce capability, equipment condition, material variability, and operational methods, a structured tool is needed to translate managerial requirements into technical and organizational actions. Traditional problem-solving approaches in agricultural manufacturing often address errors only after failures occur, offering limited support for preventive decision-making. Therefore, this study adopts the Quality Function Deployment (QFD) approach, with the House of Quality (HoQ) serving as a central analytical framework to explicitly link manufacturer and business-owner requirements—such as stable production, reliable maintenance, and reduced operational risk—to specific workforce skills, machine design considerations, and standardized procedures aimed at preventing human error.

B. Customer Voice (Manufacturer and Business Owner Requirements)

From the perspective of manufacturers and business owners, operational success in agricultural manufacturing depends strongly on workforce capability. Their primary requirements focus on stable production, controlled maintenance, and reduced risk of human error. These requirements reflect organizational and business priorities rather than individual worker preferences, aligning directly with the House of Quality (HoQ) concept, where the "customer" represents the manufacturer or business owner. From this perspective, key requirements include stable and continuous production, reduced unplanned machine downtime, consistent product quality, lower maintenance and operating costs, compliance with safety and food standards, efficient use of energy and materials, and predictable, preventive maintenance performance, all of which are essential for reducing human error and improving the overall reliability and sustainability of agricultural manufacturing systems.

C. Technical Characteristics (Worker Skills and Specifications)

To meet these requirements, workers must have specific technical characteristics. These characteristics represent measurable skills, competencies, or qualifications that directly influence error prevention: technical skill in machine setup and adjustment, ability to interpret operating parameters and process conditions, preventive maintenance knowledge, equipment inspection and fault-detection capability, understanding of material variability and process sensitivity, ability to follow standardized work procedures, safety and hygiene awareness, problem-solving and root cause analysis skill, and documentation and reporting discipline.

IV. Relationship Strength (Typical HoQ Interpretation)

This relationship mapping highlights which worker competencies most impact human error prevention. The roof of the HoQ (Fig. 3) (Correlation between Skills) illustrates interrelationships among worker skills:

- Preventive maintenance skill strongly supports fault detection ability
- Standardized work compliance reduces dependency on individual experience
- Process understanding enhances correct machine setup and material handling
- Problem-solving skills strengthen preventive decision-making

Positive correlations indicate that developing technical-school-level competencies can improve multiple performance dimensions simultaneously.

- Strong relationship (●)
  Preventive maintenance knowledge ↔ Reduced downtimeFault detection skill ↔ Stable production
- Moderate relationship (○)
  Standardized procedures ↔ Product quality Safety awareness ↔ Compliance
- Weak relationship (△)
  Documentation skill ↔ Energy efficiency

For interpretation and linking to human error, the HoQ demonstrates that human error in agricultural manufacturing is not random, but closely linked to skill gaps and unclear task requirements. Workers with technical and vocational training—especially those from technical colleges—are more likely to possess structured skills aligned with preventive maintenance, standardized procedures, and early error detection.

In contrast, workers without technical backgrounds tend to rely on experience-based judgment, increasing the likelihood that errors remain unnoticed until failure occurs. By using this HoQ, manufacturers can translate business expectations into concrete workforce skill requirements, supporting decisions on recruitment, training, and collaboration with technical education institutions.

A. Case Study: House of Quality (HoQ) for Human Error Prevention in Thailand's Starch, Sago, and Cassava Manufacturing Industries

This House of Quality translates manufacturer and business owner requirements into worker skills and technical competencies required to prevent human error in agricultural manufacturing. The framework is aligned with Thai technical and vocational education

pathways and supports preventive maintenance engineering.

For *'Roof of the House (Skill Correlation)'*, key specifications are considered as follows:

• Preventive maintenance skill (TS2) strongly supports fault detection and reduced downtime
Process understanding (TS3) improves machine setup accuracy (TS1)

• SOP compliance (TS5) reduces reliance on experience-based judgment

• Safety awareness (TS6) strengthens regulatory compliance and risk prevention

Positive correlations indicate that technical education produces multi-skill benefits for error prevention.

TABLE III
CUSTOMER REQUIREMENTS (MANUFACTURER / BUSINESS OWNER)

Co	Customer Requirements	Description	Importance(1-5)
CR1	Stable production	Continuous operation without interruption	5
CR2	Reduced machine downtime	Minimized unplanned breakdowns	5
CR3	Consistent product quality	Uniform moisture, granule size, and cleanliness	4
CR4	Lower maintenance cost	Reduced repair and replacement expenses	4
CR5	Safety and regulatory compliance	GMP, HACCP, Thai food safety laws	5
CR6	Energy efficiency	Reduced fuel and electricity consumption	3

TABLE IV
TECHNICAL CHARACTERISTICS (WORKER SKILLS / SPECIFICATIONS)

Code	Worker Skill / Specification	Description	Education Pathway in Thailand
TS1	Machine setup & adjustment	Correct setting of dryers, mills, and separators	Technical College / Vocational Certificate
TS2	Preventive maintenance skill	Inspection, lubrication, and early fault detection	Technical College / Diploma
TS3	Process parameter interpretation	Temperature, vibration, and moisture control	Technical College / Diploma
TS4	Material handling knowledge	Managing cassava/starch variability	Vocational / On-the-job training
TS5	Standard Operating Procedures (SOPs) compliance	Ability to follow standard procedures	Vocational emphasis
TS6	Safety & hygiene awareness	Food safety and machine safety	Vocational / University
TS7	Problem-solving skill	Root cause analysis of defects	Diploma / University

TABLE V
HOUSE OF QUALITY RELATIONSHIP MATRIX

Customer Requirement	TS1	TS2	TS3	TS5	TS6
Stable production (CR1)	●	●	●	○	△
Reduced downtime (CR2)	○	●	○	○	△
Product quality (CR3)	●	○	●	●	○
Maintenance cost (CR4)	○	●	○	△	△
Safety & compliance (CR5)	△	○	○	●	●
Energy efficiency (CR6)	○	○	●	△	△

(Relationship: Strong = ●, Moderate = ○, Weak = △)

Quality Function Deployment

Project title: Linking Stakeholder Needs to Worker Competencies

Project leader: SR

Date: 11-Sep-25

Correlation:

+	●	–
Positive	No correlation	Negative

Relationships:

9	5	1	
Strong	Moderate	Weak	None

1: low, 5: high

	Customer importance rating	Customer requirements - (What's) ↓	Machine setup & adjustment	Preventive maintenance skill	Process parameter interpretation	Material handling knowledge	Standard Operating Procedures (SOPs) compliance	Safety & hygiene awareness	Problem-solving skill	Weighted score
		Desired direction of improvement (↑,0,↓)	↑	↑	↑	↑	↑	↑	↑	
		Functional requirements (How's) →								
1	5	Stable production	9	9	9	9	5	1	9	255
2	5	Reduced machine downtime	5	9	5	5	5	1	9	195
3	4	Consistent product quality	9	5	9	1	9	5	5	172
4	4	Lower maintenance cost	5	9	5	1	1	1	5	108
5	5	Safety and regulatory compliance	1	5	5	1	9	9	1	155
6	3	Energy efficiency	5	5	9	1	1	1	1	69
		Technical importance score	146	186	178	86	138	82	138	954
		Importance %	15%	19%	19%	9%	14%	9%	14%	100%
		Priorities rank	3	1	2	6	4	7	4	

Fig. 3. House of Quality – linking stakeholder needs to worker competencies

B. Interpretation and Link to Thai Education Pathways

The HoQ (Fig. 3) results demonstrate that human error in starch-based manufacturing is strongly linked to workforce skill structure rather than individual negligence. Skills that most affect production stability and maintenance reliability—such as preventive maintenance, machine setup, and process interpretation—are core competencies emphasized in Thai technical and vocational education systems. Operators graduating from technical colleges and vocational institutions are typically trained through hands-on workshops, equipment-based learning, and maintenance-focused curricula. This preparation supports early error detection and preventive behavior. In contrast, workers from general education pathways often rely on experience-based decision-making, increasing the likelihood that errors remain unnoticed until failure occurs.

V. Discussion

A. Automotive Manufacturing Focus

In traditional automotive manufacturing factories [Mr. Chatchai Vorathanawat [Managing Director, Thai Saeng Charoen Service Co., Ltd. (TSS)], production systems rely heavily on manual operation, routine inspection, and maintenance activities performed by shop-floor technicians. These environments typically involve aging equipment, partial automation, and high production pressure, which together increase the likelihood of human error during machine setup, adjustment, and maintenance. As a result, workforce capability becomes a critical determinant of operational reliability, equipment availability, and product quality. In the Thai context, graduates from vocational and technical education pathways align more closely with the practical demands of automotive manufacturing than graduates from general academic education at the same level. Technical and vocational programs emphasize hands-on training, machine operation, preventive maintenance practices, and fault diagnosis. These competencies enable technicians to recognize abnormal conditions—such as vibration, noise, temperature deviation, or tool wear—early, reducing the likelihood that minor errors escalate into major breakdowns or quality defects. In contrast, general academic pathways primarily focus on theoretical knowledge and preparation for higher education, which may limit graduates' readiness for maintenance-intensive shop-floor roles.

B. A Maintenance Engineering Perspective

From *a maintenance engineering perspective*, human error in automotive factories often stems not from negligence but from insufficient technical grounding, unclear procedures, or limited experience with real equipment. Errors such as incorrect parameter settings, incomplete inspections, or delayed maintenance actions can remain unnoticed until failure occurs. Technically trained personnel are better equipped to follow standard operating procedures, perform systematic inspections, and apply preventive maintenance principles, thereby supporting a shift from corrective to preventive maintenance strategies [29].

C. Framework of Quality Function Deployment (QFD) and the House of Quality (HoQ)

Within the *Quality Function Deployment (QFD) and House of Quality (HoQ) framework,* manufacturers' requirements—such as stable production, reduced downtime, consistent quality, and controlled maintenance costs—can be interpreted as the "voice of the customer." These requirements translate into technical characteristics, which in this case correspond to workforce skills and competencies. Preventive maintenance capability, accurate machine setup, process understanding, and compliance with Standard Operating Procedures (SOPs) emerge as critical technical characteristics that directly influence human error prevention. Accordingly, the HoQ analysis supports the view that vocational and technical education pathways play a crucial role in meeting the operational needs of traditional automotive manufacturing. By aligning workforce development with manufacturer requirements, these pathways improve maintenance performance, reduce human error, and enhance the long-term sustainability of automotive production systems.

V. Some Common Mistakes

A. Automotive Industry – Examples of Human Error and Operational Failures

ISSUE I: Automotive Acceleration Problems and Recalls

One of the most widely cited cases involving vehicle defects and human interaction is the Toyota unintended acceleration incidents from 2009-2011, where floor mat placement and accelerator pedal sticking led to numerous reported accidents and safety recalls. The problem was initially attributed to driver error (e.g., pedal misapplication), highlighting how unclear procedures or failures to follow test/check protocols contributed to serious outcomes that required mass recalls and repair work [30].

ISSUE II: General Motors Ignition Switch Defect

In the early 2010s, General Motors recalled millions of vehicles because a faulty ignition switch could shut off the engine while driving, leading to crashes and fatalities. Investigations pointed to design and quality-control errors, some tied to inadequate verification of assembly specifications and testing procedures. This type of systemic error can be exacerbated when workers or supervisors with limited technical training misinterpret test results or fail to enforce quality checks [31].

B. Agricultural Industry – Examples of Operational and Safety Errors

ISSUE I: Tractor Overturn and Steering Instability

Research on tractor accidents shows that steering instability is a key factor in overturn incidents, especially on uneven terrain. While not purely education-dependent, avoiding such accidents often requires skilled training in machine operation and an understanding of vehicle dynamics—skills more likely found in vocationally trained operators [32].

ISSUE II: Human Errors in Manual Agricultural Tasks

Agricultural manufacturing industries transform raw agricultural products into materials suitable for food, industrial, and consumer applications. Among these industries, starch-based manufacturing represents a critical link between agriculture and downstream production, supplying inputs for food, pharmaceuticals, packaging, and bio-based products. While technological advances have increased efficiency and automation in modern plants, much of agricultural manufacturing—particularly starch, sago, and cassava processing—still relies on traditional factories with manual operations and human-centered decision-making.

In these environments, humans remain central to daily production and maintenance. Operators and technicians handle machine setup, material handling, inspection, adjustment, and repair, making human error a major factor affecting process stability, product quality, equipment reliability, and safety. Prior research shows that improvements in agricultural machinery management depend not only on advanced technology but also on operator skills, maintenance practices, and the quality of operational decision-making, all of which directly influence efficiency, machine downtime, and error occurrence [33].

Unlike discrete manufacturing sectors, agricultural processing deals with biological raw materials that vary in moisture content, particle size, and contamination levels. This variability increases process complexity and places additional demands on workers. Consequently, small human errors—such as incorrect machine settings, delayed maintenance,

unnoticed vibration, or improper cleaning—can propagate through the production chain, leading to quality losses, energy waste, and equipment damage. In traditional factories, people often treat these errors as isolated incidents rather than signs of underlying systemic weaknesses.

ISSUE III: Grain Entrapment and Safety Oversights

Grain entrapment, where workers are suffocated in storage bins, continues to be a major hazard in agricultural facilities worldwide. Most documented entrapments occur not because of machine failure but because workers lack training in safe grain handling, confined-space entry procedures, and emergency protocols—areas where vocational and technical education could build stronger prevention skills [34].

TABLE VI
SUMMARY OF HUMAN ERRORS IN RELATION TO EDUCATIONAL PATHWAYS

Industry	Example Error	Likely Skill Gap	Link to Education
Automotive	Toyota's unintended acceleration issues	Misapplication of test/inspection protocols; procedural gaps	Vocational training would improve hands-on diagnostic and compliance skills
Automotive	GM ignition switch recall	Inadequate verification & quality control during assembly	Technical training enhances detailed quality inspection
Agricultural	Tractor overturning	Lack of operation skills and understanding of machine behavior	Vocational schooling offers targeted machinery operation training
Agricultural	Rice transplanting errors	Multitask management and procedural oversight	Structured on-farm safety and process training improves outcomes
Agricultural	Grain entrapment	Confined-space awareness and safety procedures	Formal safety training reduces errors that may result in loss of life

Table VI summarizes the examples of human error in both industries, the associated skill gaps, and their links to education and training. A key consideration is that human error in both the automotive and agricultural sectors is not just about individual mistakes—it often reflects gaps in practical skills, task-specific training, and procedural understanding. Workers from vocational and technical education pathways generally show stronger preparation for these hands-on challenges, whereas those from general academic (12-year or bachelor's) pathways may be less practiced in real-world operations and maintenance tasks, increasing the likelihood that errors go unnoticed or uncorrected until serious consequences occur.

C. Why These Errors Relate to Educational Pathways

1) Vocational/Technical Education

This emphasizes hands-on equipment operation, recognition of abnormal conditions, and preventive maintenance. Structured training in problem-solving, SOP adherence, and early fault detection are key to reducing human error. Graduates are better prepared for repetitive, machine-intensive tasks and complex procedures that require applied skills.

2) General Academic (Grade 12 / Bachelor)

Focuses more on *theoretical knowledge* and broad conceptual education rather than applied shop-floor skills. Workers may understand principles but lack training in specific procedures, troubleshooting steps, or real-world risk indicators, leading to more unnoticed human errors during routine work.

VI. RESULTS AND DISCUSSION

This section discusses *'Human Error, Skill Gaps, and Education Pathways in Thailand.'* Agricultural and automotive manufacturing rely heavily on manual operations, making human error a key factor in process instability and equipment failure. Education shapes workforce capability: TVET programs emphasize hands-on skills and problem-solving, while general academic paths focus on theory. Vocational graduates exhibit higher employment rates, better job–skill alignment, and greater engagement in manufacturing. Using the 4M framework with QFD and HoQ, this study links manufacturer requirements to workforce competencies, promoting preventive practices and enhancing reliability, safety, and sustainability.

A. Automotive Manufacturing Context

Thailand's automotive industry operates under stringent quality and safety standards, where errors in machine setup, torque application, preventive maintenance, and process monitoring can lead to recalls, downtime, or safety incidents. Studies and industry reports indicate that maintenance-related errors—such as improper lubrication, delayed inspection, or misinterpretation of sensor signals—often stem from insufficient hands-on training rather than a lack of theoretical knowledge [35]-[36]. TVET and engineering graduates typically possess stronger competencies in *maintenance engineering, root cause analysis, and procedural compliance,* enabling them to detect early signs of failure and respond preventively. Conversely, general academic graduates

assigned to operational roles may struggle with real-time decision-making in high-pressure environments, increasing dependency on trial-and-error learning.

B. Agricultural and Starch-Based Manufacturing Context

In agricultural manufacturing—particularly in starch, sago, and cassava processing—the risk of human error is amplified by material variability and aging equipment [37]-[38]. Operators must continuously adjust process parameters such as temperature, moisture content, and separation efficiency. Errors such as incorrect dryer settings, incomplete cleaning, or overlooked vibration often originate from inadequate process understanding or weak SOP discipline. Technical and vocational graduates in Thailand are generally trained to handle such variability through repeated practice and on-site training modules. Their stronger alignment with operational tasks supports more stable production, fewer quality deviations, and reduced unplanned downtime, meeting the manufacturer's core requirements identified in the HoQ framework.

VII. Importance Scale for Human Error Prevention

The importance score reflects the severity of human error's impact on product quality, production continuity, safety, and system reliability, considering both the likelihood of failure and the likelihood of occurrence. Table VIII defines the five importance levels used to assess the impact of human error in manufacturing. In OEM automotive manufacturing, high-importance errors linked to habitual operator behaviors are typically associated with long-term familiarity, reduced vigilance, and normalization of abnormal conditions, which increase failure rates despite stable equipment. Integrating procedural controls, digital monitoring, and behavioral interventions improves MTTF and system reliability, supporting a shift from corrective to preventive manufacturing practices [39]-[42]. Table IX presents a reliability-based interpretation of the importance levels using failure rates and 24-hour reliability values.

A. Situation: Human Error in OEM Automotive Manufacturing Due to Work Habituation

Table VII illustrates that human error driven by routine normalization and reduced caution significantly impacts reliability, a pattern equally evident in OEM automotive manufacturing. These findings emphasize the need for preventive approaches—including standardized checks, parameter monitoring, job rotation, refresher training, and skill-based workforce design—rather than relying on experience alone to prevent quality degradation caused by human habituation. In OEM automotive manufacturing, especially on mature production lines with long-serving operators, human error often stems not from a lack of skill but from overfamiliarity with routine tasks. Similar failures occur when insufficient drying temperature, excessive temperature, or inadequate duration repeatedly occur due to human error [43]-[44]. Automotive production lines experience comparable issues in processes such as heat treatment, welding, painting, molding, and assembly torque application [45].

TABLE VII
HUMAN ERROR–RELATED CAUSES AFFECTING SUBSYSTEM RELIABILITY

No.	Automotive Failure Situation	Typical Process	Human Error Cause	Importance (1–5)	Priority Rank	MTTF (hr)	MTTR (hr)	MTBF (hr)	Failure Rate (1/hr)	Reliability (24 hr)	Preventive Guideline
1	Incorrect process temperature (too low)	Heat treatment, paint curing	Operator skips parameter check due to routine	5	High	355	5	360	0.0028	0.935	Mandatory digital setpoint confirmation and alarms
2	Incorrect process temperature (too high)	Welding, curing	Overcorrection based on past defects	5	High	719	1	720	0.0014	0.967	SPC-based limits with real-time feedback
3	Inadequate process duration	Bonding, curing	Time-saving shortcuts under pressure	4	High	60	0.2	60	0.0167	0.67	Automated timer interlock (no manual override)
4	Excessive process duration	Welding, coating	Habitual compensation without data	3	Medium	719	1	720	0.0014	0.967	Standard cycle enforcement via PLC
5	Improper material thickness / quantity	Coating, molding	Visual judgment replaces measurement	4	High	90	0.1	90	0.0111	0.766	Poka-yoke gauges and fixture control
6	Missed inspection steps	Assembly, in-process QC	"Nothing usually fails here" mindset	5	High	72	0.1	72	0.0139	0.716	Checklist sign-off with random audits
7	Environmental contamination	Painting, clean assembly	Failure to close covers/screens	5	Very High	24	0.03	24	0.0417	0.367	Visual status indicators + interlocks

TABLE VII
HUMAN ERROR–RELATED CAUSES AFFECTING SUBSYSTEM RELIABILITY

No.	Automotive Failure Situation	Typical Process	Human Error Cause	Importance (1–5)	Priority Rank	MTTF (hr)	MTTR (hr)	MTBF (hr)	Failure Rate (1/hr)	Reliability (24 hr)	Preventive Guideline
8	Ignored abnormal noise / vibration	Presses, conveyors	Habituation to abnormal conditions	4	High	72	0.1	72	0.0139	0.716	Early-warning dashboards and reporting
9	Repetitive minor defects	Final assembly	Reduced attention due to repetition	3	Medium	90	0.1	90	0.0111	0.766	Job rotation and fatigue management
10	Reactive maintenance behavior	All machinery	Experience replaces condition monitoring	4	High	360	5	360	0.0028	0.935	Condition-based maintenance indicators

TABLE VIII
IMPORTANCE SCALE DEFINITION FOR HUMAN ERROR PREVENTION

Score	Importance Level	Definition	Typical Impact in Manufacturing
5	Critical	Errors that can immediately cause severe quality defects, safety hazards, regulatory non-compliance, or major production shutdowns	Line stoppage, safety incidents, recalls, major equipment damage
4	High	Errors that significantly degrade product quality or system reliability and require corrective action, but do not cause immediate shutdown	Rework, scrap increase, frequent downtime
3	Moderate	Errors that affect process stability or efficiency but are detectable and correctable within normal operations	Minor defects, reduced throughput
2	Low	Errors with limited impact on quality or performance and minimal operational disruption	Small efficiency loss, cosmetic defects
1	Very Low	Errors with negligible impact and no noticeable effect on system performance or safety	No measurable impact

TABLE IX
RELIABILITY-BASED INTERPRETATION OF IMPORTANCE

Importance	Failure Rate (λ, 1/h)	24-h Reliability	Interpretation
5	≥ 0.0050	≤ 0.88	Unacceptable risk; immediate preventive action required
4	0.0030-0.0049	0.88-0.92	High risk; prioritized mitigation needed
3	0.0015-0.0029	0.92-0.95	Manageable risk; monitoring and training recommended
2	0.0005-0.0014	0.95-0.98	Low risk; routine control sufficient
1	< 0.0005	> 0.98	Minimal risk; no additional action required

TABLE X
SUMMARY OF HUMAN ERRORS IN RELATION TO EDUCATIONAL PATHWAYS

Industry	Common Human Error Type	Underlying Skill Gap	Typical Education Background	Relative Error Risk
Automotive	Incorrect machine setup or torque application	Practical machine calibration skills	General Upper Secondary / Non-engineering Bachelor	High
Automotive	Delayed fault detection	Preventive maintenance knowledge	General Academic	Moderate–High
Automotive	SOP deviation during assembly	Procedural discipline and hands-on training	Vocational / TVET	Low
Agricultural (Starch/Cassava)	Incorrect dryer or separator settings	Process parameter interpretation	General Academic	High
Agricultural (Starch/Cassava)	Incomplete cleaning and sanitation	SOP compliance and hygiene training	Vocational / TVET	Low
Agricultural (Starch/Cassava)	Unnoticed vibration or wear	Early fault recognition	Technical Diploma / Engineering	Very Low

C. Summary of Human Errors in Relation to Educational Pathways

Table X shows that human errors differ by industry and are strongly related to skill gaps and educational background. In the automotive industry, tasks such as machine setup and torque application have a high risk of error when operators lack practical calibration skills. Delayed fault detection also shows moderate-to-high risk, indicating limited knowledge of preventive maintenance. In contrast, standard Operating Procedure (SOP) deviations during assembly carry lower risk, suggesting that vocational and TVET training supports strong procedural compliance.

In the agricultural (starch/cassava) industry, incorrect dryer or separator settings are high-risk errors, mainly because workers struggle to understand process parameters. However, cleaning and sanitation errors are less frequent when workers receive proper SOP and hygiene training. Early detection of machine vibration or wear poses very low risk when workers with technical or engineering backgrounds handle it. Overall, the results indicate that matching job tasks with appropriate skills and training can significantly reduce human error.

VIII. Conclusion

From a QFD/HoQ perspective, manufacturers and business owners represent the "customer," prioritizing stable production, preventive maintenance, safety compliance, and cost control. Therefore, human error prevention is not an individual-level issue but a system-level requirement that must translate into technical characteristics, particularly workforce skills and education pathways.

Comparative evidence from Thailand's automotive and agricultural sectors supports including worker skill specifications—such as preventive maintenance capability, SOP compliance, and process interpretation—as critical "HOWs" in the House of Quality. Aligning recruitment and training strategies with vocational and technical education pathways directly reduces human error and enhances long-term operational sustainability. This evidence reinforces the view that technical and vocational education pathways function as enabling specifications within the HoQ structure. By systematically linking manufacturer requirements (WHATs) to workforce competencies (HOWs), organizations can reduce reliance on corrective actions and move toward preventive, error-resilient manufacturing systems.

Acknowledgment

The authors sincerely thank the Industrial Engineering Laboratory, School of Manufacturing Systems and Mechanical Engineering, Sirindhorn International Institute of Technology (SIIT), Thammasat University, for providing the research instruments, facilities, and valuable technical assistance that significantly contributed to completing this paper. The first author also gratefully acknowledges the financial support provided by the Excellent Thai Student (ETS) Scholarship, awarded by Sirindhorn International Institute of Technology, Thammasat University. The authors thank Mr. Vacharatorn Kitaphanich, President and Member of the Executive Board and Director of Somboon Advance Technology Public Company Limited, for sharing his extensive experience in commercial operations, business development, and research and development in the automotive and advanced manufacturing sectors. His industry insights were instrumental in evaluating the advantages and limitations of EV tri-wheel vehicle development. The authors gratefully acknowledge Mr. Wichayut Kitaphanich, Business Development Manager of Somboon Advance Technology Public Company Limited, for his valuable technical support and professional collaboration on EC tri-motor vehicle systems, which substantially contributed to the successful completion of this research study. The authors also sincerely acknowledge Mr. Supavich Vongvivat, Founder of Smiling Mad Dog Co., Ltd., for his valuable contributions from a design and business development perspective. His insights into human error considerations and customer typologies are particularly important for new-to-trend and next-generation business development, and they provide a meaningful foundation for further studies in the beverage and agricultural-based raw material industries.

References

[1] O. M. E. S. Khayal, N. M. M. Nafea, K. Ameir, and M. A. Mohammed, "Mitigating human error in maintenance operations in flour milling, aviation, and maritime industries: A review," *Excellence J. Eng. Sci.*, vol. 2, no. 1, pp. 1-18, Feb. 2025.

[2] Y. Ngadiman, B. Hussin, N. A. Hamid, R. Ramlan, and L. K. Boon, "Relationship between human errors in maintenance and overall equipment effectiveness in food industries," in *Proc. 6th Annu. Int. Conf. Ind. Eng. Oper. Manage.,* 2016, pp. 2211-2224.

[3] V. B. Emroozi, M. Kazemi, M. Doostparast, and A. Pooya, "Improving industrial maintenance efficiency: A holistic approach to integrated production and maintenance planning with human error optimization," *Process Integr. Optim. Sustain.*, vol. 8, no. 2, pp. 539-564, Jun. 2024.

[4] H. Lüttenberg, C. Bartelheimer, and D. Beverungen, "Designing predictive maintenance for agricultural machines," in *Proc. 26th Eur. Conf. Inf. Syst. (ECIS)*, 2018, pp. 1-17.

[5] OECD, *OECD Skills Strategy Thailand: Assessment and Recommendations*. Paris, France: OECD Publishing, 2025, https://doi.org/10.1787/153a1fe6-en

[6] OECD, Vocational Education and Training in Thailand. Paris, France: OECD Publishing, 2021, https://doi.org/10.1787/cc20bf6d-en

[7] W. Y. Leong, "Artificial Intelligence, automation, and technical and vocational education and training: Transforming vocational training in digital era," *Eng. Proc.*, vol. 103, no. 1, Art. no. 9, Aug. 2025, https://doi.org/ 10.3390/engproc2025103009

[8] V. Rajalakshmi and B. Reshma, "A study on AI replace human in future," *Indian J. Tech. Educ.*, vol. 18, no. 1, Jan. 2024.

[9] "Power BI report," Microsoft Power BI, [Online]. Available: https://norrin.com/what-is-microsoft-power-bi [Accessed: Feb. 26, 2026].

[10] Office of the Vocational Education Commission, "ข้อมูลพื้นฐาน สอศ. [Basic Information of the Office of the Vocational Education Commission]," *Google Looker Studio* [Online]. Available: https://lookerstudio.google.com/u/0/reporting/145a3f16-912e-4027-be5b-c713803b75f0/page/aVDeD [Accessed: Feb. 26, 2026].

[11] M. Fargnoli, M. Lombardi, N. Haber, and D. Puri, "The impact of human error in the use of agricultural tractors: A case study research in vineyard cultivation in Italy," *Agriculture*, vol. 8, no. 6, Art. no. 82, Jun. 2018.

[12] N. Chalapati and S. Chalapati, "Building a skilled workforce: Public discourses on vocational education in Thailand," *Int. J. Res. Vocat. Educ. Train.* , vol. 7, no. 1, pp. 67-90, Apr. 2020.

[13] P. Tuenpusa, S. Boonpu, and P. Chaisuk, "Technical Vocational Education and Training (TVET) model in the disruptive technology era," *Acad. Strateg. Manag. J*., vol. 21, no. 2, pp. 1-14, Jan. 2022.

[14] K. Ariansyah. "Comparing labor market performance of vocational and general school graduates in Indonesia: Insights from stable and crisis conditions," *Empir. Res. Vocat. Educ. Train.*, vol. 16, no. 1, Art. no. 5, Apr. 2024, https://link.ospringer.com/article/10.1186/s40461-024-00160-6

[15] Y. Chen, S. Li, and R. Chen, "Impact of industry and education integration on employment quality in higher vocational colleges: Moderating role of faculty qualifications and curriculum development capacity," *Educ. Sci.*, vol. 15, no. 10, Art. no. 1316, Oct. 2025, https://www.mdpi.com 2227-7102/15/10/1316

[16] D. Verhaest, J. Lavrijsen, W. Van Trier, I. Nicaise, and E. Omey, "General education, vocational education and skill mismatches: Short-run versus long-run effects," *Oxford Econ. Papers*, vol. 70, no. 4, pp. 974-993, Oct. 2018, https://doi.org/10.1093/oep/gpy026

[17] F. Musavi, R. Hekmatshoar, M. Fallahi, et al., "Identifying and preventing human error in the sugar production process: A multi-stage approach using HTA, HEC and PHEA techniques," *Heliyon*, vol. 10, no. 9, Art. no. e29687, Apr. 2024, https://doi.org/10.1016/j.heliyon.2024.e29687

[18] U. Paman, Khairizal, and S. Sutriana, "Field investigation of component failures for selected farm machinery used in small rice farming operations," *Open Agric.,* vol. 9, no. 1, Art. no. 20220292, Jan. 2024, https//doi.org/10.1515/opag-2022-0292

[19] P. Tsarouhas, "Reliability, availability and maintainability analysis in food production lines: A review," *Int. J. Food Sci. Technol.*, vol. 47, no. 11, pp. 2243-2251, Nov. 2012, https://doi.org/10.1111/j.1365-2621.2012.03073.x

[20] M. Nkosi, K. Gupta, and M. P. Mashinini, "Causes and impact of human error in maintenance of mechanical systems," *MATEC Web Conf.*, vol. 312, Art. no. 05001, 2020, https://doi.org/10.1051/matecconf/202031205001

[21] V. B. Emroozi, M. Kazemi, and M. Doostparast, "Enhancing industrial maintenance planning: Optimization of human error reduction and spare parts management," *Oper. Res. Perspect.*, vol. 14, Art. no. 100312, Dec. 2025.

[22] T. Zhao, T. Li, D. Liu, and Y. Luo, "Influential factors and interventions for repeated production violations in food enterprises: Empirical evidence from China," *J. Clean. Prod.*, vol. 447, Art. no. 141421, Apr. 2024, https://doi.org/10.1016/j.jclepro.2024.141421

[23] T. Sa-Nguanmanasak and B. Khampirat, "Comparing employability skills of technical and vocational education students of Thailand and Malaysia: A case study of international industrial work-integrated learning," *J. Tech. Educ. Train.*, vol. 11, no. 3, pp. 94-109, 2019, https://doi.org/10.30880/jtet.2019.11.03.012

[24] S. Tarat and T. Sindecharak, "The vocational education system in Thailand and Singapore: A sociological perspective," *Thammasat Rev.*, vol. 23, no. 2, pp. 192-211, Dec. 2020.

[25] OECD, Vocational Education and Training in Thailand, OECD Reviews of Vocational Education and Training. Paris, France: OECD Publishing, 2021, https://doi.org/10.1787/cc20bf6d-en

[26] S. Wongmonta, "Revisiting the wage effects of Vocational Education and Training (VET) over the life cycle: The case of Thailand," *Int. J. Educ. Dev.*, vol. 103, Art. no. 102886, Nov. 2023, https://doi.org/10.1016/j.ijedudev.2023.102886

[27] Thaisangcharoen Service Co., Ltd., *Short Trim Line Problem Analysis Report*, Jan. 25, 2023.

[28] OECD, "Improving access and quality of vocational education and training in Thailand," in Vocational Education and Training in Thailand. Paris, France: OECD Publishing, Jul. 2021, ch. 2. [Online]. Available: https://www.oecd.org/.en/publications/vocational-education-and-training-in-thailand_cc20bf6d-en/full-report/improving-access-and-quality-of-vocational--education-and-training-in-thailand_e6d52cbe.html_

[29] A. H. Farooqui, P. Bergagård, P. Falkman, and M. Fabian, "Error handling within highly automated automotive industry: Current practice and research needs," in *Proc. IEEE Int. Conf. Emerg. Technol. Factory Autom.* (ETFA), Sep. 2016, pp. 1-4, https://ieeexplore.ieee.org/document/7733628

[30] Wikipedia contributors, "2009-2011 Toyota vehicle recalls," *Wikipedia, The Free Encyclopedia*. [Online]. Available: https://en.wikipedia.org/wiki/2009%E2%80%932011_Toyota_vehicle_recalls [Accessed: Dec. 17, 2025].

[31] K. B., "Human error: A persistent challenge in manufacturing operations!" *Plutomen*, 2024. [Online]. Available: https://pluto-men.com/human-error-persistent-challenge-manufacturing-operations/ [Accessed: Dec. 17, 2025].

[32] M. Watanabe and K. Sakai, "Investigation by driving simulation of tractor overturning accidents caused by steering instability," *arXiv preprint arXiv:2101.03270*, Jan. 2021, https://doi.org/10.48550/arXiv.2101.03270

[33] D. D. Bochtis, C. G. Sørensen, and P. Busato, "Advances in agricultural machinery management: A review," *Biosyst. Eng.*, vol. 126, pp. 69-81, Oct. 2014, https://doi.org/10.1016/j.biosystemseng.2014.07.012

[34] Purdue University, "Frequently asked questions about flowing grain entrapment, grain rescue and strategies, and grain entrapment prevention measures," 2011. [online] https://www.extension.entm.purdue.edu/grainlab/content/pdf/QuestionFlowingGrainEntrap.pdf

[35] N. G. Rupp, "The attributes of a costly recall: Evidence from the automotive industry," *Rev. Ind. Organ.*, vol. 25, no. 1, pp. 21-44, 2004, https://doi.org/10.1023/B:REIO.0000040514.22968.e1

[36] J. Ni and X. Huang, "Discovery-to-recall in the automotive industry: A problem-solving perspective on investigation of quality failures," *J. Supply Chain Manag.*, vol. 54, no. 2, pp. 71-95, Apr. 2018, https://doi.org/10.1111/jscm.12160
[37] I. Melinda, A. Ahadiat, and A. Ahmad, "Analysis of quality control of tapioca flour products at PT Gunung Sugih," *Int. J. Multidiscip. Sci.*, vol. 2, no. 2, pp. 34-38, Jun. 2023, https://doi.org/10.56127/ijml.v2i2.706
[38] B. Mikolo, M. Elenga, and K. Tsoumou, "Causes of quality defects in cassava-based food production: An Ishikawa diagram analysis," *World J. Adv. Res. Rev.*, vol. 24, no. 1, pp. 750-758, Oct. 2024, https://doi.org/10.30574/wjarr.2024.24.1.2856
[39] C. Park, D. Moon, N. Do, and S. M. Bae, "A predictive maintenance approach based on real-time internal parameter monitoring," *Int. J. Adv. Manuf. Technol.*, vol. 85, pp. 623-632, May 2016, https://doi.org/10.1007/s00170-015-7981-6
[40] M. Uppal, D. Gupta, N. Goyal, A. L. Imoize, A. Kumar, S. Ojo, S. K. Pani, Y. Kim, J. Choi, and M. A. Khanesar, "A real-time data monitoring framework for predictive maintenance based on the Internet of Things," *Complexity*, vol. 2023, Art. no. 9991029, Apr. 2023, https://doi.org/10.1155/2023/9991029
[41] B. Einabadi et al., "Dynamic predictive maintenance," *IFAC-Papers OnLine*, vol. 52, no. 13, pp. 1069-1074, Jan. 2019.
[42] D. Giordano et al., "Data-driven strategies for predictive maintenance: Lesson learned from an automotive use case," *Comput. Ind.*, vol. 134, Art. no. 103554, 2022, https://doi.org/10.1016/j.compind.2021.103554
[43] Y. -C. Fu, L. Dai, and B. B. Yang, "Microwave finish drying of (tapioca) starch pearls," *Int. J. Food Sci. Technol.*, vol. 40, no. 2, pp. 119-132, Feb. 2005, https://doi.org/10.1111/j.1365-2621.2004.00898.x
[44] B. O. Akintunde and T. Y. Tunde-Akintunde, "Effect of drying method and variety on quality of cassava starch extracts," *Afr. J. Food Agric. Nutr. Dev.*, vol. 13, no. 5, pp. 8351-8367, Dec. 2013, https://doi.org/10.18697/ajfand.60.9965
[45] I. A. Memon et al., "Defect reduction with the use of seven quality control tools for productivity improvement at an automobile company," *Eng. Technol. Appl. Sci. Res.,* vol. 9, no. 2, pp. 4044-4047, Apr. 2019, https://doi.org/10.48084/etasr.2634



Wichapol Chanchiewvichai received his B.Eng. with First-Class Honors from the Industrial Engineering Program, School of Manufacturing Systems and Mechanical Engineering (MSME), Sirindhorn International Institute of Technology (SIIT), Thammasat University, Thailand. He also earned a Master of Engineering in Logistics and Supply Chain Systems Engineering (LSCSE) from the same institute. He is currently pursuing a Ph.D. degree, supported by the Excellent Thai Student (ETS) Scholarship provided by SIIT. His research interests include machine design and development, energy efficiency, process improvement, and cost analysis.



Suchada Rianmora is a lecturer in the School of Manufacturing Systems and Mechanical Engineering (MSME), Sirindhorn International Institute of Technology, Thammasat University, Thailand. She received her D.Eng. from the Asian Institute of Technology, Thailand. Her research interests are reverse engineering, rapid prototyping, image processing, industrial instruments and control systems, design and development, design for manufacture and assembly, maintenance engineering, and manufacturing processes.



Thiti Mahaboonpachai received his B.Eng. (First Class Honors) in Civil Engineering from the Sirindhorn International Institute of Technology (SIIT), Thammasat University, Thailand, and earned his M.Eng. And Ph.D. in Civil Engineering from the University of Tokyo, Japan, under Japanese Government (MEXT) Scholarships.

He is currently the Director of Pakdee College of Commerce and Technology Vocational College, Kamphaeng Phet Province, serves as the Chairman of the Kamphaengphet Chamber of Commerce (as of late 2025), and is the Secretary of the Association of Private Colleges of Technology and Vocational Education of Thailand under the Patronage of Her Royal Highness Princess Maha Chakri Sirindhorn. His research interests include vocational education policy, dual education systems, structural engineering design, and applied mechanics.



Chatchai Vorathanawat is the Managing Director of Thaisangcharoen Service Co., Ltd. (TSS), Thailand. He received his B.Eng. in Industrial Engineering from the School of Manufacturing Systems and Mechanical Engineering (MSME), Sirindhorn International Institute of Technology (SIIT), Thammasat University, Thailand. He completed additional studies at ISI School, Japan, earning a Level 2 Certificate from the International Study Institute, and participated in an internship and scholarship program with AOTS (The Association for Overseas Technical Cooperation and Sustainable Partnerships). He has extensive expertise in collaborative business development in the automotive, agricultural, and electric vehicle (EV) bus industries. He is the exclusive distributor in Thailand of the Farizon Electric Bus, developed by Farizon, a commercial vehicle brand under Geely Holding Group**,** as well as the CJNOO EV charger for community-based charging station development.



Sirawich Chanchiewvichai received his B.Eng. with first-class honors from the Industrial Engineering Program at the School of Manufacturing Systems and Mechanical Engineering (MSME), Sirindhorn International Institute of Technology, Thammasat University, Thailand. He also completed a Master of Engineering in Logistics and Supply Chain Systems Engineering (LSCSE) from the same institute. His research interests encompass machine design and development, process improvement, instrumentation and control systems, finite element analysis, and cost analysis.

Image Analysis for Hen Egg Classification and Size Estimation

Supawadee Chaivivatrakul[1*] and Jednipat Moonrinta[2]
[1]Smart Engineering Agriculture Program, Faculty of Agriculture, Ubon Ratchathani University, Warin Chamrap, Ubon Ratchathani, Thailand
[2]Asian Institute of Technology, Klong Luang, Pathumthani, Thailand
E-mail: supawadee.c@ubu.ac.th*, jednipat.moonrinta@ait.asia

Received: July 11, 2025 / Revised: November 17, 2025 / Accepted: February 2, 2026

***Abstract*—Egg size and shape are critical parameters in the poultry industry's quality grading and consumer assessment. This study presents an automated image-based system to classify and estimate hen egg size, improving quality control and operational efficiency. We assembled a dataset of 150 hen eggs under Thai agricultural standards. We employed two primary image processing techniques: binary thresholding and maximum likelihood. Binary thresholding segmented egg images based on pixel intensity values, while the maximum likelihood approach—utilizing the HSV (Hue, Saturation, and Value) color space—effectively discriminated egg regions from the background. For geometric analysis, least-squares ellipse fitting and RANSAC (Random Sample Consensus) algorithms were applied to estimate egg dimensions. The classification results showed that binary thresholding achieved true positive rates of 95% and 94% on the training and test datasets, respectively, at a threshold of 0.55. The maximum likelihood method outperformed this approach, achieving classification true positive rates of 97% and 96% on the training and test datasets, respectively. Shape estimation also demonstrated high reliability, with accuracies exceeding 95% and reaching above 98%. These findings suggest that the proposed system is both accurate and practical for automated egg quality assessment in industrial settings.**

***Index Terms*—Classification, Detection, Egg Size, Segmentation, Shape**

I. Introduction

In the modern poultry industry, grading is a fundamental mechanism for improving production efficiency and ensuring product quality, making effective detection and classification systems essential to secure market value and satisfy consumers. These tasks have been performed manually, are labor-intensive and time-consuming, and are prone to subjective variability, which undermines quality control. While an alternative mechanical grading system offers a more accurate, consistent, and faster method, it increases the risk of egg damage, affecting product quality [1], [2].

The industry has sought appropriate quality-control technology, and one non-destructive approach is image processing. Researchers have applied this method effectively across various procedures and platforms [3]. One study compared a machine learning algorithm and image processing to classify white egg size. The decision tree returned the highest result on their dataset [4]. Another study proposed a method to predict egg surface area and volume. Image analysis was used to obtain egg area, and an artificial neural network and regression were used to predict the results [5]. The modern deep learning approach was adopted and applied to single-view images to analyze and return the major and minor axes of the dataset. They used a complex algorithm that required significant resources and returned highly accurate results [6]. An introduction of a non-destructive method to calculate the volume and surface area of avian eggs using two-dimensional digital imaging and image processing. They proposed a method to transform the egg's contour into standard geometric shapes (sphere, ellipsoid, or egg-shaped ovoid), then apply established geometric formulas based on image-derived measurements (egg length and projected area) [7]. Another study by this research group developed universal mathematical formulas to calculate the volume and surface area of eggs of various shapes. To the previous weakness of precise mathematical descriptions for complex shapes, especially pyriform (pear-shaped) eggs. The proposed method analyzed a progression of egg shapes from spheres to ovoid and pyriform forms, and derived equations applicable to all avian egg geometries. The outcome produced universal formulas suitable for precise, nondestructive measurement. This work is valuable for ornithology, evolutionary biology, and the poultry industry. Supports improved breeding,

incubation, and quality [8]. Previous studies showed that image processing and machine learning have high potential to predict egg size with high accuracy. This study proposes an automatic method for classifying and estimating hen egg shape to achieve high accuracy and computational efficiency. Moreover, the proposed method has less impact on the eggs. Egg size is strongly related to weight standards and can be used to cross-check quality control. An image analysis pipeline combines detection and classification using binary thresholding and maximum likelihood approaches, with accurate dimensional estimates using an elliptical fitting algorithm based on RANSAC (Random Sample Consensus).

II. Materials and Methods

This section outlines the procedures and techniques employed to develop an automated system for hen egg detection, classification, and size estimation using image processing methods. The workflow includes collecting and preparing a dataset of hen egg images, followed by two approaches—binary thresholding and the maximum likelihood method—for egg detection. Next, the system classifies eggs by pixel count and estimates their geometric dimensions using ellipse-fitting techniques. Each stage was designed to ensure computational efficiency, accuracy, and applicability to real-world conditions in poultry production environments. Fig. 1 shows the system overview.

A. Datasets

We collected a dataset of 150 hen eggs and categorized them into five standard size classes—No. 0 through No. 4—based on the Thai agricultural standard for egg grading [9]. Each class contained 30 eggs, resulting in a balanced dataset.

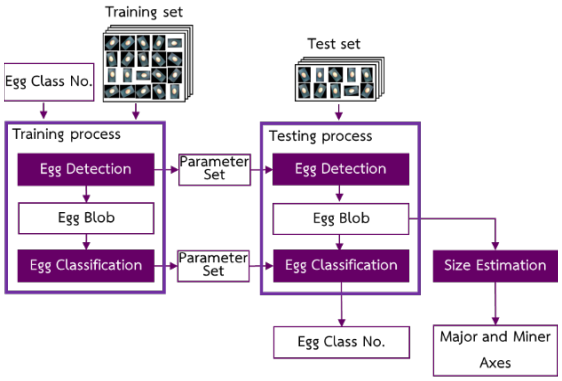

Fig. 1. System overview

For each class, 20 eggs (66.67%) were allocated to the training set and 10 eggs (33.33%) to the test set, ensuring consistent class representation across both subsets for reliable model training and evaluation (Table I). This simple proposed method requires a small dataset to demonstrate the solution, reducing computation cost and improving efficiency.

Hen egg standard in Thailand, No. 0, jumbo size, weight more than 70 g., No. 1 extra-large size, weight more than 65 g. to 70 g., No. 2 large size, weight more than 60 g. to 65 g., No. 3 medium size weight more than 55 g. to 60 g., No. 4 small size weight more than 50 g. to 55 g, and No. 5 pewee size weight more than 45 g. to 50 g. [9].

For the dataset of 150 hen egg images, each egg was taken as an image from the same angle; then the image was rotated 1- 180 degrees randomly and rescaled to get 4 datasets as 320×180 px, 160×90 px, 80×45 px, and 40×23 px, as shown in Fig. 2.

TABLE I
Dataset Proportion

Egg No.	Images in the Dataset		
	Training Set	**Test Set**	**Total**
0	20 eggs (66.67%)	10 eggs (33.33%)	30 eggs (100.00%)
1	20 eggs (66.67%)	10 eggs (33.33%)	30 eggs (100.00%)
2	20 eggs (66.67%)	10 eggs (33.33%)	30 eggs (100.00%)
3	20 eggs (66.67%)	10 eggs (33.33%)	30 eggs (100.00%)
4	20 eggs (66.67%)	10 eggs (33.33%)	30 eggs (100.00%)
Total	**100 Eggs (66.67%)**	**50 Eggs (33.33%)**	**150 Eggs (100.00%)**

B. Egg Detection

We provide 2 methods for egg detection: Binary thresholding and maximum likelihood, adopted from Chaivivatrakul [10].

1) Binary Thresholding

The binary thresholding steps include inputting an original color image, converting it to a binary image, applying a closing operation, and performing a connected-component step. Fig. 3 shows a sample output of each step.

2) Maximum Likelihood

In the maximum likelihood method, pixel values are used to calculate posterior values based on the HSV (Hue, Saturation, and Value) color model for foreground and background, as in equation (1) [11]. Fig. 4 shows a sample output of each step: Input an image, posterior calculation to return egg pixels, closing operation, and connected component.

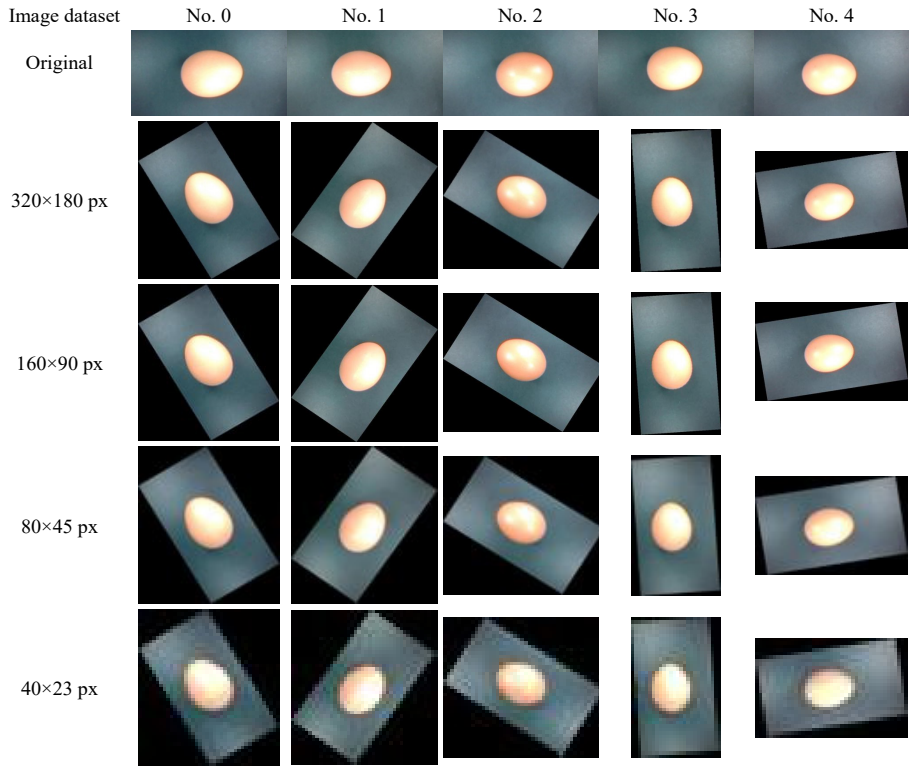

Fig. 2. Sample images of the 4 datasets

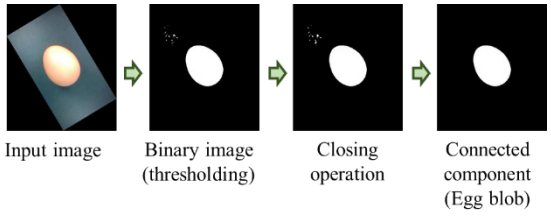

Fig. 3. Binary thresholding steps

$$P(E|x) = \frac{P(x|E)P(E)}{P(x)} \quad (1)$$

$P(E|x)$ is the probability of an egg pixel given a point x. $P(x|E)$ is the probability of a point x given an egg pixel. $P(E)$ is the probability of an egg pixel. $P(x)$ is the probability of a point x.

C. Egg Classification

Egg classes include No. 0, No. 1, No. 2, No. 3, and No. 4. The number of pixels from the detection result is used to assign egg class No. based on equations (2)-(5).

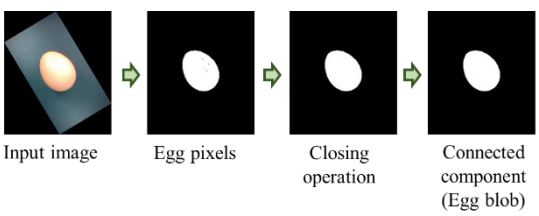

Fig. 4. Maximum likelihood steps

$$max_n = \frac{mintrain_{n+1} + maxtrain_n}{2} \quad (2)$$

$$min_n = \frac{mintrain_n + maxtrain_{n-1}}{2} \quad (3)$$

$$max_0 = maxtrain_0 \quad (4)$$

$$min_4 = mintrain_4 - 50 \quad (5)$$

n is a class No. min_n is the minimum number of pixels of class No. n in the training set. max_n is the maximum number of pixels of class No. n in the training set. $mintrain_n$ is the minimum number of pixels of class No. n in the training set. $maxtrain_{n-1}$ is the maximum number of pixels of class No. n-1 in the training set.

Formulas for classification evaluation values, the true positive rate (TP rate), the false negative rate (FN rate), the true negative rate (TN rate), the false positive rate (FP rate), Accuracy, Precision, Recall, and F-score, are provided in equations (6)-(13).

$$TP\ rate = \frac{TP}{TP+FN} \times 100 \quad (6)$$

$$FN\ rate = \frac{FN}{TP+FN} \times 100 \quad (7)$$

$$TN\ rate = \frac{TN}{TN+FP} \times 100 \quad (8)$$

$$FP\ rate = \frac{FP}{TN+FP} \times 100 \quad (9)$$

$$Accuracy = \frac{TP+TN}{TP+FN+TN+FP} \times 100 \quad (10)$$

$$Precision = \frac{TP}{TP+FP} \quad (11)$$

$$Recall = \frac{TP}{TP+FN} \quad (12)$$

$$F - score = 2 \times \frac{Precision \times Recall}{Precision + Recall} \quad (13)$$

TP is true positive, TN is true negative, FP is false positive, FN is false negative.

D. Size Estimation

We estimate the major and minor axes to estimate size. Based on the symmetrical ellipsoid assumption for egg shape, the ellipse fitting is applied to search for the major and minor axes. Algorithm 1 and Fig. 5 show the ellipse-fitting algorithm. We modified the implementation from the MATLAB File Exchange [12], [13]. Equations (14)-(17) provide the size-estimation formula.

Algorithm 1. Ransac-Ellipse-Fitting

Input: I_e: egg mask image
Output: a: major axis length
b: minor axis length
1: P_e ←SAMPLING-EGG-EDGE-POINTS(I_e,5)
2: ▶sampling 5 points on the edge of the egg mask image
3: E_j←LEAST-SQUARE-ELLIPSE-FITTING(P_e)
4: ▶j is the loop number; E_j is an ellipse for loop j
5: d_j←DISTANCE-ERROR(E_j ,P_e)
6: ▶the average perpendicular distance of all edge points P_e to the ellipse E_j
7: If d_j > 0.5 and loop j < 80
8: Go to step 1
9: If d_j <= 0.5
10: E_t←E_j
11: ▶ E_t is the taken ellipse
12: If loop j = 80
13: E_t← E_s
14: ▶E_s is the smallest average perpendicular distance ellipse
15: a, b←MAJOR-MINOR-AXIS(E_t)
16: return a,b

$$l = \frac{1}{2}\left(\frac{\sum_{e=1}^{n}\frac{h_e}{a_e}}{m} + \frac{\sum_{e=1}^{n}\frac{w_e}{b_e}}{m}\right) \quad (14)$$

$$k_e = a_e \times l \quad (15)$$

$$v_e = b_e \times l \quad (16)$$

$$r_e = \frac{k_e}{v_e} \quad (17)$$

l is the pixel size in millimeters. h_e is the height or major axis of egg e in millimeters. w_e is the width or minor axis of egg e in millimeters. a_e is the estimated ellipse major axis in pixels of egg e. b_e is the estimated ellipse minor axis in pixels of egg e. n is the number of data. k_e is the estimated egg major axis in millimeters of egg e. v_e is the estimated egg minor axis in millimeters of egg e. r_e is the estimated aspect ratio (major axis / minor axis) in millimeters of egg e.

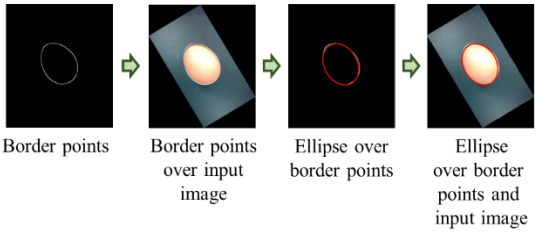

Fig. 5. RANSAC ellipse fitting steps

III. Results

The following subsections present the detection and classification results for binary thresholding and maximum likelihood, as well as the size estimation results. We chose the TP rate as the main criterion for this multi-class classification to avoid unbalanced learning effects across classes.

A. Binary Thresholding

We used the 320×180 px dataset, the highest resolution among the 4 collected datasets, and tested different threshold settings. We set the threshold to 0.50, 0.55, 0.60, 0.65, and 0.70, the disk-structure element radius to 2, and the minimum number of pixels in a connected component to 400 px.

We use image intensity to segment the background and the object. We use a grid search to find an appropriate intensity threshold, and since the 0.05 interval yields different results, we use this interval for the experiment.

Fig. 6 shows the detection sample results for binary thresholding. We evaluated the binary thresholding method at five threshold values (0.50, 0.55, 0.60, 0.65, and 0.70) using a 320×180 px dataset. Table II presents the classification results for both training and test sets, including TP rate, FN rate, TN rate, FP rate, accuracy, precision, recall, and F-score. The results show a marked improvement as the threshold increased from 0.50 to 0.55, with true positive rates rising from 27.00% to 95.00% on the training set and from 20.00% to 94.00% on the test set. A threshold of 0.55 yielded the highest overall true positive rate, making it the optimal setting for this dataset.

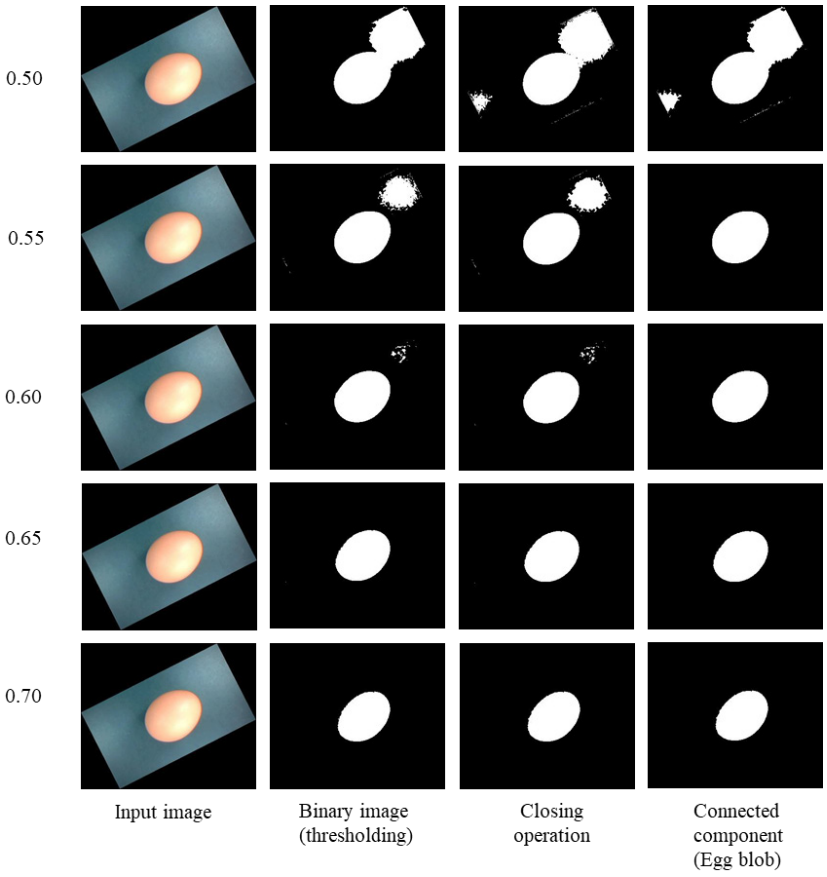

Fig. 6. Samples of the binary thresholding results with 5 threshold settings

TABLE II
CLASSIFICATION RESULTS OF BINARY THRESHOLDING ON 320×180 PX DATASET

Threshold		TP Rate (%)	FN Rate (%)	TN Rate (%)	FP Rate (%)	Accuracy	Precision	Recall	F-Score
0.50	Training Set	27.00	73.00	81.75	18.25	70.80	0.2700	0.2700	0.2700
	Test Set	20.00	80.00	80.00	20.00	68.00	0.2000	0.2000	0.2000
0.55	Training Set	95.00	5.00	98.75	1.25	98.00	0.9500	0.9500	0.9500
	Test Set	94.00	6.00	98.50	1.50	97.60	0.9400	0.9400	0.9400
0.60	Training Set	91.00	9.00	97.75	2.25	96.40	0.9100	0.9100	0.9100
	Test Set	90.00	10.00	97.50	2.50	96.00	0.9000	0.9000	0.9000
0.65	Training Set	83.00	17.00	95.75	4.25	93.20	0.8300	0.8300	0.8300
	Test Set	86.54	13.46	96.63	3.37	94.62	0.8654	0.8654	0.8654
0.70	Training Set	67.00	33.00	91.75	8.25	86.80	0.6700	0.6700	0.6700
	Test Set	74.00	26.00	93.50	6.50	89.60	0.7400	0.7400	0.7400

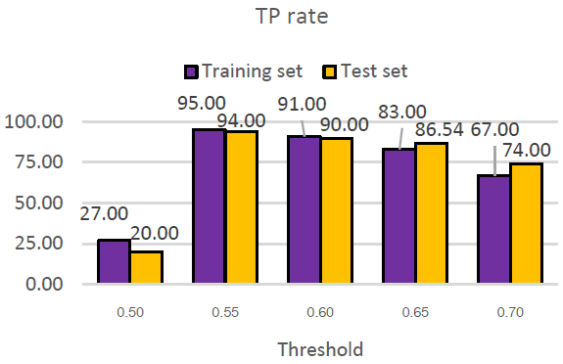

Fig. 7. TP rate of binary threshold classification results

As shown in Fig. 7, the classification TP rate began to decline beyond the 0.55 threshold. Specifically, the TP rate dropped to 91.00% at threshold 0.60, 83.00% at 0.65, and further declined to 67.00% at 0.70 for the training set. A similar pattern emerged in the test set, confirming that 0.55 represents a performance peak before over-segmentation or under-segmentation reduces the classifier's evaluation value.

Fig. 8 illustrates the confusion matrices for the binary threshold of 0.55. In both the training (Fig. 8a) and test (Fig. 8b) sets, the classifier shows strong diagonal dominance, indicating reliable class-specific predictions. Egg classes No. 0, No. 1, and No. 2 showed the highest recognition rates, while some minor confusion was observed in distinguishing class No. 3 and No. 4. Due to the number of pixels of class No.3 and No.4 being close compared to class No.1 and No.2, this confusion was observed, suggesting room for improvement through additional feature extraction or post-processing refinement.

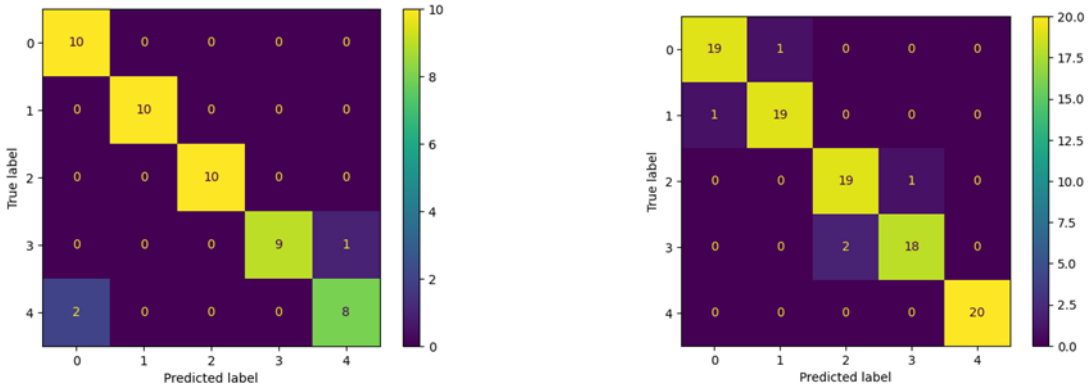

Fig. 8. Confusion matrix for the binary thresholding of 0.55 on a 320×180 px dataset (a) training set, (b) test set

B. *Maximum Likelihood*

We applied the maximum likelihood classification approach across four image resolutions: 320×180, 160×90, 80×45, and 40×23 pixels. Table III outlines the adaptive parameter sets used for each resolution, showing a decreasing disk-structure element radius and minimum pixel threshold as image resolution decreases. This scale-sensitive tuning ensured optimal region segmentation, enabling the model to balance between spatial detail and noise reduction.

TABLE III
PARAMETER SET FOR MAXIMUM LIKELIHOOD

Dataset	Radius for Disk-Structure Element	Minimum Pixel
320×180 px	4	200
160×90 px	2	100
80×45 px	1	50
40×23 px	1	25

Fig. 9 displays representative samples from the training dataset, showcasing the separability of egg and background pixels. Fig. 10 illustrates the visual results from the classification pipeline at each resolution. Table IV and Fig. 11 summarize the classification TP rate across datasets. At the highest resolution (320×180 px), the maximum likelihood method yielded an exceptional TP rate—97.00% for the training set and 96.00% for the test set. Performance declined gradually as resolution decreased, with test-set TP rates dropping to 86.00%, 78.00%, and 52.00% for 160×90, 80×45, and 40×23 px, respectively. Notably, egg Nos. 0, 1, and 4 consistently achieved high recognition rates across all resolutions, while Egg Nos. 2 and 3 performed worse, especially at lower resolutions.

Figs. 12-15 present the confusion matrices for each dataset. In the 320×180 px matrix (Fig. 12), the classification is highly accurate with minimal confusion across classes. As the resolution drops, the matrices for 160×90 px (Fig. 13), 80×45 px (Fig. 14),

and especially 40×23 px (Fig. 15), reveal increasing misclassifications, particularly between visually similar egg categories. This decline is attributed to information loss from resolution degradation, highlighting the maximum likelihood method's dependence on resolution.



(a) (b)

Fig. 9. Maximum likelihood, sample of training set for (a) egg pixels and (b) background pixels

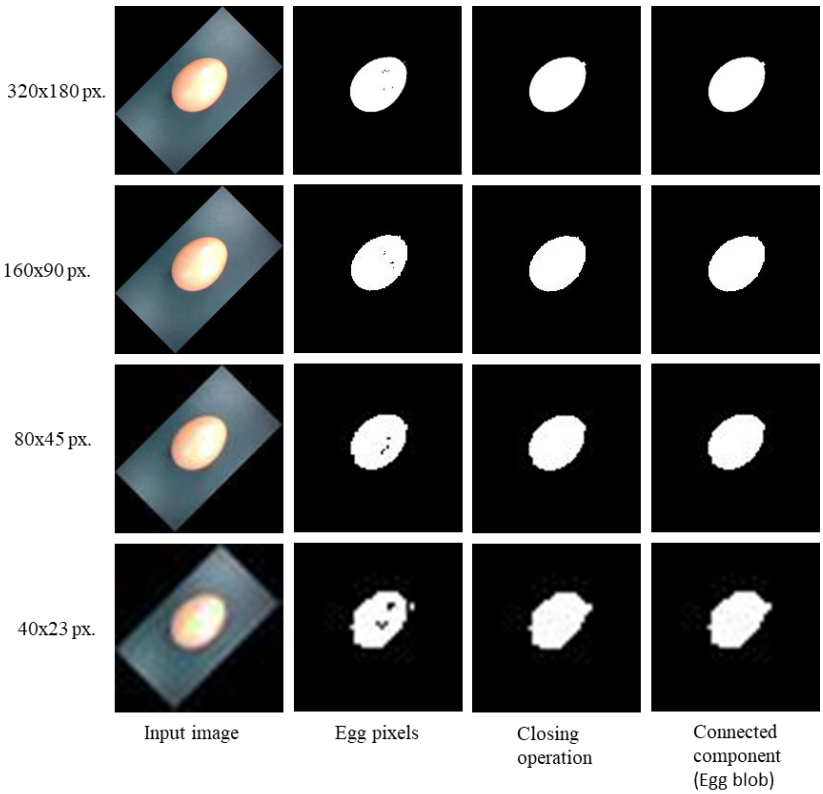

Fig. 10. Samples of the maximum likelihood results on 4 datasets

TABLE IV
CLASSIFICATION RESULTS OF MAXIMUM LIKELIHOOD ON 4 DATASETS

Dataset		TP Rate (%)	FN Rate (%)	TN Rate (%)	FP Rate (%)	Accuracy (%)	Precision	Recall	F-Score
320×180 px	Training set	97.00	3.00	99.25	0.75	98.80	0.9700	0.9700	0.9700
	Test set	96.00	4.00	99.00	1.00	98.40	0.9600	0.9600	0.9600
160×90 px	Training set	89.00	11.00	97.25	2.75	95.60	0.8900	0.8900	0.8900
	Test set	86.00	14.00	96.50	3.50	94.40	0.8600	0.8600	0.8600
80×45 px	Training set	83.00	17.00	95.75	4.25	93.20	0.8300	0.8300	0.8300
	Test set	78.00	22.00	94.50	5.50	91.20	0.7800	0.7800	0.7800
40×23 px	Training set	62.00	38.00	90.50	9.50	84.80	0.6200	0.6200	0.6200
	Test set	52.00	48.00	88.00	12.00	80.80	0.5200	0.5200	0.5200

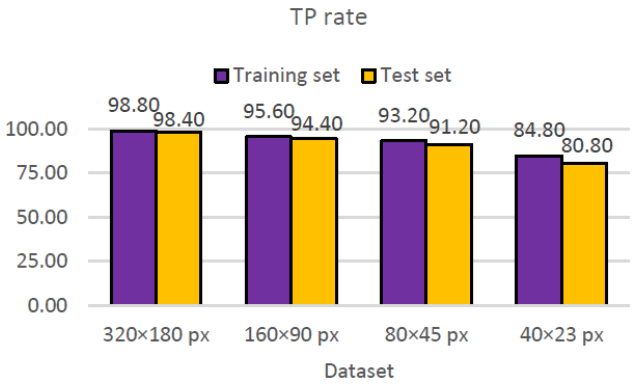

Fig. 11. Classification results of maximum likelihood

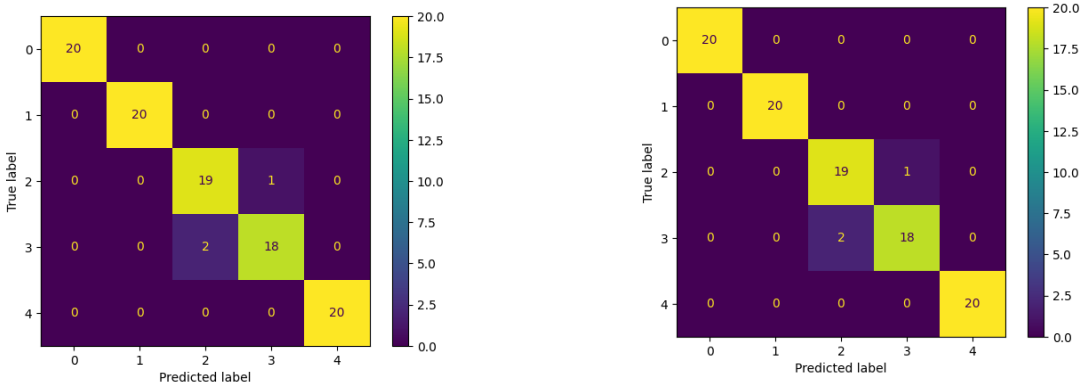

Fig. 12. Confusion matrix of 320×180 px dataset (a) training set, (b) test set

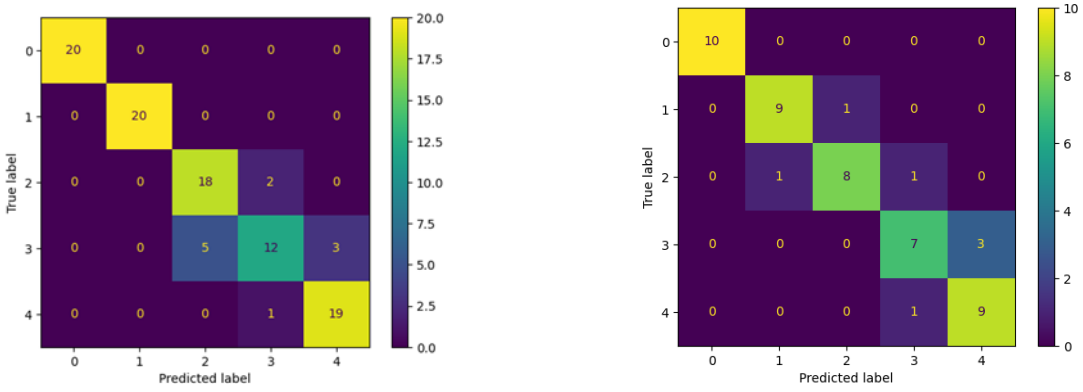

Fig. 13. Confusion matrix of 160×90 px dataset (a) training set, (b) test set

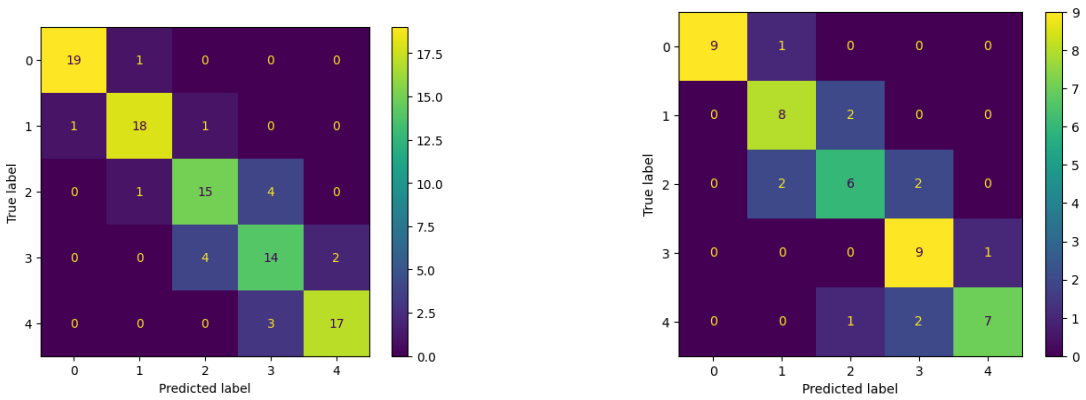

(a) (b)

Fig. 14. Confusion matrix of 80×45 px dataset: (a) training set, (b) test set

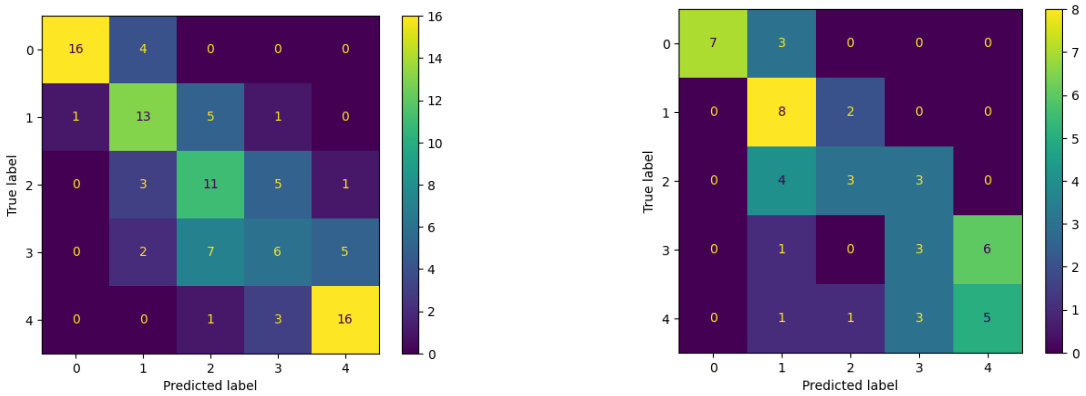

(a) (b)

Fig. 15. Confusion matrix of 40×23 px dataset: (a) training set, (b) test set

TABLE V
MAJOR AXIS AND MINOR AXIS RESULTS

Dataset	Accuracy Training Set			Accuracy Test Set		
	Major Axis	Minor Axis	Major Axis/ Minor Axis	Major Axis	Minor Axis	Major Axis/ Minor Axis
320×180 px	98.81	99.07	98.33	98.86	99.12	98.40
160×90 px	98.59	98.67	98.02	98.50	98.92	98.28
80×45 px	97.80	97.95	96.78	97.76	97.87	96.92
40×23 px	95.57	95.79	93.01	95.49	95.63	92.41

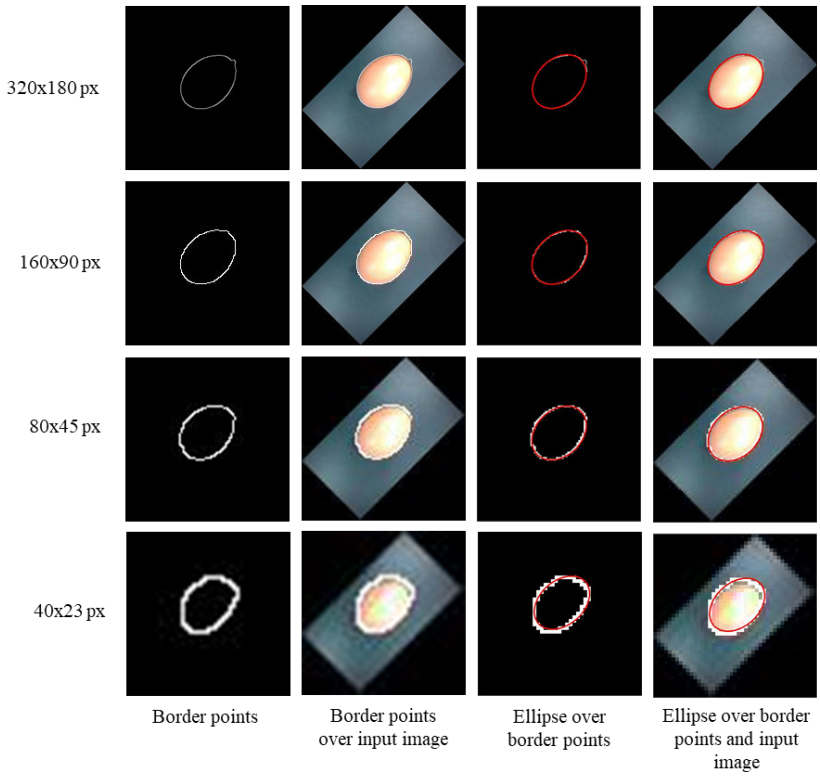

Fig. 16. Samples of the RANSAC ellipse-fitting results on 4 datasets

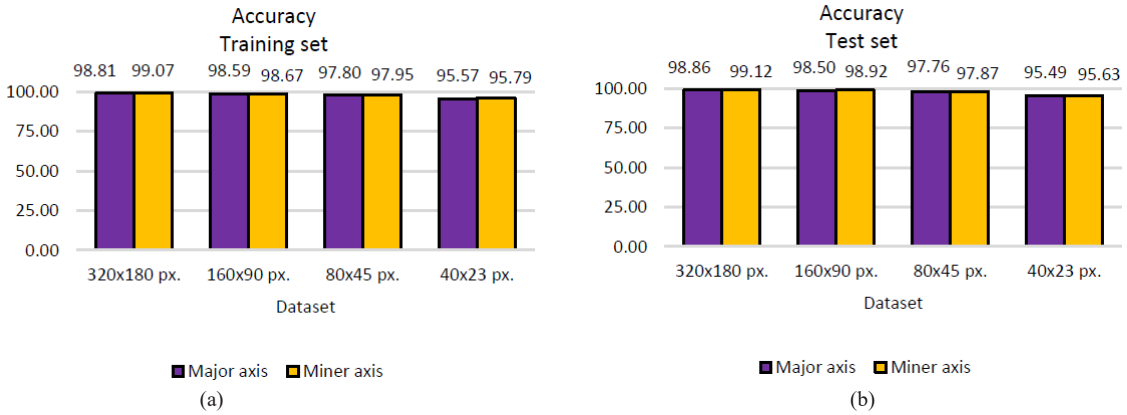

Fig. 17. Major axis and minor axis accuracy of ellipse fitting for the 320×180 px dataset (a) training set, (b) test set

IV. Conclusion and Discussion

In this paper, we looked at two main aspects of hen egg image analysis: binary thresholding and maximum likelihood estimation, which are used to detect and classify objects. We then applied RANSAC ellipse fitting to determine egg size. We assessed the accuracy, computational speed, and robustness of the methods by testing them on images at different resolutions.

Binary thresholding is a simple detection method with low processing overhead. The ideal threshold value of 0.55 yielded the most accurate results, with a TP rate of 95% for the training set and 94% for the test set. This shows that the background and foreground can be identified under the right conditions. Nevertheless, excessive or inadequate segmentation caused performance to deteriorate rapidly at suboptimal threshold levels, and the process relied heavily on the selected threshold. Because binary thresholding performs poorly when either the background or the lighting changes frequently, it should be used only where these factors are constant.

Maximum likelihood classification, on the other hand, worked better and could handle a wider range of shapes and lighting conditions. It performed better with a resolution of 320×180 px. The test set's TP rate was 96%, and the training set's was 97%. This dataset resolution also produced the best results across the other evaluation metrics: the highest TN

rate, accuracy, precision, recall, and F-score, and the lowest FP and FN rates. As resolution decreased, the TP rate dropped, although it stayed at 62% and 52% at 40×23 pixels, and the other evaluation values decreased similarly. Eggs were more likely to be assigned to the appropriate class for eggs No. 0, No. 1, and No. 4. Grouping classes with similar traits or slight differences, such as Nos. 2 and 3, was more challenging.

In applications requiring size estimation, the RANSAC ellipse-fitting method worked effectively. The accuracy of measurements on the major and minor axes was more than 98% at 320×180 px resolution. Even at the lowest resolution, accuracy remained above 95%. This illustrates that RANSAC can be used for real-time size estimation in embedded vision systems with constrained processing power and performs well with low resolution.

Overall, the results show that a key design challenge is balancing categorization strength with computational efficiency. Binary thresholding works well but is sensitive to parameter settings and cannot adjust automatically. Maximum probability approaches generalize more but require slightly more processing power. In contrast, shape estimates from RANSAC-based elliptical fitting are reliably precise and consistent. For this reason, it is useful for tasks like grading, sorting, and spotting errors.

Industries today need to balance usability, scalability, and performance in their image analysis systems. Because of their ease of use and low resource requirements, traditional computer vision techniques such as SIFT, SURF, template matching, and decision trees remain useful. As a result, they work well on the edge and in static environments [4]-[8], [14]. These typically cannot handle very complex problems.

However, deep learning methods such as Convolutional Neural Networks (CNNs), Vision Transformers (ViTs), and high-performance object detectors like YOLOv9 are the most accurate and versatile. On key benchmarks such as Cityscapes, COCO, and ImageNet, they perform well [15], [19]. They also reported strong results on an in-house collected agricultural dataset [20]. In real-time or embedded systems, they are rarely used because they require large amounts of memory, computational power, and labeled data [15], [16], [21], [22].

Hybrid approaches combine lightweight neural inference with classical preprocessing, such as quantized models or edge-optimized architectures, to address these limitations. These solutions are ideal because they enable real-time, scalable, and accurate visual inspection systems. When choosing a method, we need to consider latency, hardware limitations, data availability, and industry standards, especially in sectors like manufacturing and autonomous robots. This improves quality control and builds customer confidence.

Future studies will test the effectiveness of these strategies in a conveyor-based egg grading system to determine how well they perform in real factories. Adding additional egg types, sizes, and lighting conditions to the dataset will greatly improve the model's performance. Additionally, hybrid solutions that combine traditional image processing with novel deep learning architectures can enhance system accuracy and adaptability when resources are limited.

Acknowledgment

We thank the Faculty of Agriculture, Ubon Ratchathani University, and agricultural communities for supporting this research by providing facilities and resources.

References

[1] J. Alikhanov, Z. Shynybay, A. Moldazhanov, A. Kulmak-Hambetova, and P. Daskalov, "Machine control system operation for automatic sorting of eggs into categories," in *Proc. 5th Int. Sci. Congr. Agricultural Machinery*, 2017, pp. 222-226.

[2] I. Bagus, K. Dzinavatongaet, E. Chimana, and C. Mabuyaye, "Design and development of an IoT-based chicken egg sorting prototype based on egg weight," in *Proc. 3rd Conf. IDB Bali*, 2024, pp. 356-362.

[3] K. Limpadapun and T. Borirak, "Advancing industrial inspection through image processing techniques with OpenCV," *EAU Heritage Journal Science and Technology*, vol. 19, no. 1, pp. 63-76, Apr. 2025, https://he01.tci-thaijo.org/index.php/EAUHJSci/article/view/275593/186733

[4] D. M. Mendoza, R. G. De Luna, C. F. C. Navarro, M. R. Isada, L. Tuason, and J. M. P. Macadag-Um, "Standardized Sizing through Machine Learning (SML): Utilizing decision tree algorithm to classify white chicken egg sizes," in *Proc. IEEE Region 10 Humanitarian Technology Conf. (R10-HTC)*, 2024. pp. 66-71, https://doi.org/10.1109/R10-HTC59322.2024.10778850

[5] M. Sedghi and M. Ghaderi, "Digital analysis of egg surface area and volume: Effects of longitudinal axis, maximum breadth and weight," *Inf. Process. Agric.*, vol. 10, no. 2, pp. 229-239, Jun. 2023, https://doi.org/10.1016/j.inpa.2022.01.003

[6] C. Liu et al., "Single-view measurement method for egg size based on small-batch images," *Foods*, vol. 12, no. 5, Mar. 2023, https://doi.org/10.3390/foods12050936

[7] V. G. Narushin, G. Lu, J. Cugley, M. N. Romanov, and D. K. Griffin, "A 2-D imaging-assisted geometrical transformation method for non-destructive evaluation of the volume and surface area of avian eggs," *Food Control*, vol. 112, Jun. 2020, https://doi.org/10.1016/j.foodcont.2020.107112

[8] V. G. Narushin, J. P. Kent, A. Salamon, M. N. Romanov, and D. K. Griffin, "Density of egg interior: Looking inside an egg while keeping it intact," *Innov. Food Sci. Emerg. Technol.*, vol. 87, Jul. 2023, https://doi.org/10.1016/j.ifset.2023.103387

[9] National Bureau of Agricultural Commodity and Food Standards, *Thai Agricultural Standard (TAS 6702-2005): Hen egg*. Bangkok, Thailand: ACFS, 2005. [Online]. Available:https://faolex.fao.org/docs/pdf/tha166331.pdf

[10] S. Chaivivatrakul, "Automatic assessment of seed germination percentage," *Eng. J.*, vol. 24, no. 4, pp. 85-96, Jul. 2020, https://doi.org/10.4186/ej.2020.24.4.85

[11] K. P. Murphy, *Machine Learning: A Probabilistic Perspective*. Cambridge, MA, USA: MIT Press, 2012, pp. 1-1104.

[12] R. Brown, "fitellipse.m," *MATLAB Central File Exchange*, 2025. [Online]. Available: https://www.mathworks.com/matlabcentral/fileexchange/15125-fitellipse-m [Accessed Jun. 10, 2025].
[13] M. Arthington, "Distance from points to an ellipse," *MATLAB Central File Exchange*, 2025. [Online]. Available: https://www.mathworks.com/matlabcentral/fileexchange/26261-distance-from-points-to-an-ellipse [Accessed: Jun. 10, 2025].
[14] M. Isik, "Comprehensive empirical evaluation of feature extractors in computer vision," *Peer J Comput. Sci.*, vol. 10, p. e2415, Nov. 2024, https://doi.org/10.7717/peerj-cs.2415
[15] Y. Liu et al., "A survey of visual transformers," *IEEE Trans. Neural Netw. Learn. Syst.*, vol. 35, no. 6, 2024, https://doi.org/10.1109/TNNLS.2022.3227717
[16] R. Azad et al., "Advances in medical image analysis with vision transformers: A comprehensive review," *Med. Image Anal.*, vol. 91, Art. no. 103000, Jan. 2024, https://www.sciencedirect.com/science/article/pii/S1361841523002608
[17] C. -Y. Wang, I.-H. Yeh, and H. -Y. M. Liao, "YOLOv9: Learning what you want to learn using programmable gradient information," in *Proc. Eur. Conf. Comput. Vis. (ECCV)*, 2024, pp. 1-21.
[18] Z. Zong, G. Song, and Y. Liu, "DETRs with collaborative hybrid assignments training," in *Proc. IEEE Int. Conf. Comput. Vis. (ICCV)*, 2023, pp. 6748-6758.
[19] E. Xie, W. Wang, Z. Yu, A. Anandkumar, J. M. Alvarez, and P. Luo, "SegFormer: Simple and efficient design for semantic segmentation with transformers," in *Adv. Neural Inf. Process. Syst*., 2021, pp. 12077-12090.
[20] K. Orkphol, K. Satianpakiranakorn, J. Chaihuadjaroen, and T. Valeeprakhon, "A transfer learning-based deep convolutional neural network approach for white shrimp abnormality classification," *Int. Sci. J. Eng. Technol. (ISJET)*, vol. 8, no. 2, Dec. 2024.
[21] M. Tan and Q. V. Le, "EfficientNetV2: Smaller models and faster training," in *Proc. 38th Int. Conf. Mach. Learn. (ICML)*, 2021, pp. 10096-10106.
[22] Z. Luo, W. Yang, Y. Yuan, R. Gou, and X. Li, "Semantic segmentation of agricultural images: A survey," *Inf. Process. Agric.,* vol. 11, no. 2, pp. 172-186, Jun. 2024, https://www.sciencedirect.com/science/article/pii/S2214317323000112

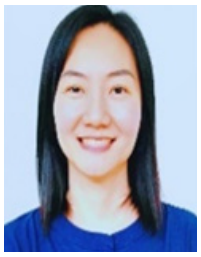

Supawadee Chaivivatrakul received the B.S. and M. S. degrees in computer science from Chiang Mai University, Chiang Mai, Thailand, in 1999 and 2003, respectively, and the Ph.D. in computer science from Asian Institute of Technology, Bangkok, Thailand, in 2014. She was a visiting scholar in Agriculture and Biosystems Engineering, Iowa State University, IA, USA, in 2010. She received a full scholarship from NSTDA for her Ph.D. Since 2005, she has been a lecturer in Information Technology for Agriculture and Rural Development and Smart Engineering Agriculture at the Faculty of Agriculture, Ubon Ratchathani University.



Jednipat Moonrinta received the B.Eng. degree in computer engineering from Chiang Mai University, Chiang Mai, Thailand, in 2008, and an M. Eng. Degree in computer science from Asian Institute of Technology (AIT), Pathumthani, Thailand, in 2010.

He worked as a research associate at the AIT Vision Lab from 2010 to 2015 before starting his doctoral studies. He is currently pursuing a Ph.D. degree in computer science at AIT and working at the AI Center. His research interests include computer vision, deep learning, and intelligent systems.

Increasing Efficiency in Pineapple Peeling Knife Sharpening through ECRS Principles

Pipat Lertkowit[1], Poom Jatunitanon[2], and Bundit Inseemeesak[3*]
[1]Faculty of Engineering, Thonburi University, Bangkok, Thailand
[2,3]Faculty of Engineering and Technology, Panyapiwat Institute of Management, Nonthaburi, Thailand
E-mail: pipatpop56@gmail.com, poomjat@pim.ac.th, banditins@pim.ac.th*

Received: March 1, 2026 / Revised: June 17, 2026 / Accepted: June 17, 2026

***Abstract*—This study aims to improve the grinding process of pineapple peeling knives by addressing repetitive and time-consuming procedures, particularly non-value-added activities. These include bottleneck delays, equipment setup inefficiencies, and the ineffective use of grinding wheels. To address these issues, the researcher applied the ECRS principle through two main approaches: (1) designing and constructing a work-holding device (JIG) to enable faster and more precise knife assembly and (2) improving the grinding process by reducing the number of grinding wheels from two to one and increasing the hardness specification of the grinding wheel, thereby enhancing grinding efficiency.**

As a result of improving the grinding process for pineapple peeling knives using the ECRS principle, processing time decreased from 151 minutes per unit to 86 minutes per unit, while the number of operational steps decreased from 17 to 9. Production capacity increased from 70 units per month to 123 units per month, grinding wheel consumption decreased from 140 units per month to 45 units per month, and grinding costs decreased from 22,400 THB per month to 7,200 THB per month.

***Index Terms*—Pineapple Peeling Knives, Grinding Process, Grinding Wheels, Sharpening, ECRS Principle, Work-holding Device (JIG)**

I. Introduction

The fruit processing industry is a key sector contributing to Thailand's economic growth, particularly the canned pineapple industry, where Thailand is highly competitive in the global market. According to data from the Office of Agricultural Economics, in 2023, Thailand ranked first in the global canned pineapple export market, accounting for 45% of total export value [1]. Maintaining this competitive advantage requires continuous development and improvement of production efficiency.

The pineapple processing industry is one of the key sectors contributing to Thailand's economy, particularly the canned pineapple industry, which demonstrates strong competitiveness in the global market. However, many manufacturing plants continue to face challenges related to production inefficiencies, operational delays, and high processing costs. These issues reduce productivity and limit long-term competitiveness.

The production process of canned pineapple generally consists of several sequential stages, including raw material procurement, washing and sorting, peeling and cutting, blanching and pretreatment, filling and syruping, sealing and sterilization, labeling and packaging, and storage and distribution. Each stage uses labour, machinery, and resources. Inadequate process management at any stage may cause excessive waste, longer production times, and higher operating costs.

From a lean manufacturing perspective, these inefficiencies are often linked to non-value-added activities and waste, including waiting time, unnecessary transportation, redundant processing, excess inventory, unnecessary motion, overproduction, and product defects. In canned pineapple production, significant waste often occurs in peeling operations, knife grinding and maintenance, machine setup, material handling, and filling processes. These inefficiencies extend lead times and reduce product quality.

To systematically address these issues, the application of the ECRS principle, consisting of Eliminate, Combine, Rearrange, and Simplify, provides a practical framework for process improvement. Unnecessary activities can be eliminated, related operations can be combined, process sequences can be rearranged to enhance workflow continuity, and complex procedures can be simplified through equipment modification and automation. Implementing ECRS reduces cycle time,

improves labor utilization, and enhances operational consistency.

Therefore, this study applies the ECRS principle to improve the production process of canned pineapple, with particular emphasis on grinding and maintenance operations for pineapple peeling knives. The objectives are to enhance operational efficiency, reduce processing time and costs, and increase overall productivity. The findings of this study are expected to provide practical guidelines for process improvement in fruit processing and related food industries facing similar operational constraints.

A. Objectives of Research

- To analyze the existing grinding process of pineapple peeling knives and identify repetitive, time-consuming, and non-value-added activities.
- To apply the ECRS principle in redesigning the grinding process through the development of a work-holding device (JIG) and the optimization of grinding wheel configuration and specifications.
- To reduce processing time and the number of operational steps in the knife grinding process.
- To evaluate the impact of ECRS-based process improvements on grinding efficiency and operational costs.

B. Research Hypothesis

- The application of the ECRS principle significantly reduces processing time in the grinding process of pineapple peeling knives.
- The implementation of a work-holding device (JIG) improves the accuracy and efficiency of knife assembly and grinding operations.
- The redesigned grinding process based on the ECRS principle reduces non-value-added activities and enhances overall process performance.

C. Scope of Research

- The scope of this research is focused on improving the grinding process of pineapple peeling knives in a selected canned pineapple processing factory for three months.
- The study is limited to the analysis and improvement of activities related to knife grinding.
- This research covers the evaluation of existing grinding procedures, identification of non-value-added activities, and application of the ECRS principle to redesign the process.
- The study evaluates process performance in terms of processing time, number of operational steps, production capacity, grinding wheel consumption, and grinding costs. Data are collected before and after the implementation of improvements for comparative analysis.

D. Benefits

- This study provides several practical and academic benefits to the pineapple processing industry and related manufacturing sectors
- The research contributes to improving operational efficiency by reducing processing time, minimizing non-value-added activities, and simplifying grinding procedures through the application of the ECRS principle**.**
- The development and implementation of a work-holding device (JIG) improves the accuracy and consistency of knife grinding operations.
- The proposed methodology serves as a practical guideline for continuous improvement initiatives.

E. Definition

- ECRS Principle means a systematic process improvement method consisting of Eliminate, Combine, Rearrange, and Simplify, used to reduce non-value-added activities and enhance operational efficiency.
- Work-holding device (JIG) means a specially designed fixture used to securely position and align pineapple peeling knives during grinding operations to improve accuracy and reduce setup time.
- Processing time means the total time required to complete one grinding cycle for a pineapple peeling knife, measured from the beginning of setup to the completion of grinding.
- Non-value-added activities mean operations that consume time and resources without directly contributing to product quality or customer value, for example, waiting, unnecessary movement, and repeated adjustments.
- Production capacity means the maximum number of pineapple peeling knives that can be processed within a specified period, measured in units per month.

II. Literature Review

In pineapple processing, peeling is a critical step that directly affects product quality and the level of raw material loss [2]. Therefore, sharp and standardized peeling knives are essential for enhancing production efficiency. A study by Ibiyeye et al. [3] reported that the quality of peeling knives influences pineapple flesh loss by approximately 15-20 % and has a direct impact on worker performance.

An investigation of the grinding process for pineapple peeling knives in the selected case-study factory identified three major issues affecting production efficiency. First, excessive time was lost in unnecessary grinding operations, which is

consistent with the findings of Kumar [4], who reported that waste reduction in manufacturing processes can improve efficiency by 20-30%. Second, inappropriate grinding wheel speed settings were observed; Kannan [5] indicated that optimal grinding parameters can extend grinding wheel service life by up to threefold. Third, significant time was consumed in workpiece alignment, a common problem in grinding operations [6].

A review of the literature indicates that the application of the ECRS principle (Eliminate, Combine, Rearrange, and Simplify) can effectively improve production efficiency. Suhardi et al. [7] reported that implementing ECRS in manufacturing industries can reduce production time by 30-40%. Furthermore, its integration with other quality improvement tools, for example, Overall Equipment Effectiveness (OEE) [8] and Six Big Losses analysis [9], contributes to systematic enhancements in operational performance.

This study focuses on the application of the ECRS principle to improve the grinding process of pineapple peeling knives, with the objectives of enhancing efficiency, reducing processing time, lowering costs, and increasing process productivity. The findings not only address existing issues in the current production process but also demonstrate potential applicability to other manufacturing operations in the fruit processing and broader food industries that face similar constraints and challenges. This contribution supports the need to respond effectively to rapid growth and evolving demands in the global food industry.

III. Methodology

A. *Pineapple Peeler Knife*

In the grinding process of pineapple peeling knives, the knife frame components are manufactured from SUS304 stainless steel and brass, as shown in Fig. 1 (a) and (b), respectively.

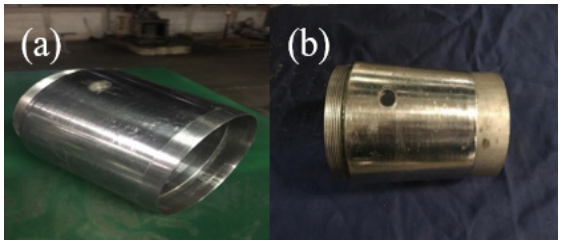

Fig. 1. Pineapple peeler knife, (a) SUS304 stainless steel and (b) brass

The blade components are made of S50C steel that has undergone a hardening process, resulting in a hardness value of 60 HRC. The hardened blades are subsequently assembled with the knife frames and then subjected to the grinding process to adjust their dimensions and geometry in accordance with the company's specified standards, as illustrated in Fig. 2.

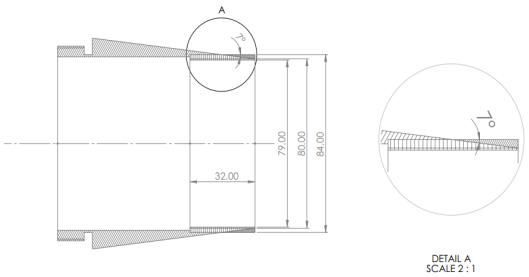

Fig. 2. Grinding specifications for pineapple peeling knives

B. *Grinding Machine*

The pineapple peeling knife grinding machine, as shown in Fig. 3, is designed to adjust the dimensions, geometry, and sharpness of the blades in accordance with specified production standards. Its operation is based on the coordinated function of seven main components, including the workpiece chuck, workpiece, rotational speed control system, grinding wheel, motor, grinding wheel turret, and belt–pulley system.

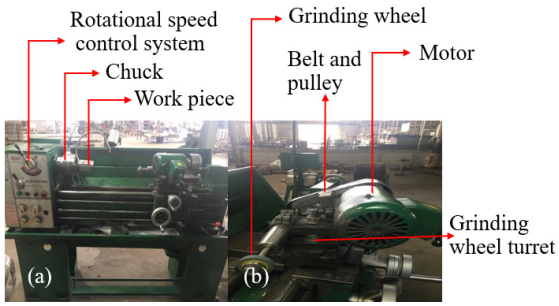

Fig. 3. Grinding machine, (a) Front view and (b) Side view

During operation, the assembled pineapple peeling knife is first secured on the workpiece chuck to ensure proper alignment and stability. This secure positioning minimizes vibration and prevents unwanted movement during the grinding process, thereby improving dimensional accuracy and surface quality. The workpiece, which consists of a hardened steel blade attached to its supporting frame, is positioned to allow both internal and external surfaces to be processed effectively.

The rotational speed control system regulates the rotational speed of the grinding wheel according to the specific grinding requirements, such as rough grinding and fine finishing. Appropriate speed adjustment is essential for maintaining consistent material removal rates, reducing thermal damage, and extending grinding wheel service life. The motor serves as the primary power source of the machine, converting electrical energy into mechanical energy

and transmitting it to the grinding wheel through the belt–pulley system. This transmission mechanism allows for flexible speed adjustment and stable torque delivery.

The grinding wheel functions as the primary cutting and finishing tool, removing excess material and refining the surface of the workpiece. Both coarse and fine grinding wheels are employed at different stages of the process to achieve the required surface roughness and dimensional accuracy. The grinding wheel turret supports and positions the grinding wheels and enables precise adjustment of their orientation and angle. This feature is particularly important for setting the cutting angle of the blade and ensuring uniform sharpening.

Throughout the grinding process, the operator adjusts the turret position and grinding parameters in accordance with process specifications. The interaction between the rotating grinding wheel and the stationary workpiece enables controlled material removal, resulting in the desired geometry and edge sharpness. After completing the rough and fine grinding stages, the workpiece is inspected to verify dimensional accuracy and surface smoothness. Once the required standards are met, the finished knife is removed from the machine and prepared for subsequent production stages.

C. Operation Process

The procedure consists of 17 main steps. The process begins with mounting the workpiece on the grinding machine chuck and performing workpiece centring, which requires approximately 20 minutes. Subsequently, the grinding wheel is assembled, followed by rough grinding of the inner surface.

After rough grinding, dimensional inspection is conducted, and the grinding wheel is replaced with a fine wheel for precision grinding. Measurements and surface smoothness inspections are then performed to ensure compliance with quality standards. The grinding wheel is later changed back to a coarse wheel for external edge grinding, and the tool post is adjusted to a 4-degree angle.

Rough grinding of the cutting edge is carried out, followed by dimensional and angular inspection. The grinding wheel is then replaced with a fine wheel for finishing operations. Final grinding, measurement, and inspection are conducted before the completed workpiece is removed and stored.

The total processing time for the entire grinding procedure is approximately 151 minutes per unit. Several stages involve repeated wheel changes and frequent inspections, which contribute to extended processing time and indicate the presence of non-value-added activities. These inefficiencies highlight the need for systematic process improvement through the application of the ECRS principle.

Table I presents an operation process chart illustrating each step of the pineapple peeling knife grinding process. The symbols represent different types of activities, including operation (Circle symbol), transportation (Arrow symbol), delay (D-shape symbol), inspection (Square symbol), and storage (Triangle symbol), which are used to analyze workflow efficiency and identify non-value-added activities.

According to Table I, the total processing time for the entire grinding procedure is approximately 151 minutes per unit. All processes can be classified into four subprocesses, namely the setup process, grinding process, inspection process, and other supporting processes. The grinding process accounts for the largest proportion of the total processing time, requiring 95 minutes. This is followed by other supporting processes, which require 26 minutes, while the setup and inspection processes require 20 and 10 minutes, respectively.

TABLE I
OPERATION PROCESS CHART FOR THE GRINDING PROCESS OF PINEAPPLE PEELING KNIVES

Order	Process	Symbols					Times (min)
		○	⇨	D	▽	□	
1	Setting on the chuck	●					1
2	Secure positioning	●					20
3	Assemble the grinding wheel	●					5
4	Rough grinding	●					45
5	Measure dimension					●	2
6	Change to fine grinding	●					5
7	Fine grinding	●					10
8	Measure dimension					●	2
9	Check surface smoothness					●	2
10	Change to rough grinding	●					5
11	Adjusted to a 4-degree	●					5
12	Rough grinding	●					30
13	Angular inspection					●	2
14	Change to a fine wheel	●					5
15	Fine grinding	●					10
16	Angular inspection					●	2
17	Removed and stored				●		-
	SUM	**11**	**0**	**0**	**1**	**5**	**151**

The grinding process of pineapple peeling knives involves multiple operational steps, and inefficiencies arising from unsuitable machine conditions and inappropriate grinding wheel selection result in excessive production time. In particular, the grinding stage requires up to 95 minutes, representing a substantial proportion of the total processing time. In addition, data on the consumption of both coarse and fine grinding wheels used in the grinding process were collected over three months, as illustrated in Fig 4.

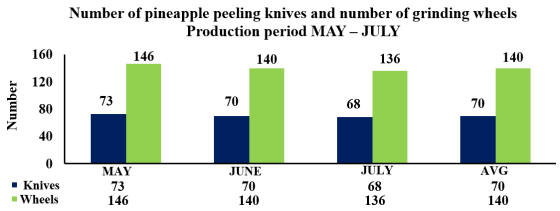

Fig. 4. Number of pineapple peeling knives and number of grinding wheels in the production period MAY-JULY.

Fig. 4 illustrates that the monthly consumption of grinding wheels exceeds the average number of workpieces produced. On average, approximately two grinding wheels are required to produce one pineapple peeling knife. Given that each grinding wheel costs 160 THB, this consumption rate results in substantial expenses associated with the pineapple peeling knife grinding process. Consequently, the total grinding wheel costs were 23,360 THB, 22,400 THB, and 21,760 THB for May, June, and July, respectively. The average grinding wheel cost over the three months was 22,506 THB.

Based on the analysis of the pineapple peeling knife grinding process, three major problems were identified. First, excessive time was consumed during the grinding operations. Second, inappropriate grinding wheel speed settings were observed, leading to inefficient material removal. Third, significant time was lost during workpiece centering and alignment. However, several studies emphasize that sustainable process improvement requires a thorough understanding of the underlying causes of problems, rather than addressing only their visible symptoms.

The **Why-Why analysis** is considered an appropriate tool for systematically identifying the root causes of operational problems, particularly those related to time losses and machine inefficiencies. In the grinding process of pineapple peeling knives, the major issues identified include excessive time consumption during grinding operations, inappropriate grinding wheel speed settings, and significant time loss during workpiece centering and alignment. These problems are complex in nature and are influenced by multiple factors, including operational methods, machine conditions, and operator skills. The insights obtained from this analysis provide a critical foundation for defining effective improvement strategies based on the ECRS principle. Such strategies aim to reduce processing time, optimize grinding wheel operating parameters, and simplify workpiece centering procedures in alignment with actual shop-floor conditions. The next section of this study presents the research methodology, detailing the procedures used to apply the **Why-Why** analysis and demonstrating how the identified root causes were translated into practical process improvement measures for the pineapple peeling knife grinding process.

While the application of ECRS principles is extensively documented across diverse manufacturing sectors, empirical research focusing on specialized supporting processes, specifically tool sharpening within the fruit processing industry, which operates under stringent hygiene and precision constraints remains markedly scarce. This study addresses this scholarly lacuna by integrating ECRS methodologies with engineering grinding techniques, thereby establishing a systematic and quantifiable framework to optimize the efficiency of the pineapple peeling knife sharpening process.

D. Why-Why Analysis

Based on the operational data collected from the production process, the researcher conducted a root cause analysis using the Why-Why analysis technique and formulated corrective measures in accordance with the ECRS principle [10]. Table II presents the analysis of the root causes associated with time losses in the grinding process.

The Why-Why analysis was conducted to identify the root causes of time losses in the grinding process of pineapple peeling knives. The analysis revealed that excessive processing time was primarily attributed to the complexity of the grinding procedure.

TABLE II
THE ROOT CAUSES ASSOCIATED WITH TIME LOSSES IN THE GRINDING PROCESS

Why I	Reson I→Why II	Reson II→Root cause
Time losses in the grinding process	The grinding process consists of multiple operational steps and requires the use of grinding wheels with various grades.	The grinding process is specified to include both rough grinding and fine grinding operations.
Solution	The improvement approach involved eliminating unnecessary operational steps by increasing the hardness of the grinding wheel to reduce redundant fine grinding operations and combining the rough and fine grinding stages into a single process.	

which consisted of multiple operational steps and required the use of grinding wheels with various grades. Further investigation indicated that the process specification mandated separate rough grinding and fine grinding operations, resulting in repeated machine setup, frequent grinding wheel changes, and extended processing time.

The analysis clearly demonstrated that the requirement for multiple grinding stages was not driven by essential quality needs but rather by traditional process design. This condition led to redundant operations and increased non-value-added time within the grinding process.

To optimize grinding wheel operating parameters, the root causes associated with machine conditions are presented in Table III.

TABLE III
THE ROOT CAUSES ASSOCIATED WITH GRINDING WHEEL OPERATING PARAMETERS

Why I	Reson I→Why II	Reson II→Root Cause
The operating parameters of the grinding wheel are not optimized	The standard operating procedure (work instruction) does not define the appropriate grinding wheel rotational speed.	No experiments have been conducted to determine the standard values for the appropriate grinding wheel rotational speed.
Solution	The improvement approach applied the principle of rearrangement by modifying the belt–pulley system to increase the rotational speed of the grinding wheel, followed by experimental testing to determine the optimal grinding wheel speed for the workpiece.	

The Why-Why analysis was conducted to investigate the root causes associated with non-optimized grinding wheel operating parameters. The analysis revealed that the primary issue was the absence of defined rotational speed values in the standard operating procedure (work instruction). Further examination indicated that this deficiency resulted from the lack of experimental studies conducted to determine appropriate grinding wheel rotational speed standards for the workpiece. Consequently, grinding wheel operating parameters were set based on operator experience rather than data-driven criteria, leading to inconsistent grinding performance and reduced process efficiency.

The third major problem relates to workpiece centering and alignment. Therefore, the root cause analysis of the centering and alignment problem during workpiece setup is presented in Table IV.

The Why-Why analysis was conducted to identify the root causes of time losses associated with workpiece centering and alignment during the setup stage. The analysis revealed that excessive setup time resulted from the need to repeatedly clamp the workpiece to the fixture. Further investigation indicated that insufficient clamping stability caused the workpiece to become dislodged during grinding operations, requiring frequent process interruptions for corrective action. These interruptions significantly increased setup time and reduced overall process efficiency.

TABLE IV
THE ROOT CAUSES ASSOCIATED WITH CENTERING AND ALIGNMENT PROBLEM DURING WORKPIECE SETUP

Why I	Reson I Why II	Reson II Root cause
Time losses associated with workpiece centering and alignment.	The workpiece must be repeatedly clamped to the fixture.	When the workpiece is not securely clamped in the fixture, it may become dislodged, requiring the grinding process to be halted for corrective action.
Solution	The improvement approach applied the simplification principle by designing a JIG to facilitate knife positioning, thereby reducing workpiece setup time and improving clamping stability.	

E. Problem – Solving Procedure

To address time losses in the grinding process, the researcher replaced the existing grinding wheels with a new specification featuring increased hardness in accordance with ISO 525:2020 [11]. Previously, a coarse grinding wheel with the specification GC 90 GV was used for rough grinding, while a fine grinding wheel with the specification GC 180 LV was applied for finishing operations. These were replaced with a newly specified grinding wheel that increased the bonding grade from G (very soft) to K (Soft) and adjusted the abrasive grain size from 90 to 100, as shown in Fig 5. Consequently, the rough and fine grinding stages were combined into a single grinding operation (Combine).



Fig. 5. Grinding wheels, (a) Grade G (very soft) and (b) Grade K (soft)

F. Experimental Investigation of Feed Rate and Rotational Speed

Following the replacement of the original grinding wheel with a new specification featuring increased hardness, grinding experiments were conducted on pineapple peeling knives to determine the grinding wheel wear rate using the minimum weight-loss method before practical application. The experiments were performed by varying the workpiece rotational speed at 70 and 115 RPM and the feed rate at 0.10, 0.15, and 0.20 mm/rev, while maintaining coolant application as a controlled variable. Each experimental condition was repeated three times, resulting in a total of 18 specimens. After each test, the grinding wheel was weighed as shown in Fig 6, and the weight loss was calculated in milligrams per hour for comparison. To minimize grinding wheel weight loss, a two-way ANOVA at a significance level of 0.05 was used to evaluate the effects of rotational speed and feed rate on grinding wheel weight loss. The grinding condition associated with the lowest weight loss was subsequently selected for implementation in actual grinding operations.



Fig. 6. The weight of the grinding wheel

G. Design and fabrication of a Work – Holding Device (JIG)

To reduce the time required for workpiece centering before grinding, which was excessively long due to direct clamping of the workpiece that could cause damage to the knife frame, a dedicated work-holding device was designed. This device was developed to prevent structural damage and to reduce workpiece setup time, as shown in Fig 7.

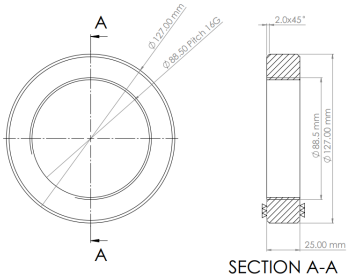

Fig. 7. The section view of the wok–holding device (JIG)

The work-holding device was fabricated from SUS304 stainless steel with an outer diameter of 127 mm and a thickness of 25 mm. It features an internal thread with a diameter of 88.5 mm and a pitch of 16G, configured as a left-hand thread to enable secure locking with the workpiece according to the design specification. The device was subsequently used to improve knife clamping stability and to function as a JIG, as illustrated in Fig 8.

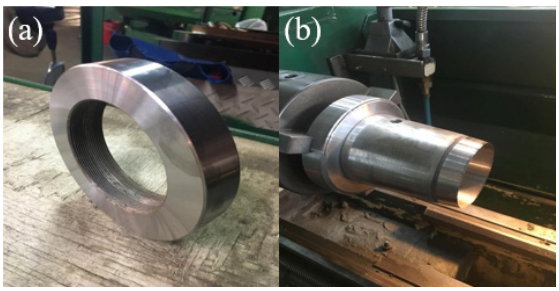

Fig. 8. A work–holding device (JIG), (a) uninstalled and (b) installed condition

IV. Research Results

The results of this study are presented in this section, highlighting the investigation of feed rate and rotational speed, their effects on grinding wheel weight loss, and the performance of the work - holding device (JIG) developed to improve workpiece centering and clamping stability in the grinding process.

A. Experimental results

For the experimental investigation of feed rate and rotational speed, Fig. 9 presents the average weight loss of grinding wheels at different rotational speeds and feed rates.

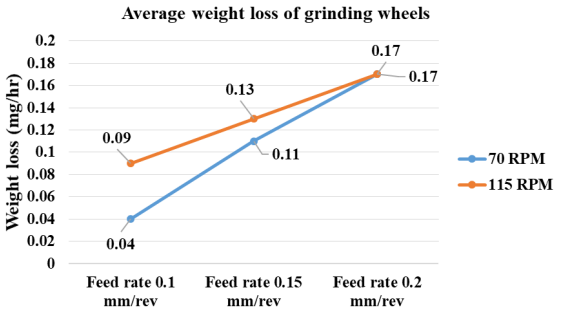

Fig. 9. Average weight loss of grinding wheels after use at different feed rate and RPM

The results show a consistent increase in grinding wheel weight loss as the feed rate increases from 0.10 to 0.20 mm/rev for both rotational speeds. This trend indicates that higher feed rates lead to greater material removal forces and increased abrasive wear. At all feed rates, grinding performed at **115 RPM** results in higher weight loss compared to **70 RPM**, demonstrating that rotational speed has a measurable influence on grinding wheel wear. The lowest weight

loss, approximately **0.04 mg/hr**, is observed at a feed rate of **0.10 mm/rev** and a rotational speed of **70 RPM**, indicating the most favorable condition for minimizing grinding wheel wear. In contrast, the highest weight loss, approximately **0.17 mg/hr**, occurs at a feed rate of **0.20 mm/rev** for both rotational speeds, suggesting that the effect of feed rate becomes dominant at higher levels.

Feed rate was identified as the most influential factor affecting grinding wheel wear. As the feed rate increased from 0.10 to 0.20 mm/rev, the average weight loss of the grinding wheel increased substantially. This trend can be attributed to the higher material removal rate and increased contact forces between the grinding wheel and the workpiece at higher feed rates, which accelerate abrasive grain fracture and bond wear. These findings are consistent with established grinding theory, which suggests that aggressive cutting conditions lead to increased tool wear.

Rotational speed also exhibited a significant effect on grinding wheel weight loss. Higher rotational speed (115 RPM) resulted in greater wheel wear compared to lower speed (70 RPM), particularly at lower feed rates. This behavior is associated with increased sliding velocity and frictional heat generation at the grinding interface, which promotes bond softening and abrasive degradation. However, the effect of rotational speed became less pronounced at higher feed rates, indicating the presence of an interaction effect between rotational speed and feed rate.

Table V presents the results of the grinding experiments, which were analyzed using a two-way analysis of variance (ANOVA) to evaluate the effects of rotational speed and feed rate on grinding wheel weight loss. The ANOVA results indicate that both main factors, namely rotational speed and feed rate, have statistically significant effects on grinding wheel wear, as well as their interaction ($p < 0.05$). This confirms that grinding wheel weight loss is influenced not only by individual process parameters but also by their combined effect.

The statistically significant interaction between rotational speed and feed rate demonstrates that the influence of rotational speed on grinding wheel wear depends on the selected feed rate. Specifically, at a feed rate of 0.10 mm/rev, increasing rotational speed led to a notable increase in weight loss, whereas at 0.20 mm/rev, the difference in wear between the two speeds was relatively small. This interaction highlights the importance of considering combined parameter settings rather than optimizing individual factors independently.

TABLE V
TWO-WAY ANOVA FOR GRINDING WHEEL WEIGHT LOSS

Source of Variation	Sum of Squares (SS)	DF	Mean Square (MS)	p-value
RPM	0.0027	1	0.0027	0.0007
Feed rate	0.0300	2	0.0150	<0.0001
Interaction	0.0012	2	0.0006	0.0317
Error	0.0016	12	0.0001	-
Total	0.0355	17	-	-

Based on the optimization objective of minimizing grinding wheel weight loss, the optimal operating condition was identified as a rotational speed of 70 RPM and a feed rate of 0.10 mm/rev. Under this condition, the grinding wheel showed the lowest average weight loss, indicating reduced abrasive wear and improved tool life. From an industrial perspective, adopting this parameter combination can lower tooling costs, improve process stability, and enhance the sustainability of the grinding operation.

B. The Performance of The Work–Holding Device (JIG)

Following implementation of the proposed corrective actions, a before–and–after comparison was conducted to evaluate process performance. As shown in Table VI, the post-improvement production process substantially reduced total processing time from 151 minutes to 86 minutes, and the number of operational steps decreased from 17 to 9, indicating a considerable simplification of the production process.

TABLE VI
OPERATION PROCESS CHART FOR THE GRINDING PROCESS OF PINEAPPLE PEELING KNIVES AFTER PROCESS IMPROVEMENTS

Order	Process	Symbols ○	⇨	D	▽	□	Times (min)
1	Setting on the Chuck	●					1
2	Secure Positioning	●					1
3	Assemble Grinding Wheel	●					5
4	Rough Grinding	●					40
5	Measure Dimension					●	2
6	Adjust to 7 Degrees	●					5
7	Fine Grinding	●					30
8	Measure Dimension					●	2
9	Removed and Stored				●		-
	SUM	**6**	**0**	**0**	**1**	**2**	**86**

After implementing process improvements, the workpiece setup stage required 20 minutes before the improvement, while no setup time was required after the improvement. In the grinding stage, processing time decreased from 95 minutes before improvement to 70 minutes after improvement. For the dimensional measurement and inspection stage, the time decreased from 10 minutes to 4 minutes. In addition, the time required for other supporting processes decreased from 26 minutes before improvement to 12 minutes after improvement, as shown in Table VII.

TABLE VII
COMPARISON OF OPERATIONAL TIME BEFORE AND AFTER PROCESS IMPROVEMENT BY WORK CATEGORY

Work Category	Times (Minute)	
	Before Improvement	After Improvement
Setting	20	0
Grinding	95	70
Measure dimension	10	4
Other	26	12
SUM	**151**	**86**

C. Production Capacity

An evaluation of production capacity in the grinding process indicates that, before process improvement, the grinding time was 151 minutes per unit with a total of 17 operational steps. After process improvement, grinding time fell to 86 minutes per unit, and the number of operational steps decreased to 9. Consequently, the reduced processing time significantly increased production capacity. Based on an average of 22 working days per month and an 8-hour working day, production output increased from 70 units per month before improvement to 123 units per month after improvement, representing an increase of approximately 75.7%, as shown in Fig 10.

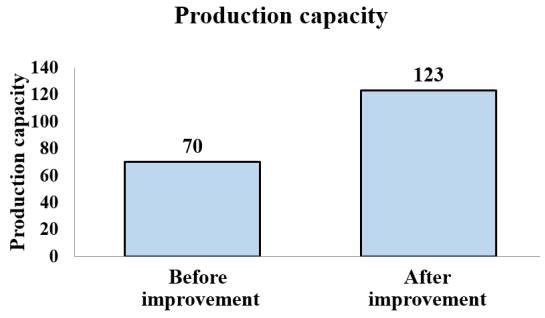

Fig. 10. Production capacity

Based on the collected data on grinding wheel consumption for pineapple peeling knife production, grinding wheel usage decreased. This reduction resulted from replacing the original grinding wheels with a new specification and decreasing processing time after process improvement. Consequently, production required fewer grinding wheels, as shown in Fig. 11.

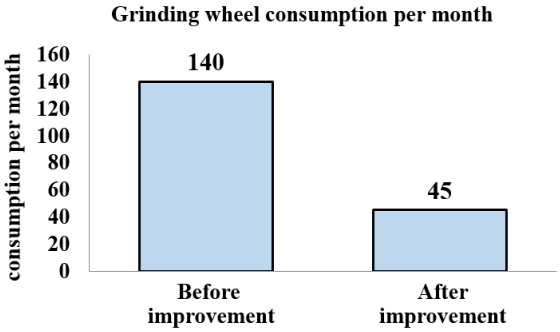

Fig. 11. Grinding wheel consumption per month

After the process improvement, grinding wheel consumption fell from 140 units to 45 units per month. Accordingly, the grinding wheel cost before improvement was 140 units at 160 THB per unit, for a total of 22,400 THB per month. After improvement, the consumption decreased to 45 units per month, corresponding to a total cost of 7,200 THB per month. This represents a cost reduction of approximately 68.01%, as illustrated in Fig. 12.

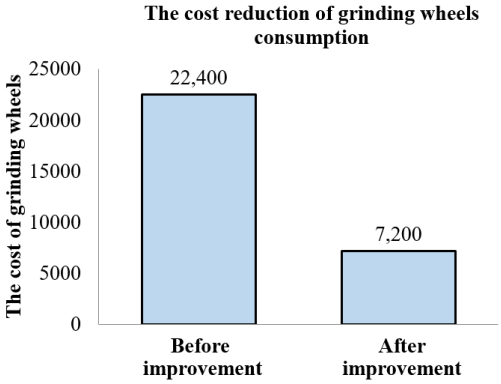

Fig. 12. The cost of grinding wheel consumption per month

V. DISCUSSION

The results show that systematic process improvement based on root cause analysis and ECRS principles can significantly improve the efficiency of the pineapple peeling knife grinding process. The initial analysis revealed that excessive processing time, high grinding wheel consumption, and unstable workpiece setup were the primary contributors to inefficiency. These issues aligned with non-value-added activities commonly reported in grinding and tool maintenance operations.

The Why-Why analysis effectively identified the fundamental causes of inefficiency rather than addressing only surface-level symptoms. In particular, the separation of rough and fine grinding operations, the lack of standardized grinding wheel rotational speed parameters, and unstable workpiece clamping

were identified as the dominant root causes of time losses and excessive tool wear. This finding highlights the importance of structured root cause analysis in guiding appropriate improvement strategies and avoiding ineffective or superficial solutions. Applying the ECRS principle provided a systematic framework for translating analytical findings into practical improvements.

Eliminating and combining grinding stages by using a single, harder grinding wheel directly reduced redundant operations and machine setup time. This modification significantly shortened the grinding cycle and simplified the overall process flow. Rearranging the belt–pulley system to increase grinding wheel rotational speed addressed machine-related inefficiencies and enabled operation under calculated optimal conditions. Experimental determination of feed rate and rotational speed further ensured that process parameters were optimized based on empirical evidence rather than operator experience. The design and implementation of a dedicated work-holding device (JIG) played a critical role in improving workpiece centering and clamping stability.

Before the improvement, workpiece setup depended heavily on operator skill and required repeated clamping, often leading to misalignment, workpiece damage, and process interruptions. The JIG effectively eliminated these issues by providing consistent positioning, reducing setup time to zero, and preventing damage to the knife frame. This result underscores the importance of fixture design in grinding operations, particularly when precision and repeatability are required. Statistical analysis using two-way ANOVA confirmed that feed rate and rotational speed significantly affected grinding wheel weight loss, with feed rate identified as the most influential factor. The statistically significant interaction between feed rate and rotational speed further indicated that optimization must consider combined parameter settings rather than individual factors in isolation.

The experimental results validated the selected optimal condition of 70 RPM and 0.10 mm/rev, which achieved the lowest grinding wheel wear and supported longer tool life. These findings are consistent with established grinding theory, where lower feed rates and controlled speeds reduce abrasive grain fracture and bond degradation. Operationally, the reduction in processing time from 151 minutes to 86 minutes per unit and the decrease in operational steps from 19 to 9 represent substantial improvements in process efficiency. These changes directly translated into increased production capacity, with monthly output rising by approximately 75.7%. In parallel, grinding wheel consumption fell by 68.01%, delivering significant cost savings. This dual improvement in productivity and cost efficiency highlights the effectiveness of the proposed approach and its practical value for industrial implementation.

Overall, the discussion confirms that integrating root cause analysis, ECRS principles, experimental optimization, and fixture design provides a robust methodology for improving grinding processes. The results not only validate the effectiveness of the proposed improvements for pineapple peeling knife manufacturing but also demonstrate their potential applicability to similar grinding and tool maintenance operations in food processing and other manufacturing industries.

VI. Conclusions

This study demonstrated that systematic process improvement based on Why-Why analysis and the ECRS principle can significantly enhance the efficiency of the pineapple peeling knife grinding process. By identifying and addressing the root causes of excessive processing time, inappropriate grinding parameters, and unstable workpiece clamping, the study successfully implemented effective improvement strategies. Integrating a redesigned work-holding device (JIG), optimizing grinding wheel rotational speed and feed rate, and consolidating grinding stages substantially reduced processing time and the number of operational steps.

Experimental optimization confirmed that a workpiece rotational speed of 70 RPM and a feed rate of 0.10 mm/rev minimized grinding wheel wear, while statistical analysis verified the significance of these parameters and their interaction. As a result of the proposed improvements, processing time was reduced from 151 minutes to 86 minutes per unit, production capacity increased by approximately 75.7%, and grinding wheel consumption decreased by 68.01%, leading to considerable cost savings.

Overall, the findings confirm that the proposed approach provides an effective and practical framework for improving grinding operations. The methodology and results offer valuable guidance for similar tool grinding and maintenance processes in food processing and related manufacturing industries.

REFERENCES

[1] Thailand Board of Investment, *Thailand's Food Industry Report 2023*. Bangkok, Thailand: Thailand Board of Investment, 2023. [Online]. Available: https://www.boi.go.th [Accessed: Mar. 15, 2026].

[2] L. Meena, A. S. Sengar, R. Neog, and C. K. Sunil, "Pineapple Processing Waste (PPW): Bioactive compounds, their extraction, and utilisation: A review," *J. Food Sci. Technol.*, vol. 59, no. 11, pp. 4152-4164, Nov. 2022, https://doi.org/10.1007/s13197-021-05271-6

[3] D. E. Ibiyeye et al., "Fabrication of a pineapple peeling machine and performance evaluation as influenced by pineapple dimensions," *J. Bioresource Manag.*, vol. 12, no. 2, pp. 67-75, Jun. 2025, https://doi.org/10.35691/JBM.5202.0017

[4] N. Kumar, M. Kumar, M. S. Alam, S. Jagtap, and V. Choubey, "Implementation of lean manufacturing principle towards improving firm performance: Evidence from the case of account book fabrication industry," *Int. J. Glob. Bus. Compet.*, May 2026, https://doi.org/10.1007/s42943-026-00151-2

[5] K. Kannan, N. Arunachalam, A. Chawla, and S. Natarajan, "Multi-sensor data analytics for grinding wheel redress life estimation—an approach towards Industry 4.0," *Procedia Manufacturing*, vol. 26, pp. 1230-1241, Jan. 2018.

[6] K. Kishore, M. K. Sinha, A. Singh, Archana, M. K. Gupta, and M. E. Korkmaz, "A comprehensive review on the grinding process: Advancements, applications and challenges," *in Proc. Inst. Mech. Eng. Part C J. Mech. Eng. Sci*., vol. 236, no. 22, pp. 10923-10952, Nov. 2022.

[7] B. Suhardi, N. Anisa, and P. W. Laksono, "Minimizing waste using lean manufacturing and ECRS principle in Indonesian furniture industry," *Cogent Engineering*, vol. 6, no. 1, Art. no. 1567019, Jan. 2019.

[8] S. Dossi, "*Enhancing Overall Equipment Effectiveness (OEE) in a Specific Food Manufacturing Process*," M.S. thesis, Dept. Mech. Ind. Eng., Univ. Illinois, Chicago, IL, USA, 2024, https://doi.org/10.25417/uic.29048645.v1

[9] M. H. I. Avichena and E. P. Widjajati, "Machine effective analysis using OEE and six big losses methods in the filter making factory," in *Proc. 1st Int. Conf. Eco-Innovation in Science, Engineering, and Technology*, 2020, Art. no. 0544, https://doi.org/10.11594/nstp.2020.0544

[10] R. Saravanan, M. S. Rao, N. Sunkara, and T. Malyadri, "Six sigma's ECRS technique to down cost and time of manufacturing—an experimental investigation," in *AIP Conf. Proc.*, 2020, Art. no. 020070.

[11] International Organization for Standardization, "Bonded Abrasive Products—Shape Types, Designation and Marking," ISO Standard 525:2020, *Geneva, Switzerland*, 2020. [Online]. Available: https://www.iso.org/obp/ui#iso:std:iso:525:ed-5:v1:en [Accessed: Mar. 15, 2026].



Pipat Lertkowit received a Master of Engineering in Manufacturing System Engineering from KMUTT University, Thailand, in 2004. Responsible as a lecturer in the Department of Industrial Engineering from 2012 to 2026 in the Faculty of Engineering at Thonburi University, Thailand, and my research specializes in work study and operational analysis in manufacturing systems.



Poom Jatunitanon received a Doctor of Engineering in Mechanical Engineering from Kasetsart University, Thailand, in 2017. Used to be a professor of automotive manufacturing engineering from 2019 to 2025 at the Faculty of Engineering and Technology at Panyapiwat Institute of Management, Thailand, and is currently the Head of Automotive Manufacturing Engineering at the Faculty of Engineering and Technology at Panyapiwat Institute of Management, Nonthaburi, Thailand.



Bundit Inseemeesak received a Doctor of Engineering in Mechanical Engineering from Kasetsart University, Thailand, in 2023. I was a professor of automotive manufacturing engineering from 2015 to 2026 at the Faculty of Engineering and Technology at Panyapiwat Institute of Management, Thailand, and my current job is maintaining internal combustion engine vehicles and electric vehicles. Composite materials from natural fibres. Biomass processing.

Integrated Lane Departure Warning and Adaptive Cruise Control for Enhanced Driving Safety in Advanced Driver Assistance Systems: A Simulation Study

Tanakorn Mongkondatsawat[1*], Panumat Rergngam[2], Wutthichai Imwong[3], Namchai Sokai[4], and Nakorn Indra-Payoong[5]

[1,2,3,4,5]Center for Future Mobility (NDrive), Faculty of Logistics, Burapha University, Chonburi

E-mail: tanakorn.mongkondatsawat@gmail.com*, phanumatrakngam@gmail.com, wutthichaiimwong@gmail.com, namchai48@gmail.com, nakorn@go.buu.ac.th

Received: June 13, 2025 / Revised: January 1, 2026 / Accepted: February 2, 2026

***Abstract*—This research aims to develop and test Advanced Driver Assistance Systems (ADAS), specifically Adaptive Cruise Control (ACC) and Lane Departure Warning (LDW), utilizing the "CARLA Simulator," an open-source driving environment simulation software for autonomous driving technology research and development. Testing results showed that the ACC system achieved 97.916% accuracy in following the speed of the vehicle ahead, maintained an average distance of 10.651 meters from the leading vehicle (exceeding the specified safety distance), and exhibited an automatic braking response time of 0.3 seconds. The LDW system correctly detected vehicle lane departures with over 75% accuracy when lane markings were complete or straight. However, in heavy rain or on roads with incomplete or dashed lane markings, the system produced false positives—incorrectly warning of lane departures departures when the vehicle remain in lane—a rate exceeding 30%.**

***Index Terms*—Advanced Driver Assistance Systems, Adaptive Cruise Control, Lane Departure Warning, CARLA Simulator**

I. Introduction

Advanced Driver Assistance Systems (ADAS) have assumed a pivotal role in the evolution of the automotive industry, with the primary objectives of enhancing safety and optimizing driving convenience. As ADAS technologies such as Adaptive Cruise Control (ACC) and Lane Departure Warning (LDW) continue to develop, they require rigorous testing and performance evaluation before real-world implementation to ensure system safety and stability.

Assessing ADAS in real environments presents numerous constraints, including substantial costs, potential accident risks during testing, and environmental limitations. Consequently, vehicle simulators are an optimal alternative for testing, as they can simulate diverse driving scenarios and allow control over various parameters. This includes the capability to evaluate ADAS performance in potentially hazardous situations or circumstances that cannot be reliably replicated in real-world environments, such as navigating dense traffic conditions, executing lane changes, or encountering obstacles.

This research employs the CARLA simulator, an open-source vehicle simulation platform with robust capabilities for realistic environmental simulation [1], [2]. Using the CARLA simulator enables the development and assessment of ADAS technologies across diverse, controlled environmental conditions. In developing countries such as Thailand, implementing and evaluating Advanced Driver Assistance Systems (ADAS) faces several challenges, including limited access to real-world testing environments, high implementation costs, diverse traffic conditions, and adverse weather scenarios. While previous studies have demonstrated the effectiveness of individual ADAS functions, such as Adaptive Cruise Control (ACC) or Lane Departure Warning (LDW), most evaluations have been conducted under controlled conditions or in developed-country contexts. Thus, a research gap remains in evaluating integrated ADAS functions under complex driving scenarios using simulation-based platforms.

This research's main contribution is developing and evaluating an integrated ADAS framework that combines Adaptive Cruise Control (ACC) and Lane Departure Warning (LDW) within the CARLA simulation environment. Unlike previous studies that primarily focus on single-function ADAS systems or theoretical modeling, this work emphasizes system-level integration, scenario-based testing, and performance evaluation under diverse conditions, including varying traffic behaviors. This study also provides a detailed analysis of velocity-tracking

accuracy, following-distance behavior, and LDW false-positive rates, highlighting practical limitations and safety implications. The findings improve understanding of ADAS performance in simulation environments and inform future improvements for real-world testing and deployment in developing countries.

II. Literature Review

A. ADAS Technology

ADAS has undergone continuous development within the automotive industry with the primary objective of enhancing driving safety [3]. These systems comprise multiple subsystems, including Adaptive Cruise Control (ACC), Lane Departure Warning (LDW), Autonomous Emergency Braking (AEB), and Lane Keeping Assist (LKA). Dosovitskiy et al. [6] showed a significant reduction in accident rates, particularly when accurate object detection and distance estimation from preceding vehicles or obstacles are achieved using diverse sensor technologies such as cameras, radar systems, and LiDAR. Furthermore, ADAS technologies have been shown to mitigate driver fatigue in high-traffic-density conditions and long-distance driving by helping drivers maintain safe vehicle operation.

B. Adaptive Cruise Control (ACC)

Adaptive Cruise Control (ACC) is an advanced driving assistance function that automatically regulates vehicle speed while maintaining a safe distance from a preceding vehicle. Anand and Ohol [1] proposed a methodology for designing and simulating ACC systems by integrating Model Predictive Control (MPC) with Decision Tree algorithms to analyze acceleration–deceleration behavior and overtaking assistance in realistic traffic conditions. Their experimental results demonstrated the effectiveness of combining radar sensor technology with intelligent control algorithms in maintaining appropriate safety distances. However, the study primarily focused on ACC as a standalone system and did not consider its interaction with other ADAS functions in an integrated framework.

C. Lane Departure Warning (LDW)

Lane Departure Warning (LDW) systems aim to detect unintended lane departures and alert drivers to potential safety risks. Ping et al. [13] developed a vision-based LDW framework using Hough transform techniques and lateral deviation ratio calculations. The system was evaluated using real-world datasets collected under both daytime and nighttime conditions. The reported results showed 94.71% lane-detection accuracy and 81.18% lane-departure detection precision. Nevertheless, the study identified performance limitations in scenarios with worn lane markings and low illumination, which increased false positive rates. These findings highlight the sensitivity of vision-based LDW systems to environmental and road conditions.

D. CARLA Simulator for ADAS Development and CARLA Selection

Driving simulators have been widely adopted for ADAS and autonomous vehicle research because they provide safe, repeatable, and cost-effective testing environments. Previous studies have used several simulation platforms, including PreScan, SUMO, LGSVL Simulator, and AirSim. PreScan offers high-fidelity vehicle dynamics and sensor modeling; however, it requires commercial licensing, which limits its accessibility for academic and research applications. SUMO is designed for traffic flow simulation and lacks the realistic sensor modeling capabilities required for perception-based ADAS evaluation. LGSVL Simulator and AirSim support sensor simulation and autonomous driving research but offer less flexibility for large-scale urban scenario customization and adverse-weather modeling than CARLA.

Dosovitskiy et al. [6] introduced the CARLA simulator as an open-source urban driving simulation platform that emulates various sensor modalities, including RGB cameras, radar, and LiDAR, within highly realistic virtual environments. In addition. Markofsky et al. [12] proposed a framework for virtual calibration of ADAS and Automated Driving Systems (ADS) using multi-scenario simulations in CARLA, demonstrating that simulation-based testing can significantly reduce real-world testing costs while enabling iterative performance optimization without safety risks.

Table I presents a comparative analysis of driving simulators used in ADAS development and identifies CARLA as the most suitable platform for developing and evaluating Adaptive Cruise Control (ACC) and Lane Departure Warning (LDW) systems. CARLA's suitability stems from its open-source architecture, realistic urban road networks, comprehensive sensor emulation, dynamic traffic generation, and advanced weather-condition modeling, including heavy rain. These features enable scenario-based testing and systematic performance evaluation of integrated ADAS functions under complex driving environments.

Unlike previous studies that primarily focus on individual ADAS functions, such as ACC and LDW, this research emphasizes the integrated evaluation of ACC and LDW within a unified ADAS framework using a simulation-based approach. The proposed study focuses on system-level performance analysis under diverse traffic and environmental conditions, which is particularly relevant for developing countries

such as Thailand, where cost, infrastructure, and safety concerns constrain real-world ADAS testing. This simulation-based evaluation provides practical insights into the applicability and limitations of integrated ADAS technologies prior to real-world deployment.

TABLE I
COMPARES CAR SIMULATOR FOR ADAS (ACC/LDW) DEVELOPMENT

Simulator	Developer	ADAS (ACC / LDW)	Reality	Sensors Support	Compatibility	Cost	Limitation
CARLA	Open-sourced by the research community	ACC and LDW in a dynamic 3D environment	High	LiDAR, Radar, Camera	Python and ROS	Free	Requires high computing resources and is difficult to set up
LGSVL Simulator	LG Electronics	ACC and LDW in urban area using ROS and Autoware	Moderate	LiDAR, Camera	ROS and Autoware	Free	Restricted vehicle models and environment
Gazebo	Open-source (OSRF)	ACC and LDW in a simulated environment using ROS	Low	Camera, LiDAR	ROS	Free	Poor graphics and user interface
PreScan	Siemens	ACC and LDW using MATLAB/Simulink with accurate sensor simulation	High	LiDAR, Radar, Camera	MATLAB and Simulink	High	Proprietary software
Ansys VRXPERIENCE	Ansys	ACC and LDW using advanced sensors and vehicle dynamics	High	LiDAR, Radar, Camera	Development across multiple platforms	High	Difficult to set up
IPG CarMaker	IPG Automotive	ACC and LDW using Hardware-in-the-loop and MATLAB	High	LiDAR, Radar, Camera	MATLAB, Hardware-in-the-loop	High	Focus on automotive engineering rather than AI development
AirSim	Microsoft Research	Unreal Engine for LDW ACC in vitural environment	High	RGB, Depth, LiDAR	Python and C++	Free	Fewer users than CARLA, and the simulation has a limit
Nvidia Drive	Nvidia	ACC and LDW using Ray-tracing technology and AI simulation	Very high	LiDAR, Radar, Camera	Nvidia Drive	High	Only simulated with Nvidia hardware

III. METHODOLOGY

As automotive technology transitions toward autonomous driving, ADAS development is expected to be a crucial component in reducing accidents and improving road safety, especially in developing countries with high accident rates. These systems must be calibrated to reflect local driver behavior across different regional contexts. However, testing ADAS on real-world roads faces numerous limitations regarding cost, time, and passenger safety risks. Therefore, this research uses the CARLA simulation program to design, test, and refine ADAS systems to ensure both safety and effectiveness.

This section examines the CARLA framework, sensor and vehicle simulation methodologies, and the ADAS development process using a simulation-driven design approach that emphasizes development based on simulated data and logic generated within the simulator environment.

A. CARLA Architecture

CARLA (Car Learning to Act) is an open-source platform for autonomous driving research and development. The platform uses Unreal Engine 4 to create highly realistic virtual environments, including sophisticated visual elements, sound reproduction, weather-condition simulation, and accurate vehicle physics. The architectural framework of CARLA is segmented into three main components [8]:

1) Server: functions as the virtual world simulator, encompassing scene rendering, map generation, actor instantiation, and diverse meteorological conditions, all implemented through Unreal Engine 4.

2) Middleware (RPC Layer): Serves as the communication intermediary between the Client and Server through a Remote Procedure Call system specifically engineered to maintain low latency values.

3) Client (Python API): The component that developers utilize to implement vehicle control algorithms, receive sensor data input, and process various behavioral parameters.

B. CARLA components

1) Actors: Vehicles, pedestrians, motorcycles, or obstacles. (Used: Any CARLA vehicle catalogue)

2) Maps: Standard simulated urban maps, such as Town01–Town10 within CARLA, or imported maps from OpenDRIVE. (Used: Town04 map)

3) Sensors: RGB camera, LiDAR, Radar, GNSS, IMU, etc. (Used: RGB Camera and Radar)

4) Traffic Manager: Traffic behavior management systems, such as braking responses to vehicle incursions or lane-changing maneuvers. (Used: Spawn-point to spawn all vehicles, Lead Vehicle: Autopilot)

IV. Experimental Results

A. Adaptive Cruise Control (ACC)

Adaptive Cruise Control (ACC) represents a critical function within Advanced Driver Assistance Systems (ADAS), automatically regulating vehicle velocity according to traffic conditions while maintaining safe distances from preceding vehicles across all speed ranges [9]-[11]. This research focuses on developing and evaluating ACC functionality within the CARLA Simulator environment, using virtual radar sensors to detect the velocity of leading vehicles and implementing PID control algorithms with safety-oriented decision logic for acceleration and braking responses. The system responds precisely to simulated scenarios that accurately reflect real-world vehicle behavior. The ACC system relies primarily on the virtual Radar Sensor (Sensor.other.radar), which detects forward objects at extended ranges and measures critical parameters including Distance, Relative Velocity, and Azimuth. The research team positioned the radar sensor at the front section of the subject vehicle (Ego Vehicle) to simulate ACC functionality in automotive applications. The system processes data frame by frame and uses median filtering to eliminate anomalous velocity readings, maintaining system stability.

The developed ACC system uses Proportional-Integral-Derivative Control (PID) algorithms to keep the Ego Vehicle's velocity within safety parameters, primarily based on the distance to the Lead Vehicle, supplemented by additional conditions that simulate human decision-making processes, as illustrated in Fig. 1.

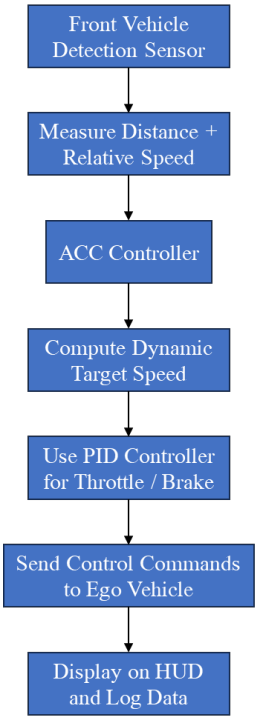

Fig. 1. Flowchart of ACC

1) Decision Criteria

• If the distance from the Lead vehicle is less than 5.5 meters, the system commands the Ego vehicle to initiate emergency braking procedures immediately.

• In conditions of extremely low velocity with proximate Lead vehicle positioning, the system instructs the Ego vehicle to execute a complete stop-and-hold maneuver.

• When the intervehicular distance falls below the calculated safety threshold (derived from velocity parameters), the system activates braking protocols. Safe_distance = max (10.0, ego_vehicle_speed x 2.0)

• In scenarios where substantial intervehicular distance exists, the system implements acceleration commands governed by PID control mechanisms.

• Under standard operating conditions, the system maintains appropriate velocity parameters.

2) PID Controller

The PID control component has been calibrated to enable rapid ego-vehicle response while maintaining smooth driving characteristics. Through parameter tuning, we determined optimal values of Kp = 1.2 (primary control), K_i = 0.08 (steady-state error reduction), and K_d = 0.15 (overshoot mitigation). The PID controller generates commands that regulate the Ego Vehicle's throttle and brake functions in real time.

The developed ADAS was tested in the CARLA Simulator, simulating driving conditions with ACC mode activated and using radar and PID control components. The acc_metrics_logger.py utility recorded all movement frames and automatically generated logs and graphical representations. Fig. 2 illustrates ACC system operations



Fig. 2. Testing ACC in CARLA simulator

Fig. 3 presents the performance assessment results for the developed ACC, and Table II summarizes the Performance Matrices for the ACC system.

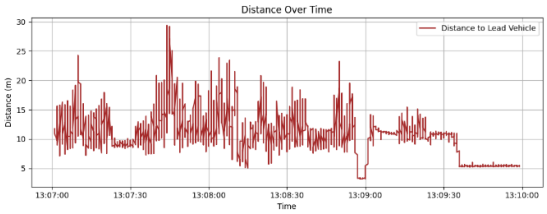

Fig. 3 (a). Distance to lead vehicle

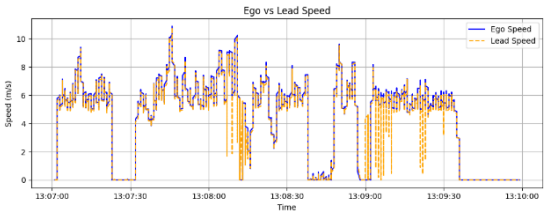

Fig. 3 (b). Ego vs. lead speed

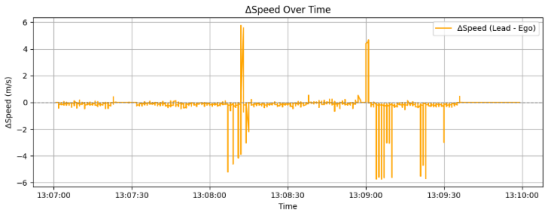

Fig. 3 (c). Delta speed

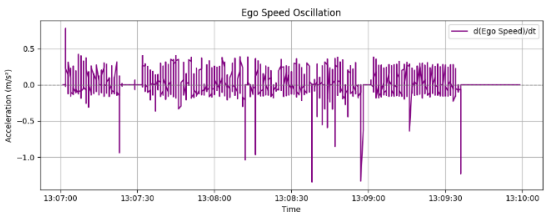

Fig. 3 (d). Eco speed oscillation

TABLE II
SUMMARY OF ACC PERFORMANCE MATRICES

Metric	Value
mean_delta_speed	-0.095
std_delta_speed	0.558
mean_ego_acceleration	0.000
std_ego_acceleration	0.131
max_ego_speed	10.877
max_lead_speed	10.793
speed_following_accuradcy (%)	97.916
afjust_reaction_match_rae (%)	58.306
emergency_brake_count	740
mean_distance	10.651
min_distance	3.191
max_distance	29.376

Testing results from the developed ACC system in the CARLA Simulator demonstrate its ability to maintain safe distances in dynamic situations. The system achieved 97.916% velocity accuracy in tracking the Lead Vehicle and maintained an average distance of 10.651 meters from the Lead Vehicle, exceeding the specified safety distance threshold. Additionally, the system exhibited an automatic braking Reaction Time of 0.3 seconds, indicating rapid response when detecting braking actions from the Lead vehicle.

This PID with Logic-Based Control approach is appropriate for implementation as an automotive engineering prototype and presents opportunities for future expansion. Potential development pathways include integration with Autonomous Emergency Braking (AEB) systems and incorporation into Full Autopilot systems or Lane Keeping Assist (LKA) technologies.

B. Lane Departure Warning (LDW)

LDW is another essential ADAS system that aims to reduce accidents caused by drowsiness, unintentional lane deviation, or driver inattention. An effective LDW system must accurately detect the vehicle's position on the road, respond in real-time, and provide precise warnings [2], [9]. This research focuses on developing and evaluating an LDW system using the CARLA Simulator, with a simulated front-facing RGB camera as the primary sensor. The system incorporates Computer Vision techniques and geometric logic to assess lane deviation and transmits warning signals through a Heads-Up Display (HUD), color indicators, and auditory alerts in situations where the vehicle is at risk of departing from its lane Operational Principles of LDW.

1) The system utilizes images from the sensor. camera.rgb mounted at the front of the vehicle (with a Field of View of 110° at a resolution of 1280 x 720 pixels) to capture real-time road and lane marking data [5].

2) The LDW employs the following image processing procedures:

• Grayscale → Gaussian Blur → Canny Edge Detection to decrease noise and detect lane markings efficiently

• Perspective Transform (Bird's Eye View) to adjust the image viewpoint to render lane markings as straight lines.

• Sliding Window Search + Polynomial Fitting to utilizes image window segmentation to detect left and right lane markings, followed by curve fitting to determine lane curvature [10].

• To compute the lane center point in relation to the vehicle position to measure lane deviation.

Fig. 4 illustrates the flowchart of the developed LDW.

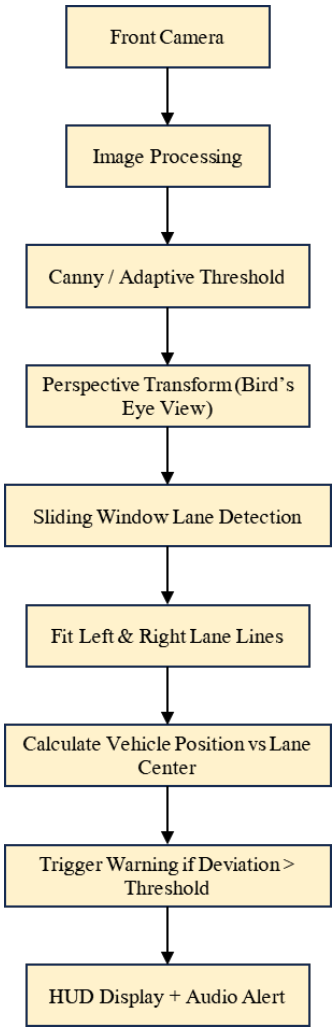

Fig. 4. Flowchart of LDW

Notification and Heads-up Display (HUD): When the system detects lane deviation exceeding the predetermined threshold values, it initiates driver notifications through multiple channels:

- Notification message "LDW: Lane Departure!" on HUD (red text).
- A flashing red bar displayed at the side of the screen to indicate danger.
- Beep.wav sound to notify the driver.
- Lane Overlay in green to follow the correct lane (bird's-eye overlay).

We tested the LDW system on the Town04 map in CARLA, simulating a route with extended continuous curves and implementing periodic transitions between driving modes, alternating between Manual mode (user-controlled) and Autopilot (automated driving system). We incorporated both intentional and unintentional lane deviations to observe LDW functionality across various scenarios. Figs. 5-7 illustrate examples of LDW system alerts during vehicle lane deviation. Fig. 8 shows the LDW simulation over time.

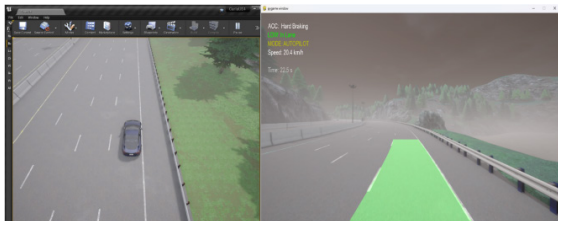

Fig.5. LDW test: Vehicle in lane (with complete or straight lane markings: Show Display = LDW: In Lane)



Fig. 6. LDW test: Lane departure (with complete or straight lane markings: Show Display = LDW: Lane Departure! and display a red frame to the right and left of the display frame.)

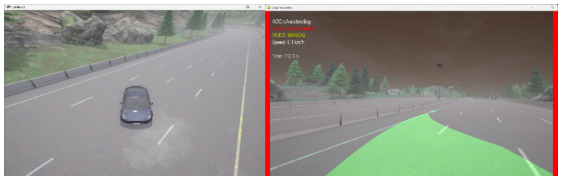

Fig. 7. LDW test: Lane departure (with incomplete or dashed lane markings: Show Display = LDW: Lane Departure! and display a red frame to the right and left of the display frame.)

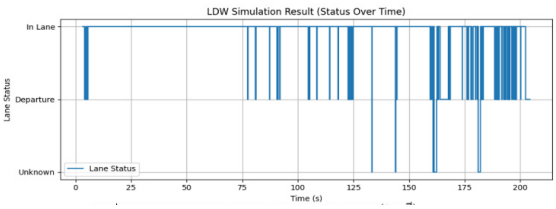

Fig. 8. LDW simulation over the time period

In Lane = vehicle in lane, Lane Departure = vehicle deviates from lanes, Unknown = LDW cannot detect, caused by unclear images or poor lighting, etc.

The developed LDW system demonstrates effective lane-deviation detection using data from a single RGB camera, employing geometric principles alongside fundamental image-processing techniques. The system provides real-time feedback through a Heads-Up Display (HUD) and auditory alerts, and is compatible with all driving modes. However, testing revealed that under certain conditions, such as heavy precipitation or roads with indistinct lane markings, the LDW system generates frequent false positives—error notifications exceeding 30% of instances. This error rate results from the system's inability to differentiate between clear and indistinct lane markings, particularly during adverse weather conditions like heavy rainfall. Future development of the LDW system could incorporate Deep learning methodologies within constrained computational resources.

V. Conclusions

This research focuses on developing Advanced Driver Assistance Systems (ADAS), specifically two primary systems: Adaptive Cruise Control (ACC) and Lane Departure Warning (LDW). Both ACC and LDW systems were developed and evaluated using the CARLA Simulator, a platform that provides a highly realistic automotive driving environment simulation and facilitates efficient algorithm development for control and sensor data processing.

The ACC system incorporates acceleration and braking force calculations utilizing data from a Radar sensor capable of detecting the distance and velocity of the Lead vehicle. A PID controller manages the driving system in real time to maintain safe distances from the Lead vehicle, enhancing driving convenience and safety. Testing results show that the system effectively adjusts the ego vehicle's behavior in response to the lead vehicle's movement, achieving a velocity tracking accuracy of 97.916%. The system maintains an average distance from the Lead vehicle of 10.651 meters, exceeding the specified safety threshold of 10.0 meters, with an automatic braking response time of 0.3 seconds. Additionally, the ACC system can initiate automatic braking when necessary, resulting in safe driving performance and appropriate responses to traffic conditions across all testing scenarios.

The LDW system uses forward-facing camera imagery and image-processing techniques, including Canny edge detection and Hough transform, to identify lane markings. The system incorporates a Heads-Up Display (HUD) and auditory alerts when it detects vehicle lane departure. Testing results indicate that the LDW system can continuously monitor lane positioning and departures throughout the testing period. When lane markings are intact or straight, the system demonstrates correct lane departure warning accuracy exceeding 75%. However, in heavy rainfall or on roads with incomplete or dashed lane markings, the LDW system produces false positives—incorrect warnings when the vehicle has not left its lane—exceeding 30%. Future LDW development could incorporate Deep learning in resource-constrained processing environments to improve detection accuracy by implementing confidence-level assessment for each frame. Because of the limitations of RGB camera technology, rainy weather degrades performance, resulting in over 30% false lane departure warnings. This could potentially be addressed by using deep learning methods instead of the Canny edge detection and Hough transform used in this experiment.

References

[1] S. Anand and S. S. Ohol, "Modelling and simulation of adaptive cruise control and overtake assist system," *Mater. Today Proc.*, vol. 72, pp. 1353-1360, 2023, https://doi.org/10.1016/j.matpr.2022.09.330

[2] Angelkim88, "CARLA-Lane_Detection," *GitHub repository*, 2020. [Online]. Available: https://github.com/angelkim88/CARLA-Lane_Detection [Accessed: Dec. 10, 2024].

[3] CARLA, "Quickstart start package instalbtion," *Carla Documentation*. [Online]. Available: https://carla.readthedocs.io/en/latest/start_quickstart [Accessed: Dec. 10, 2024].

[4] Carla Simulator, "scenario_runner", *GitHub repository*, 2018. [Online]. Available: https://github.com/carla-simulator/scenario_runner [Accessed: Dec. 10, 2024].

[5] Da-frank2, "Carla-object-detection-using-yolo," *GitHub repository*, 2022. [Online]. Available: https://github.com/Da-frank2/Carla-Object-Detection-Using-YOLO [Accessed: Dec. 10, 2024].

[6] A. Dosovitskiy, G. Ros, F. Codevilla, A. Lopez, and V. Koltun, "CARLA: An open urban driving simulator," in *Proc. 1st Annu. Conf. Robot Learn. (CoRL)*, 2017, pp. 1-16.

[7] *Intelligent transport systems—Adaptive cruise control systems—Performance requirements and test procedures*, ISO 15622:2018, Sep. 2018. [Online]. Available: https://www.iso.org/standard/71515.html

[8] *Intelligent transport systems—Forward vehicle collision warning systems—Performance requirements and test procedures,* ISO 15623:2013, Jul. 2013. [Online]. Available: https://www.iso.org/standard/56655.html

[9] *Intelligent transport systems—Lane Departure Warning systems—Performance requirements and test procedures*, ISO 17361:2017, Jun. 2017. [Online]. Available: https://www.iso.org/standard/72349.html

[10] C. Kedmanee, "Kalman filter modeling for trajectory prediction of cartraveling through Straight and curved lane boundaries," *Sripatum Rev. Sci. Technol*., vol. 5, no.1, pp. 57-66, Dec. 2013.
[11] KochlisGit, "Autonomous-Vehicles-Adaptive-Cruise-Control," *GitHub repository*, 2021. [Online]. Available: https://github.com/kochlisGit/Autonomous-Vehicles-Adaptive-Cruise-Control [Accessed: Dec. 10, 2024].
[12] M. Markofsky, M. Schäfer, and D. Schramm, "Use cases and methods of virtual ADAS/ADS calibration in simulation," *Vehicles*, vol. 5, no. 3, pp. 802-829, Jul. 2023, https://doi.org/10.3390/vehicles5030044
[13] E. P. Ping, J. Hossen, F. Imadudin, and W. E. Kiong, "Vision-based lane departure warning framework," *Heliyon*, vol. 5, no. 8, Art. no. e02169, Aug. 2019, https://doi.org/10.1016/j.heliyon.2019.e02169
[14] Siraphobk, "xd_senior2019_adas_selfdrive", *GitHub repository*, 2020. [Online]. Available: https://github.com/siraphobk/xd_senior2019_adas_selfdrive/tree/master [Accessed: Feb. 5, 2025].



Tanakorn Mongkondatsawat received a Bachelor of Science (B.Sc.) in Logistics and Supply Chain Management from Burapha University, Thailand, in 2024. He is currently pursuing a Master of Science program in Logistics and Supply Chain Management. His research interests include artificial intelligence development, logistics, and supply chain management.



Phanumat Rakngam received her B.Sc. degree in Logistics and Supply Chain Management from Burapha University, Thailand, in 2024. She currently works in the private sector in logistics and supply chain management. Her interests span intelligent transportation and supply chain process design.



Wutthichai Imwong earned a B.Sc. degree in Logistics and Supply Chain Management from Burapha University, Thailand, in 2024. As an undergraduate, he gravitated toward data-center projects—building proof-of-concept ADAS functions in the CARLA simulator, writing Python scripts for data cleaning and visualisation, and experimenting with machine-learning models for small research assignments. He is now looking at graduate study and early-career roles that combine data analytics, AI modelling, and software development. His current interests include applied machine learning, open-source software engineering, digital-twin simulation, and data engineering.



Namchai Sokai received a Master of Science in Logistics and Supply Chain Management from Burapha University, Thailand. He was a lecturer at the Faculty of Logistics at Burapha University, Thailand. His research interests are in future mobility, artificial intelligence, and optimization.



Nakorn Indra-Payoong received a Ph.D. in Computing from the University of Leeds. He is currently with the Faculty of Logistics, Burapha University, Thailand, where he serves as an associate professor in logistics and supply chain management. His research interests include large-scale network optimization and future mobility.

Measuring What Matters: Sustainable Performance Indicators and STI's Role in Achieving the SDGs

Kaewkarn Manosudprasit[1], Suchada Rianmora[2,*], and Pisal Yenradee[3]
[1,2,3]School of Manufacturing Systems and Mechanical Engineering (MSME),
Sirindhorn International Institute of Technology, Thammasat University, Pathumtani, Thailand
E-mail: d6622300132@g.siit.tu.ac.th, suchada@siit.tu.ac.th*, pisal@siit.tu.ac.th

Received: June 13, 2025 / Revised: January 1, 2026 / Accepted: February 2, 2026

***Abstract*—This study examines the pivotal role of Science, Technology, and Innovation (STI) organizations in advancing the United Nations Sustainable Development Goals (SDGs) and proposes a structured framework to assess their contributions through Sustainable Performance Indicators (SPIs). STI organizations are key enablers of progress in areas such as clean energy, healthcare, education, and climate resilience; however, existing measurement systems often overlook their broader societal and environmental impacts. This study evaluates the performance of three Thai STI organizations—NRCT, NSTDA, and TSRI—by applying the proposed SPI framework and assessing alignment with global sustainability frameworks, including ESG, GRI, Circular Economy (CE), BS 8001:2017, and ISO standards. The framework was validated through expert review panels and pilot testing within NSTDA, ensuring its relevance, reliability, and practical applicability. The research develops 26 SPIs linked to 81 SDG indicators, providing a practical roadmap for STI institutions to monitor and enhance their impact. The paper offers key recommendations for STI organizations, governments, and stakeholders to strengthen transparency, strategic alignment, and accountability in national and global sustainability agendas. The findings underscore the transformative potential of validated SPIs in guiding science and innovation toward inclusive, measurable, and sustainable development outcomes.**

***Index Terms*—Sustainable Development Goals (SDGs), Science, Technology and Innovation (STI), Sustainable Performance Indicators (SPIs), ESG, Circular Economy (CE), GRI, ISO Standards, BS 8001:2017, Impact Measurement; STI Policy, R&D Evaluation, Sustainability Reporting, Innovation for Development, NSTDA**

I. Introduction

The Sustainable Development Goals (SDGs), adopted by the United Nations in 2015, highlight the pivotal role of Science, Technology, and Innovation (STI) in driving progress across a wide range of targets, particularly those related to human well-being—such as health, access to clean water and sanitation, climate action, clean energy, decent work, and responsible consumption and production. As STI encompasses the creation, dissemination, and application of knowledge, it serves as a powerful tool for generating evidence to better understand the complex challenges associated with each SDG. Furthermore, STI can help identify and implement effective solutions, particularly in navigating the trade-offs that arise from the interconnected and systemic nature of the SDGs [1].

STI organizations—such as research councils, innovation agencies, and national laboratories—play a pivotal role in national development. These institutions fund and conduct research, promote stakeholder collaboration, and translate scientific knowledge into solutions that advance economic, social, and environmental progress. In Thailand, key agencies such as the National Research Council of Thailand (NRCT), the National Science and Technology Development Agency (NSTDA), and Thailand Science Research and Innovation (TSRI) align their work with strategic national frameworks, including the 20-Year National Strategy and the 13th National Economic and Social Development Plan. These strategies aim to enhance national competitiveness and sustainable development, with clear linkages to the SDGs.

STI is explicitly emphasized in SDG 9 (Industry, Innovation, and Infrastructure) and SDG 12 (Responsible Consumption and Production). The Addis Ababa Action Agenda (AAAA) also outlines over 20 STI-related commitments. The global STI Forum has repeatedly underscored the cross-cutting role of science and innovation in advancing nearly all

SDGs. Notably, STI holds great potential for developing countries by enabling homegrown innovation, strengthening technological capacity, and tailoring solutions to local challenges [2]. The Organization for Economic Co-operation and Development (OECD)'s Science, Technology, and Innovation (STI) indicators provide a detailed picture of a country's strengths, weaknesses, and unique characteristics in its science and innovation system. They are based on a collection of statistics that track innovation activities and outcomes among firms across OECD member countries and other economies [3]-[5].

At the regional level, the ASEAN Plan of Action on Science, Technology and Innovation (APASTI) 2016-2025 envisions an integrated, innovative, and sustainable ASEAN community. APASTI explicitly supports the SDGs through initiatives aimed at inclusive growth, strengthened STI infrastructure, and innovation-driven economies [6]. Thailand's commitment to the SDGs is reflected in its development planning framework guided by the principle of "leaving no one behind." The National Economic and Social Development Council (NESDC) [7], while not the lead STI policymaker, provides strategic guidance that informs the direction of STI-related agencies. Current national priorities, such as the Bio-Circular-Green (BCG) Economy Model, air pollution control, and plastic waste management, are closely intertwined with the SDGs [8]. Thailand has also pledged to reduce Greenhouse Gas (GHG) emissions by 20-25% by 2030 under the Paris Agreement, with a long-term vision for net-zero emissions between 2030 and 2040. However, operationalizing the BCG model and aligning environmental targets with other development goals remain ongoing challenges requiring stronger cross-sectoral coordination and concrete action plans [8].

ESG (Environmental, Social, and Governance), CE (Circular Economy), GRI (Global Reporting Initiative), BS 8001, and ISO standards offer structured approaches to corporate and institutional responsibility. However, a key challenge for local STI organizations lies in effectively adopting and integrating these frameworks to meaningfully support the achievement of the SDGs. In practice, many organizations implement these standards assuming they are equivalent to the SDGs. While these frameworks may align in some areas, they are not the same; adhering to them does not necessarily ensure the full realization of the SDGs. Consequently, indicators that effectively show how research contributes to specific SDG targets are lacking.

Despite STI organizations' critical role, measuring their actual contribution to the SDGs remains complex and underdeveloped. This study addresses this gap by developing a nationally contextualized framework of Sustainable Performance Indicators (SPIs) specifically tailored to Thai STI organizations, ensuring relevance to local institutional contexts and national priorities. By analyzing and comparing standards such as ESG, CE, GRI, BS 8001, and ISO, the research highlights key gaps and opportunities to improve current measurement systems. Ultimately, it advocates a more holistic, context-sensitive approach to evaluating STI performance that reflects their transformative potential in achieving the 2030 Agenda. This study aims to:

1) Analyze the role and impact of STI organizations in supporting and advancing the SDGs.

2) Identify and examine existing global sustainability frameworks (e.g., ESG, GRI, CE, BS 8001, ISO) as essential tools for evaluating and aligning organizational efforts with the SDGs.

3) Develop a set of Sustainable Performance Indicators (SPIs) and align them with global frameworks and 2030 SDG indicators to enhance accountability, transparency, and comparability.

4) Propose policy and implementation recommendations for STI institutions, governments, and stakeholders to adopt SPIs for more strategic planning and effective performance evaluation.

II. Literature Review

This study focuses on STI organizations, using the National Science and Technology Development Agency (NSTDA) as a case study and examining the impact of its research projects. As one of Thailand's leading STI organizations, NSTDA contributes significantly to the country's socio-economic development.

A. Linking STI Outcomes with Sustainable Goals:

STI is pivotal in addressing the complex, interconnected challenges outlined in the 2030 Agenda for Sustainable Development. More than just advancing new technologies, STI catalyzes systemic change, shaping economies, societies, and environmental outcomes. Global policy frameworks such as the Addis Ababa Action Agenda and Agenda 2030 highlight the importance of inclusive governance, knowledge-sharing, and capacity-building to unlock STI's full potential in driving sustainable development.

However, traditional STI approaches often face structural limitations. Aktar, Harun, and Alam [9] identify four key systemic failures that hinder STI's transformative impact: A lack of clear directionality, poor policy coordination, weak articulation of societal demand, and insufficient reflexivity in adapting to evolving challenges. Addressing these issues requires a shift toward more inclusive, sustainability-oriented innovation policies that promote diverse innovation

pathways and support long-term, cross-sectoral change [1].

To translate this vision into action, meaningful measurement tools are essential. SPIs provide a structured way to assess how well STI systems contribute to sustainable development outcomes. As the OECD notes [4], effective SPIs should go beyond conventional metrics, such as patent counts or publication volume, to encompass broader dimensions, including green technology adoption, social inclusion, and economic resilience. These indicators help capture both tangible outputs (e.g., new product revenues, technology transfer agreements) and intangible contributions (e.g., talent development, knowledge diffusion, and improvements in quality of life).

Zemlickienė and Turskis [10] identify key financial indicators for assessing R&D performance, including profit generated from R&D, budget adherence, and R&D spending as a percentage of sales. These indicators support SDG 12 (Responsible Consumption and Production) by promoting efficient resource utilization. Complementary efficiency metrics, such as project timelines, time-to-market, and R&D staffing changes, enhance operational assessment. Additionally, customer satisfaction measures, such as the new product acceptance rate, contribute to SDG 3 (Good Health and Well-being) and SDG 12 by reflecting the impact on consumer well-being and sustainable consumption.

Innovation-specific metrics, including the number of patents filed and new product sales as a share of total sales, align with SDG 9 (Industry, Innovation, and Infrastructure) and provide insights into technological advancement and market competitiveness (Ponta [11]). As R&D evaluations increasingly adopt multidimensional approaches, these indicators offer a more holistic view of both organizational efficiency and societal contribution.

Lee and Lee [12] further propose an evaluation model for public research institutions, emphasizing broader goals beyond profitability. Their framework includes academic publications, journal impact factors, technology transfer agreements, granted patents, and user satisfaction. Public R&D is also evaluated by its role in national capacity building, such as supercomputing infrastructure and workforce development, aligning with SDGs 4 (Quality Education) and 9 (Industry, Innovation, and Infrastructure).

Recognizing the different missions of public and private R&D institutions is also critical. While private R&D often emphasizes profit-driven innovation, public R&D typically focuses on delivering wider societal value. Lee and Lee [12] propose SPI frameworks tailored to these differences. For public research institutes, key indicators may include the number and impact of scientific publications, granted patents, the effectiveness of technology transfer, and the societal relevance of research outcomes, particularly in relation to SDGs 4 (Quality Education) and SDG 9 (Industry, Innovation, and Infrastructure).

In summary, aligning STI efforts with well-designed, context-sensitive SPIs offers a promising path to strengthen strategic planning, increase transparency, and ensure that innovation systems contribute meaningfully to both national priorities and global sustainable development goals.

B. Exploring Sustainable Practices and Global Frameworks Alignment

The reviewed literature reveals a broad spectrum of approaches and frameworks that aim to advance sustainability across sectors and geographies. Central to many studies is the alignment of organizational practices with the United Nations' SDGs. Research by Ikram [13] and Journeault [14] emphasizes how sustainability reporting frameworks, particularly the Global Reporting Initiative (GRI) [15], play a crucial role in promoting transparency and stakeholder engagement. For instance, Journeault [14] examined more than 50 documents to analyze how frameworks like GRI address social and environmental concerns, including their impact on indigenous communities. These efforts highlight the importance of effectively embedding SDG-aligned principles into business operations. R&D performance is another prominent theme. Zemlickienė and Turskis [10] proposed a detailed framework for evaluating R&D projects through indicators such as profitability, budget adherence, patent filings, and sales from new products. These financial and innovation-focused metrics are aligned with SDG 12 (Responsible Consumption and Production). Lee and Lee [12] expanded this perspective by categorizing R&D indicators based on their relevance and timing, especially within public-sector institutions. They argued for a clear distinction between public and private R&D objectives, with public initiatives often targeting societal outcomes such as talent development and improved quality-of-life goals that align with SDGs 4 and 9.

The transition from linear to CE models is also well-documented in the literature. De Jesus Pacheco [16] evaluated CE practices in 87 Brazilian SMEs using the BS 8001:2017 standard [17]. Their findings offer practical insights into applying CE principles in resource-constrained environments. Kirchherr [18] highlighted conceptual ambiguity in CE implementation by reviewing 221 definitions and emphasized the need for a unified framework. Alhawari et al. [19] showed how CE can integrate with Industry 4.0 technologies to improve resource

efficiency and sustainability outcomes. Together, these studies reinforce CE's potential to drive progress on SDGs 9, 12, and 13.

The role of policy frameworks in advancing sustainability goals is underscored in studies by [1] Niyommaneerat [20] and Journeault [14]. Niyommaneerat [20] assessed Corporate Social Responsibility (CSR) driven sustainability initiatives in Thailand, such as biogas and solar-powered water-pumping systems. These efforts not only align with SDG objectives but also deliver tangible environmental and social benefits. Meanwhile, Journeault [14] emphasized accountability and stakeholder engagement through adherence to sustainability standards. Moraga [21] and Martinho [22] provided further insights into industrial transitions toward CE. Moraga [21] identified 20 CE indicators designed to enhance both economic and societal outcomes, while Martinho [22] conducted a systematic review of over 1,000 academic papers to map trends and inform evidence-based policy development. These standards underscore the importance of integrating robust indicators, transparent reporting systems, and management for green to support the SDGs [23].

C. Research Gaps and Opportunities in SPI Adoption and R&D Alignment with the SDGs

Despite the increasing global recognition of the pivotal role that Science, Technology, and Innovation (STI) play in achieving the SDGs, a significant gap remains in the adoption and development of Sustainable Performance Indicators (SPIs) that accurately capture this relationship—particularly in developing countries like Thailand. Existing frameworks such as ESG, Circular Economy (CE), GRI, BS 8001, and ISO standards provide structured approaches for corporate sustainability reporting and responsibility [9], [15]-17], [24], [34]-[36]. However, these frameworks primarily target traditional business operations and often lack the specificity needed to assess the unique contributions of STI organizations, such as knowledge generation, technology transfer, innovation diffusion, and evidence-based policy-making. While these frameworks may align with certain SDG targets, they do not automatically reflect the transformative impact of STI activities, and adherence alone does not guarantee meaningful contributions toward national or global sustainability goals. While these frameworks provide valuable guidance for corporate sustainability, they are primarily designed for traditional businesses rather than for STI organizations that conduct research, innovation, and knowledge transfer. Key gaps include:

1) Activity vs. Outcome Measurement: Existing corporate frameworks focus on organizational activities, outputs, or compliance, rather than on measuring the transformative outcomes of research and innovation.

2) Sector-Specific Relevance: ESG, GRI, and CE metrics do not fully capture the unique contributions of STI organizations toward SDG-related goals such as technological capacity building, knowledge dissemination, or science-based policy support.

3) Integration with SDGs: While global frameworks provide high-level alignment, they lack tailored indicators that reflect the specific functions, programs, and outputs of STI institutions.

4) Contextualization for National Priorities: Current indicators do not account for local development strategies, institutional capabilities, or sector-specific challenges, leaving a gap in actionable, context-sensitive performance measurement.

As a result, STI institutions—despite their central role—struggle to demonstrate their direct and indirect impact on the SDGs. The absence of integrated SPI systems that explicitly connect STI outputs and outcomes to SDG targets undermines strategic alignment, institutional accountability, and evidence-based decision-making. In Thailand, no existing framework comprehensively measures the impact of public STI organizations against the SDGs, underscoring the urgent need for a nationally contextualized, outcome-oriented SPI system.

This context presents a critical opportunity to design and implement SPIs tailored specifically to the roles and functions of STI organizations. To address the identified gaps, this study develops 26 new Sustainable Performance Indicators (SPIs) for STI organizations in Thailand, linking their research and innovation activities directly to 81 SDG indicators. By leveraging insights from global sustainability frameworks—ESG, GRI, CE, BS 8001, and ISO—and adapting them to the operational and strategic realities of STI institutions, these SPIs provide outcome-oriented, context-sensitive metrics that complement existing corporate frameworks. Such SPIs enhance visibility, transparency, and strategic alignment, enabling STI organizations to demonstrate how research and innovation investments generate societal value. In Thailand, agencies like NSTDA are key examples, where adopting robust SPI frameworks can improve impact measurement, support evidence-based policy development, and strengthen national and international collaboration. Developing these 26 SPIs bridges the gap between global sustainability ambitions and the operational realities of STI organizations, providing a practical roadmap for a knowledge-based, resilient, and sustainable approach to national and international development.

This research shows how using SPIs can make it easier to evaluate and plan strategies more effectively, making national and international efforts to use STI

for sustainable development clearer, more transparent, and more impactful. Utilizing standard implementation tools to connect all the pieces—like a jigsaw puzzle—toward achieving the SDGs.

III. Research Methodology

This study employs a multi-step qualitative research methodology to develop SPIs for STI organizations aligned with the SDGs. The process begins with a comprehensive understanding of the SDG framework, which consists of 17 Goals, 169 Targets, and 231 unique indicators. It then explores the mandates and operational scope of STI institutions, evaluating the outcomes and impacts of their research projects and related activities. Subsequently, the study examines institutional missions to identify strategic priorities and analyzes how existing impacts align with SDG objectives. A thorough literature review is conducted to assess relevant global frameworks and standards—such as ESG, GRI, CE, ISO standards, and BS 8001:2017—to evaluate their applicability and relevance within the SDG context. It then compares these international frameworks with the SDG targets and assesses global methodologies used to measure R&D performance. The study also compares existing R&D indicators within STI institutions to SDG indicators, identifying overlaps and gaps through a detailed mapping process. Building on insights from NSTDA's existing activities and core capabilities, the research proposes mechanisms and activities that support all 17 SDGs in a practical, actionable way. It also develops tailored R&D project-level SPIs that can be used to explicitly measure contributions to specific SDG targets.

Finally, the study offers policy and implementation recommendations to facilitate the institutional adoption of these SPIs, ensuring that STI organizations are better equipped to contribute effectively and measurably to sustainable development.

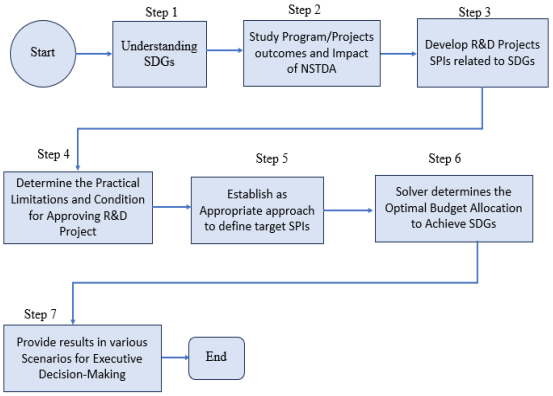

Fig. 1. The steps for Sustainable Performance Indicators (SPIs) as SDG-aligned tools to assess STI initiatives

IV. Global Standards and Frameworks with SDGS

This section explores key theories and frameworks related to the Sustainable Development Goals (SDGs) by examining global standards such as the Circular Economy (CE), Environmental, Social, and Governance (ESG), ISO standards [24], BS 8001:2017 [17], and the Global Reporting Initiative (GRI) [15]. It highlights their scope, relevance, and practical application, and compares their similarities and differences in supporting SDG implementation. The discussion highlights both the commonalities and distinctions among these frameworks, emphasizing how they support SDG implementation.

A. SDGs with ESG

ESG is a structured framework for assessing a company's sustainability performance and ethical practices. It evolved from the earlier concept of CSR, shifting from voluntary goodwill efforts to measurable, accountable business practices. This shift reflects growing expectations from investors, regulators, and society for transparency and long-term risk management. The rise of ESG was shaped by key milestones, such as the 2004 UN report *Who Cares Wins*, which emphasized the financial relevance of non-financial factors [25]. ESG became especially prominent in capital markets as a tool for evaluating business and managing sustainability [26]. While it began in developed countries and the finance sector, ESG has since gained global relevance, particularly as a corporate counterpart to the broader, society-level SDGs, introduced by the United Nations in 2015.

The SDGs provide a universal framework with 17 goals to tackle poverty, inequality, environmental degradation, and more, guiding national and global sustainable development efforts through 2030. ESG and SDGs differ in scope. ESG focuses on business-level practices, while the SDGs focus on global priorities; the two are complementary. Companies increasingly align ESG strategies with SDG targets to demonstrate their contribution to global sustainability. For example, a PTT's emission reduction efforts under ESG directly support SDG 13 (Climate Action), reflecting its integration of ESG principles with the SDGs [27]. However, ESG lacks a universal measurement and reporting standard, leading to inconsistencies across organizations. Scholars like Saetra argue that ESG frameworks often fall short in capturing the complex sustainability impacts of emerging technologies, such as Artificial Intelligence (AI). To address this, Saetra [28] proposes integrating ESG with the SDGs to better assess risks and benefits across micro to macro levels. Meanwhile, Delgado-Ceballos [29] emphasizes the

importance of the "double materiality" concept, considering both financial impact (on the company) and societal impact (on stakeholders and the environment). This dual perspective helps businesses navigate sustainability challenges more holistically and align their ESG activities with the SDGs.

In Thailand, Niyommaneerat [20] illustrates how CE indicators can enhance the integration of CSR and ESG in real-world projects like renewable energy and waste management. They advocate using CE-based KPIs aligned with ISO and GRI standards to bridge gaps in environmental and social performance and support the achievement of SDG targets.

In summary, ESG serves as a practical business tool to guide responsible investment and operational decisions, while the SDGs offer a global blueprint for sustainable development. Aligning ESG with the SDGs enables businesses not only to reduce risks and improve performance but also to contribute meaningfully to global goals, making sustainability a shared agenda for both the private sector and society at large.

B. SDGs with CE

CE initiatives in the EU effectively drive sustainability, helping most EU countries lead in SDG fulfillment [30]. According to Alhawari [19], CE is a strategic approach in which organizations design and manage products, components, and materials to retain their highest value for as long as possible. This is achieved by efficiently utilizing natural and economic resources and closing the loop across ecosystems and product life cycles. In essence, CE aims to extend product use beyond its initial life, thereby minimizing waste and maximizing resource efficiency.

However, their study also highlights a key challenge: The lack of a unified, system-wide definition of CE. Kirchherr [18] reinforces this point, identifying over 221 different CE definitions in academic literature, making it difficult to standardize measurement and guide consistent implementation. Despite this, CE is increasingly recognized as a powerful enabler of the SDGs, particularly SDG 12 (Responsible Consumption and Production), by promoting sustainable resource use, waste reduction, and circular production models.

Moreover, integrating CE indicators with SDG targets offers an opportunity to monitor and enhance progress. Yet, as Corona [31] argues, the effectiveness of this integration depends on harmonizing CE metrics and establishing clearer definitional standards. The CE significantly supports SDG achievement, with several CE indicators showing strong correlations with multiple SDGs [32].

In summary, the CE serves as a transformative strategy to accelerate SDG progress by encouraging resource efficiency, waste minimization, and sustainable production.

C. SDGs with GRI

The Global Reporting Initiative (GRI) [15], established in 1997 and formally launched in 2000 in collaboration with the United Nations Environment Programme (UNEP), is the second-largest international non-profit organization focused on sustainability reporting Journeault [14]. GRI plays a pivotal role in advancing economic, social, and environmental sustainability by providing comprehensive reporting guidelines and global standards. These standards promote transparency and accountability in corporate disclosures, addressing the evolving needs of diverse stakeholders [15]. GRI has become a de facto global benchmark for sustainability reporting, adopted by organizations in over 90 countries. Its wide user base spans multinational corporations, SMEs, NGOs, government bodies, and international initiatives such as the UN Global Compact [33]. Since 2016, GRI has actively aligned its standards with the United Nations Sustainable Development Goals, thereby strengthening the link between corporate sustainability performance and global development priorities. To support SDG integration, GRI has developed specific disclosures mapped to individual goals. For example:

GRI Standards 207:1-4, 203-2, and 207-2 correspond to SDG 1 (No Poverty).

GRI Standard 403 supports SDG 3 (Good Health and Well-being).

GRI Standard 404 aligns with SDG 4 (Quality Education).

GRI Standard 201 addresses SDG 8 (Decent Work and Economic Growth).

GRI Standard 302 contributes to SDG 13 (Climate Action).

GRI Standard 403 also supports SDG 16 (Peace, Justice, and Strong Institutions).

GRI Standard 303 supports SDG 6 (Clean Water and Sanitation).

The most recent update to GRI's SDG mapping was released in May 2022, further refining how sustainability disclosures align with the global goals [15]. GRI serves as a voluntary reporting framework for organizations, and the SDGs provide a broader roadmap for global sustainability, with the GRI helping companies align and measure their contributions toward these goals [33].

D. SDGs with ISO standard

The International Organization for Standardization (ISO) [34] plays a pivotal role in advancing sustainable development by providing a globally recognized framework for consistent, transparent practices [35]. With over 22,000 standards implemented in 170 countries, ISO contributes directly to achieving the SDGs by addressing environmental, social, and economic dimensions

(ISO, 2018a). These standards enable effective knowledge transfer across borders, promote responsible production and consumption, and support international trade partnerships [13]. ISO standards support SDGs by improving industry practices and aligning with specific targets like sustainable agriculture [36]. Key ISO standards are directly aligned with specific SDGs. For example, ISO 14001 (Environmental Management Systems) supports SDGs 13 (Climate Action) and 15 (Life on Land); ISO 26000 (Social Responsibility) addresses SDGs 2 (Zero Hunger), 5 (Gender Equality), and 10 (Reduced Inequalities); ISO 20400 (Sustainable Procurement) contributes to SDGs 1 (No Poverty), 2, and 12 (Responsible Consumption and Production); and ISO 50001 (Energy Management Systems) supports SDG 7 (Affordable and Clean Energy). Through these standards, ISO provides practical tools to guide governments, industries, and consumers toward more sustainable practices in line with Agenda 2030 (ISO, 2018b).

To enhance impact, it is essential to strengthen the alignment between the SDG Index and the ISO Standards Index. Doing so ensures that all stakeholders, including policymakers, businesses, and civil society, can effectively leverage ISO standards to monitor, manage, and improve their contributions to the SDGs. The strategic application of ISO's quality management principles serves as a vital mechanism for embedding sustainability into organizational operations and decision-making processes worldwide.

E. SDGs with BS 8001:2017

BS 8001:2017, developed by the British Standards Institution (BSI), provides practical guidance for organizations across various sectors in adopting CE practices [16], [28]. These standards bridge the gap between CE theory and implementation, making it accessible to businesses regardless of their level of experience with CE. By optimizing resource use, BS 8001 delivers significant environmental benefits while also contributing to economic growth, innovation, and social value, such as job creation and enhanced opportunities [16]. Introduced in May 2017, BS 8001's development began with research in 2013, which revealed a gap in specific CE standards. This led BSI to form a committee dedicated to sustainable resource management, resulting in a framework that was refined through consultations with global stakeholders. Developed over 18 months and refined through public consultation, the final standard reflects a comprehensive effort to ensure relevance and applicability across industries [17].

BS 8001 aligns closely with key SDGs, including SDG 12 (responsible consumption and production), SDG 14 (Life Below Water), and SDG 15 (Life on Land). By providing a structured approach to resource efficiency and waste reduction, it helps organizations meet these global sustainability targets. The standard is also particularly valuable for Small and Medium-Sized Enterprises (SMEs), which are vital to economic development, especially in emerging economies where SMEs account for over 70% of employment (UN, 2023). As de Jesus Pacheco [16] notes, BS 8001 offers valuable insights for managers and policymakers in navigating the challenges of implementing CE practices, thereby advancing sustainable development in these critical sectors. BS 8001 plays a crucial role in advancing sustainability by providing a practical framework for applying circular economy principles that align directly with several SDGs. It is particularly valuable for businesses in emerging and developing economies, helping them transition toward more sustainable practices and align operations with global sustainability goals.

In summary, the SDGs offer a global blueprint for sustainable development, while ESG provides a corporate-level lens to align business ethics and risks with organizational goals. CE supports SDG 12 by promoting resource efficiency and waste reduction. GRI translates SDGs into measurable corporate disclosures, enhancing transparency and accountability [31]. ISO standards guide consistent practices that align with economic, social, and environmental SDG targets. BS 8001:2017 operationalizes CE in organizations, especially SMEs, supporting SDGs 12, 14, and 15. Together, these frameworks integrate sustainability into strategy, operations, and reporting. Their synergy enables organizations to deliver measurable impact and accelerate SDG achievement.

V. Towards Sustainable Innovation Performance

Measurement dimensions vary by the purpose of the measurement. This study offers multifaceted perspectives on indicators, providing a rich understanding of their role in enhancing performance and the economic, environmental, and social responsibility of sustainable development. Research and Development (R&D) and innovation performance indicators are essential for assessing the success and impact of R&D projects, particularly in advancing technological progress, market competitiveness, and sustainability. A comprehensive framework of these indicators covers dimensions such as financial outcomes, project efficiency, customer satisfaction, and market success, aligning them with broader societal and sustainability goals. Integrating these indicators with the SDGs underscores the potential of R&D activities to contribute positively to economic, environmental, and social goals. By linking R&D performance with sustainable practices, organizations not only enhance their innovative outcomes but also address critical global challenges in line with sustainability objectives. Consequently, performance

in R&D that aligns with SDG practices will be referred to as the Sustainable Performance Indicators.

To analyze R&D metrics and the SDGs, these indicators provide a detailed, comprehensive assessment of R&D project performance at the project level. In contrast, the SDGs, established by the United Nations, comprise a set of global objectives designed to address diverse social, economic, and environmental challenges. Broader in scope, the SDGs provide a framework to guide international efforts toward a more sustainable and equitable future by 2030. They cover a wide array of issues, including poverty, hunger, health, education, gender equality, clean water, climate action, and more, with specific targets and metrics for tracking progress. While there may be overlaps between R&D performance indicators and certain SDG targets, the SDGs address systemic, global challenges that go beyond the scope of individual projects. Many studies recognize that specific projects may contribute to broader SDG goals. However, typical project-level output Indicators, such as the number of patents or publications, do not always directly reflect alignment with the wider SDG framework (Fig. 2).

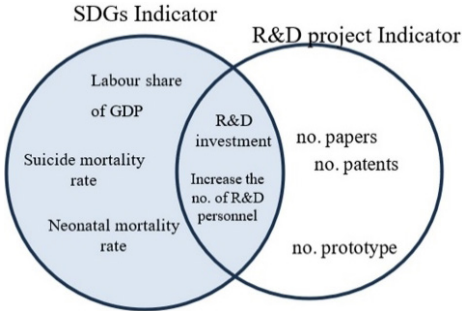

Fig. 2. SDGs Indicator and R&D Project Indicator

This diagram illustrates the overlap and distinction between SDG Indicators and R&D Project Indicators. The left circle represents SDG metrics—broad, global measures addressing societal, economic, and environmental challenges (e.g., Labour Share of GDP, Suicide Mortality Rate, Neonatal Mortality Rate aligned with SDG 3).

The right circle shows R&D Project Indicators, which assess specific research outputs such as the Number of Papers, Patents, and Prototypes, reflecting scientific and technological progress. The intersection highlights shared metrics where R&D efforts contribute to SDG targets. For example, R&D Investment aligns with SDG 8 (Economic Growth), while growth in R&D Personnel supports SDG 4 (Education) and 9 (Industry and Innovation). The diagram highlights that while many R&D indicators are project-specific, there are key overlaps where R&D activities align with SDG targets. This highlights the need to align project outcomes with broader sustainability objectives.

This study provides an in-depth analysis of all 17 SDGs, linking project-level indicators to global development objectives. It presents an opportunity to enhance efficiency and deliver high-impact outcomes in STI organizations, supporting economic growth, social well-being, and environmental sustainability.

VI. Guidelines for Graphics Preparation and Submission

A. Comparison of Global Frameworks with SDG Alignment

Table I, when comparing the SDGs, ESG criteria, CE principles, GRI, BS 8001:2017, and ISO standards, it's important to recognize their differences in scope, applicability, specificity, and other factors. The SDGs have a broad scope, addressing a wide range of global challenges across environmental, social, and economic dimensions. In contrast, ESG criteria, CE, GRI, BS 8001:2017, and ISO standards each have more specific focuses, tailored to organizations aiming to implement sustainability, CE practices, or comply with best practices in particular domains.

The choice of framework or standard depends largely on an organization's specific goals and priorities. These frameworks share similarities in their alignment with certain SDG goals and targets, emphasizing environmental, social, and economic considerations. However, they differ significantly in their specific focus and approach. The SDGs stand out for their wide-ranging and interconnected approach to global issues, whereas ESG criteria focus more narrowly on evaluating a company's ethical and sustainability performance. CE principles focus on promoting CE practices, and the GRI primarily focuses on sustainability reporting with defined indicators, offering a narrower scope than the SDGs. ISO standards, while varying in scope by standard, are generally more specialized, addressing particular aspects of business practices or management systems. BS 8001:2017, for instance, provides a framework for implementing CE principles within an organization and offers specific guidance on this topic.

Moreover, SDGs and ESG differ in several ways: ESG lacks a unified global definition and framework, is more process-focused than target-oriented, and lacks standardized metrics. This contrasts with the SDGs, which are globally recognized, target-oriented, and provide a comprehensive framework for addressing a wide range of interconnected global challenges. These distinctions underscore the broader, more inclusive nature of the SDGs in tackling global issues, compared to the more specialized and focused nature of ESG, CE, GRI, BS 8001:2017, and ISO standards. They overlap in their focus on sustainability and corporate responsibility, but each framework and standard serves a distinct purpose. The SDGs are a global blueprint for sustainable development, while

ESG criteria are primarily used for investment and reporting. CE standards and ISO standards focus on specific areas such as environmental management and quality control. GRI and BS 8001:2017 provide guidelines for sustainability reporting and CE practices, respectively. The choice of framework or standard depends on an organization's objectives, industry, and stakeholder needs. The audience for the SDGs is primarily governments and international organizations, while businesses and organizations use ESG, CE, GRI, BS 8001:2017, and ISO standards to measure and report their sustainability and corporate responsibility efforts. ESG, CE, GRI, BS 8001: 2017, and ISO standards provide more specific guidance and indicators for organizations to follow in their respective areas, whereas the SDGs offer a broader framework with global indicators.



Fig. 3. Align ESG, CE, GRI, ISO, and BS 8001:2017 frameworks with the SDGs

By aligning with the SDGs, frameworks like ESG, CE, GRI, ISO, and BS 8001:2017 help organizations turn global sustainability goals into actionable strategies, drive measurable impact, foster accountability, and accelerate the transition to a more sustainable and inclusive world, as shown in Fig. 3.

B. Key Framework

In summary, while the SDGs offer a broad and globally recognized framework for sustainable development, other standards and frameworks provide more specific guidance for measuring and reporting on corporate responsibility. Although many of these frameworks support sustainability assessment and reporting, a clear gap remains in standardized tools that directly measure contributions to SDG targets. This study addresses that gap by proposing a structured SPI that is explicitly aligned with the SDG indicator system, enabling organizations to evaluate and validate their impact more effectively. STI organizations play a vital role in driving progress toward the SDGs by promoting innovation, scientific research, and technological development that support social, economic, and environmental sustainability. Through their initiatives, these organizations align their efforts with the global SDG framework and address key areas such as clean energy, sustainable agriculture, healthcare innovation, and climate resilience. By collaborating with industry, academia, and government, STI organizations not only drive the development of technological solutions but also contribute to policymaking and capacity-building efforts [1]. These combined actions help ensure long-term, sustainable impacts across multiple sectors. The following section presents selected examples of how Science and Technology (S&T) initiatives align with the 17 SDGs, with reference to activities and projects undertaken by the National Science and Technology Development Agency (NSTDA). While these projects were not always initially designed with SDGs as the primary framework, many of them nonetheless contribute directly or indirectly to the SDG targets. Through years of work in areas such as advanced research, technology deployment, innovation support, and capacity building, NSTDA has built a foundation of programs and mechanisms that reflect its potential to support national and global sustainable development priorities.

VII. Sustainable Performance Indicators (SPIS)

This can serve as an essential tool for evaluating the performance and broader impact of STI initiatives, particularly in relation to the SDGs. This study underscores the significance of SPIs in offering a multidimensional assessment of R&D activities, moving beyond conventional metrics such as research outputs, patents, and R&D publications. Instead, SPIs provide a more holistic perspective by linking technological outputs with economic, environmental, and social objectives.

TABLE I
COMPARE THE SDGS, ESG, CE, GRI, BS 8001:2017, AND ISO STANDARDS

Items	Sustainable Development Goals (SDGs)	Environmental, Social, and Governance (ESG)	Circular Economy (CE)	Global Reporting Initiative (GRI)	BS 8001:2017	ISO Standards
Scope	The SDGs have a broad and comprehensive scope, covering a wide range of global challenges, including poverty, hunger, healthcare, education, gender equality, clean water, climate action, and more.	ESG criteria focus primarily on the environmental, social, and governance aspects of an organization's operations. ESG lacks a global definition and framework, is process-focused rather than target-oriented, and lacks standardized metrics.	CE principles focus on optimizing resource use, reducing waste, and managing the product life cycle. No single definition of CE or standard definition of CE.	GRI provides guidelines for organizations to report on their economic, environmental, and social impacts.	This British standard provides guidelines for implementing CE principles in organizations, focusing on minimizing waste, reusing resources, and improving resource efficiency.	ISO standards cover a wide range of topics, including quality management, environmental management, energy management, and many others. They provide specific guidelines and best practices for various aspects of an organization's operations.
Applicability	The SDGs are applicable globally and are intended for all countries and organizations, emphasizing shared responsibility and collaboration.	Businesses and investors primarily use ESG criteria to assess a company's environmental, social, and governance practices.	CE principles are relevant to businesses and organizations looking to transition from linear to circular consumption and production models.	Organizations use the GRI framework for sustainability reporting, and it applies to a wide range of industries.	BS 8001 is designed for organizations implementing circular economy practices and is particularly relevant to businesses aiming to reduce waste and improve resource efficiency.	ISO standards are applicable to organizations seeking to implement best practices in various domains, depending on the specific ISO standard.
Specificity	The SDGs provide a broad framework with 17 overarching goals, each with specific targets, but they allow flexibility for nations to adapt them to their specific contexts.	ESG criteria focus on environmental, social, and governance aspects, with individual companies defining their own ESG goals and metrics.	CE principles focus on resource efficiency, waste reduction, and product life cycle management.	GRI provides detailed sustainability reporting guidelines, offering specific indicators and metrics for measuring an organization's environmental, social, and economic impacts.	BS 8001 provides specific guidance on implementing CE principles, including strategies for resource efficiency and waste reduction.	ISO standards are highly specific to their respective areas, providing detailed requirements and guidance for organizations seeking to comply, such as environmental management (ISO 14001) or quality management (ISO 9001).
Differences	The SDGs address a broad spectrum of global issues, making them highly comprehensive. They emphasize interconnectedness among these challenges.	ESG criteria are narrower in scope compared to the SDGs. They concentrate on assessing a company's ethical and sustainability performance.	The scope of CE is specific to CE practices and principles, with an emphasis on sustainable resource management	GRI primarily focuses on sustainability reporting, offering specific indicators and metrics for measuring an organization's impacts, making it narrower in scope than the SDGs.	Its scope differs from the broad spectrum of the SDGs by focusing on CE practices.	ISO standards are highly specific to their respective areas, and their scope varies by standard.
Similarities	Like ESG and sustainability frameworks, the SDGs encompass environmental, social, and economic aspects, aligning with sustainability and responsible business practices.	ESG criteria are aligned with some of the goals and targets within the SDGs, especially those related to social and environmental aspects.	CE principles align with the environmental and economic aspects of the SDGs, particularly those related to responsible consumption and production (SDG 12).	GRI aligns with SDG reporting requirements, helping organizations measure and communicate their contributions to sustainability goals.	BS 8001:2017 aligns with the environmental and economic aspects of the SDGs, particularly those related to responsible consumption and production.	ISO standards may align with certain aspects of the SDGs, particularly those related to environmental and quality management, depending on the specific ISO standard in question.

TABLE II
STI INSTITUTE CONTRIBUTIONS TO SUSTAINABLE DEVELOPMENT GOALS (SDGS)

DG No.	SDG	Relevant STI Contribution	Explanation
1	No Poverty	Enhances economic prospects using scientific knowledge to develop local products and services. Promotes sustainable tourism based on unique local resources.	Empowers underprivileged populations and drives communities toward integrated, value-added initiatives.
2	Zero Hunger	Integrates technology, innovation, and local wisdom to improve agricultural production, food quality, nutritional value, and safety. Uses data-driven systems and biobank resources.	Strengthens food security and hygiene standards in Thai cuisine, enabling precise and modern management of the entire food supply chain
3	Good Health and Well-being	Promotes access to treatment, prevention, and rehabilitation services. Combats diseases and enhances overall healthcare outcomes for society.	Applying advanced genetic technologies, precision medicine, and research in vaccines, biopharmaceuticals, pharmaceuticals, medical devices, and digital health.
4	Quality Education	Provides lifelong learning, expands access to education, and nurtures talented youth in science for a future-ready workforce.	Provides accessible online and on-site learning, especially in remote areas, and develops young scientific talent through research, innovation skills, and applied scientific knowledge.
5	Gender Equality	Promotes equal opportunities and empowerment for women in leadership and research roles.	Contributes to a more inclusive and equitable scientific community.
6	Clean Water and Sanitation	Designs technologies to ensure safe and reliable water, detect contamination, and maintain supply.	Improves water quality management sustainably for households, communities, and agriculture.
7	Affordable and Clean Energy	Supports research innovations in low-carbon energy, renewables, energy management, storage, fossil energy, and smart grids.	Applies research to communities, supporting sustainable transportation and energy efficiency.
8	Decent Work and Economic Growth	Creates jobs throughout the value chain, boosts competitiveness, and drives nationwide economic growth.	Encourages entrepreneurs to return to their hometowns using infrastructure, workforce, and R&D support. Offers tax incentives and skill development.
9	Industry, Innovation and Infrastructure	Fosters tech businesses, scales research outcomes, and develops innovative cities with advanced infrastructure.	Ensures environmental sustainability, compliance with product safety and other regulations, and promotes growth in technology sectors.
10	Reduced Inequalities	Enhancing self-reliance and reducing economic, health, and educational inequalities to foster a more balanced socio-economic landscape, supported by Thai research reaching both domestic and international markets.	Promotes high-value Thai goods and services, fair income distribution, and access to standardized medical equipment, facilitating access to information and educational resources.
11	Sustainable Cities and Communities	Using advanced technology enhances urban living, resilience, and sustainable management of natural resources.	Develop smart cities that address health, pollution, waste, risks, emergency response, crime prevention, and cultural preservation.
12	Responsible Consumption and Production	Advances in technology and innovation to boost production efficiency, optimize food processing, improve consumption quality, and support sustainable food production and consumption	Create value-added products from leftovers, ensure traceability, improve waste management, and extend food shelf life.
13	Climate Action	At every stage of disaster management, technology plays a key role in reducing disaster impacts through a proactive approach to natural and climate-related challenges.	Creating technology to help communities before a crisis, reduce damage during it, and efficiently support recovery afterward.
14	Life Below Water	Supports the sustainable use of marine resources by preventing erosion and protecting ecosystems, helping to preserve the environment, biodiversity, and coastal areas.	Protecting ecosystems like mangroves, beaches, seagrasses, algae, corals**,** and local fisheries by preventing erosion, managing waste, and reducing microplastic impact**.**
15	Life on Land	Improving the protection, care, and restoration of ecosystems, natural resources, rare plants and animals, and biodiversity through scientific advancements.	Promote sustainability in forests, geology, unique species, and wildlife; restore damaged soil; and add value to conservation efforts.
16	Peace, Justice and Strong Institutions	Build trust among stakeholders and ensure transparent, ethical practices.	Implement good governance, anti-corruption, biosecurity, and ethical standards in science and AI.
17	Partnerships for the Goals	Establishes networks across government, private, academic, and civil sectors to share knowledge and collaborate both locally and globally.	Accelerates the application of research and joint innovation or investment for greater societal impact.

TABLE III
ALIGNMENT OF SUSTAINABLE PERFORMANCE INDICATORS (SPIS) WITH THE UN 2030 SUSTAINABLE DEVELOPMENT GOALS (SDGS)

SDGs	UNSD Indicator Codes	SPI no.	SPI Name
1, 2, 10, 14	C010101, C140701, C020302, C100101	SPI 1	Increment in population income (THB)
2	C020301, C020401	SPI 2	Increase in the productivity of smallholder production (tons)
2, 15	C020501, C020503, C150501, C200206, C150801	SPI 3	The number of plant and animal breeds or genetics that have been improved to have the potential to have characteristics such as increased yield, disease resistance, and stability in conservation settings over the medium or long term. (breeds or genetics)
3	C030301-5	SPI 4	Reduce medical expenditure per year (THB)
3	C030301-5, C030b01	SPI 5	Lower the import costs of medical products and pharmaceuticals (THB).
3	C030401-2, C030601, C030901-3	SPI 6	Reduce death rate (persons)
4, 8, 9, 10	C040301, C040401, C200306, C080201, C080601, C090202, C090502, C100401	SPI 7	Research Workforce and Job Market Readiness (persons)
5	C050502, C050C01	SPI 8	Proportion of Senior Executives (Female not less than male) ± 10 %
5	C050502, C050C01	SPI 9	Researcher proportion (Female not less than male) ± 10 %
3, 6	C060303, C060302, C06040, C030902	SPI 10	Amount of safely treated wastewater (cubic meters)
6	C060402, C060501	SPI 11	The no. of areas that receive sufficient water for consumption (rais)
3, 6	C060402, C060101, C030902	SPI 12	The no. of areas that receive sufficient water for consumption (households)
7	C070201,C200208	SPI 13	Increase standard and volume of biodiesel/ethanol production (tons)
7, 9, 13	C130202, C090401, C070201	SPI 14	Total CO_2 and Greenhouse Gas Emissions Reduction (tCO2e)
2, 8, 9, 12	C020301, C080101, C080901, C090301, C120b02	SPI 15	Increase entrepreneurial income (THB)
1, 8, 9, 11, 12, 14, 17	C200211, C080903, C090201, C090301, C090b01, C200211, C120b02, C140701, C170101, C170102	SPI 16	Economic development value (THB)
1, 3, 4, 6, 8, 10, 11	C010401, C030801, C040501, C060201, C080502, C200204, C110201, C110701	SPI 17	Opportunity to access affordable treatment, education, learning, information, and good standard products (case/person)
11	C110602	SPI 18	PM 2.5 emissions reduction (tons)
11, 12, 14	C110603, C140101	SPI 19	Waste Reduction and Effective Waste Management (tons)
5, 11, 16	C050202, C110702, C160101, C160103, C160402, C160501	SPI 20	The number of times security surveillance systems or technology devices can quickly alert and report incidents (cases)
12	C120301, C120501, C200208, C140401	SPI 21	Reduce 7 wastes (THB)
1, 11, 13	C200303	SPI 22	The no. of illnesses and deaths resulting from natural disasters decreased (persons)
6, 11, 14, 15	C060601, C110401, C140201, C140501, C150201, C150301, C150401, C150501	SPI 23	Sustainable ecosystem restoration and utilization (RAIS)
16	C160502	SPI 24	The average score for Integrity and Transparency (ITA) in NSTDA's operation is not less than 85
16	C160602	SPI 25	Referral score from NSTDA project service
15, 17	C200210, C170101, C170304, C170701, C170801	SPI 26	Income from NSTDA research work and services (THB)

By aligning SPIs with global sustainability frameworks such as the SDGs, STI organizations can better ensure that their initiatives contribute not only to economic growth and technological competitiveness but also to societal well-being. STI plays a key role in achieving the SDGs, particularly targets related to human well-being, such as health, clean water and sanitation, climate change, clean energy, decent work, and responsible production, among others. Because STI comprises the production, dissemination, and use of knowledge, it can expand the evidence available to appraise the challenges associated with each SDG. Moreover, STI can inform possible solutions to address the trade-offs that the systemic nature of the SDGs presents.

Integrating SPIs into performance evaluations enables organizations to track their contributions to pressing global challenges, such as poverty alleviation, gender equality, climate action, and inclusive development. This study advocates for the continued development and use of SPIs that reflect the expanded role of STI in advancing all 17 SDGs. Such indicators can guide strategic planning, improve accountability, and enhance the societal impact of

STI systems in both public and private sectors. This study supports the development and use of SPIs that reflect this broader STI role, aiming to guide and assess how effectively STI organizations contribute to eliminating poverty and hunger, reducing inequalities, protecting the environment, and fostering inclusive and sustainable development.

Table III shows 26 unique SPIs have been developed, each designed to correspond with 81 unique indicators from the United Nations Statistics Division (UNSD). These SPIs serve as tools to measure how effectively STI outcomes contribute to specific SDG targets. By applying a systematic mapping approach, STI activities are analyzed and linked to relevant SDGs based on their objectives and measurable benefits. This process not only shows potential alignment but also validates each activity's actual contribution to sustainable development outcomes.

For example:

Case 1: *NSTDA Research on Vaccine Development*

NSTDA has contributed to vaccine research and development efforts to combat diseases such as tuberculosis and malaria. This activity is directly aligned with SDG 3: Good Health and Well-being, specifically supporting Target 3.3, which aims to "*end the epidemics of AIDS, tuberculosis, malaria, and other communicable diseases*." It corresponds to the UN indicator that tracks the incidence rate of Tuberculosis, Malaria, and Hepatitis B per 100,000 population, identified under the code C030302-4.

The associated SPIs that validate this contribution include:

1) Reduction in import costs of medical products and pharmaceuticals related to the aforementioned diseases (THB).

2) Annual reduction in national medical expenditures due to domestically developed vaccines (THB/year).

These indicators confirm not only alignment with SDG 3, but also the tangible economic and health-related benefits derived from STI investments.

Case 2: *NSTDA research Clean Water Purification Innovation from Solar Energy*

NSTDA has developed an innovative clean water purification system that harnesses solar energy, providing an environmentally friendly and sustainable solution for communities with limited access to safe drinking water. This project aligns with multiple SDGs, including:

SDG 3: *Good Health and Well-being* – by reducing the incidence of waterborne diseases (Target 3.9), which aims to reduce deaths and illnesses caused by hazardous water, inadequate sanitation, and poor hygiene. The official UNSD Indicator Code: C030902 – *Mortality rate attributed to unsafe water, unsafe sanitation, and lack of hygiene*. The aligned SPI is SPI 4 – Reduction in annual medical expenditure (in THB) for waterborne diseases in communities.

SDG 6: *Clean Water and Sanitation* – by increasing access to safe and affordable drinking water, particularly in rural and underserved areas (Target 6.1), which aims to ensure universal and equitable access to safely managed drinking water services. The official UNSD Indicator Code: C060101 – *Proportion of population using safely managed drinking water services*. The aligned SPI 12 – Number of households gaining access to safe water through NSTDA-supported technological solutions.

SDG 13: *Climate Action* – by replacing conventional fossil fuel-based systems with solar-powered alternatives in water treatment processes (Target 13.2), which focuses on integrating climate change measures into national policies, strategies, and planning. The official UNSD Indicator Code: C130202 – *Total greenhouse gas emissions per year*. The aligned SPI 14 – Total CO_2 and greenhouse gas emission reduction (tCO_2e), reflecting annual reductions from the use of solar energy in place of fossil fuel-based systems. These examples show how SPIs go beyond general alignment—they act as validation tools by capturing specific, measurable outcomes that directly link NSTDA's benefits to SDG targets. The mapping ensures relevance, while the SPIs bring evidence and accountability to the contribution of research and innovation to sustainable development. Below are the SPIs derived from studying NSTDA's research projects and mapping their context to align with the SDGs by linking them to relevant UNSD Indicator Codes [36].

VIII. Discussion

Science, Technology, and Innovation (STI) organizations play an important role in supporting the Sustainable Development Goals (SDGs) by encouraging new ideas, promoting fair development for all, and helping protect the environment. However, this study identifies key challenges in measuring and enhancing their contributions, largely due to fragmented indicator systems, the lack of standardized SPI frameworks, and limited integration of global sustainability standards within institutional operations. The following discussion elaborates on these findings and outlines actionable recommendations for STI organizations, government bodies, and relevant stakeholders.

1) Fragmentation and Misalignment of SPI Systems: A significant challenge faced by STI organizations in contributing to the SDGs is the fragmentation and misalignment of SPI systems. Many organizations adopt internally developed or nationally contextualized indicators that, while useful for local performance assessment, often lack

alignment with internationally recognized frameworks such as ESG criteria, GRI, CE principles, BS 8001, and various ISO standards. This lack of harmonization hampers the comparability of performance outcomes across organizations and countries. Consequently, it impedes meaningful international benchmarking and reduces the transparency and credibility of sustainability reporting. Furthermore, the absence of standardized metrics complicates efforts to aggregate data for regional or global assessments, thereby weakening the evidence base for policy development and international collaboration. Bridging this gap requires integrating global frameworks into local SPI systems to ensure both contextual relevance and alignment with broader sustainability goals.

2) Limited Focus on Outcome-Oriented Metrics: A key limitation of current SPIs in STI organizations is their predominant focus on inputs and outputs—such as funding levels, number of publications, or completed projects—rather than long-term outcomes aligned with the SDGs. This emphasis fails to capture the broader societal and environmental impacts, such as reduced inequality, improved health, or ecological resilience. The absence of outcome-oriented metrics weakens the ability to assess the true effectiveness of STI initiatives in advancing sustainable development. It also constrains strategic decision-making and accountability, as stakeholders lack clear evidence of long-term impact. Shifting to outcome-based indicators is essential to align STI performance with transformative SDG objectives.

3) Insufficient Capacity and Awareness: Many STIs

Organizations in developing countries face significant institutional and technical limitations that hinder effective integration of SPIs into strategic planning and decision-making. These constraints often include limited human and financial resources, weak data management systems, and a lack of trained personnel to implement or interpret sustainability metrics. Moreover, awareness and understanding of global sustainability frameworks such as the SDGs, GRI, or ISO standards are often low. As a result, STI organizations may struggle to align their activities with international sustainability benchmarks or to report their contributions in a globally comparable manner. This combination of limited capacity and low awareness not only reduces the effectiveness of sustainability efforts but also diminishes opportunities for international collaboration, funding, and benchmarking. Strengthening institutional capabilities, improving technical infrastructure, and promoting knowledge exchange are therefore critical steps toward enabling STI organizations to meaningfully engage with sustainability agendas.

IX. Conclusion and Recommendations

To strengthen sustainability performance, STI organizations should first build clear, practical foundations for measurement and reporting. One essential step is to adopt structured approaches that guide how sustainability practices are planned, monitored, and evaluated.

1) Adopt and Localize Global SPI Frameworks

STI organizations should adopt and adapt globally recognized SPI frameworks—such as ESG, ISO standards, and Circular Economy (CE) principles—and tailor them to local contexts, organizational capacities, and sector-specific needs. Integrating these localized frameworks into routine planning, monitoring, and reporting helps improve consistency, comparability, and transparency. This approach strengthens internal decision-making, builds stakeholder trust, and ensures alignment with international sustainability standards. Ultimately, this supports a more coherent and effective STI agenda for long-term sustainable development.

2) Develop Outcome- and Impact-Based Indicators

Shift from measuring only activities and outputs to assessing real outcomes and long-term impact. For example, evaluate how R&D initiatives improve clean energy access, enhance food security, or support healthcare innovation.

3) Strengthen Capacity Building and Institutional Learning

Provide training programs, workshops, and strategic partnerships to improve institutional skills in sustainability measurement, impact assessment, and SDG-aligned data governance.

4) Provide Regulatory and Policy Support

Create supportive policies that encourage or require STI organizations to integrate SPIs. This may include national SDG strategies, STI roadmaps, or conditions tied to public funding.

5) Invest in National SPI Infrastructure

Support the development of digital platforms and national SPI databases that enable real-time tracking, reporting, and comparison of SDG contributions. Support pilots and innovation funds: Offer seed funding and technical assistance for STI-led SDG pilot projects to test new approaches and develop high-impact models that can be scaled up.

For future development, STI organizations should consider the combined strengths of three key models (Fig. 4): SPI coverage optimization – ensuring all priority areas are addressed. Cost-efficiency prioritization – maximizing impact while minimizing resource use. Time-discounted planning – considering long-term benefits and sustainability over time.

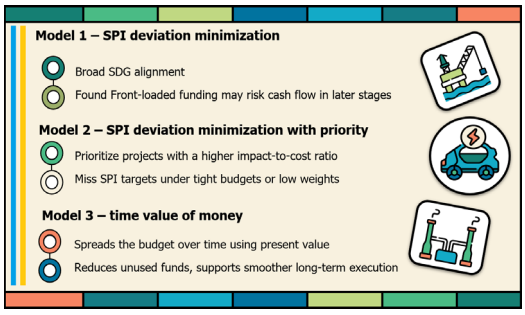

Fig. 4. Three key models for supporting future work

ACKNOWLEDGMENTS

The authors sincerely thank the Industrial Engineering Laboratory, School of Manufacturing Systems and Mechanical Engineering, Sirindhorn International Institute of Technology (SIIT), Thammasat University, for providing the necessary equipment and support throughout this research. Special thanks are extended to the Product Design and Development Research Team for their valuable assistance and insights into selecting and applying analytical methods for different types of data. The first author gratefully acknowledges the Half Faculty's Quota Scholarship awarded by SIIT, Thammasat University.

REFERENCES

[1] United Nations Industrial Development Organization (UNIDO) and United Nations Inter-Agency Task Team on Science, Technology and Innovation for the SDGs, *Science, Technology and Innovation for Achieving the SDGs: Guidelines for Policy Formulation*, Vienna, Austria, Apr. 2022, pp. 11-12, 27, 46.

[2] United Nations Inter-Agency Task Team on Science, Technology and Innovation for the SDGs, *Guidebook for the Preparation of Science, Technology and Innovation (STI) for SDGs Roadmaps*, 2nd ed. New York, NY, USA: United Nations, 2021, pp. 2, 19, 94.

[3] Organisation for Economic Co-operation and Development (OECD), *Governance of Innovation Systems: Synthesis Report*, vol. 1. Paris, France: OECD Publishing, 2005, pp. 28-29.

[4] Organisation for Economic Co-operation and Development (OECD), *Science, Technology and Innovation Indicators in a Changing World: Responding to Policy Needs*. Paris, France: OECD Publishing, Jan. 2007, pp. 19-20.

[5] Organisation for Economic Co-operation and Development (OECD), *Agenda for Transformative Science, Technology and Innovation Policies*, OECD Science, Technology and Industry Policy Papers, no. 16. Paris, France: OECD Publishing, Apr. 2024, pp. 11, 26-27, 29.

[6] Association of Southeast Asian Nations (ASEAN), *ASEAN Plan of Action on Science, Technology and Innovation (APASTI) 2016-2025*. Jakarta, Indonesia: ASEAN Secretariat, 2016. [Online]. Available: https://asean.org/book/asean-plan-of-action-on-science-technology-and-innovation-apasti-2026-2035/ [Accessed: Oct. 10, 2024].

[7] Office of the National Economic and Social Development Council (NESDC), *The thirteenth national economic and social development plan (2023-2027)*. Bangkok, Thailand: Office of the Prime Minister, 2023. [Online]. Available: https://www.nesdc.go.th/wp-content/themes/plant3-child/assets/pdf/13/article_file_20230615134223.pdf [Accessed: Jan. 14, 2025].

[8] National Science and Technology Development Agency (NSTDA), *BCG Model: Fostering sustainable development in Thai economy*. Pathum Thani, Thailand: NSTDA, 2024. [Online]. Available: https://www.nstda.or.th/en/images/pdf/BCG_Booklet1.pdf [Accessed: Nov. 6, 2025].

[9] M. A. Aktar, M. Harun, and M. M. Alam, *Science, Technology and Innovation (STI) policy for sustainable development*. Cham, Switzerland: Springer, Aug. 2020, pp. 1-12, https://doi:10.1007/978-3-319-71057-0_59-1

[10] V. Zemlickienė and Z. Turskis, "Performance measurement in R&D projects: Relevance of indicators based on US and German experts," *Sustainability*, vol. 14, no. 18, p. 11737, Sep. 2022.

[11] L. Ponta, G. Puliga, and R. Manzini, "A measure of innovation performance: The innovation patent index," *Manag. Decis.*, vol. 59, no. 13, pp. 73-98, Dec. 2021.

[12] K. Lee and S. Lee, "Enhancing R&D performance management: A case of R&D projects in South Korea," *Sustainability*, vol. 15, no. 15, p. 11752, Jul. 2023.

[13] M. Ikram, Q. Zhang, R. Sroufe, and M. Ferasso, "Contribution of certification bodies and sustainability standards to sustainable development goals: An integrated grey systems approach," *Sustain. Prod. Consum.*, vol. 28, pp. 326-345, May 2021.

[14] M. Journeault, Y. Levant, and C. F. Picard, "Sustainability performance reporting: A technocratic shadowing and silencing," *Crit. Perspect. Account.*, vol. 74, p. 102145, Jan. 2021.

[15] Global Reporting Initiative (GRI), "Global Reporting Initiative," [Online]. Available: https://www.investeurope.eu/invest-europe-esg-reporting-guidelines/mapping-of-voluntary-frameworks-and-standards/who-is-who/global-reporting-initiative-gri/ [Accessed: Jan 1, 2026]

[16] D. A. de Jesus Pacheco, I. S. Rampasso, G. S. Michels, S. M. Ali, and J. D. Hunt, "From linear to circular economy: The role of BS 8001:2017 for green transition in small business in developing economies," *J. Clean. Prod.*, vol. 439, p. 140787, Jan. 2024.

[17] STIP Compass, "The British Standards Institution," 2025. [Online]. Available: https://stip.oecd.org/stip/interactive-dashboards/policy-initiatives/2023%2Fdata%2FpolicyInitiatives%2F2783 [Accessed: Aug. 11, 2025].

[18] J. Kirchherr, N. H. N. Yang, F. Schulze-Spüntrup, M. J. Heerink, and K. Hartley, "Conceptualizing the circular economy (revisited): An analysis of 221 definitions," *Resour. Conserv. Recycl.*, vol. 194, p. 107001, Apr. 2023.

[19] O. Alhawari, U. Awan, M. K. S. Bhutta, and M. A. Ülkü, "Insights from circular economy literature: A review of extant definitions and unraveling paths to future research," *Sustainability*, vol. 13, no. 2, p. 859, Jan. 2021.

[20] W. Niyommaneerat, K. Suwanteep, and O. Chavalparit, "Sustainability indicators to achieve a circular economy: A case study of renewable energy and plastic waste recycling Corporate Social Responsibility (CSR) projects in Thailand," *J. Clean. Prod.*, vol. 391, p. 136203, Jan. 2023.

[21] G. Moraga et al., "Circular economy indicators: What do they measure?" *Resour. Conserv. Recycl.*, vol. 146, pp. 452-461, Jul. 2019.

[22] V. J. P. D. Martinho, "Insights into circular economy indicators: Emphasizing dimensions of sustainability," *Environ. Sustain. Indic.*, vol. 10, p. 100119, May 2021.

[23] L. Fonseca, F. Carvalho, and G. Santos, "Strategic CSR: Framework for sustainability through management systems standards—Implementing and disclosing sustainable development goals and results," *Sustainability*, vol. 15, no. 15, p. 11904, Aug. 2023.

[24] International Organization for Standardization, *Sustainable Development Goals* [Online]. Available: https://www.iso.org/sdg?utm_source=chatgpt.com [Accessed: Aug. 15, 2025].

[25] United Nations Global Compact, *Who cares wins: Connecting financial markets to a changing world*. Geneva, Switzerland: United Nations Global Compact and Swiss Federal Department of Foreign Affairs, 2004. [Online]. Available: https://documents1.worldbank.org/curated/en/280911488968799581/pdf/113237-WP-WhoCaresWins-2004.pdf [Accessed: Sep. 23, 2024].
[26] M. Gebhardt, T. W. Thun, M. Seefloth, and H. Zülch, "Managing sustainability—Does the integration of environmental, social and governance key performance indicators in the internal management systems contribute to companies' environmental, social and governance performance?" *Bus. Strategy Environ.*, vol. 32, no. 4, pp. 2175-2192, May 2023.
[27] PTT Public Company Limited, "Sustainability strategy, policy, and management, 2025-2029," *PTT PLC*, [Online]. Available: https://www.pttplc.com/en/sustainability/OVJXUXZoTGxMJTJmUHBpbTZDWjZhWG13JTNkJTNk [Accessed: Aug. 12, 2025].
[28] H. S. Saetra, "A framework for evaluating and disclosing the ESG-related impacts of AI with the SDGs," *Sustainability*, vol. 13, no. 15, p. 8503, Jul. 2021.
[29] J. Delgado-Ceballos, N. Ortiz-De-Mandojana, R. Antolín-López, and I. Montiel, "Connecting the sustainable development goals to firm-level sustainability and ESG factors: The need for double materiality," *BRQ Bus. Res. Q.*, vol. 26, no. 1, pp. 2-10, Jan. 2023.
[30] J. M. Rodriguez-Anton, L. Rubio-Andrada, M. S. Celemín-Pedroche, and M. D. M. Alonso-Almeida, "Analysis of the relations between circular economy and sustainable development goals," *Int. J. Sustain. Dev. World Ecol.*, vol. 26, no. 8, pp. 708-720, Nov. 2019.
[31] B. Corona, L. Shen, D. Reike, J. R. Carreón, and E. Worrell, "Towards sustainable development through the circular economy—A review and critical assessment on current circularity metrics," *Resour. Conserv. Recycl.*, vol. 151, p. 104498, Dec. 2019.
[32] A. K. Sah and Y. M. Hong, "Circular economy implementation in an organization: A case study of the Taiwan Sugar Corporation," *Sustainability*, vol. 16, no. 17, p. 7865, Sep. 2024.
[33] R. N. Archer and M. Mardiana, "Implementation of GRI and SDGs achievements in MSMEs sustainability report," *J. Akunt.*, vol. 17, no. 1, pp. 65-77, May 2025.
[34] International Organization for Standardization (ISO), *Contributing to Sustainable Development Goals with ISO Standards*. Geneva, Switzerland: ISO, 2018. [Online]. Availablehttps://www.iso.org/files/live/sites/isoorg/files/store/en/PUB100429.pdf [Accessed: Nov. 10, 2025].
[35] E. Ceko, "On the relationship between ISO standards and sustainable development," *Probl. Ekorozwoju*, vol. 18, no. 2, pp. 148-158, Jul. 2023.
[36] X. Zhao, P. Castka, and C. Searcy, "ISO standards: A platform for achieving sustainable development goal 2," *Sustainability*, vol. 12, no. 22, p. 9332, Nov. 2020.
[37] United Nations, *Global Indicator Framework for the Sustainable Development Goals and Targets of the 2030 Agenda for Sustainable Development*, 2025. [Online]. Available: https://agenda2030lac.org/estadisticas/global-indicator-framework-sdg.html [Accessed: Nov. 10, 2025].



Kaewkarn Manosudprasit is a Senior Officer at NSTDA, specializing in Policy and Planning Analysis. She received her B.Eng. in Industrial Engineering from the School of Manufacturing Systems and Mechanical Engineering (MSME), Sirindhorn International Institute of Technology (SIIT). She also holds an M.Sc. from the University of Hertfordshire. She is currently pursuing a Ph.D. in Engineering in Logistics and Supply Chain Systems Engineering (LSCSE) at SIIT. Her research interests include sustainable Research and Development (R&D) portfolio selection in Science and Technology organizations.

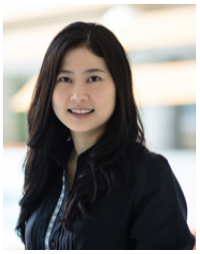

Suchada Rianmora is an Associate Professor at the School of Manufacturing Systems and Mechanical Engineering (MSME), SIIT, Thammasat University, Thailand. She received her D. Eng. in Design and Manufacturing from the Asian Institute of Technology. Her research focuses on product design and development, reverse engineering, rapid prototyping, image processing, industrial instrumentation, and manufacturing systems.



Pisal Yenradee is an Associate Professor at the School of Manufacturing Systems and Mechanical Engineering (MSME), Sirindhorn International Institute of Technology, Thammasat University, Thailand. He received his D.Eng. in Industrial Engineering and Management from the Asian Institute of Technology (AIT), Thailand. He has expertise in the analysis of production and inventory control problems in industrial settings and has spent nearly 35 years in this field.

Miniaturized Electrostatic Size Classifier (mESC): Development and Validation of Nanometer Aerosol Classification

Papol Sardyoung[1] and Panich Intra[2*]
[1]Department of Industrial Electrical Technology, Faculty of Industrial Technology, Thepsatri Rajabhat University, Mueang Lopburi, Lopburi, Thailand
[2]Research Unit of Applied Electric Field in Engineering College of Integrated Science and Technology, Rajamangala University of Technology Lanna, Chiang Mai, Thailand
E-mail: papol.s@lawasri.tru.ac.th, panich.intra@rmutl.ac.th[*]

Received: January 26, 2026 / Revised: April 10, 2026 / Accepted: April 22, 2026

***Abstract*— This study focuses on developing and testing the preliminary performance of a miniaturized electrostatic classifier for nanometer-sized aerosol particles. Designed with a parallel-plate configuration, the prototype classifies aerosols up to 300 nm in diameter. We first developed a mathematical model to accurately predict particle trajectories across sizes within the classifier. The physical prototype was then evaluated for its size-classification capabilities. Experimental findings showed strong agreement with theoretical predictions, confirming the model's effectiveness in designing such electrostatic classifiers. Furthermore, the prototype demonstrates promising potential for accurately classifying nanometer-sized aerosol particles.**

***Index Terms*— Aerosol, Nanoparticle, Miniature, Electrostatic, Size Classifier**

I. Introduction

Nanoparticles are particles characterized by diameters in the nanometer size range [1], [2], resulting from various chemical, physical, or biological processes. These particles are widely recognized for their technological importance across numerous disciplines. They are integral to fields such as materials synthesis, biotechnology, semiconductor manufacturing, pharmaceutical development, nanocomposites and ceramics, emission control, health effects studies, measurement and instrumentation, and fundamental investigations into transfer processes.

As particle size is a key physical characteristic that profoundly influences their behavior and dynamics, accurate measurement and classification are crucial. These activities are essential for better understanding particle transport, controlling contamination, and generating monodisperse particle samples needed for research.

Among the diverse techniques established for nanoscale aerosol particles, the electrical mobility analyzer has become the gold-standard instrument for both classifying and generating monodisperse particles. Electrical mobility measurements have a long history, dating back to the early twentieth century. This method of determination was initially applied to measure gaseous ions [3] and atmospheric ions [4]-[6]. Subsequently, Rohmann [7] was instrumental in utilizing this technique to quantify airborne particles in the atmosphere.

A typical electrical mobility analyzer (often referred to as a Differential Mobility Analyzer, or DMA) is generally constructed with two concentric electrodes between which a voltage is applied. An aerosol containing charged particles is introduced near one of the electrodes. Crucially, a particle-free sheath airflow separates the aerosol from the opposing electrode. The electric field established across the gap causes charged particles to migrate toward the opposing electrode. Since a particle's migration speed is directly proportional to its electrical mobility (which correlates with its size), particles exit the analyzer at different axial positions according to their size.

The electrical mobility analyzer has been the subject of continuous investigation and innovation, with recent developments comprehensively summarized by Flagan [8] and Intra and Tippayawong [9].

A significant portion of earlier research [10]-[16] has focused on refining performance through single-size channel identification, enhancing measurement capabilities, and expanding the instrument's operational size range.

More recently, the scientific community has seen a growing trend toward miniaturization of these analytical instruments. This shift aims to create instruments that are more portable, less expensive, and easier to deploy in various field settings while

maintaining high analytical accuracy. Such miniaturized DMAs (mDMAs) address the limitations of conventional benchtop instruments, which are often bulky and power-intensive.

This study contributes to the field by developing a miniature electrostatic classifier that accurately classifies nanometer-sized aerosol particles, operating on principles similar to those of its predecessors. However, the present analyzer distinguishes itself from existing instruments through the following key innovations:

1) Compact Design and Portability: The instrument was specifically engineered to be a small, cost-effective, and highly portable device. To minimize particle diffusion, we intentionally adopted a short classifier length. Its optimized dimensions and light weight improve handling and field mobility.

2) Controlled Operating Voltage: The applied voltage was maintained at a low level, significantly below the corona initiation voltage, to prevent any inadvertent or undesirable charging of particles within the classifier volume.

This research began by establishing a mathematical model to accurately predict particle trajectories inside the classifier for different particle sizes. This model then served as the foundation for designing the complete aerosol size spectrometer system. The final step involved experimentally testing the physical classifier prototype to comprehensively evaluate its aerosol size-classification performance.

Research Objectives: The primary goal of this study is to develop and validate a high-performance miniature electrostatic classifier. The specific objectives are as follows:

A. Design and Instrumentation

1) Mechanical Design: Develop a compact parallel-plate (or radial) classifier geometry optimized for a target size range of X-Y nm.

2) Flow Dynamics: Engineer the internal manifold to maintain stable, laminar sheath-to-aerosol flow ratios at Z flow rates, ensuring a distinct separation between particle trajectories.

3) Voltage Regulation: Implement a control system to maintain operating voltages significantly below the corona discharge threshold to prevent unintended particle charging and electrical noise.

B. Mathematical Modeling and Validation

1) Trajectory Prediction: Derive a robust mathematical model based on the balance of electrical drag and convective forces to predict the exit particle diameter (nm) as a function of the applied voltage (kV) and flow rate liters per minute (lpm).

2) Model Validation: Validate the theoretical transfer function against numerical simulations to account for non-ideal effects such as flow distortions at the inlet/outlet.

C. Performance Evaluation

1) Classification Accuracy: Determine the Geometric Standard Deviation (GSD) of the output aerosol to assess the instrument's ability to generate truly monodisperse samples.

2) System Reliability: Conduct longitudinal testing to evaluate the repeatability of measurements across multiple duty cycles and environmental conditions.

3) Loss Analysis: Quantify internal particle losses caused by diffusion and electrostatic attraction to non-target surfaces, particularly for particles under 20 nm.

D. Comparative Benchmarking

1) Standard Correlation: Perform side-by-side experimental runs with a commercial-grade DMA/SMPS (Scanning Mobility Particle Sizer) to correlate sizing accuracy and concentration measurements.

2) Efficiency Analysis: Compare the power consumption, weight, and response time of the prototype against the standard benchtop system to justify its use in portable applications.

Table I is a comparison between the prototype Miniaturized Electrostatic Size Classifier (mESC) evaluated in the study and conventional benchtop Differential Mobility Analyzers (DMAs):

TABLE 1
TECHNICAL SPECIFICATIONS COMPARISON: MESC PROTOTYPE VS. CONVENTIONAL BENCHTOP DMAS

Feature	mESC Prototype	Conventional Benchtop DMA
Device Type	Miniature Electrostatic Size Classifier (mESC)	Differential Mobility Analyzer (DMAs) / Standard Benchtop System
Geometry	**Parallel-plate configuration** consisting of two metal plates separated by a 2.5 mm gap	Generally constructed with **two concentric electrodes**
Size Range	Designed to classify nanometer-sized aerosol **up to 300 nm** in diameter	Measures broad nanoscale aerosol particles (specific numerical range is not detailed in the sources)
Flow	Engineered for a **1.0 L/min sheath flow rate**, and tested using a 0.6 L/min aerosol flow with total flow rates ranging up to 2.4 L/min	Utilizes a particle-free sheath air flow to separate the aerosol from the opposing electrode

TABLE 1
TECHNICAL SPECIFICATIONS COMPARISON: MESC PROTOTYPE VS. CONVENTIONAL BENCHTOP DMAS (CONT.)

Feature	mESC Prototype	Conventional Benchtop DMA
Voltage	Tested at low-level applied DC voltages from **0.5 kV to 2.5 kV** to prevent inadvertent particle charging, though the physical gap allows for a theoretical breakdown limit of roughly 7.5 kV	Operates by applying a voltage between the two concentric electrodes to establish an electric field (specific operational voltages are not listed)
Footprint	Highly compact and portable, measuring exactly **120 mm (L) × 80 mm (W) × 40 mm (H)**	Larger, standard benchtop systems that are generally less portable, heavier, and more expensive to deploy in field settings

II. SCHEMATIC DESCRIPTION OF THE MINIATURE ELECTROSTATIC SIZE CLASSIFIER

The schematic diagram of the prototype miniature electrostatic classifier is illustrated in Fig. 1, Classifier Core and Structure. The classifier utilizes a parallel-plate configuration, consisting of two metal plates separated by a 2.5 mm gap. This gap defines the height of the size classification zone. To minimize electrostatic particle losses during aerosol transport, the metal plates were designed with separate channels for polydisperse and classified aerosol flows. For safety, these two metal electrode plates are housed in a Teflon enclosure and electrically insulated.

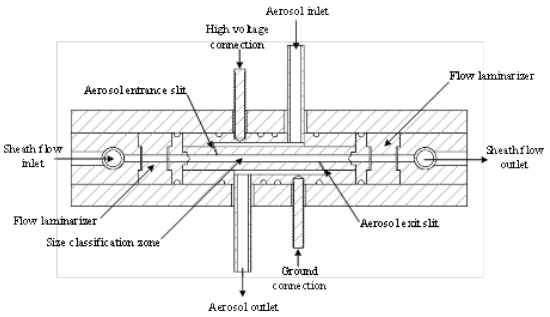

Fig. 1. Schematic diagram of the studied miniature electrostatic classifier

A. Aerosol and Sheath Flow Configuration

1) Aerosol Inlet: The polydisperse aerosol flow is introduced at the top inlet of the classifier. It subsequently passes through a triangular-shaped flow channel before entering the classification zone via the Aerosol entrance slit.

2) Electrodes and Field: A positive high DC voltage is applied to the top electrode plate (high-voltage connection), while the bottom electrode plate is electrically grounded (Ground connection). This setup establishes a uniform electric field within the particle-size classification zone.

3) Sheath Flow: Sheath air enters the classifier through the left inlet, passing through a screen-type flow linearizer to ensure a smooth, stable flow profile before reaching the classification zone. The excess flow then exits the classifier through the right-side outlet (Sheath flow outlet).

4) Classified Aerosol Outlet: The channel for the classified aerosol (Aerosol outlet) in the bottom metal plate is designed symmetrically to the inlet channel.

B. Design Parameters and Performance Goal

The geometry of the core components was precisely engineered:

1) Slits: The slits for aerosol entrance and exit are 2 mm long and 0.5 mm wide. Using a shorter slit length relative to the classification zone width helps keep aerosol flow away from the classifier's side walls, mitigating particle wall loss. The center-to-center distance between the entrance and exit slots is 40 mm.

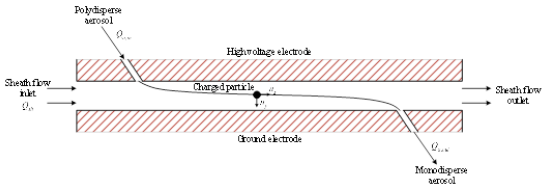

Fig. 2. Schematic diagram of particle trajectory in studied miniature electrostatic classifier

Performance: The prototype M-EC was engineered to classify particles up to 300 nm in diameter at a sheath flow rate of 1.0 liters per minute (lpm).

Footprint: The prototype's overall dimensions are remarkably compact, measuring 120 mm in length, 80 mm in width, and 40 mm in height, underscoring its miniature, portable design.

Fig. 2 illustrates the fundamental principle of particle classification by depicting a schematic of a charged particle's trajectory within the miniature electrostatic classifier. Particle Motion Dynamics: The movement of a particle inside the classification zone is governed by two primary forces, resulting in two distinct velocity components:

a) Axial Motion (u_z): The particle's motion along the length of the classifier (z-axis) is dictated by the fluid velocity profile of the combined sheath and aerosol flows. Since the flow is typically laminar, the particle is carried axially along the flow streamlines.

b) Radial Motion (u_r): The particle's lateral movement (r-axis) is primarily driven by the electric force. For nanometer-sized aerosols, the electric force is significantly stronger than other lateral forces, such as gravity or diffusion, making it the dominant factor in radial transport. Classification Mechanism, when a charged particle enters the size classification zone, the

applied electric field causes it to acquire an electrical mobility. This mobility, inversely proportional to the particle's size, determines how quickly the particle migrates radially toward the grounded electrode.

As shown in the diagram, polydisperse aerosol (Q_a,in) is introduced, and depending on a particle's electrical mobility (and thus its size), it follows a specific curved path. Only particles with a narrow range of mobilities will successfully exit through the Aerosol outlet (Q_a,out), resulting in a monodisperse aerosol sample. Particles outside this range will either deposit on the collection electrode or be carried out with the sheath-flow outlet.

It is assumed that: The flow and electric fields are axisymmetric and steady, the flow in the classifier is laminar, fully developed, and incompressible ($\nabla \cdot u = 0$), the space charge effect is negligible ($\nabla \cdot E = 0$), and the gravitational and Brownian diffusion effects are negligible. The total volumetric flow rate,Q_t, through the classifier column is

$$Q_t = Q_{sh} + Q_a \tag{1}$$

where Q_{sh} is the particle-free sheath air flow rate and Q_a is the aerosol flow rate. For the particular case of annular geometries where the charged aerosol sample enters the classifier on an axial flow, and the charged particles migrate along the radial direction of the electric field, the motion of the charged particles within the classification zone can be described by the system of differential equations as [17].

$$\frac{dy}{dt} = u_y + Z_p E_y \tag{2}$$

$$\frac{dz}{dt} = u_z + Z_p E_z \tag{3}$$

Where y and z are the radial and axial dimensions of the classifier, u_y and u_z are the radial and axial components of the air flow velocity. Similarly, E_y and E_z are the radial and axial components of the electric field and Z_p is the electrical mobility of particles. When a uniform electric field is established between the two electrodes of the classifier, the electric field components are given by the following relations

$$E_y = \frac{V}{h} \quad \text{and} \quad E_z \approx 0 \tag{4}$$

where V is the applied electrode voltage and h is the height of the classifier. Assuming uy = 0 and uz = uz(y). Substituting into Equations (2) and (3) gives the following differential equations describing the trajectory of an aerosol particle in a viscous flow [17],

$$\frac{dy}{dt} = \frac{Z_p V}{h} \tag{5}$$

$$\frac{dz}{dt} = u_z(y) \tag{6}$$

where:

$$u_z(y) = \frac{h^2}{2\mu}\left(-\frac{dp}{dz}\right)\left(\frac{1}{4} - \frac{y^2}{h^2}\right) \tag{7}$$

dp/dz represents the constant pressure gradient, defined by equations

$$\frac{dp}{dz} = -\frac{\rho \bar{U}^2 f}{2D_h} \tag{8}$$

Where:

$$D_h = 2h, \tag{9}$$

$$f = \frac{96}{Re} \tag{10}$$

$$Re = \frac{\bar{U}\rho D_h}{\mu}, \tag{11}$$

D_h Is the hydraulic diameter for an annular flow area f is the friction factor, $\bar{U}$ is the mean axial flow velocity, ρ is the gas density and Re is the Reynolds number in the annular flow. Using Equations (5) and (6), the trajectory of the charged particle in a viscous flow is given by

$$\frac{dy}{dz} = \frac{\frac{dy}{dt}}{\frac{dz}{dt}} = \frac{Z_p V}{u_z(r)h} \tag{12}$$

Integrating Equation (12), the migration paths of the charged particles can be determined. Their landing location downstream of the aerosol inlet is given in terms of their electrical mobility, the flow velocity profile, and the electric field strength:

$$\frac{h^2}{2\mu}\left(-\frac{dp}{dz}\right)\int_0^y \left(\frac{1}{4} - \frac{y^2}{h^2}\right) dy = \frac{VZ_p}{h}\int_0^z dz \tag{13}$$

The particle entering the classifier at a radial position of has a trajectory taking it to an axial position of z, which can be obtained as

$$z = -\frac{y}{VZ_p}\left(-\frac{h^2}{2\mu}\frac{dp}{dz}\left(\frac{y}{4} - \frac{y^3}{3h^2}\right)\right) \tag{14}$$

Which rearranges in terms of the critical electrical mobility of y a particle that is collected on the electrode at a distance z downstream of the aerosol inlet can be calculated as

$$Z_p = -\frac{y}{Vz}\left(-\frac{h^2}{2\mu}\frac{dp}{dz}\left(\frac{y}{4} - \frac{y^3}{3h^2}\right)\right) \tag{15}$$

C. Experimental Setup for Performance Evaluation

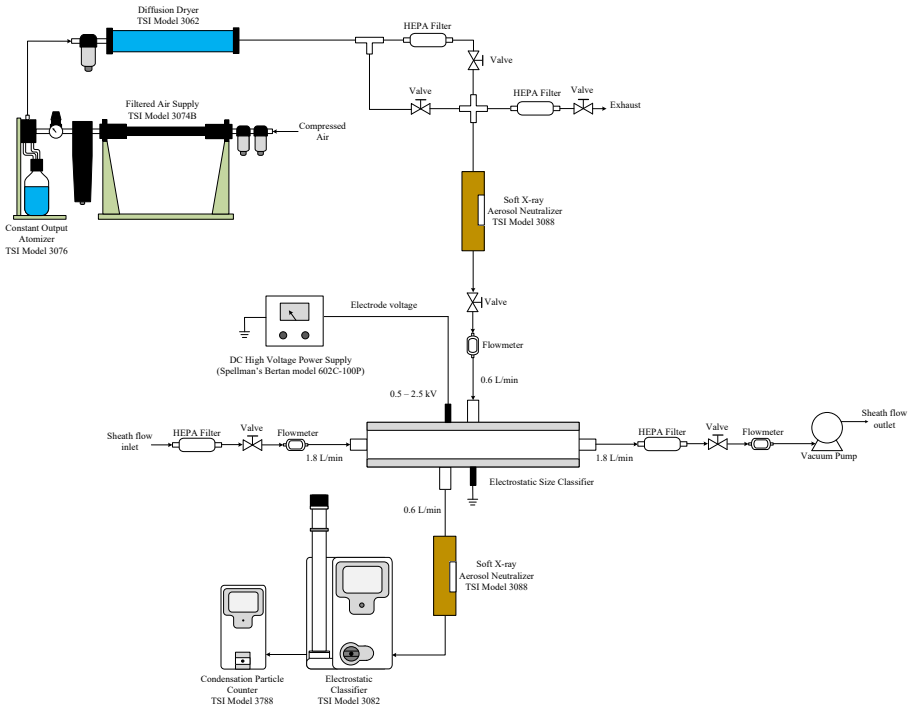

Fig. 3. Experimental setup for the performance evaluation of the miniature electrostatic classifier

Fig. 3 presents the comprehensive experimental setup used to evaluate the performance of the miniature electrostatic size classifier. System Components and Aerosol Generation The integrated system comprises several standard components, including an aerosol atomizer, a filtered air supply, an aerosol neutralizer, concentration adjustment valves, a HEPA filter, a diffusion dryer, flowmeters, a vacuum pump, a DC high-voltage power supply, the electrostatic classifier under investigation, and an Ultrafine Condensation Particle Counter (UCPC). Sodium Chloride (NaCl) polydisperse particles were generated by atomizing a 0.1% (w/w in water) NaCl solution using an Aerosol Atomizer (TSI Model 3076) paired with a Filtered Air Supply (TSI Model 3074B). The resulting wet NaCl particles were then passed through a Diffusion Dryer (TSI Model 3062) to reduce the relative humidity to below approximately 30% RH. Aerosol Conditioning and Characterization.

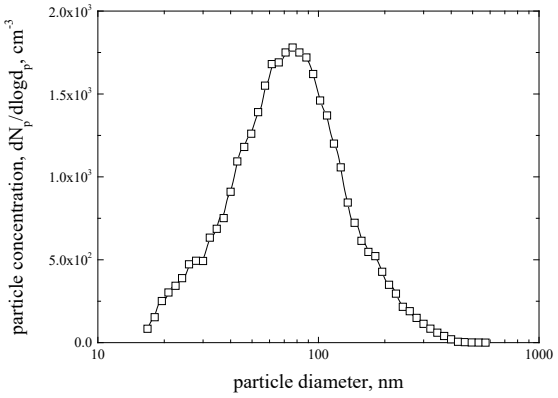

Fig. 4. Particle concentration and size distribution of sodium chloride particles generated from an atomizer

The generated NaCl particles inherently carry some electric charge. Failure to neutralize these charges could lead to significant particle losses due to electrostatic deposition on the inner walls of the tubing and other surfaces within the system. Therefore, a Soft X-ray Aerosol Neutralizer (TSI Model 3088) was employed to bring the particles to their Boltzmann charge equilibrium state. Particle number concentration could be precisely regulated by adjusting the concentration adjustment valves in combination with a HEPA capsule filter. Fig. 4 presents the particle concentration and size distribution of the polydisperse sodium chloride (NaCl) aerosol generated by the atomizer and conditioned by the system.

Analysis of the generated aerosol confirms that the particles follow a log-normal distribution. Specifically, the polydisperse NaCl aerosol utilized for the performance evaluation exhibited a mean particle diameter of 98.8 nm, a total number concentration of 1.74 x 10^3 particles/cm^3, and a geometric standard deviation (sigma_g) of 2.0. This distribution served as the input challenge aerosol for the miniature electrostatic classifier. Classifier Operation and Measurement

The prepared polydisperse NaCl particles were introduced into the classifier under study for size classification based on their electrical mobility. The classifier was operated at a target aerosol flow rate (Q_a,in) of 0.6 L/min and a sheath flow rate (Q_sh) of 1.8 L/min. The high voltage applied to the classifier electrodes was supplied by a DC High Voltage Power Supply (Spellman & Bertran model 602C-10P), with a sweep range of 0.5-2.5 kV.

At a specific applied voltage, the particles exiting the examined classifier constitute an almost singly charged, monodisperse aerosol flow. We then introduced this classified monodisperse flow into a Scanning Mobility Particle Sizer (SMPS) system to measure particle size distribution. The SMPS configuration included a second aerosol neutralizer, a standard Electrostatic Classifier (TSI Model 3082) equipped with a long Differential Mobility Analyzer (DMA) (TSI Model 3081, operated at a 3.0 L/min sheath airflow), and an Ultrafine Condensation Particle Counter (UCPC) (TSI Model 3788). This downstream SMPS system enabled accurate measurement of the particle size distribution, with a mobility-diameter selection range spanning 10 to 700 nm.

The performance evaluation of the miniature electrostatic size classifier is based on several key operational parameters and aerosol characteristics.

Input Challenge Aerosol Metrics: The classifier was tested using polydisperse Sodium Chloride (NaCl) particles generated from a 0.1% NaCl solution. Before entering the classifier, these particles were dried to below 30% relative humidity and neutralized to their Boltzmann charge equilibrium state to prevent electrostatic deposition losses. The resulting challenge aerosol followed a log-normal distribution with the following specific metrics:

1) Mean particle diameter: 98.8 nm

2) Total number concentration: 1.74 x 10^3 particles/cm^3

3) Geometric standard deviation: 2.0

Classifier Operating Parameters: To evaluate its classification capabilities, the device was operated under precisely controlled flow and voltage metrics:

1) Aerosol flow rate (): 0.6 L/min

2) Sheath flow rate (): 1.8 L/min

3) Applied electrode voltage: Swept across a range of 0.5 to 2.5 kV using a DC high-voltage power supply.

Output and Measurement Metrics: The primary performance outcome is the classifier's ability to produce an almost singly-charged, monodisperse aerosol flow at a specific applied voltage. We measured the accuracy of this size classification using a downstream Scanning Mobility Particle Sizer (SMPS) system. This system tracked the output particle size distribution across a mobility-diameter range of 10-700 nm.

Particle normalization is performed using a soft X-ray aerosol neutralizer to stabilize charge. The concentration efficiency is then evaluated across the 10-700 nm range using a UCPC integrated with an SMPS system.

The system's repeatability is determined by the consistency of the monodisperse aerosol output and the stability of the particle size distribution across multiple measurements at the same applied voltage.

D. Mitigation of Particle Loss and Diffusion

The experiments used instruments to manipulate factors affecting particle movement and dispersion, as follows:

1) To ensure stable distribution, wet NaCl particles are processed through a diffusion dryer to maintain relative humidity below 30%RH.

2) A Soft X-ray Aerosol Neutralizer is utilized to reach a Boltzmann charge equilibrium state.

3) This neutralization step is critical to prevent significant particle losses caused by electrostatic deposition on the internal surfaces of the system.

Table II presents an uncertainty budget: voltage ±%, flow rate ±%, dimensional tolerance ±mm, and the expected impact on the classified diameter.

TABLE II
UNCERTAINTY BUDGET TABLE AND IMPACT ON PARTICLE CLASSIFICATION

Source of Uncertainty	Estimated Uncertainty	Expected Impact on Classified Particle Diameter (d_p)
Applied Voltage	±1% to ±2%	**Moderate:** Directly affects electrical mobility. If the voltage is unstable, it shifts the selected d_p, leading to sizing inaccuracies.
Flow Rates	±3% to ±5%	**High:** The ratio of sheath flow (1.8 L/min) to aerosol flow (0.6 L/min) determines resolution. Flow fluctuations cause "peak broadening" in the size distribution.
Physical Dimensions	±0.05 to ±0.1 mm	**Constant:** Uncertainties in electrode spacing or classifier geometry create a systematic bias, causing the actual d_p to deviate from theoretical values.

III. RESULTS AND DISCUSSION

Calculation Setup and Governing Parameters: The particle trajectories within the classifier cavity, situated between the two parallel electrodes, were calculated across a range of operating conditions: Particle sizes from 50 to 200 nm, electrode voltages from 0.5 to 2.5 kV, and total flow rates from 1.8 to 3.0 L/min, all at a constant operating pressure of 1 bar. The calculated results predicted the precise locations where the charged particles were deflected radially and subsequently collected at the electrode surface. Influence of Particle Size (Fig. 5).

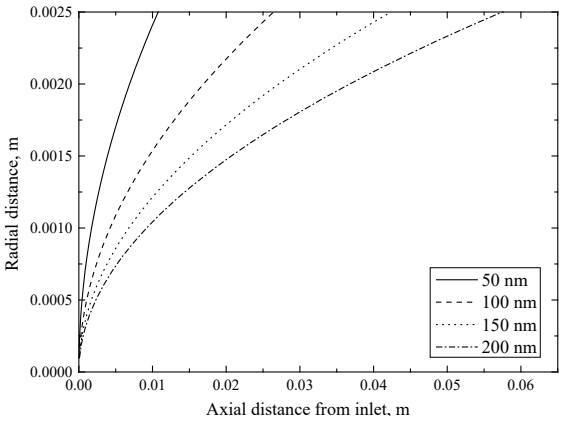

Fig.5. Variation of particle trajectories along the classifier with particle sizes (1.0 kV electrode voltage, 0.6 l/min aerosol flow and 1.2 l/min sheath air flow)

Fig. 5 illustrates how particle size influences the trajectory along the classifier under fixed operating parameters: 1.0 kV inner electrode voltage, 0.6 L/min aerosol flow, and 1.2 L/min sheath air flow. The results clearly indicate that, at a given electrode voltage, smaller particles are collected closer to the classifier entrance slit. This behavior is consistent with their higher electrical mobility, which enables faster migration toward the electrode. Influence of Electrode Voltage (Fig. 6).

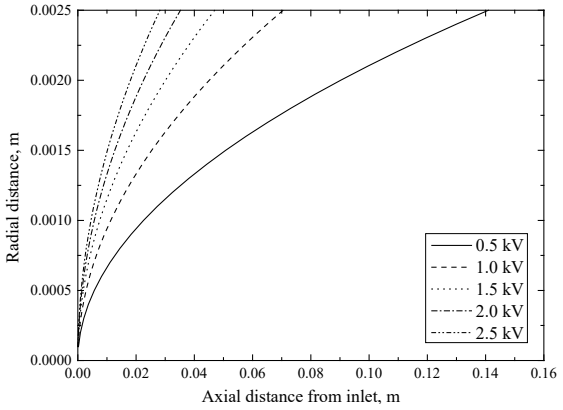

Fig. 6. Variation of particle trajectories along the classifier with electrode voltage (100 nm particle diameter, 0.6 l/min aerosol flow, and 1.2 l/min sheath air flow)

Fig. 6 shows how particle trajectories vary with electrode voltage (100-nm particle diameter, 0.6 l/min aerosol flow, and 1.2 l/min sheath air flow). Increasing the electrode voltage causes a particle of a given size to deposit closer to the entrance slit. This behavior is expected because the applied electrical force primarily determines radial particle motion. A higher voltage intensifies the electric field, increasing the particle's radial velocity. Limitation by Breakdown Voltage: The breakdown voltage imposes an upper limit on the maximum applied electrode voltage.

Given that the breakdown voltage of air is approximately 30 kV/cm under standard conditions (20 °C and 1 bar). Therefore, a 2.5 mm gap between parallel electrodes corresponds to a theoretical breakdown voltage of about 7.5 kV. By applying a significant safety margin to prevent electrical discharge, the electrode system can operate reliably over the 3-5 kV range. Range. Influence of Total Flow Rate (Fig. 7).

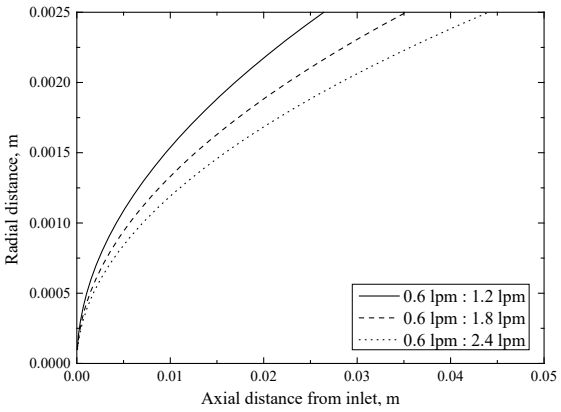

Fig.7. Variation of particle trajectories along the classifier with total flow rate (1.0 kV electrode voltage and 100 nm particle diameter)

Fig. 7 illustrates the variation in particle trajectories as a function of the total flow rate (electrode voltage: 1.0 kV, particle diameter: 100 nm). At higher flow rates, particles of a given size tend to contact the electrode wall further downstream, closer to the exit. This behavior arises because the increased axial flow velocity shortens the particle's residence time within the classification zone, thereby requiring a longer distance to achieve the necessary radial migration. Importantly, the results show that the collection positions for different particle sizes are clearly separated, confirming the classifier's effectiveness. Relationship between Voltage, Flow Rate, and Particle Diameter (Fig. 8).

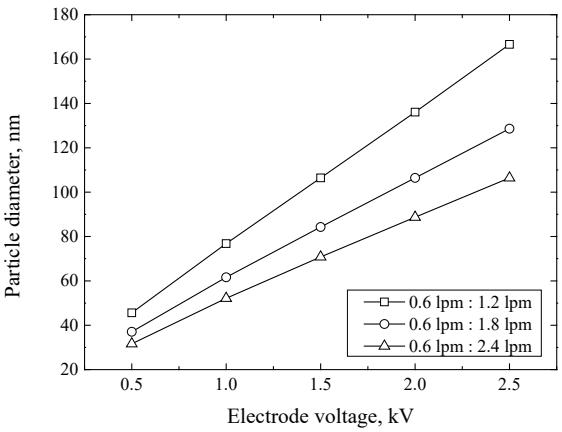

Fig. 8. Variation of the electrode voltage with particle diameter at the aerosol exit slit of the studied classifier at different flow rates

Fig. 8 shows the theoretical and experimental dependence of classified particle diameter on electrode voltage at total flow rates from 1.8 to 3.0 L/min.

The results show two key relationships, consistent with the principles of electrical mobility:

1) Effect of Voltage: Increasing the applied electrode voltage systematically increases the classified particle diameter at the classifier's aerosol exit slit. A higher voltage creates a stronger electric field, enabling larger (lower mobility) particles to migrate toward the collection electrode within the classification zone.

2) Effect of Flow Rate: Conversely, increasing the total flow rate results in a decrease in the classified particle diameter for a constant voltage. A higher flow rate reduces the residence time of the particles within the classification zone, meaning only smaller (higher mobility) particles can complete the necessary migration distance before exiting.

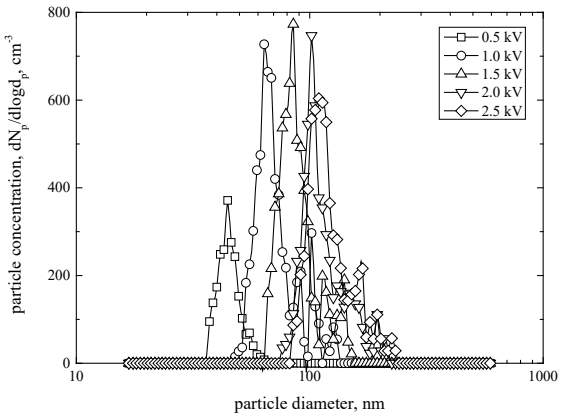

Fig. 9. Particle size distribution of the studied miniature electrostatic classifier at different electrode voltages

This behavior confirms that the classified particle size depends on electrode voltage, total flow rate, and the particle's electrical mobility. Since smaller particles have higher electrical mobility than larger ones, the classifier can precisely select the desired size by controlling the applied voltage and flow parameters. Monodisperse Particle Generation (Fig. 9)

Fig. 9 presents the size distribution of particles exiting the classifier, obtained by sweeping the applied electrode voltage from 0.5 to 2.5 kV. Throughout this experiment, the total operating flow rate was maintained at approximately 1.8 L/min.

The results clearly demonstrate that the particles exiting the classifier at any given voltage are highly monodisperse. This validates the effectiveness of the developed miniature electrostatic classifier for precise particle-size selection. As shown in Fig. 10, the particle-size distribution of the monodisperse aerosol exiting the classifier was evaluated at various applied electrode voltages. Classification Performance: The experimental results confirm that the miniature electrostatic classifier produced an approximately monodisperse size distribution at the aerosol exit slit.

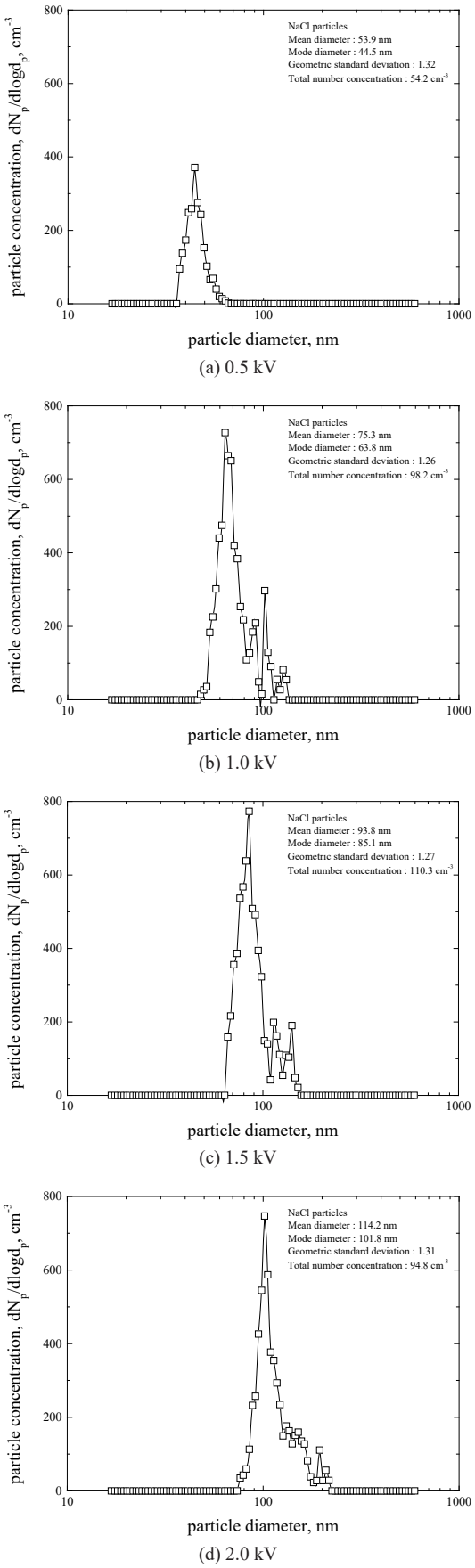

Fig. 10. Particle size distribution of monodisperse aerosol at different electrode voltages

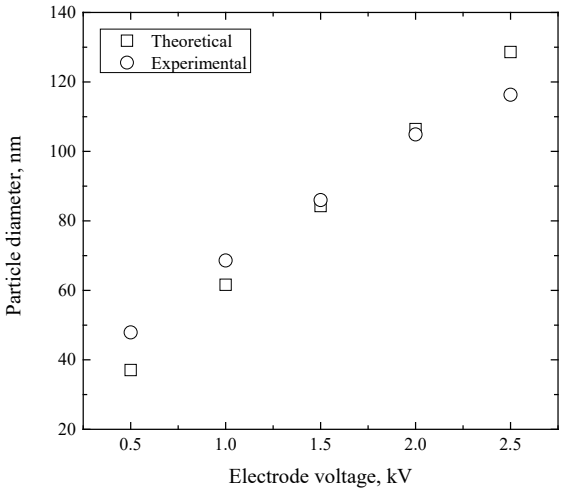

Fig. 11. Theoretical and experimental variation of the electrode voltage with particle diameter (0.6 l/min aerosol flow and 1.2 l/min sheath air flow

For applied electrode voltages of 0.5, 1.0, 1.5, 2.0, and 2.5 kV, the corresponding mean particle diameters ($D_{p,\text{mean}}$) were approximately 53.9, 75.3, 93.8, 114.2, and 126.7 nm, respectively. The geometric standard deviations (sigma_g) calculated for these classified mean diameters were 1.32, 1.26, 1.27, 1.31, and 1.28, respectively. These low sigma_g values clearly indicate the classifier's high efficiency at generating a narrow, monodisperse output. Observation of Multiply-Charged Particles

Multiply-charged particles began to appear in the classified aerosol distribution when classifying particles larger than 100 nm. This phenomenon is typical of electrical mobility classifiers and is a critical factor when interpreting size-classification data in this range.

Fig. 11 illustrates the theoretical and experimental relationship between the applied electrode voltage (kV) and the resulting classified particle diameter (nm) under fixed operating conditions: 0.6 L/min aerosol flow and 1.2 L/min sheath air flow. Key Findings and Discussion

1) Agreement in Trend: The overall trend observed in the experimental measurements (circles) closely mirrors the tendency predicted by the theoretical model (squares). Both curves show a clear positive correlation: as the electrode voltage increases, the classified particle diameter increases, consistent with the fundamental principles of electrical mobility classification.

2) Magnitude Discrepancy: While the trends align, a systematic deviation is observed between the two datasets. The discrepancy is smallest at 2.0 kV but becomes more pronounced at both lower and higher voltages. In general, the experimental particle diameters are consistently lower than the theoretically predicted diameters for the same voltage.

3) Potential Cause of Discrepancy: This disparity between the experimentally measured mean particle diameter and the theoretical prediction is primarily attributed to the influence of multiply-charged particles entering the classification zone. Multiply charged particles (e.g., a 2q particle) would be measured to have an electrical mobility diameter smaller than their true size at a given voltage, thus shifting the experimental data downward. Further investigation is warranted to fully explore and quantify the underlying causes for this discrepancy in both the theoretical assumptions and experimental conditions.

V. Conclusion

In summary, your argument is very valid. This article shows that experimental trends strongly agree with theoretical models for sizes up to 126.7 nm at 2.5 kV. However, the device has not yet been empirically proven to operate at the 300 nm level, consistent with the design's potential. To demonstrate its capability in the 300 nm range, further research is needed, as the author suggests, including modifications to the experimental methods, such as using larger starting aerosols or employing techniques to remove multi-charge fractions before measurements.

Experimental evaluation of the prototype using NaCl particles (0.6 L/min aerosol flow, 1.8 L/min sheath flow) and an applied voltage ranging from 0.5 to 2.5 kV demonstrated initial nanoparticle classification capabilities. However, SMPS measurements showed a significant magnitude discrepancy relative to theoretical predictions, indicating that the current mathematical model does not fully account for real-world particle behavior. Further refinement of both the physical design and theoretical framework is required to enhance classification accuracy.

Table III and Fig. 12 summarize the data, demonstrating that as the voltage rises from 0.5 kV to 2.5 kV, the measurement error drops substantially from 45.7% down to 1.0%.

TABLE III
PROVIDE A SUMMARY TABLE: VOLTAGE, PREDICTED DP, MEASURED DP (MEAN/MODE), SIGMA_G, ERROR (%)

Voltage (kV)	Mean d_p (nm)	Mode d_p (nm)	GSD (σ_g)	Predicted d_p (nm)	Error (%)
0.5	53.9	44.5	1.32	37	45.7
1.0	75.3	63.8	1.26	62	21.5
1.5	93.8	85.1	1.27	84	11.7
2.0	114.2	101.8	1.31	107	6.7
2.5	126.7	113.2	1.28	128	1.0

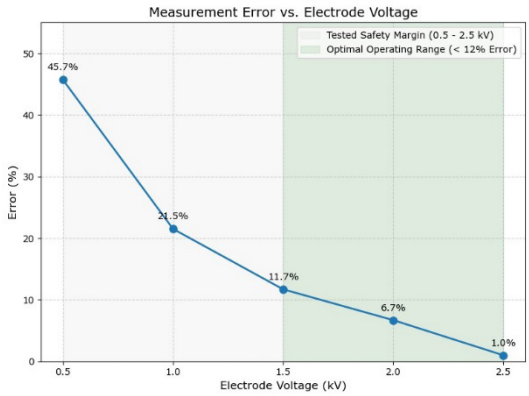

Fig. 12. Effect of Electrode Voltage on Measurement Error

VI. Recommendations for Future Research

Based on this work, the following specific directions are recommended for future research, covering both theoretical and experimental aspects of electrical mobility analyzer development:

1) Expand Detection Range and Multi-Parameter Sensing: Future work should focus on expanding the measurable size range to allow a single sensor to cover a broader spectrum of naturally occurring particles. Furthermore, integrating the mESC with other measurement techniques would enable multi-parameter investigations, facilitating the simultaneous quantification of nanoparticles (from molecular clusters up to 100 nm) and analysis of characteristics beyond size, such as composition.

2) Design Optimization and Manufacturing Precision: Further investigation is essential to refine the analyzer's design. This research should quantify the impact of several critical factors on classification performance and accuracy, including design configuration; limitations imposed by manufacturing precision and practical materials; non-ideal flow conditions; electrode eccentricity; component misalignment; and the accuracy of flow-setting mechanisms.

3) Non-Spherical Particle Analysis: The performance and accuracy of the analyzer must be evaluated when classifying non-spherical aerosol particles, such as asbestos fibers, soot aggregates, or bio-aerosols, commonly found in nature. Because particle shape strongly influences drag, settling velocity, and electrical mobility (non-spherical particles generally have lower electrical mobility than spherical particles), understanding this effect is crucial for real-world applications.

4) Enhanced Temporal Response: To accurately assess the transient behavior of airborne particles, such as those found in automotive exhaust gas, the temporal responsiveness (response time) of the instrument should be significantly improved.

Acknowledgements

The authors gratefully acknowledge the financial support provided by the Thailand Center of Excellence for Life Sciences (TCELS) under Research Contract No. TC-A (ERP) 15/2564.

References

[1] P. R. Sune et al., "Nanoparticles: Classification, types and applications: A comprehensive review," *GSC Biol. Pharm. Sci.*, vol. 29, pp. 190-197, Dec. 2024.

[2] Z. Sung et al., "Direct observation of nanometer size hydride precipitations in superconducting niobium," *J. Springer,* vol.14, pp. 1-12, Nov. 2024, https://doi.org/10.1038/s41598-024-77905-6

[3] S. M. Tham and M. Daley, "Measurement of gas concentrations," *J. Sci.*, vol. 25, p.128-132, Feb. 2024.

[4] I. Ueta, "Gas chromatographic determination of volatile compounds," *J. Springer,* vol. 38, pp. 737-738, Apr. 2022, https://doi.org/10.1007/s44211-022-00108-4

[5] X. Kong, M. Ammann, C. George, and D. Knopf, "Atomic and molecular ions in atmospheric chemistry: Interfacial reactivity, emerging mechanisms, and future perspectives," *J. Geophys. Res.: Atmos.*, vol. 130, no. 20, Art. no. e2025JD044379, Oct. 2025, https://doi.org/10.1029/2025JD044379

[6] Y. Li, W. Yang, H. Lin, and Z. Kuang, "Research on suspended particle size measurement based on ultrasonic backscattered amplitude analysis," *J.* MDPI, vol. 16, pp. 2-13, Jun. 2024, https://doi.org/10.3390/w16141973

[7] R. C. Flagan, "History of electrical aerosol measurements," *Aerosol Sci. Technol.*, vol. 28, no. 4, pp. 301-380, Apr. 1998, https://doi.org/10.1080/02786829808965530

[8] P. Intra and N. Tippayawong, "An overview of differential mobility analyzers for size classification of nanometer-sized aerosol particles," *J. Science and Technology*, vol. 30, no. 2, pp. 243-256, Mar. 2008.

[9] K. T. Whitby and W. E. Clark, "Electric aerosol particle counting and size distribution measuring system for the 0.015 to 1 μ size range," *Tellus*, vol. 18, no. 2-3, pp. 573-586, Aug. 1966, https://doi.org/10.3402/tellusa.v18i2-3.9340

[10] K. Vasilatou et al., "Aerosol physical characterization: A review on the current state of aerosol documentary standards and calibration strategies," *J. Aerosol Sci.*, vol. 183, Art. no. 106483, Jan. 2025, https://www.sciencedirect.com/science/article/pii/S0021850224001502

[11] A. Barba-Lobo, E. G. San Miguel, and J. P. Bolívar, "A new procedure to validate and optimize ^210Po measurements in atmospheric aerosols," *J. Aerosol Sci*., vol. 183, Art. no. 106469, Jan. 2025, https://www.sciencedirect.com/science/article/pii/S0021850224001368

[12] S. Basnet, A. Jäntti, P. Yli-Pirilä, M. Kortelainen, O. Sippula, and A. Lähde, "Performance of dry electrostatic precipitator for the removal of CsI aerosol particles under simulated severe nuclear accident conditions," *Nucl. Eng. Des*., vol. 445, Art. no. 114440, Dec. 2025, https://www.sciencedirect.com/science/article/pii/S002954932500617X

[13] J. Wu et al., "Effect of filter rod structure on aerosol particle size distribution in electrically heated cigarettes," *Atmos. Environ.: X*, vol. 29, Art. no. 100412, Jan. 2026, https://doi.org/10.1016/j.aeaoa.2025.100412

[14] H. Hagino, "Winter emission factors of ultrafine total and solid particle numbers and PM2.5 near a major arterial road in Tokyo," *Atmos. Environ.: X*, vol. 28, Art. no. 100382, Dec. 2025, https://doi.org/10.1016/j.aeaoa.2025.100382

[15] A. Bianco et al., "Separation of isomers using a Differential Mobility Analyser (DMA): Comparison of experimental vs modelled ion mobility," *Talanta*, vol. 243, Art. no. 123339, Jun. 2022, https://doi.org/10.1016/j.talanta.2022.123339

[16] C. Hagwood, Y. Sivathanu, and G. Mulholland, "The DMA transfer function with Brownian motion: A trajectory/ Monte-Carlo approach," *Aerosol Sci. Technol.*, vol. 30, no. 1, pp. 40-61, Jan. 1999, https://www.tandfonline.com/doi/abs/10.1080/027868299304877

[17] M. Carsí and M. Alonso, "A simple correlation to estimate the resolution of concentric cylindrical DMAs for diffusive particles," *J. Aerosol Sci.*, vol. 167, Art. no. 106089, Jan. 2023, https://doi.org/10.1016/j.jaerosci.2022.106089



Papol Sardyoung is currently an Assistant Professor in the Department of Industrial Electrical Technology, Faculty of Industrial Technology, Thepsatri Rajabhat University, Lopburi, Thailand.

He researches pulsed electric fields, Energy Conversion, energy-saving for Industry, and solar cell design and Simulation.



Panich Intra is currently an Associate Professor working at the Electro-Aerosol Instrument Laboratory (EAIL), Research Unit of Applied Electric Field in Engineering (RUEE), the College of Integrated Science and Technology, Rajamangala University of Technology Lanna, Chiang Mai, Thailand.

He researches aerosol electrical mobility analysis, Corona discharge-based aerosol charging, Electrostatic precipitation, and Pulsed electric field and electroporation. Current projects include "Modification, calibration, and field testing of an electrical particulate matter monitor towards commercialization" and "Development of a microorganism inactivation system in beverage production processes for industrial use using a pulsed electric field technique."

Review of DonkeyCar Platform: From Deep Learning to Autonomous Driving Implementation

Ning Wang[1] and Jian Qu[2*]
[1,2]Faculty of Engineering and Technology, Panyapiwat Institute of Management, Nonthaburi, Thailand
E-mail: 6672100041@stu.pim.ac.th, jianqu@pim.ac.th*

Received: September 2024 / Revised: June 12, 2026 / Accepted: June 16, 2026

***Abstract*—This review paper examines explainable image captioning techniques for autonomous driving. It focuses on natural language explanations to improve transparency and explainability. We review more than 20 studies published from 2015 to 2024. These include foundational models, attention mechanisms, Transformer-based methods, and integrations with large language models. The review traces the progress from basic textual descriptions to chain-based reasoning and multimodal fusion. Because of resource limits and the need for low-cost experimentation, we chose the open-source DonkeyCar platform to replicate models. We replicated the ADAPT (Action-aware Driving Caption Transformer) model and compared it with prior methods using standard metrics: BLEU-4, CIDEr, and METEOR. The results show that ADAPT outperforms previous state-of-the-art methods, with CIDEr gains of 31.7 in narration and 33.1 in reasoning. We also successfully reproduced lane-following and obstacle-avoidance tasks on DonkeyCar. Multimodality supports more natural learning for future AI models, but accuracy is limited in most scenarios.**

***Index Terms*—Image Captioning, Explainable Autonomous Driving, Deep Learning, DonkeyCar**

I. Introduction

With the rapid development of computers and the Internet, Artificial Intelligence (AI) has become a crucial part of human life. From deep mathematical and algorithmic research in the 1950s and 1960s, through the development of complex systems in the 1990s, to extensive applications in autonomous driving today, AI has moved from theoretical exploration to practical use. In autonomous driving, AI plays a key role in transforming how we understand transportation, enhancing safety, and increasing convenience [1].

The widespread adoption of autonomous vehicles has led to an urgent need for interpretability. This need arises from several factors. First, autonomous vehicles' role in road accidents presents a fundamental practical issue. Negligence and hazardous driving in traditional vehicles directly affect the safety of passengers and bystanders, making transportation system safety crucial. Furthermore, understanding the motives behind decisions is a fundamental human psychological need. Users are likely to avoid using a system if they cannot understand or trust it. Research shows that systems that are both understandable and perceptible significantly increase user confidence. Frequent system malfunctions without reliable explanations can severely undermine user and public trust. Restoring trust once it is damaged is extremely challenging. Therefore, users need to understand the key decisions autonomous vehicles make in specific situations to build confidence in their decision-making. Confidence in a vehicle's smart decisions will further bolster transparency.

Transparency not only enhances explainability but also ensures the system's decisions and actions comply with current regulations and standards. This is crucial for ensuring fairness, ethical scrutiny, and rational justification of the system's key decisions. These interconnections are essential for the widespread adoption of autonomous vehicles [2].

Specifically, interpretability in autonomous driving systems must account for users' backgrounds and knowledge levels. For example, a user unfamiliar with autonomous driving technology might need a simple, clear explanation of the system's decisions and outcomes to feel satisfied. In contrast, autonomous systems engineers need more detail to understand the vehicle's current functionality and when to activate existing systems. Therefore, analyzing the audience's domain expertise and knowledge traits is crucial to providing appropriate, knowledgeable, and comprehensible explanations.

Recent research and practice have also advanced this field. For instance, "Explaining Explanations: An Overview of Interpretability of Machine Learning" (2019) explores model interpretability and introduces techniques such as Local Interpretable Model-agnostic Explanations (LIME) and integrated gradients, which help enhance the interpretability of autonomous driving systems. Additionally, "Towards Transparent

and Explainable AI: From Interpretability to Explainability" (2021) further expands understanding of AI transparency by emphasizing the relationship between model interpretability and explainability. These findings provide important references for interpreting autonomous driving systems, making their decision-making processes more transparent and understandable [3].

In summary, as autonomous driving technology evolves, the demand for system interpretability grows. By continuously improving explanation techniques and considering user backgrounds and needs, researchers can enhance the transparency and explainability of autonomous driving systems, facilitating broader acceptance in practical applications.

II. Related Studies

A. The Development of Explaining in Autonomous Driving

In recent years, autonomous driving research has increasingly focused on system interpretability and transparency in decision-making processes [4]. From early visual scene descriptions to chain-based reasoning and large language models for natural language explanations, research has deepened, driving the evolution of explainable autonomous driving systems. Below is a chronological review of representative papers in this field, with a detailed analysis of how each study builds on or improves its predecessors [5]. First, "Textual Explanations for Self-Driving Vehicles" is an early study on explainability in autonomous driving. This paper introduced generating natural language explanations for autonomous driving behaviors through visual scene understanding. The system provided a simple yet effective framework that generated coherent textual explanations from perception to decision-making, allowing external observers to clearly understand the vehicle's decision-making process. Its main contribution was establishing a model that converts visual information into natural language, laying the foundation for future studies on generating explanations through language [6].

Building on this, "Reason2Drive: Towards Interpretable and Chain-based Reasoning for Autonomous Driving" extended and improved the previous work [7]. This research introduced a chain-based reasoning model that constructs causal chains tracing each step from sensor data to the final driving behavior. Compared with "Textual Explanations for Self-Driving Vehicles," Reason2Drive not only generated natural-language descriptions of driving behaviors but also emphasized the causal relationships and logical reasoning behind each decision. This significantly enhanced the system's transparency, allowing systematic tracing of the entire decision-making process and increasing trust in autonomous driving systems.

Next, "Advancing Explainable Autonomous Vehicle Systems: A Comprehensive Review and Research Roadmap" offers a thorough examination of explainability technologies in autonomous driving [8]. This paper systematically summarizes current technological developments, focusing on how multimodal fusion and behavior prediction can improve the transparency of autonomous driving systems. Unlike earlier model-specific research, this paper took a macro-level view of the explainability problem, highlighting the strengths and weaknesses of existing methods while outlining challenges and future directions in complex driving scenarios. It provided theoretical guidance for subsequent research and emphasized the importance of multimodal data fusion in enhancing system interpretability.

As technology advanced, "ADAPT: Action-aware Driving Caption Transformer" introduced the Transformer model and significantly improved the accuracy and contextual relevance of driving scene descriptions [9]. ADAPT proposed an "action-aware driving caption transformer" that combined visual input with driving behavior actions to generate natural language explanations related to driving scenes. Compared with earlier methods, ADAPT not only described driving behaviors but also effectively integrated dynamic scene information, making the generated explanations more context-aware and reflective of real-world driving scenarios. The innovation lies in using a Transformer model to enhance contextual understanding and add depth and detail.

Building on this, "DRIVEGPT4: Interpretable End-to-End Autonomous Driving via Large Language Model" uses Large Language Models (LLMs) such as GPT-4 to create even more natural and highly interactive explanations [10]. By incorporating GPT-4, this system could generate more complex natural-language explanations that cover subtle changes in driving scenes. Compared to ADAPT, DRIVEGPT4 emphasized flexibility and adaptability in explanations, especially in complex driving environments, where LLMs gave the system more powerful language-generation capabilities. It not only generated descriptions of driving behaviors but also dynamically explained driving logic across scenarios, demonstrating LLMs' vast potential in autonomous driving.

Finally, "Driving with LLMs: Fusing Object-Level Vector Modality for Explainable Autonomous Driving" further improved explanation precision and detail compared with DRIVEGPT4 [11]. This study fused object-level vector modalities with large language models to generate more precise explanations of driving scenes. Specifically, the system could not only produce global driving-behavior explanations but also provide detailed descriptions of each object

in the driving environment. This object-level explanatory ability significantly improved the system's understanding of complex scenes and offered more actionable insights. Compared with DRIVEGPT4's global scene explanations, "Driving with LLMs" focused more on multimodal fusion, particularly combining visual perception with language generation, and achieved new breakthroughs.

Research on explainability in autonomous driving systems has evolved from simple visual-to-text generation models to integrating reasoning chains and multimodal data. The introduction of Transformer models and large language models has significantly enhanced the system's ability to provide explanations. In particular, LLMs have greatly improved the flexibility and adaptability of explanations, enabling the system to handle complex, dynamic driving scenarios. Future work will continue to improve the accuracy and efficiency of explainability, especially in object-level explanation generation [12].

This review traces the evolution of explainable autonomous driving and compares core transparency techniques. Early methods (e.g., Textual Explanations) provided basic visual-to-text descriptions but lacked explanatory depth. Reason2Drive improved this with chain-based reasoning for better logical traceability, though it was less flexible. ADAPT advanced further by using action-aware Transformers for context-rich captions, outperforming prior models in relevance but requiring more computation. DriveGPT4 introduced LLMs for adaptive, nuanced explanations, addressing earlier rigidity in complex scenes. LLM-driven driving added object-level multimodal fusion, achieving higher precision. Overall, the field has progressed from static text to dynamic, multimodal reasoning with steady gains in interpretability; however, challenges in scalability, real-time performance, and resource efficiency persist for low-cost platforms. Our earlier study on explainable captioning for traffic sign recognition confirms this trend, showing that resource-limited hardware can produce readable justifications for individual road objects [12].

B. The Development of Image Captioning

In recent years, image captioning technology has garnered significant attention and developed rapidly. With the introduction of deep learning models, researchers have continuously optimized image-to-text generation. Below is a review of several representative image captioning papers, presented in chronological order, focusing on their key contributions and developments.

First, "Show and Tell: A Neural Image Caption Generator" is a foundational work in image captioning. Vinyals et al. combine Convolutional Neural Networks (CNNs) for image feature extraction with Recurrent Neural Networks (RNNs) to generate textual descriptions, achieving end-to-end image captioning. This model integrates image representation with a language model, significantly improving the coherence and semantic relevance of generated captions. The innovation lies in merging CNN and RNN and training the model using maximum likelihood estimation. This work laid a solid foundation for subsequent deep learning-based image captioning techniques [13].

Next, "Show, Attend and Tell: Neural Image Caption Generation with Visual Attention" builds upon the previous work by introducing the attention mechanism. Xu et al. proposed a model that dynamically focuses on different image regions as it generates each word, producing more precise captions that match specific image features. Compared with "Show and Tell," attention greatly improves the model's ability to handle complex scenes, allowing it to capture image details more effectively. This innovation introduced new ideas to image captioning, particularly excelling at generating descriptions in multi-object scenes [14].

Subsequently, "Self-critical Sequence Training for Image Captioning" introduced self-critical training for sequence-generation tasks. Rennie et al. addressed image caption evaluation by proposing reinforcement learning optimization using metrics like BLEU and CIDEr. This training method lets the model focus more on caption quality rather than relying solely on maximum likelihood estimation. Unlike previous training methods, reinforcement learning improves performance during evaluation, especially for long sequences. This advancement addresses earlier models' tendency to get stuck in local optima during generation [15].

Following this, "Bottom-Up and Top-Down Attention for Image Captioning and Visual Question Answering" introduced bottom-up and top-down attention mechanisms, further improving the model's ability to capture complex information from images [16]. Anderson et al. proposed this dual attention mechanism, which considers global image features and extracts local details, leading to more accurate, content-rich captions. Compared with "Show, Attend, and Tell," this model better balances global information and local features, making the generated captions more aligned with human visual perception.

Building on these advances, "Meshed-Memory Transformer for Image Captioning" introduced a Transformer-based image captioning model. Traditional RNNs struggle with training efficiency and long dependencies, but the Transformer model, with its fully attention-based architecture, addresses these issues. Cornia et al. showed that Transformers can process sequence data in parallel while capturing long-range dependencies between images and text, improving both efficiency and accuracy. This study showed that Transformer-based models

handle complex image information better and scale more effectively [17].

Finally, "Oscar: Object-Semantics Aligned Pre-training for Vision-Language Tasks" combined object semantic information with visual features and proposed a new pre-training method. Li et al. jointly pre-trained visual and language information, enabling the model to better understand objects' attributes and relationships in images. This approach effectively addressed the issue of separately processing semantic and visual information in traditional methods. Compared with earlier work, Oscar achieved better semantic consistency, improving both the accuracy and diversity of image caption generation [18].

Image captioning technology has evolved from early CNN-RNN models to attention mechanisms and, more recently, to Transformer models and object-semantics pre-training methods. Each step has improved these models' precision, coherence, and efficiency. Future research may focus on better integrating visual and language information, enhancing caption generation in complex scenes, and expanding the use of pre-training methods in multimodal tasks.

C. DonkeyCar

DonkeyCar is an open-source platform designed for small-scale autonomous vehicle experiments, valued for its low cost and flexibility in autonomous driving research. The 2018 paper "Training Neural Networks to Pilot Autonomous Vehicles" showed how Convolutional Neural Networks (CNNs) trained on camera data could control steering and acceleration in DonkeyCar, demonstrating deep learning's potential in small cars.

DonkeyCar's affordability makes it ideal for researchers, educators, and enthusiasts to explore autonomous driving without the expense of commercial platforms. Its open-source design allows for customization and adaptation to diverse research needs.

Building on this, the 2019 paper "End-to-End Deep Learning for Autonomous Driving" proposed an advanced model incorporating Generative Adversarial Networks (GANs) to improve the car's performance in varied environments. Additionally, the 2020 paper "Real-Time Deep Learning for Autonomous Vehicles" optimized real-time performance through edge computing to reduce latency and improve image processing [19].

In 2021, "Multi-Modal Sensor Fusion for Autonomous Vehicles" integrated data from multiple sensors, such as cameras and LiDAR, to improve environmental perception and offered new insights into multi-modal data processing on DonkeyCar [20]. The platform's flexibility enables rapid iteration and testing, making it an excellent tool for developing and validating algorithms in controlled environments. As research progresses, DonkeyCar is likely to support more advanced sensor fusion and real-time processing techniques, expanding its use in education and research.

D. Multi-Modal Technology

Multi-modal technology, which combines image recognition and Natural Language Processing (NLP), has gradually become a key area in artificial intelligence. By integrating visual and linguistic modalities, systems can better understand and generate explanatory content.

Early research primarily focused on image captioning tasks. The 2015 paper "Show, Attend and Tell" combined Convolutional Neural Networks (CNNs) with attention mechanisms to generate natural language descriptions of images, laying the foundation for integrating image and language modalities.

Later, researchers focused on cross-modal learning. The 2018 paper "Bottom-Up and Top-Down Attention" used a dual attention mechanism to link image recognition with language generation, enabling more accurate processing of visual details and improving image captioning and visual question-answering tasks [16].

Generative models further advanced multimodal technology. The 2019 paper "Image Captioning: Transforming Objects into Words" was among the first to apply Transformers to image captioning, showing the power of combining visual and linguistic modalities to produce richer text generation [21].

Recent studies have focused on unified multimodal frameworks. The 2020 paper "Unified Vision-Language Pre-Training for Image Captioning and Visual Question Answering" proposed a unified pre-training model that integrates image captioning and visual question answering, enhancing cross-task performance [22].

Looking ahead, multi-modal technology will increasingly focus on real-time capabilities and generation quality, driving deeper integration of visual and language modalities in practical applications. Recent work on matching traffic sign images with textual captions illustrates this direction on a concrete driving task [23].

III. Research Methodology

We searched Google Scholar, IEEE Xplore, arXiv, and Scopus using keywords such as "explainable autonomous driving," "image captioning autonomous," "multimodal autonomous driving," and "DonkeyCar." We searched for papers published between 2015 and 2024. We included only peer-reviewed papers or high-impact preprints focused on explainability in autonomous driving and image-to-text generation. After screening about 35 papers, we selected 22 core

studies: 10 on autonomous driving explainability, 8 on image captioning, and 4 on multimodal methods and DonkeyCar.

In the experimental part, we replicated the ADAPT model using the pre-processed BDD-X dataset. The setup included Python 3.8, PyTorch, and NVIDIA Apex, with pretrained weights downloaded from Google Drive. We trained for 40 epochs using the default hyperparameters. We evaluated performance on narration and reasoning tasks using BLEU-4, CIDEr, and METEOR metrics. In addition, we successfully reproduced the lane-following and obstacle-avoidance tasks on the DonkeyCar platform. This lays the foundation for integrating explainable image captioning into the DonkeyCar end-to-end autonomous driving system.

IV. Experiments and Results

We replicated the ADAPT model by strictly following the official GitHub repository instructions. ADAPT takes a short driving video clip as input and generates two sentences: A narration describing the vehicle's current action and a reasoning sentence explaining why the action is taken. Fig. 1 shows two examples of this output on BDD-X video clips. In the first example, the model describes the behavior as "the car is turning left" and gives the reason "because the car is making a left turn onto a different street." In the second example, it describes the behavior as "the car is slowing down and coming to a stop" and explains it with "because there is a stop sign."

We began by cloning the repository to obtain the source code and project structure. Next, we created a Conda virtual environment with Python 3.8, installed PyTorch with CUDA support, and then installed NVIDIA Apex to accelerate mixed-precision training. We then installed additional dependencies, including mpi4py and OpenMPI for distributed processing, along with the remaining packages listed in the requirements file. We also prepared a Docker environment, as shown in Fig. 2. We installed Docker, pulled the prebuilt ADAPT image (jxbbb/adapt: Latest), and launched the container with the launch_container.sh script provided in the repository.

We created the necessary folders for checkpoints and models. We downloaded the pretrained weights from the provided Google Drive link and placed them in the checkpoints folder. We also obtained the base Video-Swin Transformer models and caption evaluation tools from their respective Google Drive links and organized them into the appropriate directories. Fig. 3 shows the resulting ADAPT-main/checkpoints/basemodel directory, which contains a checkpoints subfolder for the pretrained weights and a log subfolder for the training logs. Fig. 4 shows the ADAPT-main/models directory, which holds the basemodel, captioning, and Video Swin Transformer subfolders. Fig. 5 shows the ADAPT-main/src/evalcap directory, which contains the caption evaluation tools, including the cider and coco_caption packages and the caption_eval.py and evaluate.py scripts used to compute the metrics.

For the dataset, we downloaded and extracted the preprocessed BDD-X dataset from the provided Baidu link. We then arranged it into the datasets/BDDX/ directory with the required file structure, including frame data and captions. Finally, we split the data into train, validation, and test sets.

We trained for 40 epochs using the multitask script with default hyperparameters for both the Driving Caption Generation and Control Signal Prediction tasks. Finally, we evaluated the model on the BDD-X test split using the provided test script, computing standard metrics BLEU-4, CIDEr, and METEOR separately for the narration (action description) and reasoning (explanation of causes) tasks.

Table I compares state-of-the-art methods. Results adapted from the original paper and confirmed in our replication show that ADAPT achieved superior performance, with CIDEr improvements of 31.7 on narration and 33.1 on reasoning over previous best baselines. This successful replication validates the model's functionality and reproducibility, making it a strong baseline for action-aware driving captioning and explainable autonomous driving research.



Fig. 1. The effect of forming the description

```
#step1: 一键安装docker
#参考: https://blog.csdn.net/qq_27865227/article/details/127246251
wget http://fishros.com/install -O fishros && . fishros

#step2:拉取docker镜像
docker pull jxbbb/adapt:latest

#step3:运行docker镜像（即readme中的命令）
sh launch_container.sh
```

Fig. 2. Prepare the environment for Docker

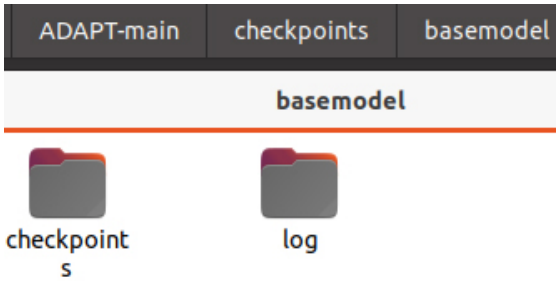

Fig. 3. Prepare the ADAPT-main/checkpoints file and copy the file directory as shown in the figure

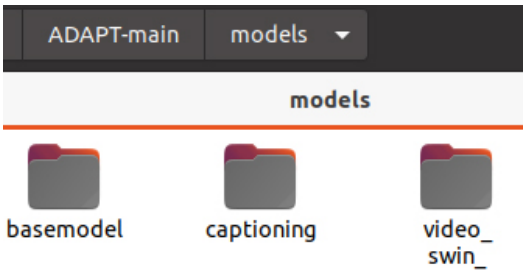

Fig. 4. Prepare the ADAPT-main/models file and copy the file directory as shown in the figure

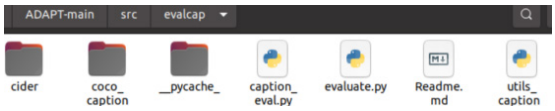

Fig. 5. Prepare the ADAPT-main/src/evalcap file and copy the file directory as shown in the figure

This reproduction of the ADAPT model validates its functionality and demonstrates its capability in video understanding and text generation tasks. The process provides a solid foundation for further model optimization and research into multimodal relationships between video and language, supporting future work in video content understanding.

Compared with existing advanced methods, ADAPT achieves SOTA results in machine evaluation. For example, on the CIDEr indicator, ADAPT is 31.7 higher than previous state-of-the-art methods for action description and 33.1 higher for cause explanation, as shown in Table I.

However, the accuracy is still not high enough for real-world use.

Multimodal fusion makes human-machine interaction more natural, but it needs too much computing power for low-resource devices.

TABLE I
COMPARISON OF RESULTS WITH STATE-OF-THE-ART

Method	Narration			Reasoning		
	BLEU4	CIDEr	METEOR	BLEU4	CIDEr	METEOR
S2VT	30.2	179.8	27.5	6.3	53.4	11.2
S2VT++	27.1	157.0	26.4	5.8	52.7	10.9
SAA	31.8	214.8	29.1	7.1	66.1	12.2
WAA	32.3	215.8	29.1	7.3	69.5	12.2
ADAPT	34.6	247.5	30.6	11.4	102.6	15.0

In the future, we plan to integrate explainable captioning directly into the DonkeyCar platform.

V. Conclusion

Our research systematically reviews explainable image captioning for autonomous driving. First, we explore the necessity of explainability in autonomous driving. Next, we introduce the tasks of explainable autonomous driving and image captioning. After establishing the need for explainability in autonomous driving, we chose the DonkeyCar platform to collect experimental data under our conditions. We also investigated image feature extraction methods, modalities, and datasets. Existing research indicates that multimodality can fully achieve free-form natural language explanations for autonomous driving. Implementing natural language explanations for autonomous driving also suggests greater flexibility in human-machine interaction. Additionally, we validated currently well-performing models through experimental replication. The results show that although related models have improved, their accuracy still does not reach a high level. Therefore, natural language-based explainability for autonomous driving still requires more time and effort. Meanwhile, existing research remains incomplete.

Author Contributions

Conceptualization, N. W. and J. Q.; Methodology, N. W. and J. Q.; Software, N.W. and J. Q.; Validation, N. W. and J. Q.; Formal Analysis, N. W. and J. Q.; Investigation, N. W. and J. Q.; Data Curation, N. W. and J. Q.; Writing—Original Draft Preparation, N.W. and J. Q.; Writing—Review and Editing, N. W. and J. Q.; Visualization, N. W. and J. Q.; Supervision, J. Q.; All authors have read and agreed to the published version of the manuscript. J. Q. is the corresponding Author. The first Author received scholarship support from CPALL for conducting this research in PIM.

References

[1] M. Bojarski et al., "End to end learning for self-driving cars," *arXiv preprint arXiv:1604.07316*, 2016, https://doi.org/10.48550/arXiv.1604.07316

[2] F. Nesti, G. Roossolini, S. Nair, A. Biondi, and G. Buttazzo, "Evaluating the robustness of semantic segmentation for autonomous driving against real-world adversarial patch attacks," in *Proc. IEEE/CVF Winter Conf. Appl. Comput. Vis. (WACV)*, 2022, pp. 2280-2289.

[3] S. Ding and J. Qu, "Research on multi-tasking smart cars based on autonomous driving systems," *SN Comput. Sci.*, vol. 4, no. 3, p. 292, Mar. 2023, https://doi.org/10.1007/s42979-023-01740-1

[4] F. Zheng and J. Qu, "TIDCB: Text image dangerous-scene convolutional baseline," *ECTI Trans. Comput. Inf. Technol. (ECTI-CIT)*, vol. 18, no. 3, pp. 280-294, May 2024.

[5] Y. Li and J. Qu, "A novel neural network architecture and cross-model transfer learning for multi-task autonomous driving," *Data Technol. Appl.*, vol. 58, no. 4, pp. 579-598, Apr. 2024.

[6] J. Kim, A. Rohrbach, T. Darrell, J. Canny, and Z. Akata, "Textual explanations for self-driving vehicles," in *Proc. Eur. Conf. Comput. Vis. (ECCV)*, 2018, pp. 577-593.

[7] M. Nie et al., "Reason2Drive: Towards interpretable and chain-based reasoning for autonomous driving," in *Proc. Eur. Conf. Comput. Vis. (ECCV)*, 2024, pp. 292-308.

[8] S. Tekkesinoglu, A. Habibovic, and L. Kunze, "Advancing explainable autonomous vehicle systems: A comprehensive review and research roadmap," *ACM Trans. Human-Robot Interact.*, vol. 14, no. 3, pp. 1-46, Mar. 2025, https://arxiv.org/abs/2404.00019

[9] B. Jin et al., "ADAPT: Action-aware driving caption transformer," in *Proc. IEEE Int. Conf. Robot. Autom.* (ICRA) 2023, pp. 7554-7561, https://arxiv.org/abs/2302.00673

[10] Z. Xu, E. Xie, Z. Zhao, Y. Guo, and K. -Y. Wong, "DriveGPT4: Interpretable end-to-end autonomous driving via large language model," *IEEE Robot. Autum. Lett.*, vol. 9, no. 10. pp. 8186-8193, Oct. 2024, https://doi.org/10.1109/LRA.2024.3440097

[11] L. Chen et al., "Driving with LLMs: Fusing object-level vector modality for explainable autonomous driving," *arXiv preprint arXiv:2310.01957*, 2023, https://doi.org/10.48550/arXiv.2310.01957

[12] N. Wang and J. Qu, "Explainable image captioning for autonomous driving: A traffic sign recognition task," in *Proc. 10th Int. Conf. Bus. Ind. Res. (ICBIR)*, 2025, pp. 35-40.

[13] O. Vinyals, A. Toshev, S. Bengio, and D. Erhan, "Show and tell: A neural image caption generator," in *Proc. IEEE Conf. Comput. Vis. Pattern Recognit. (CVPR)*, 2015, pp. 3156-3164.

[14] K. Xu et al., "Show, attend and tell: Neural image caption generation with visual attention," in *Proc. 32nd Int. Conf. Mach. Learn. (ICML)*, 2015, pp. 2048-2057.

[15] S. J. Rennie, E. Marcheret, Y. Mroueh, J. Ross, and V. Goel, "Self-critical sequence training for image captioning," in *Proc. IEEE Conf. Comput. Vis. Pattern Recognit. (CVPR)*, 2017, pp. 1179-1195.

[16] P. Anderson et al., "Bottom-up and top-down attention for image captioning and visual question answering," in *Proc. IEEE/CVF Conf. Comput. Vis. Pattern Recognit. (CVPR)*, 2018, pp. 6077-6086.

[17] M. Cornia, M. Stefanini, L. Baraldi, and R. Cucchiara, "Meshed-memory transformer for image captioning," in *Proc. IEEE/CVF Conf. Comput. Vis. Pattern Recognit. (CVPR)*, 2020, pp. 10575-10584.

[18] X. Li et al., "Oscar: Object-semantics aligned pre-training for vision-language tasks," in *Proc. Eur. Conf. Comput. Vis. (ECCV)*, 2020, pp. 121-137, https://arxiv.org/abs/2004.06165

[19] M. Bechtel, E. McEllhiney, M. Kim, and H. Yun, "DeepPicar: A low-cost deep neural network-based autonomous car," in *Proc. IEEE 24th Int. Conf. Embedded Real-Time Comput. Syst. Appl. (RTCSA)*, 2018, pp. 11-21, https://arxiv.org/abs/1712.08644

[20] K. Huang, B. Shi, X. Li, X. Li, S. Huang, and Y. Li, "Multi-modal sensor fusion for auto driving perception: A survey," *arXiv preprint arXiv:2202.02703*, 2022, https://doi.org/10.48550/arXiv.2202.02703

[21] S. Herdade, A. Kappeler, K. Boakye, and J. Soares, "Image captioning: Transforming objects into words," in *Proc. Adv. Neural Inf. Process. Syst. (NeurIPS)*, 2019, pp. 11137-11147. https://arxiv.org/abs/1906.05963

[22] L. Zhou, H. Palangi, L. Zhang, H. Hu, J. J. Corso, and J. Gao, "Unified vision-language pre-training for image captioning and VQA," in *Proc. AAAI Conf. Artif. Intell. (AAAI)*, 2020, pp. 13041-13049, https://arxiv.org/abs/1909.11059

[23] N. Wang and J. Qu, "Research on deep learning-based methods for matching traffic sign images with textual captions," *ECTI Trans. Comput. Inf. Technol. (ECTI-CIT)*, vol. 19, no. 3, pp. 379-391, Jul. 2025, https://doi.org/10.37936/ecti-cit.2025193.262155



Ning Wang is currently pursuing a dual-degree Ph.D. at SIIT, Thammasat University, Thailand, and the Japan Advanced Institute of Science and Technology, Japan. He received an M.Eng. from the Faculty of Engineering and Technology, Panyapiwat Institute of Management, Thailand, in 2025. His research primarily focuses on end-to-end autonomous driving, with a particular emphasis on collecting data for explainable autonomous driving using the DonkeyCar platform. He is also committed to developing secure and reliable autonomous driving systems using Deep Reinforcement Learning.



Jian Qu is an Assistant Professor at the Faculty of Engineering and Technology, Panyapiwat Institute of Management. He received a Ph.D. in 2013 with an Outstanding Performance award from the School of Information Science, Japan Advanced Institute of Science and Technology, Japan. He earned a B.B. with Summa Cum Laude honors from the Institute of International Studies, Ramkhamhaeng University, Thailand, in 2006, and an M.S.I.T. from the Sirindhorn International Institute of Technology, Thammasat University, Thailand, in 2010. He has been a member of the THAI Super AI house committee since 2020. His research interests are natural language processing, intelligent algorithms, machine learning, machine translation, information retrieval, image processing, autonomous driving, and multi-modal AI.

PAPER FORMAT (IEEE Style)

I. Format

- Your paper must use a paper size corresponding to A 4 which is 210 mm (8.27 inch) Wide and 297 mm (11.69 inch)
- Your paper must be in two column format
- Articles not more than 15 pages in length, single-sided A4 paper, margins (top, bottom, left, right) are 1 inch (2.54 cm)
- Abstract and References and content set to double columns,
- English font is Times New Roman, as follows:

TABLE I
Font Sizes for Papers

Content	Font Size	Labelling
Title (Single column)	18 (CT)	bold
Authors (Single column)	11 (CT)	bold
Authors Information (Single column)	10 (CT)	regular
Abstract	10 (LRJ)	bold
Index Terms (Keywords)	10 (LRJ)	bold
Content	10 (LRJ))	regular
Heading1	10 (CT)	regular (Capitalization)
Heading 2	10 (LJ)	regular
Table Title (Place above the Table)	8 (CT)	regular
Table content	8 (CT)	regular
Figure caption (Place below the figure)	8 (LJ)	regular
Reference Head	10 (CT)	regular (Capitalization)
Reference	8 (LJ)	regular
Author Profiles	10 (LRJ)	bold author name/ profile regular

CT=Centre Text, LJ=Left Justified, RJ=Right Justified, LRJ=Left & Right Justified

II. Composition of the Article

A. Article title

B. Authors information, Write (all) the author's name, affiliation, department, city, country and E-mail (set to Single Column) all.

C. Abstract, Must be under 200 words and not include subheadings or citations. Define all symbols used in the abstract. Do not delete the blank line immediately above the abstract.

D. Index Terms, Enter key words or phrases in alphabetical order, separated by commas.

E. Content

1) Academic article, should include: Introduction, Content, and Conclusion.

2) Research article, should include: introduction, literature review, Materials methods, Results, Discussion, and conclusion.

Clearly summarize the important findings of the paper. It should contain such as objectives, methods and major results.

F. Introduction

The Introduction section of reference text expands on the background of the work (some overlap with the Abstract is acceptable). The introduction should not include subheadings.

G. Pictures, table, etc., Must be use in numerical order in the article, provided the source correctly, cannot use other people' copyright.

Chart should be colored contrastingly or in black and white.

H. Reference

1) Cited in the main text. Indicate the number in the [ ] mark at the end of the text or the name of the referring person. Let the numbers be in the same line of content as [1].

2) Cited after the article. Put all bibliographical reference after articles, and order according to the author's name, please refer IEEE format. The footer reference format is as follows.

III. Rererences

References in research articles and scholarly articles. For academic and research journals, INTERNATIONAL SCIENTIFIC JOURNAL OF ENGINEERING AND TECHNOLOGY (ISJET). The technology defines referrals according to the IEEE format. All references should be listed at the end of the paper using the following.

Basic format for books:

J. K. Author, "Title of chapter in the book," in *Title of His Published Book,* xth ed. City of Publisher, Country if not USA: Abbrev. of Publisher, year, ch. x, sec. x, pp. xxx–xxx.

Examples:

[1] G. O. Young, "Synthetic structure of industrial plastics," in *Plastics,* 2nd ed., vol. 3, J. Peters, Ed. New York: McGraw-Hill, 1964, pp. 15-64.

[2] W.-K. Chen, *Linear Networks and Systems.* Belmont, CA: Wadsworth, 1993, pp. 123-135.

Basic format for periodicals:

J. K. Author, "Name of paper," *Abbrev. Title of Periodical*, vol. x, no. x, pp. xxx-xxx, Abbrev. Month. year.

Examples:

[3] J. U. Duncombe, "Infrared navigation—Part I: An assessment of feasibility," *IEEE Trans. Electron Devices*, vol. ED-11, no. 1, pp. 34-39, Jan. 1959.

[4] E. P. Wigner, "Theory of traveling-wave optical laser," *Phys. Rev*., vol. 134, pp. A635-A646, Dec. 1965.

[5] E. H. Miller, "A note on reflector arrays," *IEEE Trans. Antennas Propagat*., to be published.

Basic format for reports:

J. K. Author, "Title of report," Abbrev. Name of Co., City of Co., Abbrev. State, Rep. xxx, year.

Examples:

[6] E. E. Reber, R. L. Michell, and C. J. Carter, "Oxygen absorption in the earth's atmosphere," Aerospace Corp., Los Angeles, CA, Tech. Rep. TR-0200 (4230-46)-3, Nov. 1988.

[7] J. H. Davis and J. R. Cogdell, "Calibration program for the 16-foot antenna," Elect. Eng. Res. Lab., Univ. Texas, Austin, Tech. Memo. NGL-006-69-3, Nov. 15, 1987.

Basic format for handbooks:

Name of Manual/Handbook, x ed., Abbrev. Name of Co., City of Co., Abbrev. State, year, pp. xxx-xxx.

Examples:

[8] *Transmission Systems for Communications*, 3rd ed., Western Electric Co., Winston-Salem, NC, 1985, pp. 44-60.

[9] *Motorola Semiconductor Data Manual*, Motorola Semiconductor Products Inc., Phoenix, AZ, 1989.

Basic format for books (when available online):

Author. (year, month day). *Title.* (edition) [Type of medium]. *volume (issue).* Available: site/path/file

Example:

[10] J. Jones. (1991, May 10). *Networks.* (2nd ed.) [Online]. Available: http://www.atm.com

Basic format for journals (when available online):

Author. (year, month). Title. *Journal.* [Type of medium]. *volume (issue),* pages. Available: site/path/file

Example:

[11] R. J. Vidmar. (1992, Aug.). On the use of atmospheric plasmas as electromagnetic reflectors. *IEEE Trans. Plasma Sci.* [Online]. *21(3),* pp. 876-880. Available: http://www.halcyon.com/pub/journals/21ps03-vidmar

Basic format for papers presented at conferences (when available online):

Author. (year, month). Title. Presented at Conference title. [Type of Medium]. Available: site/path/file

Example:

[12] PROCESS Corp., MA. Intranets: Internet technologies deployed behind the firewall for corporate productivity. Presented at INET96 Annual Meeting. [Online]. Available: http://home.process.com/Intranets/wp2.htp

Basic format for reports and handbooks (when available online):

Author. (year, month). Title. Comp any . City, State or Country. [Type of Medium]. Available: site/path/file

Example:

[13] S. L. Talleen. (1996, Apr.). The Intranet Archi-tecture: M anaging information in the new paradigm. Amdahl Corp., CA. [Online]. Available:http://www.amdahl.com/doc/products/bsg/intra/infra/html

Basic format for computer programs and electronic documents (when available online):

ISO recommends that capitalization follow the accepted practice for the language or script in which the information is given.

Example:

[14] A. Harriman. (1993, June). Compendium of genealogical software. *Humanist.* [Online]. Available e-mail: HUMANIST @NYVM.ORG Message: get GENEALOGY REPORT

Basic format for patents (when available online):

Name of the invention, by inventor's name. (year, month day). *Patent Number* [Type of medium]. Available: site/path/file

Example:

[15] Musical toothbrush with adjustable neck and mirror, by L.M.R. Brooks. (1992, May 19). *Patent D 326 189* [Online]. Available: NEXIS Library: LEXPAT File: DESIGN

Basic format for conference proceedings (published):

J. K. Author, "Title of paper," in *Abbreviated Name of Conf.*, City of Conf., Abbrev. State (if given), year, pp. xxxxxx.

Example:

[16] D. B. Payne and J. R. Stern, "Wavelength-switched pas- sively coupled single-mode optical network," in *Proc. IOOC-ECOC,* 1985, pp. 585-590.

Example for papers presented at conferences (unpublished):

[17] D. Ebehard and E. Voges, "Digital single sideband detection for interferometric sensors," presented at the 2nd Int. Conf. Optical Fiber Sensors, Stuttgart, Germany, Jan. 2-5, 1984.

Basic format for patents:

J. K. Author, "Title of patent," U.S. Patent x xxx xxx, Abbrev. Month. day, year.

Example:

[18] G. Brandli and M. Dick, "Alternating current fed power supply," U.S. Patent 4 084 217, Nov. 4, 1978.

Basic format for theses (M.S.) and dissertations (Ph.D.):

J. K. Author, "Title of thesis," M.S. thesis, Abbrev. Dept., Abbrev. Univ., City of Univ., Abbrev. State, year.

J. K. Author, "Title of dissertation," Ph.D. dissertation, Abbrev. Dept., Abbrev. Univ., City of Univ., Abbrev. State, year.

Examples:

[19] J. O. Williams, "Narrow-band analyzer," Ph.D. dissertation, Dept. Elect. Eng., Harvard Univ., Cambridge, MA, 1993.

[20] N. Kawasaki, "Parametric study of thermal and chemical nonequilibrium nozzle flow," M.S. thesis, Dept. Electron. Eng., Osaka Univ., Osaka, Japan, 1993.

Basic format for the most common types of unpublished references:

J. K. Author, private communication, Abbrev. Month, year.

J. K. Author, "Title of paper," unpublished.

J. K. Author, "Title of paper," to be published.

Examples:

[21] A. Harrison, private communication, May 1995.

[22] B. Smith, "An approach to graphs of linear forms," unpublished.

[23] A. Brahms, "Representation error for real numbers in binary computer arithmetic," IEEE Computer Group Repository, Paper R-67-85.

Basic format for standards:

Title of Standard, Standard number, date.

Examples:

[24] IEEE Criteria for Class IE Electric Systems, IEEE Standard 308, 1969.

[25] Letter Symbols for Quantities, ANSI Standard Y10.5-1968.



First A. Author and the other authors may include biographies at the end of regular papers. Biographies are often not included in conference related papers. The first paragraph may contain a place and/or date of birth (list place, then date). Next, the author's educational background is listed. The degrees should be listed with type of degree in what field, which institution, city, state, and country, and year the degree was earned. The author's major field of study should be lower-cased.

The second paragraph uses the pronoun of the person (he or she) and not the author's last name. It lists military and work experience, including summer and fellowship jobs. Job titles are capitalized. The current job must have a location; previous positions may be listed without one. Information concerning previous publications may be included. Try not to list more than three books or published articles. The format for listing publishers of a book within the biography is: title of book (city, state: publisher name, year) similar to a reference. Current and previous research interests end the paragraph.

The third paragraph begins with the author's title and last name (e.g., Dr. Smith, Prof. Jones, Mr. Kajor, Ms. Hunter). List any memberships in professional societies. Finally, list any awards and work for committees and publications. If a photograph is provided, the biography will be indented around it. The photograph is placed at the top left of the biography, and should be of good quality, professional-looking, and black and white (see above example). Personal hobbies will be deleted from the biography. Following are two examples of an author's biography.



Second B. Author was born in Greenwich Village, New York City, in 1977. He received the B.S. and M.S. degrees in aerospace engineering from the University of Virginia, Charlottesville, in 2001 and the Ph.D. degree in mechanical engineering from Drexel University, Philadelphia, PA, in 2008. From 2001 to 2004, he was a Research Assistant with the Princeton Plasma Physics Laboratory. Since 2009, he has been an Assistant Professor with the Mechanical Engineering Department, Texas A&M University, College Station. He is the author of three books, more than 150 articles, and more than 70 inventions. His research interests include high-pressure and high-density nonthermal plasma discharge processes and applications, microscale plasma discharges, discharges in liquids, spectroscopic diagnostics, plasma propulsion, and innovation plasma applications. He is an Associate Editor of the journal *Earth*, *Moon*, *Planets*, and holds two patents.

Mr. Author was a recipient of the International Association of Geomagnetism and Aeronomy Young Scientist Award for Excellence in 2008, the IEEE Electromagnetic Compatibility Society Best Symposium Paper Award in 2011, and the American Geophysical Union Outstanding Student Paper Award in Fall 2005.



Third C. Author received the B.S. degree in mechanical engineering from National Chung Cheng University, Chiayi, Taiwan, in 2004 and the M.S. degree in mechanical engineering from National Tsing Hua University, Hsinchu, Taiwan, in 2006. He is currently pursuing the Ph.D. degree in mechanical engineering at Texas A&M University, College Station.

From 2008 to 2009, he was a Research Assistant with the Institute of Physics, Academia Sinica, Tapei, Taiwan. His research interest includes the development of surface processing and biological/ medical treatment techniques using nonthermal atmospheric pressure plasmas, fundamental study of plasma sources, and fabrication of micro- or nanostructured surfaces.

Mr. Author's awards and honors include the Frew Fellowship (Australian Academy of Science), the I. I. Rabi Prize (APS), the European Frequency and Time Forum Award, the Carl Zeiss Research Award, the William F. Meggers Award and the Adolph Lomb Medal (OSA).

Remark: More detail information, Pleases read Preparation of Papers for INTERNATIONAL SCIENTIFIC JOURNAL OF ENGINEERING AND TECHNOLOGY (ISJET), https://ph02.tci-thaijo.org/index.php/isjet/index